UNIVERSIDAD COMPLUTENSE DE MADRID

FACULTAD DE FARMACIA

Departamento de Microbiología II

TESIS DOCTORAL

Role of cortactin and the adaptor proteins NCK and CRK in pedestal formation by entherpathogenic *Escherichia coli* enteropatógena (EPEC)

Papel de cortactina y de las proteínas adaptadoras Nck y Crk en la formación del pedestal por *Escherichia coli* enteropatógena (EPEC)

MEMORIA PARA OPTAR AL GRADO DE DOCTOR

PRESENTADA POR

Elvira Nieto Pelegrín

Directora

Narcisa Martínez Quíles

Madrid, 2013

UNIVERSIDAD COMPLUTENSE DE MADRID
FACULTAD DE FARMACIA
DEPARTAMENTO DE MICROBIOLOGÍA II

ROLE OF CORTACTIN AND THE ADAPTOR PROTEINS NCK AND CRK IN PEDESTAL FORMATION BY ENTEROPATHOGENIC *ESCHERICHIA COLI* (EPEC)

Papel de cortactina y de las proteínas adaptadoras Nck y Crk en la formación del pedestal por *Escherichia coli* enteropatógena (EPEC)

Thesis submitted in fulfillment of the requirements for the degree of Doctor

Memoria presentada para optar al Grado de Doctor

ELVIRA NIETO PELEGRIN

Supervisor
Directora

NARCISA MARTINEZ QUILES

Madrid, 2012

Dª. CONCEPCIÓN GIL GARCÍA, Directora del Departamento de Microbiología II de la Facultad de Farmacia de la Universidad Complutense de Madrid

CERTIFICA: Que Dª. **ELVIRA NIETO PELEGRIN** ha realizado en el Departamento de Microbiología II de la Facultad de Farmacia de la Universidad Complutense de Madrid, bajo la dirección de la doctora **NARCISA MARTINEZ QUILES**, el trabajo que presenta para optar al grado de Doctor con el título: "Role of cortactin and the adaptor proteins Nck and Crk in pedestal formation by enteropathogenic *Escherichia coli* (EPEC)".

Y para que así conste, firmo la presente certificación en Madrid, 2012

Fdo. Catedrática. Dª Concepción Gil García

Dª. NARCISA MARTÍNEZ QUILES, Profesor Contratado Doctor del Departamento de Microbiología I-Inmunología de la Facultad de Medicina de la Universidad Complutense de Madrid

CERTIFICA: Que Dª. **ELVIRA NIETO PELEGRIN** ha realizado bajo mi dirección el trabajo que presenta para optar al grado de Doctor con el título: "Role of cortactin and the adaptor proteins Nck and Crk in pedestal formation by enteropathogenic *Escherichia coli* (EPEC)".

Y para que así conste, firmo la presente certificación en Madrid, 2012

Fdo. Dra. Narcisa Martínez Quiles

Este trabajo ha sido financiado por:

- Proyecto Comunidad Europea "Marie Curie International Reintegration Grant" (MIRG-CT-2005-028995).
- Proyecto del Instituto de Salud "Carlos III". Fondo de Investigación Sanitaria (FIS). PI06-0004.
- Proyecto Fundación Médica Mutua Madrileña (FMMM-01754/2008).
- Proyecto del Instituto de Salud "Carlos III". Fondo de Investigación Sanitaria (FIS). PS09/00080

La doctoranda ha sido financiada por:

- Proyecto Comunidad Europea "Marie Curie International Reintegration Grant" (MIRG-CT-2005-028995) durante dos años.
- Proyecto Fundación Médica Mutua Madrileña (FMMM-01754/2008) durante cinco meses.
- Beca de Formación Investigador de la Universidad Complutense de Madrid (UCM-FPI) durante cuatro años.

"Cuando enseñes algo a alguien, enséñale también a dudar de ello"

(Jose Ortega y Gasset)

A mis padres.

A Maria, Teresa, Lucia y Noelia.

A Cris.

ACKNOWLEDGEMENTS

ACKNOWLEDGEMENTS

(Agradecimientos)

Siempre es un alivio escribir los agradecimientos, primero porque es bonito dedicarle unas líneas a todos los que de un modo u otro te han ayudado durante este largo camino, y segundo porque significa que el duro periodo de escritura de la tesis está próximo a su fin.

En primer lugar quiero agradecer a mi directora, Narcisa, por darme la oportunidad de realizar la tesis doctoral y por enseñarme todo lo aprendido en el laboratorio. Me llevo tu enseñanza que en ciencia, y en todo en la vida, hay que ser insistente y paciente, de este modo hemos podido entender muchos de los resultados obtenidos a lo largo de todos estos años. Gracias además por la rapidez y la dedicación en estos últimos meses de intensas correcciones.

A continuación quiero agradecer al programa Europeo "Marie Curie Reintegration Grant", a la "Fundación Médica Mutua Madrileña" y en especial a la Universidad Complutense de Madrid, por la financiación recibida gracias a la cual ha sido posible la realización de la presente tesis doctoral.

Quiero agradecer a todos los miembros del departamento de Microbiología II por estos años vividos allí. A todos los profesores y compañeros, pasados y presentes, que constituís esa gran familia donde la función de cada uno es necesaria para el funcionamiento del conjunto. Gracias por todo lo que cada uno de vosotros ha aportado. Gracias a los que durante estos años han sido mis compañeros de unidad, en especial a Miguel por la ayuda recibida, por tan buenos consejos y tardes de intentar solucionar el mundo, y a Pablo por todos los días de charlas y experimentos en el laboratorio. Gracias a todos los chicos de las demás unidades por las divertidas cenas de navidad, de verano, cañitas (me encantó la quedada del Gula Gula!)… y por todo el apoyo y el ánimo durante estos últimos meses de escritura. Os deseo todo lo mejor en el futuro. Gracias también a Benito y Jose Alberto, sin los cuales el departamento no se

mantendría como lo conocemos, gracias por arreglos de cajones, por solucionar emergencias de CO_2 y una y mil cosas a lo largo de estos años.

En especial quería agradecer a las que han sido mis compañeras de grupo y he tenido la oportunidad de enseñarles algo: Maria, Preetie, Lidia y sobre todo a Eugenia, gran compañera y mejor amiga, gracias por toda la ayuda con los experimentos en estos últimos meses y por todos los días de conversaciones, confesiones y buenos consejos. Gracias también por los momentos fuera del laboratorio, estoy segura que después de la tesis todo te irá muy bien porque eres una persona que persigue sus objetivos con ahínco.

Agradecer también a las siguientes personas: Dr. Steffen Backert (School of Biomolecular and Biomedical Sciences, University College Dublin, Ireland), Dr. Philip R. Hardwidge (University of Kansas Medical Center, Kansas City), Dr. Brett B. Finlay (University of British Columbia, Vancouver, Canadá), Dr. Scott B. Snapper (Massachusetts General Hospital, Boston, USA), Dr. Tony Pawson (Mount Sinai Hospital, Toronto, Canadá), Dr. Thomas Curran (The Children's Hospital of Philadelphia, Pennsylvania, USA), Dr. Akira Imamoto (The University of Chicago, USA), Dr. Peter Greer (Queen´s University. Ontario. Canadá), Dr. Brett B. Finlay (University of British Columbia, Vancouver, Canadá), Dr. Michiyuki Matsuda (Osaka University, Japón), Dr. Isabel Rodriguez Escudero (Microbiología II. Fac. Farmacia. UCM. Madrid) y Dr. Chihiro Sasakawa (Institute of Medical Science. The University of Tokyo, Japón) por los reactivos suministrados sin los cuales la realización de esta tesis no hubiera sido posible.

I would also like to thank Dr. Marie-France Carlier and Dr. Christophe LeClainche (CNRS. Gif-sur-Yvette. France) to give me the opportunity to learn actin polymerisation assays in their lab. Also thanks the members of their laboratory for Arp2/3 and actin purification. Also thank Christophe for the technical support and the valuable comments during my period there and for being my thesis reviewer. The month in France was also a unique occasion to live in a French castle; I want thank my castle friend, Nikie, for the basketball matches (never played again) and for keeping me company during those days. I wish you all the best with your physics doctorate.

Dr. Brendan Kenny deserves a special thank you to give me the opportunity to be part of his laboratory during three months, and for all the help and support trying to understand thousands of western blots bands. Working in your lab has been a rewarding experience. Thank you also for being my thesis reviewer. A big thank-you goes to Sabine because without her help it would not have been possible to obtain so many results during my period in the lab. Also thanks Lorna for all the help in the lab and outside the lab; you are one of the most enthusiastic people that I have ever met. Thank you both, Sabine and Lorna, for keeping me company, it was really nice to have you around during my period in NC and I wish you all the luck in the future. Thanks also to Paul, for your help with my experimental problems and for your technical advices. Also thanks to Marc to make the days funnier in the lab and specially for agreeing to be a substitute member of my thesis committee. Finally, I would like to thank Susanne to be a really good flat mate, having such a good talks. Thank you for listening to me and for your advices.

I would like to thank to Dr. Ilan Rosenshine for the helpful comments about my results and for the involvement during the process of applying for the European fellow.

Quería agradecer también a la Dr. Susana Alemany, la primera investigadora que me dio la oportunidad de empezar a trabajar en ciencia formando parte de su laboratorio cuando aun no era ni licenciada. Gracias también a todas las chicas del B-15 donde aprendí muchas cosas que me han servido en lo profesional y en lo personal.

Mención especial requieren mis padres porque sin ellos esto no habría sido posible. En primer lugar, gracias papis por haberme dado la oportunidad de estudiar una carrera, de aprender inglés (sin el cual ahora no habría sido posible presentar así esta tesis) y por la educación y los valores recibidos. Gracias también por apoyar todas las decisiones que he tomado en mi vida, por difíciles que hayan sido. Sois unos padres admirables. Os quiero. Agradecer también a mis abuelos por enseñarme que la juventud está en el espíritu y por toda vuestra ayuda, os quiero. A mi hermanito, al que adoro aunque a veces no hablemos en días, gracias por ser mi informático 24 horas,

por responder a mis llamadas para solucionar tonterías con paciencia y por estar ahí cuando realmente se te necesita.

A mis amigas, gracias por estos doce años de amistad apoyándome día tras día, por todas las tardes de sanedrín y vips en las que hemos acabado hablando de ciencia muchas veces. Gracias también por divertidísimas noches de fiesta y vacaciones juntas. A Noelia, ha sido un placer ser tu compañera de aula, de laboratorio y de barrio. Te voy a echar mucho de menos cuando ya no estés en el laboratorio de al lado. Gracias por toda la ayuda durante estos años y por estar ahí siempre cuando se te necesita. A Maria, gracias por tu gran apoyo, por estar siempre al otro lado del "whatsapp" para cualquier cosa, por tu ayuda técnica y los miles de artículos sin los que habría sido mucho más difícil escribir esta tesis. A Teresa, gracias por estar siempre dispuesta a ayudar en lo que esté en tu mano y por habernos presentado a grandes amigos como Álvaro, Carlos, Juanjo y al resto de componentes de "pataliebre production" y colaboradores a los cuales quiero agradecer también todos los días de cumples y fiestas juntos. Y por último, y no menos importante, a Luci, gracias por tu ayuda durante estos años y por esos consejos tan válidos. Sois muy buenas amigas y me siento muy orgullosa de poder contar con vosotras para todo. Espero que superemos con éxito esta dura época de meternos en el mercado laboral y que sigamos siendo amigas para siempre.

A mis primos y amigos de mi queridísimo pueblo porque aunque a veces dicen que la familia te toca y no se elige, si tuviera que elegir unos primos tened por seguro que os elegiría a vosotros. Gracias por tener siempre esas ganas de fiesta y por ser tan divertidos. Es un gusto tener a alguien siempre dispuesto a pasar un buen rato aunque solo sea comiendo pipas y "dándole a la húmeda" en el salón, aunque generalmente elijamos la barra de un bar. Gracias a Elvira, Aurelio, Luisa, Cristina, Thierry, Arturo, Miguel, Amparo, Angelito, Ton, Juanma, Paco, Esther, Amara y un largo etc... A los sobris, Mariona, Paquito, Manuel y "bolita suapel" y al que está en camino, deseo que tengáis tan buena relación como tenemos nosotros. Os quiero.

Gracias a Laura M. por los años de carrera vividos juntas, por quedadas y viajes tan divertidos. A Alvarito por tu amistad durante estos años y por escuchar siempre mis historias, te echo de menos ahora que estás tan lejos. A Luzma, gracias por estar siempre ahí para darme tus consejos y tu interesante punto de vista. Gracias también por cuidarme a la Cristi cuando yo no estoy. Gracias a Javichu y a Rubén. A Marga por esa gran portada de tesis. A Tania y Vicky por tantas cenitas y comidas de interesante conversación, y a sus pequeños a los que quiero mucho. Gracias también a Sonia y Tania por vuestra amistad desde la infancia. Gracias a Clara por todos los momentos que vivimos fuera y dentro del laboratorio, echamos de menos tenerte por aquí siempre dispuesta a cualquier plan con nosotras. También a Laura, un placer compartir tardes de patines y esquí contigo.

Y por último gracias a ti, Cris, por tantas cosas que no cabrían en esta hoja. Gracias por ser tan buena persona, por estar a mi lado cada día, por ayudarme incondicionalmente, por entender y compartir mis debilidades, y en definitiva por haber creado lo que siempre he buscado. No imagino la vida sin ti. Te quiero.

TABLE OF CONTENTS

TABLE OF CONTENTS

SUMMARY

SUMMARY

The adherence of enteropathogenic *Escherichia coli* (EPEC) to human intestinal cells triggers the formation of actin-rich pedestals. This process requires the translocation of the bacterial translocated intimin receptor (Tir) into host cells through a type III secretion system. The insertion of Tir into the plasma membrane and its tyrosine-phosphorylation leads to the recruitment of the host cell adaptor Nck, following Tir interaction with its ligand -the EPEC intimin surface protein. Nck in turn activates the neural Wiskott-Aldrich syndrome protein (N-WASP) initiating actin polymerisation mediated by the actin-related (Arp)2/3 complex. Interestingly, the host cortactin protein activates the Arp2/3 complex and N-WASP promoting actin polymerisation by two different mechanisms.

Here, we interrogate a suggested role for cortactin in Tir-mediated actin nucleation events and reveal a critical role. We propose that cortactin binds Tir through its N-terminal part in a phosphorylation independent manner. On the other hand, the SH3 domain binding and activation of N-WASP is regulated by tyrosine and serine mediated phosphorylation of cortactin. Moreover, Tir-cortactin interaction promotes Arp2/3 complex-mediated actin polymerisation *in vitro*. Therefore, cortactin could act on Tir:Nck:N-WASP signalling pathway and control a possible cycling activity of N-WASP underlying pedestal formation.

We also demonstrate that Crk family adaptor proteins have a redundant inhibitory role in regulating actin polymerisation in actin pedestals. Furthermore, we have observed that Nck-deficient mouse embryonic fibroblasts (MEFs) have significantly reduced amounts of Tir whereas the levels of other translocated effectors, EspF and EspB, are normal. In addition, the levels of Map effector are also reduced in these cells. Importantly, we establish that the absence of Tir in Nck-deficient cells implies a decrease in pedestal formation and bacterial attachment to these cells. We investigated whether the drastic reduction in the amount of Tir in the absence of Nck is due to protein degradation or to a defective delivery process. Interestingly, the treatment with TSA, a known deacetylase and autophagy inhibitor, results in a significant increase in the amount of Tir in Nck-deficient cells. Although our results point to a selective defective delivery of Tir and Map proteins, the only two effectors whose efficient translocation is dependent on the chaperone CesT, we cannot discard a possible degradation of both effectors inside the host cell.

ABBREVIATIONS AND ACRONYMS

ABBREVIATIONS AND ACRONYMS

A/E: Attaching and effacing

Ab: Antibody

Abl: Tyrosine kinase: Abelson tyrosine kinase

ABR: Actin-binding region

ADF: Actin depolymerising factor

ADP: Adenosine diphosphate

ARF: ADP-ribosylation factor

Arp: Actin-related protein

ATEC: Atypical enteropathogenic *E. coli*

ATP: Adenosine triphosphate

BFP: Bundle-forming pili

CBD: Chaperone-binding domain

Cdc42: Cell division cycle 42

CML: Chronic myelogenous leukaemia

CR: *Citrobacter rodentium*

CRIB domain: Cdc42/Rac-interactive binding domain

Crk: CT10 (chicken tumour virus no. 10) regulator of kinase

CrkL: Crk-like

C-terminal: Carboxyl-terminal

DAEC: Diffusely adhering *E. coli*

dS mutant: p*tir*S434/463A

dY mutant: p*tir*Y474F/Y454F

EAEC: Enteroaggregative *E. coli*

EGF: Epidermal growth factor

EHEC: Enterohaemorrhagic *E. coli*

EIEC: Enteroinvasive E. coli

EPEC: Enteropathogenic *E. coli*

Erk: Extracellular signal-regulated kinase

Esc: *E. coli* secretion component

Esp: *E. coli* secretion protein

ETEC: Enterotoxigenic *E. coli*

Etk: Epithelial and endothelial tyrosine kinase

FA: Focal adhesion

F-actin: Filamentous actin

FAK: Focal adhesion kinase

Fer tyrosine kinase: Feline sarcoma-related tyrosine kinase

FGF: Fibroblast growth factor

FL: Full-length

G-actin: Globular monomeric form

GBD: GTPase-binding domain

GEF: Guanine exchange factor

GST: Glutathione S-transferase

GTP: Guanosine triphosphate

GTPase: Guanosine triphosphatase

HDAC6: Histone deacetylase 6

HDACi: Histone deacetylase inhibitor

HS1: Haematopoetic-specific protein 1

I-BAR: Inverse Bin-amphiphysin-Rvs167

IF: Immunofluorescence

IRSp53: Insulin receptor tyrosine kinase substrate p53

IRTKS: Insulin receptor tyrosine kinase substrate

IVOC: *In vitro* organ cultures

LA: Localised adherence

LEE: Locus of enterocyte effacement

Map: Mitochondrial-associated protein

MEFs: Mouse embryonic fibroblasts

Mo Ab: Monoclonal antibody

MOI: Multiplicity of infection

NC: Needle complex

Nck-/-: Nck-deficient MEFs

Nck: Non-catalytic tyrosine kinase

NF-kB: Nuclear factor kB

Nle: Non-LEE effectors

NMR: Nuclear magnetic resonance

NPF: Nucleation-promoting factor

NPY motif: Asn-Pro-Tyr motif

NSD domain: N-terminal signal domain

NTA: N-terminal acidic domain

N-WASP-/-: N-WASP-deficient MEFs

N-WASP: Neural Wiskott Aldrich Syndrome Protein

p130Cas: p130 Crk-associated substrate

Pak: p21 activated kinase 1

PCAF: Histone acetyltransferase p300/CBP-associated factor

PDGF (R): Platelet-derived growth factor (receptor)

PI3K: Phosphoinositide 3-kinase

PIP_2: Phosphatidylinositol 4,5-bisphosphate

PKA: Protein kinase A

Poly Ab: Polyclonal antibody

PRD: Proline-rich domain

p*tir*: pACYC184 based plasmid carrying the 3´*map*, *tir* and *cesT*

quad: p*tir*Y474F/Y454F S434/463A

REPEC: Rabbit-specific enteropathogenic *E. coli*

S405,418A (2A) mutant: Erk non-phosphorylatable mutant

S405,418D (SD) mutant: Erk-phosphorylation-mimicking mutant

SEM: Scanning electron micrograph

Sep: Secreted *E. coli* proteins

SGTL-1: Sodium-dependent glucose co-transporter

SH2 domain: Src homology-2 domain

SH3 domain: Src homology-3 domain

siRNA: Small interference RNA

SNX9: Sortin nexin 9

Src tyrosine kinase: Sarcoma tyrosine kinase

Tccp: Tir cytoskeleton coupling protein (also known as EspFu)

TCR: T-cell receptor

Tir: Translocated intimin receptor

TJ: Tight-junction

TNF- α: Tumor necrosis factor-α

TTSS: Type III secretion system

VCA domain: Verprolin homology, central hydrophobic and acidic regions

W22A mutant: Arp2/3 activation mutant (W22A)

W525K mutant: SH3 domain mutant

WASPs: Wiskott-Aldrich syndrome family of proteins

WAVE: WASP-family verprolin homologue

WB: Western blot

WCA domain: see VCA domain

WH1 domain: WASP-homology 1 domain

WIP: WASP-interacting protein

WT: Wild type

Y421,466,482D (3D) mutant: Src-phosphorylation-mimicking mutant

Y421,466,482F (3F) mutant: Src non-phosphorylatable mutant

INTRODUCTION

INTRODUCTION

1. Actin polymerisation promoted by the Arp 2/3 complex

The actin cytoskeleton is a dynamic network composed of actin filaments that remodels to accomplish many cellular processes and therefore exhibits significant changes during cell migration, adhesion, endocytosis and bacterial invasion. Actin polymerisation occurs when the globular monomeric form (G-actin) undergoes cycles of self-assembly into filamentous actin (F-actin) in a tightly regulated process. Actin filaments are polar structures that contain fast-growing barbed ends and less active pointed ends. The initial formation of a dimeric or a trimeric nucleus is kinetically unfavourable being promoted and controlled by proteins that facilitate the process, such as the actin-related protein (Arp) 2/3 complex and formin proteins. The Arp2/3 complex has the ability to organise the actin filaments into branched networks (Figure 1A) (reviewed in (Pantaloni et al., 2001)) whereas formins produce unbranched actin filaments (Figure 1B). Apart of *the novo* nucleation of monomers, cells initiate actin assembly creating free barbed ends by uncapping or severing pre-existing filaments. Cells need to maintain a high concentration of monomeric actin to support the rapid and constant actin polymerisation at their leading edge. Proteins of the cofilin/ADF (actin depolymerising factor) family play a major role in this process by disassembling the actin network. It has been proposed that ADF acts by severing actin filaments (reviewed in (Pollard and Cooper, 2009)) or by increasing the dissociation rate of monomers at the pointed end of actin filaments (reviewed in (Pantaloni et al., 2001)).

The Arp2/3 complex is comprised of seven subunits, including the two actin-related proteins 2 and 3. This complex is able to add a 'branch' to the side of a pre-existing actin filament, giving rise to branched filaments with a characteristic 70-degree angle (Pollard and Cooper, 2009) (Figure 1A). By itself, the Arp2/3 complex is inactive and requires the action of the so-called nucleation-promoting factors (NPFs) to efficiently nucleate filaments.

The first described activators of the Arp2/3 complex are the Wiskott-Aldrich syndrome family of proteins (WASPs) (Marchand et al., 2001). The representative member of the family, WASP, which is expressed exclusively in the immune system, is mutated in the immune deficiency called Wiskott-Aldrich syndrome (WAS) (Derry et al., 1994). Neural WASP (N-WASP), first discovered in brain, is more ubiquitous than WASP and is coexpressed with this protein in some cell types, such as macrophages and dendritic cells (Miki et al., 1996). WASPs proteins belong to a group of NPFs called Class I that promotes actin polymerisation through the binding to G-actin and activating the Arp2/3 complex through a conserved carboxyl terminal VCA domain (or WCA domain) named for its three sub-elements, the Verprolin homology (also called WASP homology 2), Central hydrophobic (previously known as cofilin-homology) and Acidic regions (Machesky and Insall, 1998) (reviewed in (Kurisu and Takenawa, 2009)).

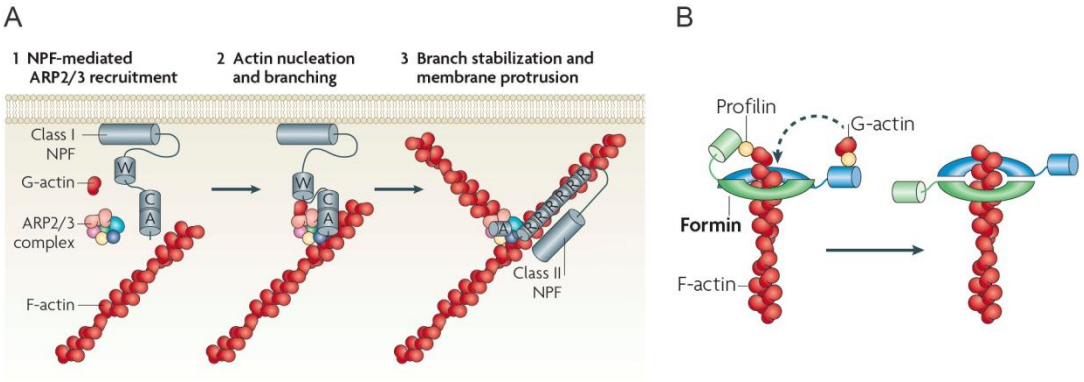

Figure 1. (A) Model of Arp2/3-dependent actin polymerisation. 1. The WCA domains of Class I NPFs, such as N-WASP, recruit the Arp2/3 complex. **2.** The collective activities of WCA domain serve for bringing Arp2/3 together with the first actin subunit in the new filament to generate a 70º branch on the side of a pre-existing filament. **3.** Arp2/3 branch points can be stabilised by filamentous actin (F-actin)-binding class II NPFs, such as cortactin. (Abbreviations used: G-actin, globular actin; W, WASP homology 2 domain; C, central hydrophobic region; A, acidic region; R, repeat). **(B) Model of formin-mediated actin polymerisation.** In contrast to the Arp2/3 complex, formins nucleate formation of unbranched actin filaments. The formin closed conformation prevents capping by other factors. Figure adapted from (Campellone and Welch, 2010).

In addition to Class I NPFs, many animals possess a second type of Arp2/3 activator, termed Class II activators. This category includes cortactin and the haematopoetic-specific protein 1 (HS1). These proteins have Arp2/3-binding acidic motifs and

repetitive sequences that interact with F-actin influencing the stability of F-actin branch points (Weaver et al., 2001) (Figure 1A).

WASP family proteins

WASP family proteins are categorised into two groups: (1) WASP and N-WASP, and (2) three WASP-family verprolin homologue (WAVE; also known as SCAR) isoforms. All of them have a modular organisation. WASP and N-WASP present an N-terminal WASP homology 1 domain (WH1) followed by a basic region, a GTPase-binding domain (GBD) and a proline-rich domain (PRD). In the C-terminus they have the conserved VCA domain that directly binds to and activates the Arp2/3 complex.

WASP and N-WASP present an inactive conformation because its VCA region is inhibited by intramolecular interactions with the autoinhibitory portion of the GBD (Kim et al., 2000; Padrick and Rosen, 2010), and require the interaction with other proteins and possibly post-translational modifications to be fully active. Thus, the complex regulation of N-WASP implies the interaction of multiple cellular proteins with its GBD or PRD domains. For example, the autoinhibition is released by the competitive binding of the small GTPase cell division cycle 42 (Cdc42) to the GBD domain. This activation mechanism is enhanced by phosphatidylinositol 4,5-biphosphate (PIP2) binding to the basic region amino-terminal to the GBD domain that synergises with cdc42 to activate WASPs and N-WASPs (Rohatgi et al., 2001). In addition, Src homology 3 (SH3)-domain containing proteins such as Nck (Rivero-Lezcano et al., 1995) or Grb2 (She et al., 1997) binds to the numerous proline motifs in the PRD and also activates N-WASP by destabilising the inhibitory interactions. It is currently thought that the activation of N-WASP occurs in a cooperative way; therefore WASPs proteins are able to integrate multiple signalling inputs that promote their maximal activity.

The inactive conformation is stabilised by the binding of WASP-interacting protein (WIP) to WH1 domain of WASP and N-WASP. Although the role of WIP *in vivo* requires further investigations (reviewed in (Noy et al., 2012)), *in vitro* WIP inhibits N-WASP (Martinez-Quiles et al., 2001).

2. Cortactin, a cytoskeletal oncoprotein targeted by pathogens

Cortactin was originally described as a substrate of the sarcoma (Src) kinase located primarily at the cell cortex (Wu et al., 1991). Almost simultaneously, cortactin was cloned as the product of the CTTN gene (formerly EMS1), located in chromosomal region 11q13, which is frequently amplified in different human carcinomas (Schuuring et al., 1993). Today, cortactin is considered an oncoprotein and a *bona fide* marker of actin-rich protusions of the cell membrane that degrade the extracellular matrix, called invadopodia (Weaver, 2008) (Caldieri et al., 2009).

Cortactin is a key regulator of the actin cytoskeleton that participates in many cellular functions emerging as an important node in the network regulating the cytoskeleton during numerous biological processes (Daly, 2004; Ren et al., 2009). Thus, cortactin is involved in several pathogenic processes, such as actin-based motility of *Listeria monocytogenes, Shigella flexneri* and *vaccinia* virus (Frischknecht and Way, 2001), cell scattering induced by *Helicobacter pylori* (Selbach et al., 2003), invasion of *Shigella flexneri* (Dehio et al., 1995) and others (*Neisseria meningitides* (Hoffmann et al., 2001), *Rickettsia conorii* (Martinez and Cossart, 2004) etc.) and pedestal formation of enteropathogenic *E. coli* (EPEC) and enterohaemorrhagic *E. coli* (EHEC) (Cantarelli et al., 2006). Hence, it was called by our collaborators the Achilles´ heel of the actin cytoskeleton targeted by pathogens (Selbach and Backert, 2005).

2.1. Structure of cortactin

Cortactin is composed of several domains. It contains an N-terminal acidic domain (NTA) which harbours a $_{20}$DDW$_{22}$ motif that directly binds and activates the Arp2/3 complex, thereby behaving as a nucleation-promoting factor (NPF) as previously mentioned. The NTA domain is followed by six and a half amino acids repeats which bind to filamentous actin and define the actin-binding region (ABR) (Weed and Parsons, 2001). The ABR is followed by a helical, proline-rich region, and a final C-terminal SH3 domain (Figure 2).

Cortactin only weakly activates the Arp2/3 complex *in vitro* (Uruno et al., 2001), therefore it is unclear whether cortactin requires post-translational modifications to be fully active. On the other hand, cortactin and N-WASP can be found as components of molecular complexes in cells as first described by (Mizutani et al., 2002). In addition, it was demonstrated that *in vitro* cortactin binds directly to N-WASP through its SH3 domain and activates it (Martinez-Quiles et al., 2004). Thus, cortactin can promote actin nucleation in two different ways, firstly by activating the Arp2/3 complex and secondly by activating N-WASP.

Moreover, cortactin binds various proteins through its SH3 domain, such as WIP [(Kinley et al., 2003) and (Martinez-Quiles *et al.*, unpublished results)] and Nck (Okamura and Resh, 1995) (Figure 2) that are also implicated in actin dynamics.

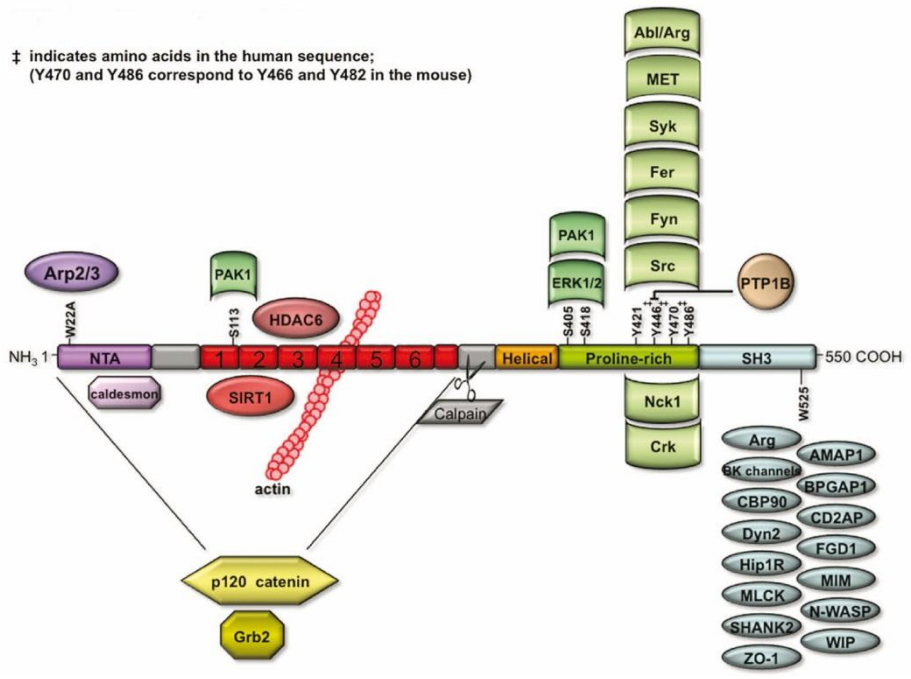

Figure 2. Cortactin and its binding partners. Schematic of cortactin domains (Abbreviations used: NTA, N-terminal acidic domain; SH3, Src homology 3 domain). Amino acids that are essential for the interaction with cortactin binding proteins are shown (W22 in the NTA domain and W525 within SH3 domain). Interacting proteins are shown in the same colour as the domain on cortactin. Proteins in yellow bind the amino terminus of cortactin. The kinases known to phosphorylate cortactin are shown above the respective sites they have been shown to phosphorylate. Figure adapted from (Kirkbride et al., 2011).

2.2. Regulation of cortactin

The understanding of the regulation of cortactin is far from clear (reviewed in (Ammer and Weed, 2008)). Although cortactin has been described as a substrate of Src family kinases (Wu et al., 1991), it can also be phosphorylated by other tyrosine kinases such as feline sarcoma-related protein (Fer) (Sangrar et al., 2007) and Abelson (Abl)-family kinases Abl and Abl-related gene (Arg) (Boyle et al., 2007) (Figure 2). Interestingly, it is thought that Src family kinases act upstream of Arg in phosphorylating cortactin (Mader et al., 2011). Tyrosine phosphorylation of cortactin by Src occurs at residues 421, 466 and 482 (Huang et al., 1998) during numerous physiological conditions, such as integrin-mediated cell adhesion, fibroblast growth factor (FGF) 1-mediated cell migration and others (reviewed in (Lua and Low, 2005)).

The effects of tyrosine phosphorylation on cortactin structure and function remain largely unknown. One group described that tyrosine phosphorylation of cortactin decreases its F-actin binding and cross-linking activity *in vitro* (Huang et al., 1997). Moreover the binding of cortactin to F-actin is required for cortactin activation of the Arp2/3 complex (Weaver et al., 2001). By using tyrosine non-phosphorylatable cortactin mutants, it was shown that Src-mediated phosphorylation of cortactin is involved in endothelial cell migration (Huang et al., 1998). Similarly, tyrosine phosphorylation of cortactin is also required for inducing bone metastasis of breast cancer cells in nude mice (Li et al., 2001).

Studies have demonstrated that tyrosine phosphorylation of cortactin is essential for generation of free barbed ends to promote actin polymerisation in invadopodia (Bowden et al., 1999; Oser et al., 2009) and for efficient extracellular matrix degradation (Clark et al., 2007). Moreover, it has been described that the tyrosine kinase Arg mediates epidermal growth factor (EGF)–induced cortactin phosphorylation in invadopodia, promoting actin polymerisation. Notably, it was suggested that Src indirectly regulates the process through Arg activation. Hence, they propose that the EGFR–Src–Arg–cortactin pathway is responsible for mediating functional maturation of invadopodia and breast cancer cell invasion (Mader et al., 2011).

Considering the many molecular complexes that must be formed *in vivo*, cortactin actions are difficult to analyse *in vitro*. Thus, it was proposed that the tyrosine phosphorylation of cortactin promotes the efficient actin polymerisation *in vitro* by facilitating the assembly of an Nck1–N-WASP–WIP–Arp2/3 signalling complex (Tehrani et al., 2007).

Hence, tyrosine phosphorylation of cortactin has to be tightly regulated since tyrosine phosphorylation-dephosphorylation of cortactin may regulate its ability to form complexes with other proteins. In fact, protein phosphatase 1B (PTP-1B) dephosphorylates cortactin (Mertins et al., 2008; Stuible et al., 2008), suggesting a reversible regulation.

On the other hand, tyrosine-phosphorylated cortactin is involved in bacterial invasion of cells. The entry of *Shigella flexneri* (Dehio et al., 1995) is accompanied by an increase in the phosphorylation of cortactin. In contrast, *Helicobacter pylori* infection induces the tyrosine-dephosphorylation of cortactin (Selbach et al., 2003). Many other pathogens have been shown to alter the tyrosine phosphorylation of cortactin (reviewed in (Selbach and Backert, 2005)).

Cortactin is also the target for serine-threonine kinases, including extracellular signal-regulated kinase (Erk) that phosphorylates cortactin at serine residues 405 and 418 (Campbell et al., 1999). The stimulation with epidermal growth factor (EGF) of tumour cells leads to phosphorylation of these sites and induces a shift in cortactin electrophoretic mobility from 80 kDa to 85 kDa in SDS-PAGE. The member of the p21 activated kinase family (Pak) 1 also phosphorylates cortactin at residues 405 and 418. In addition, Pak3 phosphorylates cortactin at serine residue 113 (Grassart et al., 2010; Webb et al., 2006). Phosphorylation of serine residues of cortactin enhances binding of the cortactin SH3 domain to N-WASP, stimulating Arp2/3-mediated actin polymerisation *in vitro* (Martinez-Quiles et al., 2004) (see below).

Besides the previously mentioned sites, phosphoproteomic analysis of cortactin has revealed numerous new phosphorylation sites, most of which are serines and

threonines (Martin et al., 2006). However, the functional implications of these sites need to be studied.

Adding another level of complexity to cortactin regulation, studies have shown that the protein is also regulated by reversible acetylation. The protein can be acetylated by histone acetyltransferase p300/CBP-associated factor (PCAF) and deacetylated mainly by Histone Deacetylase 6 (HDAC6) and SIRT1 (Zhang et al., 2007; Zhang et al., 2009). Acetylation of lysine residues in the ABR of cortactin was shown to reduce binding to F-actin, which inhibits cell migration (Zhang et al., 2007).

Our group has recently described a competition between acetylation and tyrosine phosphorylation of cortactin and that tyrosine phosphorylation inhibits cell spreading. Furthermore, we demonstrated that cell spreading promotes the association of cortactin and focal adhesion kinase (FAK) and that tyrosine phosphorylation of cortactin disrupts this interaction, which may explain how it inhibits cell spreading (Meiler et al., 2012). This will be the subject of the Ph.D. dissertation from Eugenia Meiler. In accordance with our results it has been demonstrated that focal adhesion (FA) remodelling may occur through the formation of a FAK-cortactin complex and cortactin tyrosine phosphorylation results in FAK-cortactin complex dissociation associated with FA turnover (Tomar et al., 2012).

2.3. Cortactin as a cytoskeletal switch

As previously mentioned, Src kinase targets tyrosine residues 421, 466 and 482 of cortactin while Erk phosphorylates serines 405 and 418 (Campbell et al., 1999), which lie in a proline rich area. Cortactin promotes actin polymerisation through two pathways: directly, by activating the Arp2/3 complex; and indirectly, when the SH3 domain binds and activates N-WASP (Martinez-Quiles et al., 2004). The interaction between cortactin and N-WASP was studied using *in vitro* actin polymerisation assays involving both phosphomimetic mutants and non-phosphorylatable mutants of cortactin, as well as recombinant cortactin phosphorylated i*n vitro*. Erk phosphorylation of cortactin or the

double mutation S405,418D in cortactin that mimics this phosphorylation enhance the binding and activation of N-WASP. Conversely, Src phosphorylation inhibits the ability of both Erk-phosphorylated cortactin and that doubly mutated S405,418D cortactin, to activate N-WASP. Furthermore, phospho-mimetic mutation of the three tyrosine residues targeted by Src (Y421,Y466, and Y482) inhibited the ability of S405,418D cortactin to activate N-WASP. Thus, cortactin binds and activates N-WASP only when phosphorylated on serines by Erk, whereas phosphorylation by Src terminates cortactin activation of N-WASP, which suggests that phosphorylation indeed affects cortactin structure. Based on these studies by the P.I. of our group (Martinez-Quiles et al., 2004) and previous studies (Campbell et al., 1999), it was proposed a model in which serine/tyrosine phosphorylation of cortactin controls the ability of cortactin to activate N-WASP (Figure 3).

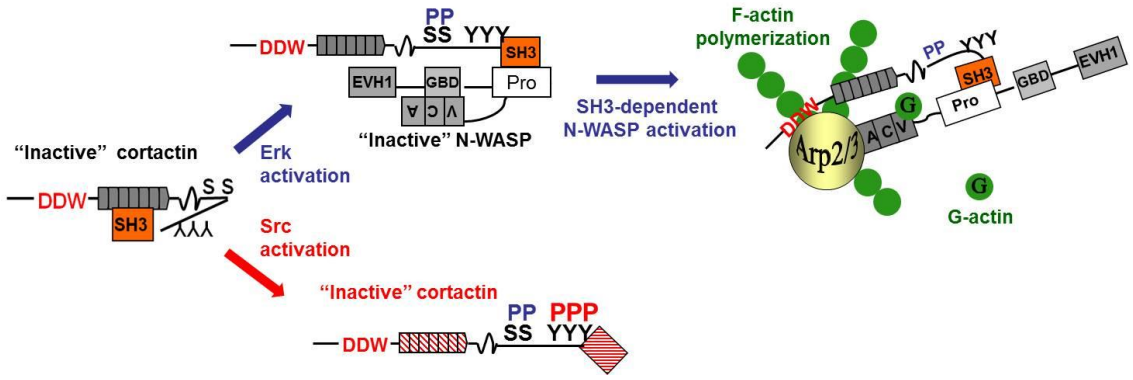

Figure 3. Coupled cortactin-N-WASP activation according to the 'S-Y Switch' model proposed by (Martinez-Quiles et al., 2004). In non-phosphorylated cortactin, the SH3 domain folds back and binds the repeats region (Cowieson et al., 2008). The phosphorylation of serine residues by Erk could interrupt the intramolecular interaction and induce a conformational change. This could liberate the SH3 domain for binding N-WASP, which can stimulate the activity of the Arp2/3 complex. Phosphorylation on tyrosines residues by Src induces another conformational change and the interaction of the cortactin SH3 domain with N-WASP is terminated. Taken together, Erk and Src phosphorylation of cortactin might act as a 'switch on/off' mechanism that controls the activity of cortactin via its ability to bind F-actin and activate N-WASP. Figure adapted from (Nieto-Pelegrin et al., 2010).

This model was subsequently reviewed by Lua and Low, who renamed it as the 'S-Y Switch' model (Lua and Low, 2005). Until that moment the study by Campbell and colleagues (Campbell et al., 1999) was the sole report on cortactin phosphorylation by Erk that was brought to light by the study of Martinez-Quiles *et al*. Interestingly, the

former report was the first one using the expression of phospho-mimetic cortactin tyrosine and serine mutants, not only the non-phosphorylatable cortactin forms.

One of the most important prediction of the model is that cortactin can be regulated by a conformational change, that would liberate the SH3 domain from intramolecular interactions. Soon after the proposal of the model, the structure of unmodified cortactin using circular dichroism revealed a closed, globular conformation achieved mainly through interactions between the SH3 domain and the ABR region (Cowieson et al., 2008). This study is in contrast to the previously described elongated monomeric form of cortactin (Weaver et al., 2002). Currently both conformations are accepted to exist (reviewed in (Ammer and Weed, 2008)).

As an immediate consequence of the proposal of cortactin mode of regulation and of the use of the phospho-mimetic mutants, many studies were carried out to understand the functional consequences of serine and tyrosine phosphorylation of cortactin.

Indeed, Kruchten and colleagues proposed that different cortactin phosphoforms have distinct cellular functions (Kruchten et al., 2008). In this study, tyrosine-phosphocortactin mainly regulates FA turnover and leads to stress fiber disassembly, whereas serine-phosphocortactin promotes the assembly of branched actin networks. More recently, antibodies specific for phospho-serine cortactin have been used to study the implications of serine phosphorylation in regulating lamellipodia actin dynamics (Kelley et al., 2010). The production of planar protrusive extensions of the plasma membrane at the leading edge of the cell named lamellipodia is essential for carcinoma cell migration (Small et al., 2002). Lamellipodia extension drives cell migration through cycles of actin polymerisation and depolymerisation and cortactin, that it is highly enriched in lamellipodia, regulates the actin dynamics in these structures (reviewed in (Cosen-Binker and Kapus, 2006)). Kelley and colleagues have shown that serine phosphorylation of cortactin is implicated in carcinoma motility and adhesion and is also essential for lamellipodial persistence (Kelley et al., 2010).

Finally, the importance of studying the different states of cortactin phosphorylation during bacterial invasion has been highlighted (Selbach and Backert, 2005). A recent study to which our group has contributed has demonstrated the importance of serine phosphorylation of cortactin in cell scattering induced by *Helicobacter pylori* (Tegtmeyer et al., 2011). Thus, phosphorylation of cortactin at serine residue 405 is required for the interaction of cortactin and FAK whose activity is involved in regulating cell adhesion processes.

3. Nck family adaptor proteins

Non-catalytic tyrosine kinases (Nck) 1 and 2 are ubiquitously expressed adaptor proteins that regulate a variety of cellular processes linking phosphotyrosine signals to actin cytoskeletal reorganisation. Nck1 and Nck2 (collectively termed "Nck") bind to specific phosphotyrosine-containing sites on activated receptors and scaffolds proteins, through its SH2 domain, and to proline-rich motifs in downstream effectors, through its SH3 domain (Buday et al., 2002).

The two isoproteins possess one SH2 domain and three SH3 domains (Buday et al., 2002). They represent the prototype of regulatory proteins called adaptors, composed of SH2 and SH3 domains separated by linker sequences that act as building blocks to assemble multiprotein complexes (Figure 4). SH2 domain recognises targets in a phosphotyrosine-dependent manner, binding phosphorylated tyrosine with the consensus pTyr-X-X-Pro (where X is any amino acid) (Songyang et al., 1993). SH3 domains bind to proline-rich sequences (Cicchetti et al., 1992) and also have specific preferences for arginine and leucine residues (Yu et al., 1994).

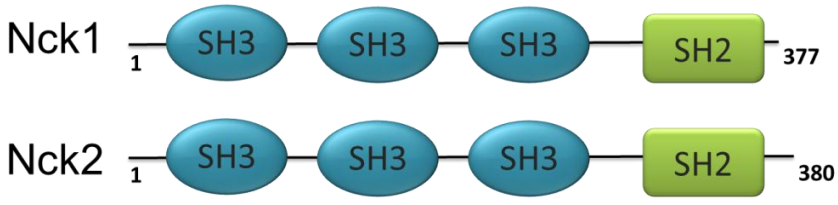

Figure 4. Schematic of Nck adaptor proteins. Nck1 and Nck2 are composed of three SH3 domains followed by one SH2 domain.

Nck1 and Nck2 are thought to be functionally redundant in many aspects (Bladt et al., 2003). Notably, both proteins display 68% identitiy at the amino acid level, and the largest differences are mainly located in the linker regions between the interaction domains. In like manner, neither Nck1 nor Nck2 knockout mice exhibit an apparent phenotype whereas double knockout mice have profound defects in the development of mesodermal structures causing embryonic lethality (Bladt et al., 2003).

The SH3 domains of Nck bind many proteins functionally associated with the regulation of actin cytoskeleton, including N-WASP (Rivero-Lezcano et al., 1995) and WIP (Anton et al., 1998).

Rohatgi and colleagues demostrated that the SH3 domains of Nck stimulate the rate of Arp2/3-dependent actin nucleation by purified N-WASP (Rohatgi et al., 2001). Several Nck ligands bind to more than one SH3 domain suggesting that a cooperative interaction is necessary for the formation of complexes (Wunderlich et al., 1999). Accordingly, each SH3 domain can bind and activate N-WASP individually, but their native tandem configuration results in cooperative N-WASP activation, leading to high levels of actin polymerisation *in vitro* (Rohatgi et al., 2001). Interestingly, artificially clustering of the SH3 domains of Nck at the plasma membrane, using an antibody-based system, triggers actin polymerisation in cultured cells (Rivera et al., 2004).

The isolated SH2 domain of Nck was shown to bind cortactin in pull-down assays with cell lysates (Okamura and Resh, 1995). In addition, the SH2 domain of Nck has been shown to associate with activated receptor-tyrosine kinases such as the EGF receptor (EGFR), PDGF receptor (PDGFR) and with the Ephrin receptor EphB1. In T lymphocytes, Nck mediates a role in the T cell receptor (TCR)-induced reorganisation of the actin cytoskeleton and the formation of the immunological synapse (reviewed in (Lettau et al., 2009)). Moreover, via binding to phosphorylated transmembrane adhesion protein nephrin, Nck promotes the reorganisation of the actin cytoskeleton in protusions known as podocytes of kidney epithelial cells (Jones et al., 2006). This signalling pathway to induce actin polymerisation targeting Nck, has been hijacked by pathogenic

microorganism, such as EPEC and *vaccinia virus*, which have evolved a similar strategy to promote their infection (Frischknecht et al., 1999; Gruenheid et al., 2001).

4. Crk family adaptor proteins

The CT10 regulator of kinase (Crk) protein was originally identified as a product of the oncogene *v-crk* in a CT10 chicken retrovirus system (Mayer et al., 1988a; Mayer et al., 1988b). v-Crk and its cellular homologous, CrkI, CrkII, and the paralog Crk-like (CrkL) are adaptor proteins. CrkII and CrkL consist of one SH2 domain followed by two SH3 domains while CrkI lacks the carboxyl-terminal SH3 domain (Figure 5) (reviewed in (Birge et al., 2009)). CrkI and CrkII are derived from alternative splicing from a single gene locus (Matsuda et al., 1992) in chromosome 17p13 (Fioretos et al., 1993), whereas the CrkL protein is expressed by a distinct gene in chromosome 22q11 (ten Hoeve et al., 1993).

This ubiquitously expressed family of proteins plays an important role in intracellular signal transduction integrating signals from a wide variety of sources, including growth factors, extracellular matrix molecules and bacterial pathogens. Crk proteins are involved in cell spreading, actin reorganisation and cell migration (reviewed in (Birge et al., 2009)). In fact, Crk proteins are required for remodelling of actin cytoskeleton induced by PDGF and for the formation and turnover of focal adhesions (Antoku and Mayer, 2009). Some of the key partners of Crk include the p130 Crk-associated substrate (p130Cas) and paxillin, both of which are FA proteins (Birge et al., 1993; Sakai et al., 1994). Crk proteins are also dysregulated in several human malignancies (reviewed in (Sriram and Birge, 2010)).

CrkL shares high sequence identity with CrkII, and the two proteins have been shown to compensate to each having overlapping functions in certain cases. However, several studies have demonstrated that they also have distinct physiological roles. In fact, the study of knockout mouse models indicates that these proteins have non-overlapping roles during embryonic development. Crk knockout mice, which lack both CrkI and

CrkII, die perinatally due to defects in cardiac and craniofacial development (Park et al., 2006). CrkL knockout mice exhibit defects in multiple cranial and cardiac neural crest derivatives, and they do not survive embryogenesis. Interestingly, mice homozygous for a null mutation of CrkL provide a model for studying the congenital birth defects seen in the DiGeorge syndrome (Guris et al., 2001).

4.1. Regulation of Crk proteins

Crk signalling acts through the assembly of protein-protein complexes and requires both SH2 and SH3 domains (Matsuda et al., 1991). As mentioned before, SH2 domain recognises phosphotyrosine-containing targets. The consensus sequence for the N-terminal SH3 (designated hereafter as nSH3) domain was determined to be Pro-X-Leu-Pro-X-Lys (where X is any amino acid) (Wu et al., 1995). In contrast, the C-terminal SH3 domain (cSH3) of CrkII and CrkL is atypical lacking the binding determinants of polyproline type II binding SH3 domains (Muralidharan et al., 2006). Indeed, it is thought that the cSH3 domain of CrkII functions as an autoregulatory element (Kobashigawa et al., 2007).

Both CrkII and CrkL are regulated by phosphorylation on tyrosine residue Y221 in CrkII (or Y207 in CrkL) (Figure 5) via the activity of the tyrosine kinase Abl (de Jong et al., 1997; Feller et al., 1994). It has been described that the phosphorylation of Y221 in CrkII and Y207 in CrkL causes intramolecular binding of the linker region to the SH2 domain, preventing SH2 and nSH3 from binding target proteins, determined by the binding affinities (Kobashigawa et al., 2007; Rosen et al., 1995). However, a recent nuclear magnetic resonance (NMR) spectroscopy study has revealed that the SH2 and SH3 domains of CrkL are organised in a different architecture from that in CrkII. They corroborate that upon phosphorylation of Y207 in CrkL, the linker region interacts with the SH2 domain, inhibiting the binding of phosphotyrosine effectors. However, this intramolecular interaction has little effect on the nSH3 domain of CrkL, which is fully accessible, in contrast to CrkII, when phosphorylation of Y221 results in nSH3 autoinhibition (Jankowski et al., 2012).

The authors also show differences in the assembled structure between the unphosphorylated forms of CrkL and CrkII. Moreover, they demonstrate that CrkL forms a constitutive complex with Bcr-Abl, the oncogenic kinase that causes chronic myelogenous leukaemia (CML), independently of phosphorylation (Colicelli, 2010). In contrast, the association of CrkII with the kinase is repressed in various conformational states of the protein (Jankowski et al., 2012; Kobashigawa and Inagaki, 2012). Thus, the differences in the structural organisation of the two adaptors confer specific functions of both proteins. However, CrkL is thought to bind many or all of the same partners of CrkII, pointing to overlapping functions of both proteins in certain processes.

The C-terminus of CrkI ends prior to the regulatory Y221 site and lacks the carboxyl-terminal SH3 domain (Matsuda et al., 1992) (Figure 5). Thus, CrkI signalling cannot be regulated by tyrosine phosphorylation (Kobashigawa et al., 2007), a possible explanation for the greater transforming activity of this protein (Feller et al., 1994).

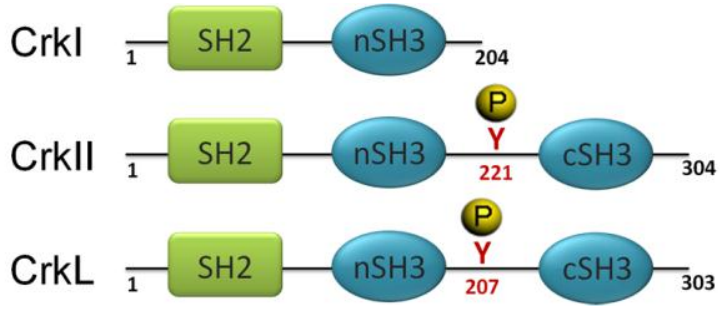

Figure 5. Schematic of CrkI, CrkII and CrkL proteins. CrkII and CrkL are composed of one SH2 domain followed by two SH3 domains. CrkI lacks the carboxyl-terminal SH3 domain (cSH3). Phosphotyrosine residues Y221 in CrkII and Y207 in CrkL are shown.

4.2. Crk adaptor proteins contribute to bacterial pathogenesis

Many studies suggest that Crk may contribute to bacterial pathogenesis by participating in bacterial internalisation or being a target for bacterial virulence factors.

A role for Crk in bacterial uptake was demonstrated in *Yersinia pseudoturbeculosis* infection into epithelial cells. The binding of *Yersinia* to β1 integrin receptor initiates a

cascade of signalling events involving tyrosine phosphorylation of p130Cas and the subsequent formation of p130Cas-Crk complexes (Weidow et al., 2000).

Crk is also involved in *Shigella flexneri* infection as a target for Abl kinases. Thus, it was shown that a phosphorylation-deficient Crk mutant significantly inhibits bacterial uptake (Burton et al., 2003). Moreover, in a subsequent study Bougneres *et al.* demonstrated that *Shigella* uptake promotes the interaction of Crk with tyrosine phosphorylated cortactin which was necessary for cortactin-dependent actin polymerisation required for bacterial uptake (Bougneres et al., 2004).

A role for Crk as a target for a bacterial factor is exemplified by the interaction of Crk with CagA, a major virulence factor from *Helicobacter pylori* (Suzuki et al., 2005). As mentioned before, cortactin phosphorylation is also implicated in *H. pylori* infection. It has been demonstrated that *H. pylori* induces cortactin tyrosine dephosphorylation in a CagA-dependent manner (Selbach et al., 2003) followed by serine phosphorylation in a CagA-independent manner (Tegtmeyer et al., 2011).

In the case of enteropathogenic *E. coli* (EPEC), the focus of our study, is a single report where immunofluorescence analysis suggested that CrkII localised to actin pedestals induced by EPEC (Goosney et al., 2001) (Figure 6).

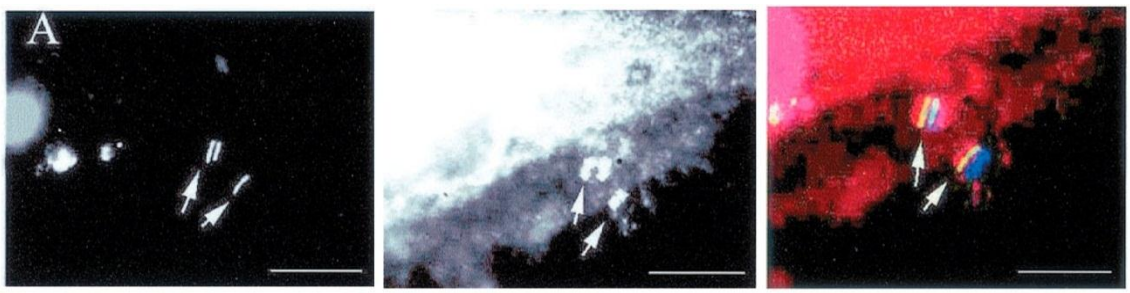

Figure 6. Immunofluorescence analysis of CrkII in EPEC pedestal formed in HeLa cells infected with EPEC. Right panel represent a merger of Tir (green), CrkII (red), and DAPI-stained EPEC (blue). Bars, 5 μm. Figure from (Goosney et al., 2001).

5. Enteropathogenic *Escherichia coli* manipulates the actin cytoskeleton

5.1. Pathogenic *Escherichia coli*

Escherichia coli was first isolated from the faeces of newborns in 1885 by Theodor Escherich and was then named *Bacterium coli commune*. It was later renamed *Escherichia coli*, and for many years the bacterium was simply considered to be a commensal organism of the large intestine. In the 1940s *E. coli* was characterised as a cause of diarrhoea for the first time in United Kingdom, based on epidemiological investigations of infantile gastroenteritis outbreaks (Bray, 1945).

E. coli belongs to the large family of enteric bacteria -*Enterobacteriacea*- which are facultatively anaerobic gram-negative rods that live in the intestinal tracts of animals. The family *Enterobacteriaceae* is among the most important bacteria medically having a great number of human intestinal pathogens within the family (e.g. *Salmonella*, *Shigella*, *Yersinia*). Several others are normal commensal of the human gastrointestinal tract (e.g., *Klebsiella, Enterobacter, Escherichia*) but may occasionally be associated with diseases of humans. Thus, several *E. coli* strains have acquired specific virulence factors, which confer abilities to cause a broad range of diseases in human (reviewed in (Kaper et al., 2004)).

Pathovar is a group of strains of a single specie defined based on common virulence factors and its characteristics of pathogenicity. The various species of *E. coli* tend to be clonal groups that are characterised by shared O (lipopolysaccharide, LPS) and H (flagellar) antigens that define serogroups (O antigen only) or serotypes (O and H antigens) (Nataro and Kaper, 1998).

Intestinal pathogenic (or diarrhoeagenic) *E. coli* is categorised into seven pathovars: enteropathogenic *E. coli* (EPEC), enterohaemorrhagic *E. coli* (EHEC), enterotoxigenic *E. coli* (ETEC), enteroinvasive *E. coli* (EIEC), enteroaggregative *E. coli* (EAEC), atypical enteropathogenic *E. coli* (ATEC) and diffusely adhering *E. coli* (DAEC) (reviewed in (Kaper et al., 2004)). In addition, there are other human pathovars, such as adherent

invasive *E. coli* (AIEC) and others not yet well defined, like the novel strain of *E. coli* O104:H4 bacteria that caused a serious outbreak of foodborne illness in northern Germany in 2011. EHEC was the first suspected cause of the outbreak, but it was later shown that the causative agent was an EAEC strain that had acquired the genes to produce Shiga toxins. This fact highlights the high plasticity of the genome of *E. coli* facilitating the emergence of new pathotypes.

5.2. Enteropathogenic *E. coli*, an attaching and effacing (A/E) bacterial pathogen

The term enteropathogenic *E. coli* (EPEC) was first used in 1955 to describe strains associated with infantile gastroenteritis (Neter, 1955). In 1978, studies with human volunteers using the EPEC O127:H6 strain E2348/69 clearly demonstrated the pathogenic potential of EPEC. Based on these studies, EPEC E2348/69 became the prototype EPEC strain (Levine et al., 1978) and the one used in this study.

Today, EPEC is one of the leading causes of diarrhoea worldwide, contributing to an overall burden of two million annual deaths in children in developing countries (Bryce et al., 2005). EPEC primarily cause prolonged watery diarrhoea, which is usually self-limited, but can be chronic, often accompanied by low-grade fever, dehydration and vomiting. EPEC is transmitted person-to-person via the fecal-oral route being an important agent of water and food contamination. Although this bacterium is not a major concern in developed nations, outbreaks of EPEC-related pathogens infections, as the one occurred last year in Europe, demonstrate the importance of studying the pathogenic mechanisms of this family of bacteria.

EPEC is the prototypic member of a closely related family of pathogens that induce the formation of characteristic attaching and effacing (A/E) lesions on the apical surface of intestinal epithelial cells. The members of this family of non-invasive extracellular pathogens are so called A/E pathogens, and include the human pathogen EHEC and a number of animal pathogens such as the mouse-specific *Citrobacter rodentium* (CR)

and rabbit-specific enteropathogenic *E. coli* (REPEC). Attaching and effacing lesions are characterised by a localised loss of epithelium microvilli (Figure 7A), close adherence of the bacteria to the host cell membrane and the generation of filamentous (F)-actin-rich structures beneath these bacteria called pedestals (Figure 7B and 7C) ((Knutton et al., 1989), reviewed in (Croxen and Finlay, 2010; Hayward et al., 2006)).

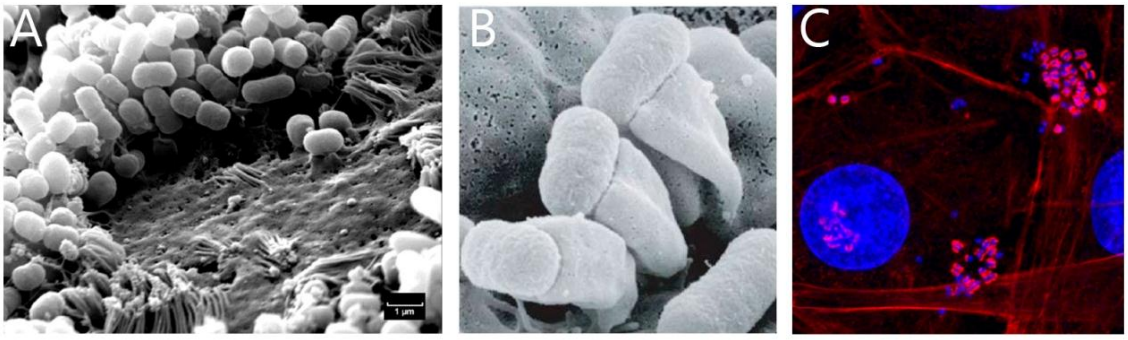

Figure 7. (A) Scanning electron micrograph (SEM) of extensive loss of microvilli of Caco-2 cell surface around EPEC infection site (taken from (Dean et al., 2006)). **(B)** SEM of pedestals formed by EPEC on the surface of HeLa cells (taken from (Finlay and Cossart, 1997)). **(C)** Immunofluorescence image of pedestals formed by EPEC on murine embryonic fibroblast. Actin is stained with TRITC-phalloidin (in red) and bacteria and cell nuclei are stained with DAPI (in blue).

Pedestal structures are dynamic, promoting bacterial motility along the surface of the cultured cells. The dynamic polymerisation and breakdown of F-actin beneath the cell surface induced by EPEC permit the movement of the bacteria across the surface of the cell and perhaps cell to cell spread (Sanger et al., 1996). Though the biological purpose of these pedestals still remains unclear, the ability of EPEC to form pedestals has been correlated with the extent of the diarrhoea that was induced in human volunteers (Donnenberg et al., 1993a). In addition, the disruption of genes critical for the formation of these structures, such as genes that encode bacterial proteins intimin and the translocated intimin receptor (Tir), has been shown to diminish colonisation and disease in experimental animals (Donnenberg et al., 1993b; Marches et al., 2000; Schauer and Falkow, 1993; Tzipori et al., 1995).

The pedestals may provide an advantage for EPEC growth and residence inside the intestine, by allowing the bacteria to remain attached to the epithelium during

peristalsis and during the host response to infection (Hecht, 1999). An additional view is that pedestals formation is an antiphagocytosis mechanism. The authors Darkoh and DuPont have proposed, based on recent results (Lin et al., 2011), that internalisation is blocked by hijacking the host endocytosis-associated proteins to remain extracellular and to avoid the host defense mechanism (Darkoh and Dupont, 2011). These and other hypotheses await future experimental work.

5.3. The locus of enterocyte effacement (LEE)

Pathogenic bacteria have large clusters of virulence genes called pathogenicity islands integrated in the chromosome. Hence, the capacity for A/E lesions formation is encoded mainly on the 35 Kb-pathogenicity island termed the locus of enterocyte effacement (LEE) that was identified in 1995. The overall organisation and the gene content of the LEE are highly conserved among different A/E pathogens (McDaniel et al., 1995).

The regulation of LEE gene expression is complex, controlled through complicated regulatory cascades involving quorum sensing, host and environmental factors and several regulators (Hughes and Sperandio, 2008). The LEE contains 41 genes, most of which are organised in 5 operons that encode (Figure 8):

- The outer membrane adhesin, intimin (Jerse et al., 1990).
- Structural components of the type III secretion system (TTSS) (Jarvis et al., 1995).
- Several secreted proteins, including the translocated intimin receptor (Tir) (Kenny et al., 1997), secreted translocators (Elliott et al., 1999) and transcriptional regulators (Elliott et al., 2000).
- Type-III specific chaperones (Abe et al., 1999).

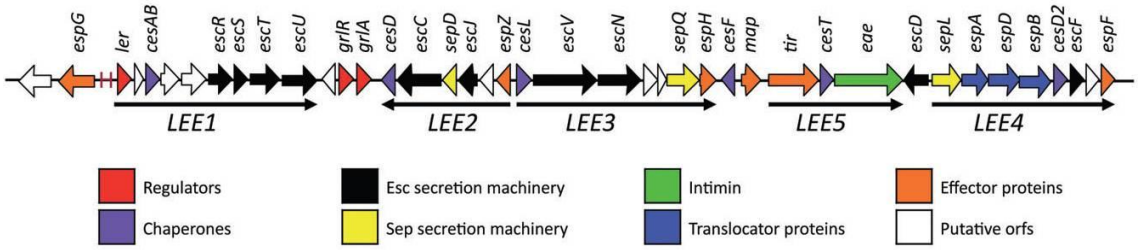

Figure 8. Diagram of the genetic organization of the locus of enterocyte effacement region (LEE). This image has been reproduced from (Wong et al., 2011).

5.3.1. Intimin

The outer membrane adhesin intimin, encoded by the LEE-*eae* gene, is essential for colonisation by A/E pathogens (Donnenberg et al., 1993a; Ritchie et al., 2003). The principal function of intimin is to interact with the extracellular region of Tir protein that is exposed on the surface of the cell. In this way, the bacteria inject its own receptor to achieve a "lock and key" adhesion mechanism.

The N-terminus of the protein promotes intimin localisation in the bacterial outer membrane, forming a β-barrel-like structure, and mediates dimerisation (Touze et al., 2004) (see figure 10 in section 5.5), whereas the intimin C-terminus interacts with receptors in the host cell plasma membrane (Batchelor et al., 2000; Frankel et al., 1995).

It has been postulated that in addition to binding Tir, intimin can bind one or more host receptors to promote bacterial adhesion. On the other hand, results also suggest the contribution of intimin to the disruption of epithelial barrier function (Dean and Kenny, 2004). The epithelial barrier is achieved by cell–cell contact through the tight junctions. Tight junctions are dynamic structures composed of many different proteins, which enable regulation of this intestinal barrier function. Disruption of tight junction integrity enhances the diarrhoea phenotype and, accordingly, is a mechanism used by several bacteria (Balkovetz and Katz, 2003).

5.3.2. Type III Secretion System (TTSS)

EPEC modulates cell traits by translocating proteins directly into the interior of host cells through the type III secretion system (TTSS). The TTSS is found among gram-

negative bacteria and is responsible for the transport of proteins, termed effectors, into the host cell cytoplasm. The bacterial effectors modify signalling pathways within the host cell contributing to the pathogenicity of EPEC.

The TTSS is a multiprotein apparatus assembled from the products of approximately 20 genes. Most of these 20 structural components are highly conserved among several pathogens and are also evolutionarily related to proteins of the flagellar system (reviewed in (Cornelis, 2006)). The TTSS apparatus of A/E pathogens is made up of a needle complex (NC, composed of a basal body that spans the inner and outer membranes and a needle that projects from the bacterial surface) and a filamentous extension of the NC that interacts with the host cell plasma membrane (reviewed in (Garmendia et al., 2005)) (Figure 9).

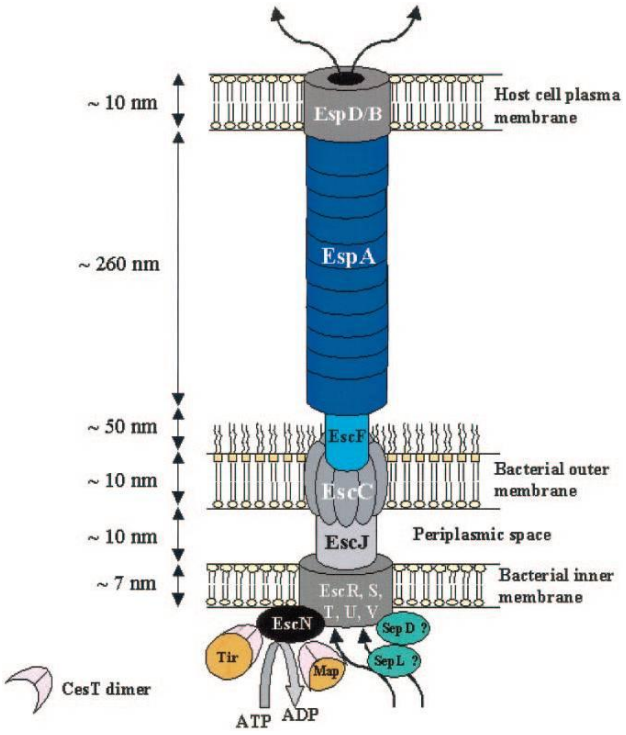

Figure 9. Schematic representation of the EPEC type III secretion system (TTSS). The basal body of the TTSS is mainly composed of EscC and EscV, and the EscJ lipoprotein that spans the periplasm forming a cylindrical structure. EscF constitutes a short needle structure that forms a projection channel that is extended by a long filament formed by EspA subunits. EspA filament is a hollow tube through which proteins are delivered form the bacteria to the cell being also an important adhesion factor. The translocator proteins EspB and EspD form the pore in the host cell plasma membrane, connecting the bacteria with the cell. The cytoplasmic ATPase EscN provides the energy to the system by hydrolysing ATP into ADP. The functional switch from secreting components of the translocator apparatus (EspA, B and D) to secreting effector proteins is regulated by two proteins, SepD and L, which sense environmental conditions, such as Ca^{+2} concentration. Image from (Garmendia et al., 2005).

5.3.3. LEE effectors

Historically, the LEE effectors were the first to be identified and until now a total of seven proteins delivered into the host cell have been characterised, namely Tir, Map, EspF, EspG, EspZ, EspH and EspB. More recently, many effectors encoded outside the LEE region, which utilise the TTSS for delivery into host cells, have been found and recent functional studies on these "non-LEE" effectors have started to ascribe cellular functions to these proteins. Although the list of known type III secreted effectors proteins continues to expand, currently EPEC is predicted to encode 21 effector proteins (Iguchi et al., 2009).

5.4. The four-stage model for EPEC lesion formation

The pathogenesis of EPEC infection has been proposed to occur in four different stages (Donnenberg et al., 1997; Nougayrede et al., 2003). In the first step, EPEC adheres non-intimately to the host epithelium in discrete microcolonies, the so-called localised-adherence (LA) phenotype that is mediated by the fimbriae named "bundle-forming pili" (BFP). Apart of BFP, this first stage of adherence is supported by multiple other adhesins, including the fimbrial *E. coli* common pilus, flagella and the EspA filament and intimin (reviewed in (Humphries and Armstrong, 2010)).

In the second stage, EPEC injects Tir and others effector proteins into the host cells via the TTSS. These effector proteins induce cytoskeletal restructuring leading to depolymerisation of the apical host cell actin cytoskeleton and the effacing of the epithelium microvilli. Tir is modified by the action of host kinases and inserted into the membrane.

In the third stage, following effector translocation, EspA filaments and the type III secretion organelles are eliminated from the bacteria cell surface. This is necessary for the intimate attachment to the host cell through intimin-Tir interactions (Frankel et al., 1998; Knutton et al., 1998).

The fourth and final step involves the intimate adherence of EPEC and the massive accumulation of cytoskeletal proteins at the site of bacterial attachment resulting in the actin polymerisation and formation of the pedestal-like structure.

5.5. Translocated intimin receptor (Tir)

Translocated intimin receptor (Tir) is the most studied and the best characterised LEE effector. Tir contains two transmembrane domains and upon injection is inserted in the plasma membrane in a hairpin-loop conformation, with both its C and N termini located within the host cell and the region between the two transmembrane domains forming an extracellular loop (Figure 10).

The extracellular portion of Tir is exposed on the surface of the cell and interacts with intimin (Kenny, 1999). Intimin forms a dimer within the bacterial outer membrane (Touze et al., 2004), as occurs with Tir in the plasma membrane (Luo et al., 2000). Each of the two Tir-binding domains of the intimin dimer interacts with Tir molecules of different Tir dimers (Figure 10). This binding pattern generates a reticular conformation resulting in the clustering of Tir in the plasma membrane beneath adherent bacteria. The interaction between intimin and Tir appears to trigger downstream signalling events leading to the formation of actin-rich pedestals (Kenny and Finlay, 1997) in a manner dependent on Tir tyrosine phosphorylation (Kenny et al., 1997). However, tyrosine phosphorylation of Tir occurs in cells infected with an EPEC strain lacking intimin (Kenny and Finlay, 1997) (Kenny et al., 1997). Hence, is not clear whether the phosphorylation of Tir is directly related to intimin–Tir interaction (reviewed in (Frankel et al., 1998)).

The currently accepted major pathway for actin polymerisation in EPEC pedestals takes place as follows. Tir becomes phosphorylated on tyrosine residue 474 (Y474) within the C-terminal cytoplasmic domain (Kenny, 1999) by redundant mammalian tyrosine kinases including c-Fyn (Phillips et al., 2004), Abl, Arg and epithelial and endothelial tyrosine kinase (Etk) (Swimm et al., 2004a). This phosphotyrosine is the binding site for

the SH2 domain-containing host cell adaptor proteins Nck1 and Nck2 (hereafter referred to collectively as Nck) (Gruenheid et al., 2001). Nck in turns recruits N-WASP, which initiates actin polymerisation by binding and activating the Arp2/3 complex (Kalman et al., 1999; Lommel et al., 2001) (Figure 10).

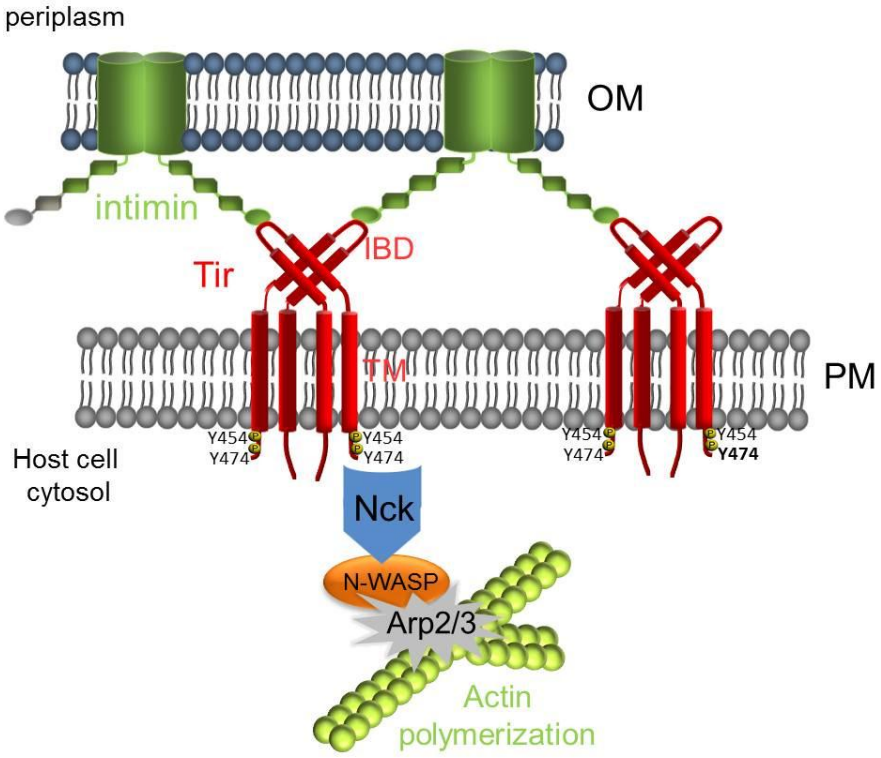

Figure 10. Major pathway for actin polymerisation in EPEC pedestals. Intimin (in green) is localised in the bacterial outer membrane (OM). Tir (in red) is shown as a dimer inserted in the host plasma membrane (PM). Tir is composed of the extracellular intimin binding domain (IBD) and the two transmembrane (TM) domains. The model for intimin-Tir interaction is adapted from (Luo et al., 2000; Touze et al., 2004). The phosphorylation of Tir in Y474 by host kinases recruits the adaptor protein Nck that activates N-WASP, which initiates actin polymerisation mediated by the Arp2/3 complex.

Although the predominant site of tyrosine phosphorylation is Y474, a second tyrosine residue Y454 can also be phosphorylated. This residue Y454 forms part of a conserved Asn-Pro-Tyr (NPY) motif (Campellone and Leong, 2005), which has been recently demostrated to recruit the insulin receptor tyrosine kinase substrate p53 (IRSp53) (Weiss et al., 2009) and insulin receptor tyrosine kinase substrate (IRTKS, a homologue of IRSp53) (Vingadassalom et al., 2009), promoting weak Nck-independent actin polymerisation.

In addition, the bacterial effector Tir is also phosphorylated at serine residues S434 and S463 by a host cell kinase (Warawa and Kenny, 2001)(see below) and has intimin-independent functionality (Dean et al., 2010; Ruchaud-Sparagano et al., 2011).

Phosphorylation of Tir

As mentioned before, tyrosine phosphorylation of Tir by host cell tyrosine kinases represents a crucial step leading to actin polymerisation and pedestal formation (Kenny, 1999). The identity of the cell kinases implicated in this process has been controversial. The Src-family tyrosine kinase c-Fyn has been reported to associate transiently with Tir within minutes of Tir clustering (Phillips et al., 2004). However, evidences suggest that c-Fyn is not sufficient for pedestal formation (Swimm et al., 2004a; Swimm et al., 2004b).

Interestingly, the Abl-family kinases Abl and Arg, and the Tec-family kinase Etk have also been shown to phosphorylate Tir (Bommarius et al., 2007; Swimm et al., 2004a). Unlike c-Fyn, these kinases appear to endure in the pedestal as a result of their ability to associate with an N-terminal proline-rich peptide of Tir using their SH3 domains (Bommarius et al., 2007). Collectively, these studies suggest a molecular mechanism that helps to maintain long-term Tir signalling by ensuring that it is persistently phosphorylated.

The bacterial effector Tir is also phosphorylated at serine residues that are also required for efficient pedestal formation. The phosphorylation at serine residues of Tir *in vitro* has been linked to the observed shift in the apparent molecular mass of the protein (Kenny, 2001; Kenny and Finlay, 1997). This shift can be mimicked by *in vitro* protein kinase A (PKA)-mediated phosphorylation of two serine residues, 434 and 463 (Warawa and Kenny, 2001). It has been proposed that these serine residues may induce changes in the three-dimensional structure of Tir. These changes might aid additional kinase-dependent modification and/or promote Tir insertion into the plasma membrane (Race et al., 2007; Warawa and Kenny, 2001).

Co-infections experiments with *H.pylori* and EPEC demonstrated a function for protein kinase A (PKA)-mediated phosphorylation of Tir at serine residues 434 and 463. It was shown that EPEC infection activates PKA which phosphorylates the Rho GTPase member Rac1 inactivating it. The authors proposed that the phosphorylation of Rac1 by PKA during EPEC infection could contribute to the formation of A/E lesions and subsequently disruption of epithelial cell-cell interactions (Brandt et al., 2009).

5.6. Nck-mediated actin assembly stimulated by Tir

Once clustered and phosphorylated, a 12-residue Tir peptide that harbours the tyrosine residue Y474, binds to Nck (Campellone et al., 2004a; Gruenheid et al., 2001). In addition, Tir is phosphorylated to a lesser extent at tryosine residue Y454 (Campellone and Leong, 2005).

Nck is crucial for recruiting N-WASP whose localisation diminishes drastically in the absence of this protein (Gruenheid et al., 2001). Although Nck binds directly to the PRD domain of N-WASP through it SH3 domain (Rohatgi et al., 2001), it is not completely clear whether N-WASP is recruited to Tir via direct binding of Nck to N-WASP or indirectly through another cell host protein. Lommel and colleagues observed that the PRD of N-WASP is dispensable, while the WASP-homology 1 (WH1) domain of N-WASP is essential for EPEC pedestal formation (Lommel et al., 2001). However, recently it has been demonstrated that both PRD domain and WH1 domain are important regions for pedestal formation (Wong et al., 2012).

N-WASP is absolutely required for actin pedestal formation by EPEC, as demostrated by the absence of pedestal formation on N-WASP-deficient murine embryonic fibroblasts (Lommel et al., 2001). The genetically modified murine fibroblast-like cells (FLCs) that lack N-WASP (Snapper et al., 2001) used in the present study, have been also assessed for the deficiency of EPEC-induced pedestals (Mousnier et al., 2008; Vingadassalom et al., 2010). The required role of N-WASP in pedestal formation lies in its ability to promote the actin nucleation activity of the Arp2/3 complex.

Moreover, the clustering of Tir in the host cell membrane initiates the recruitment of a large number of cytoskeletal-related proteins. These proteins include focal adhesion (α-actinin, vinculin, talin and ezrin), cytoskeletal (actin and cytokeratins 8 and 18) (reviewed in (Caron et al., 2006)), endocytic (dynamin 2, clathrin, adaptor protein-2, epsin1 and Eps15) (reviewed in (Darkoh and Dupont, 2011)) and actin assembly-regulating proteins that include cortactin (Cantarelli et al., 2000), apart from the two previously mentioned N-WASP and the Arp2/3 complex.

5.7. Nck-independent functions of Tir

Several activities of Tir aside from Nck recruitment might modulate actin pedestal formation. In like manner, the N-terminus of Tir can interact with the SH3 domain of tyrosine kinases (Bommarius et al., 2007). In addition, the second phosphotyrosine Y454 of Tir stimulates low levels of actin assembly independent of Y474 and Nck recruitment (Campellone and Leong, 2005). The mutation of tyrosine residue 474 results in an approximately 95% reduction in the frequency of pedestal formation, establishing the signalling pathway Y474:Nck:N-WASP as the primary mechanism by which EPEC triggers actin assembly in cultured cells (reviewed in (Hayward et al., 2006)).

Interestingly, the phosphotyrosine 454 was recently shown to bind to the SH3 domain of phosphoinositide 3-kinase (PI3K) (Sason et al., 2009). In addition, there is increasing evidence that additional Tir residues can coordinate actin signalling pathways modulated by phosphoinositide metabolism (Sason et al., 2009; Selbach et al., 2009). As mentioned before, the tyrosine residue 454 is also involved in the recruitment of IRSp53/IRTKS (Vingadassalom et al., 2009; Weiss et al., 2009), promoting weak Nck-independent actin polymerisation.

5.8. Contribution of cortactin to pedestal formation by EPEC

At the start point of our study it was known that cortactin localises to actin pedestals induced by EPEC (Cantarelli et al., 2000) and that the overexpression of a truncated form of cortactin that lacks the NTA domain blocks pedestal formation (Cantarelli et al., 2002). Furthermore, it was also shown by immunoprecipitations assays that complexes of Tir contain cortactin (Cantarelli et al., 2002). However, the direct interaction between Tir and cortactin was not demonstrated since it could be mediated by others proteins, such as N-WASP. In conclusion, although it was clear that cortactin could play an important role in pedestal actin dynamics, the underlying mechanism was not well understood.

5.9. Formation of pedestals by enterohaemorrhagic *E. coli* (EHEC)

Enterohaemorrhagic *E. coli* (EHEC) is a A/E pathogen that causes bloody diarrhoea, haemorrhagic colitis and haemolytic uremic syndrome. EHEC generates pedestals by a mechanism distinct from EPEC, because Tir_{EHEC} does not recruit or require Nck for actin assembly (Gruenheid et al., 2001) and is not tyrosine phosphorylated (Deibel et al., 1998; DeVinney et al., 1999; Kenny, 1999). Instead, utilises the conserved Asn-Pro-Tyr (NPY458) motif to recruit the host factors IRSp53 and IRTKS. These two factors are members of the inverse Bin-amphiphysin-Rvs167 (I-BAR) family, a group of proteins that possesses an I-BAR domain that binds membranes to induce membrane protrusion, and contains also an SH3 domain (reviewed in (Scita et al., 2008)).

EHEC requires a second translocated effector, EspFu (also known as Tir cytoskeleton coupling protein, Tccp) (Campellone et al., 2004b; Garmendia et al., 2004), which contains multiple almost identical 47-amino-acid proline-rich repeats that bind IRTKS/IRSp53 (Vingadassalom et al., 2009) and the GBD of N-WASP (Campellone et al., 2004b; Garmendia et al., 2004). Rather than mimicking cdc42 activation, each EspFu repeat mimics an auto-inhibitory element within the GBD, thus competitively binding to

the GBD to relieve N-WASP autoinhibition, triggering actin polymerisation via the Arp2/3 complex (Cheng et al., 2008; Sallee et al., 2008).

Notably, IRTKS/IRSp53 might have additional functions in actin pedestal formation as I-BAR domains may be important for deforming the membrane during pedestal protusion.

5.10. Role of Tir:Nck and Tir:IRTKS/IRSp53 signalling pathways *in vivo*

Tir is essential for A/E lesion formation on mucosal surfaces, and *in vitro* cultured cells appear to be a selective pressure for the preservation of the Tir Y474 or Y454 signalling pathways responsible for actin polymerisation. However, neither the Tir:Nck nor Tir:IRTKS/IRSp53 signalling complexes are necessary for A/E lesion formation or N-WASP recruitment during *Citrobacter rodentium* (CR) infection of mice (Crepin et al., 2010) or EPEC infection of human intestinal *in vitro* organ cultures (IVOC)(Crepin et al., 2010; Schuller et al., 2007). Although not essential, Tir residues Y454 (Y451 in CR) and Y474 (Y471 in CR) play an important role, and these signalling pathways provide the bacterium with competitive advantage and fitness *in vivo* (Crepin et al., 2010).

Cortactin is recruited to the sites of EHEC bacterial adhesion in human IVOC via an EspFu- and N-WASP-independent pathway, in contrast to the EspFu dependent recruitment of cortactin in cultured cells (Mousnier et al., 2008). These results indicate that cortactin might have a more influential role during EHEC infection of mucosal surfaces than of cultured cells *in vitro*, and its role in mediating A/E lesion formation needs further investigation.

Collectively, all these data are suggestive of important signalling differences between *in vitro* and *in vivo* conditions.

5.11. Other LEE-effectors

Map (mitochondrial-associated protein) is targeted to the mitochondria where it disrupts the mitochondrial membrane potential, triggering mitochondrial damage (Kenny and Jepson, 2000). At the initial stages of EPEC infection, Map induces the formation of finger-like protrusive structures that contain actin bundles called filopodia at the bacterial attachment sites (Kenny and Jepson, 2000). Moreover, Map is essential for disruption of intestinal barrier function and alteration of tight junctions, and inactivates the sodium-dependent glucose co-transporter 1 (SGTL-1) affecting enterocyte fluid uptake (Dean and Kenny, 2004; Dean et al., 2006).

EspH represses the formation of filopodia and is involved in promoting the formation and elongation of actin pedestals (Tu et al., 2003). Recently, it has been demonstrated that EspH promotes the recruitment of N-WASP and the Arp2/3 complex independently of the Tir:Nck and Tir:IRTKS/IRSp53 signalling pathways (Wong et al., 2012). On the other hand, EspH blocks the activation of Rho GTPases by inactivating endogenous Rho guanine exchange factors (GEFs) to inhibit phagocytosis (Dong et al., 2010).

EspB is a translocon component that spans the cytoplasmic membranes of host cells to form pores through which effectors are translocated (Wolff et al., 1998). In addition, EspB has an effector activity. Cytosolic EspB localises to the region of bacterial attachment (Taylor et al., 1998), and when expressed in host cells, EspB induces a dramatic loss of actin stress fibers altering the morphology of the cells (Taylor et al., 1999). EspB binds to myosin inhibiting its function and facilitates microvillus effacing and antiphagocytosis (Iizumi et al., 2007).

EspZ promotes cell survival and the maintenance of the epithelium and it has been identified as essential for virulence of the murine A/E pathogen CR (Deng et al., 2004; Kanack et al., 2005). Moreover, EspZ localises to host mitochondria and its role may be to stabilise the epithelium during bacterial colonisation, thereby reducing the cytotoxic effect of the infection (Shames et al., 2010). Thus, EspZ and the anti-apoptotic non-LEE

effector H (NleH) (Hemrajani et al., 2010), would promote cell adherence and epithelial integrity.

The two effectors **EspG** and **EspG2** (EspG2 is encoded outside of the LEE) belong to a class of proteins involved in microtubule network disruption underneath adherent bacteria during EPEC infection (Hardwidge et al., 2005; Matsuzawa et al., 2004). However, it has been recently described that EspG appears to possess a dual function where it forms a GTPase-kinase signalling complex with ADP-ribosylation factor (ARF) GTPases ARF1 and 6 and Pak family members. EspG inhibits GTPase signalling and stimulates PAK being a regulator of endomembrane trafficking (Germane and Spiller, 2011; Selyunin et al., 2011). Moreover, EspG and EspG2 induce a detaching phenotype in host cell by activating the host cysteine protease calpain, process that is maintained in check by Tir protein (Dean et al., 2010).

EspF is a proline-rich effector protein that have the greatest number of reported functions among the A/E pathogens effectors known (reviewed in (Holmes et al., 2010)). EspF plays a role in antiphagocytosis and mitochondrial disruption, induces tight junction breakdown and promotes degradation of anti-apoptotic proteins playing a direct role in apoptosis (McNamara et al., 2001; Nougayrede and Donnenberg, 2004). Moreover, EspF coordinates membrane remodelling and F-actin polymerisation by binding to the SH3 domain of the host protein sorting nexin 9 (SNX9). In addition, EspF binds to the Cdc42/Rac-interactive binding (CRIB) domain of N-WASP contributing to its activation (Alto et al., 2007).

5.12. Type III secretion chaperones

The efficient secretion and translocation of many secreted proteins is often dependent of a specific family of type III chaperones (Hueck, 1998; Wattiau et al., 1996). A typical effector contains two regions required for its translocation: the N-terminal signal domain (NSD) and the chaperone-binding domain (CBD) (reviewed in (Ghosh, 2004)).

Chaperones are low molecular mass proteins, cytosolic or membrane-associated, that bind to the N-terminal CBD of effectors and remain in the bacterial cell following translocation of effectors into the host cell. Many chaperones show structural similarity, even in the absence of primary sequence homology (Delahay and Frankel, 2002; Wattiau et al., 1996). Chaperones promote translocation by stabilising the effectors, maintaining them in a secretion-competent conformation, and by targeting the bound effector to the TTSS (summarised in (Ghosh, 2004)). The effector-chaperone interaction is required for efficient translocation.

Two classes of TTS chaperones have been distinguished according to whether they associate with a single effector (class I) or two translocators (class II). Class I is subdivided on the basis if the chaperone binds one effector (class IA) or several effectors (class IB) (Parsot et al., 2003). In the case of EPEC, five TTS chaperones have been identified. One example is CesT, a class IA chaperone that binds and enhances the translocation of Tir and Map (Creasey et al., 2003; Elliott et al., 1999) and probably also influences the translocation of EspH, EspZ, and some non-LEE efectors (Thomas et al., 2005). One class IB chaperone is CesF, which binds to EspF and enhances its translocation (Elliott et al., 2002).

5.13. Non-LEE effectors

The effector repertoire of A/E pathogens is much larger than previously thought as it is not restricted to LEE-encoded proteins, however EPEC appears to have a much smaller non-LEE effector repertoire than its related pathogen EHEC. The non-LEE effector genes are clustered in six pathogenicity islands. Due to the more recently discovery of non-LEE effectors (Nle), their cellular functions are beginning to be elucidated. NleA is reported to inhibit protein secretion and tight-junction disruption (Kim et al., 2007; Thanabalasuriar et al., 2010), EspJ inhibits phagocytosis (Marches et al., 2008), whilst NleE and NleH activate innate inmune responses (Hemrajani et al., 2008; Zurawski et al., 2008). The antagonism of pro-apoptotic effects by EPEC is mediated by the translocation of a set of anti-apoptotic effectors such as NleH1/2 and NleD. NleD may

complement the activities of NleH to promote overall cell survival protecting infected cells form the activation of pro-death pathways. The concerted activity of the effectors NleE, NleB, NleC, NleD and NleH, prevents host cells from mounting an effective inflammatory respone (reviewed in (Wong et al., 2011)).

OBJECTIVES

Our first goal was to determine the contribution of the protein cortactin in the actin polymerisation process during pedestal formation by enteropathogenic *E. coli* (EPEC). This aim takes into account the new prism of the 'S-Y Switch' model for regulation of cortactin, that proposes that serine and tyrosine phosphorylation modulates cortactin activity *in vitro*. The knowledge over the contribution of cortactin to pedestal formation at the start point of the thesis was solely based on the publications of one group. In 2000, Cantarelli and colleagues demonstrated by confocal microscopy studies, that cortactin is accumulated at the sites of EPEC infection in cultured HeLa cells (Cantarelli et al., 2000). In 2002, the same group reported that the overexpression of a truncated form of cortactin lacking the NTA domain blocks pedestal formation suggesting that cortactin was necessary for pedestal formation. Furthermore, they also showed by immunoprecipitation assays that complexes of Tir contain cortactin (Cantarelli et al., 2002). Based **on these data our initial hypothesis was that cortactin plays a role in the Tir:Nck:NWASP signalling pathway for actin polymerisation in pedestal formation by EPEC.**

EPEC recruits a large number of host cell proteins although their specific function in the process of pedestal formation has not been yet clarified. That it is the case for the adaptor protein Crk, which despite being localised in EPEC pedestals (Goosney et al., 2001), its function is completely unknown. Moreover, it was shown that Crk is involved in *Shigella* entry by interacting with tyrosine phosphorylated cortactin, which is necessary for cortactin-dependent actin polymerisation required for bacterial uptake. Taking into consideration the former data, we intended to investigate the **role of Crk during pedestal formation by EPEC aiming to understand the significance of its EPEC-induced recruitment.**

Murine embryonic fibroblasts that lack Nck were used as basis to study the role of cortactin in EPEC-induced pedestal formation. Our experimental results demonstrated that unexpectedly **reduced amounts of the bacterial effector Tir were present in Nck-deficient infected cells**. Due to the importance of Tir:Nck:N-WASP pathway in actin polymerisation by EPEC, we decided to study in depth this phenomenon.

OBJECTIVES

Part I

- Study the role of cortactin and its regulation by protein kinases Erk and Src in pedestal formation induced by enteropathogenic *Escherichia coli*.
- Analysis of the contribution of cortactin to the activation of Arp2/3-mediated polymerisation in pedestals.

Part II

- Analysis of the role of the host adaptor proteins Crk in pedestal formation induced by enteropathogenic *Escherichia coli*.

Part III

- Study of the role of the host adaptor protein Nck in the injection or stability of the bacterial effector protein Tir.

MATERIALS AND METHODS

MATERIALS AND METHODS

1. Cell culture

The human cervical epithelial cancer cell line HeLa was obtained from American Type Culture Collection (ATCC). Wild type (WT) mouse embryonic fibroblasts (MEFs), N-WASP-deficient MEFs and N-WASP-deficient MEFs that were retrovirally reconstituted with N-WASP (Rescued N-WASP) (Snapper et al., 2001) were obtained from Dr. Scott B. Snapper (Massachusetts General Hospital, Boston, USA). Nck1/2-deficient MEFs and Nck1/2-deficient MEFs that were retrovirally reconstituted with EGFP-Myc-tagged Nck1 vector (Rescued Nck) (Bladt et al., 2003) were obtained from Dr. Tony Pawson (Mount Sinai Hospital, Toronto, Canada). CrkI/II-deficient MEFs and the corresponding WT MEFs (Park et al., 2006) were obtained from Dr. Thomas Curran (The Children's Hospital of Philadelphia, Pennsylvania, USA). CrkL-deficient MEFs, the corresponding WT MEFs and CrkL-deficient MEFs reconstituted with CrkL (Guris et al., 2001) were obtained from Dr. Akira Imamoto (The University of Chicago, USA). Calpain 4-deficient MEFs, Calpain 4-deficient MEFs that were transduced with lentiviruses encoding calpain 4 and the corresponding WT MEFs (Tan et al., 2006) were obtained from Dr. Peter Greer (Queen´s University. Ontario. Canada).

All cell lines were maintained in Iscove´s Modified Dulbecco´s medium (IMDM, Invitrogen) supplemented with 10% heat-inactivated foetal bovine serum (FBS, Lonza BioWhittaker, FisherScientific), antibiotics (penicillin 100 U/ml and streptomycin 100 µg/ml, Invitrogen) at 37 ºC in a humidified atmosphere with 5% CO_2. Cell lines were routinely subcultured twice a week by detaching the monolayer with 0.25% trypsin-0.03% ethylenediaminetetraacetic acid (EDTA) solution. The cell passage was recorded and cells were discarded after about 25 passages. Frozen cell stocks were stored in liquid nitrogen using a freezing solution containing 20% of dimethyl sulfoxide (DMSO) as a cryoprotectant.

2. Bacterial strains

Strains used in this study were *E. coli* BL21 (DE3) (Genotype: *hsd*S, *gal (λc*I*ts*857 *ind*1 *S*am7 *nin*5 *lac*UV5-T7 gene *1*); *E. coli* DH5α (Genotype: *supE*44 Δ*lac*U169 *(Φ*80*lac*ZΔM15*) hsd*R17 *rec*A1 *end*A1 *gyr*A96 *thi*-1 *rel*A1).

Enteropathogenic *E. coli* strains used were WT EPEC 0127:H6 strain E2348/69 (Levine et al., 1978) (provided by Dr. Brett B. Finlay. University of British Columbia, Vancouver, Canada), Δ*tir* mutant (strain E2348/69 with in frame deletion within *tir* gene (Kenny et al., 1997) and the Δ*eae* (intimin) mutant CVD206 (Donnenberg and Kaper, 1991) that were provided by Dr. Brendan Kenny (University of Newcastle. Newcastle-upon-Tyne. England). Δe*ae* and Δ*tir* mutant were nalidixic acid-resistant strains. All strains were cultured in Luria-Bertani (LB) broth at 37 ºC with shaking at 200 r.p.m.

3. Molecular methods

3.1. Preparation of DH5α competent cells using rubidium chloride method

A single fresh colony of *E. coli* DH5α was inoculated into 5 ml of LB medium and incubated at 37 ºC with shaking for 16 hrs. A volume of 5 ml of this overnight culture was inoculated into 500 ml of LB medium and incubated at 37 ºC with shaking to an optical density of 0.5 at a wavelength of 600 nm (O.D. 600). 250 ml of the bacterial culture were transferred to pre-chilled tubes and kept on ice for 15 min, the cells were then pelleted at 1,500 x g for 15 min at 4 ºC. The supernatant was completely drained and the pellet was gently resuspended in 80 ml of ice cold buffer R1 (100 mM RbCl, 50 mM $MnCl_2.4H_2O$, 30 mM potassium acetate, 10 mM $CaCl_2.2H_2O$, 15% glycerol) and incubated on ice for 15 min. The cells were then pelleted at 1,500 x g for 10 min at 4 ºC and the pellet was gently resuspended in 20 ml of ice cold buffer R2 (10mM 4-morpholinopropanesulfonic acid (MOPS), 10 mM RbCl, 75 mM $CaCl_2.2H_2O$, 15% glycerol) and incubated on ice for 15 min. The competent cells were then distributed into pre-chilled 1.5 ml tubes in 500 µl aliquots, quick frozen in liquid nitrogen and stored at -80 ºC.

3.2. Transformation of bacteria using heat-shock procedure

After thawing DH5α competent bacteria on ice, 20 ng of purified plasmid DNA were added to 50 µL competent cells in a pre-chilled 1.5 mL tube (for BL21 competent cells β-mercaptoethanol was added to a final concentration of 0.287 mM). Then competent bacteria were mixed gently with the DNA and kept on ice for 30 min. The bacteria were then heat-shocked at 37 °C for 45 seconds, incubated on ice for 1 min and 200 µL of LB medium were added. The bacteria were incubated at 37 °C with shaking for 60 min. Selection of transformed bacteria by the desired plasmid was done by plating 100 µL of the bacterial suspension on antibiotic-containing LB agar plates that were allowed to grow at 37 ºC for 16-20 h. A single colony was then grown in 4 ml of LB medium with antibiotics and used for preparing frozen glycerol stock cultures, DNA preparation or protein production. For storage of bacteria, a glycerol stock culture was prepared by adding sterile glycerol to a final concentration of 15% and subsequently frozen at -80 ºC.

3.3. Preparation of electrocompetent EPEC cells and electroporation

The following protocol was kindly provided by Brendan Kenny (University of Newcastle. Newcastle-upon-Tyne. England). 100 ml of LB medium were inoculated with 100 µl of an overnight culture of EPEC strain and grown at 37 °C with shaking till the O.D. 600 reached 0.4-0.6. Then, 50 ml of bacterial culture were pelleted by centrifugation at 1,200 x g for 15 min at 4 ºC and the pellet was washed three times with 50 ml of cold sterile water. The pellet was finally resuspended in 100 µl of cold sterile water. 40 µl of these competent bacteria were transfected with 3 µl of DNA plasmid by electroporation at 2KV in 1 mm-gap electroporation cuvettes (Cell Project) using a BTX Electro Cell Manipulator 600. As soon as the electroporation was completed, the electroporated bacteria were kept on ice and 1 ml of SOC media (2% tryptone, 0.5% yeast extract, 10 mM sodium chloride, 2.5 mM potassium chloride, 10 mM magnesium chloride, 20 mM glucose, p.H=7) was added by mixing gently. Selection of bacteria that have taken up the desired plasmid was done by plating 50 µL and 500 µL of electroporated bacteria on antibiotic-containing LB agar plates incubating at 37 ºC for 16-20 h.

3.4. DNA constructs

Plasmid DNAs were purified with the High Pure Plasmid Isolation Kit for mini preparation (Roche) according to the manufacture's instruction.

Murine wild type cortactin construct and selected mutants (Martinez-Quiles et al., 2004) were subcloned in frame with GFP at the N-terminus into the pC2-EGFP vector (Invitrogen) by Narcisa Martinez Quiles and verified by sequencing in the UCM facility. The constructs used in this study were full-length wild type cortactin (FL), and the following derivatives: the single point mutants W22A and W525K; the double mutant S405,418D; the triple mutant Y421,466,482D; an N-terminal fragment of cortactin (NH2) containing residues 1-333, and a cortactin fragment (residues 458-546) containing the SH3 domain (SH3). Two new cortactin mutants: S405,418A and Y421,466,482F were generated by PCR with QuikChange site-directed mutagenesis kit (Stratagene) with glutathione S-transferase (GST)-FL as the template. PCR products were cloned into pC2-EGFP vector by Narcisa Martinez Quiles and verified by sequencing. pC2-EGFP plasmids were selected with kanamycin (30 µg/ml, final concentration).

pCAGGS-myc-CrkII encodes myc-tagged rat CrkII protein and pCAGGS-myc-CrkII-R38V encodes myc-tagged rat CrkII protein with a single amino acid substitution in the SH2 domain (Hashimoto et al., 1998). Both DNA plasmids were obtained from Dr. Michiyuki Matsuda (Osaka University, Japan). pCAGGS plasmids were selected with ampicillin (100 µg/ml, final concentration).

pGEMT-*tir* DNA was obtained from Dr. Isabel Rodriguez Escudero (Dpto. Microbiología II. Facultad de Farmacia. Universidad Complutense, Madrid) and *tir* was sub-cloned into the pcDNA3.1HisB. The pcDNA3.1HisB-*tir*Y474D mutant was produced using the QuikChange kit according to the manufacture's instruction. Both pcDNA3.1HisB-*tir* and *tir*Y474D were produced by Narcisa Martinez Quiles and verified by sequencing.

The EPEC strains were transformed by electroporation (see section 3.3) with different DNA plasmids, p*tir* is a pACYC184 based plasmid, which is low-copy-number plasmid carrying the 3´*map*, *tir* and *cesT* (Kenny and Warawa, 2001). p*tir*Y474F/Y454F (referred as dY) is a p*tir* plasmid harbouring a double substitution converting tyrosine residues 474 and 454 to phenylalanine residues. p*tir*S434/463A (referred as dS) is a p*tir* plasmid harbouring a double substitution converting serine residues 434 and 463 to alanine

residues. p*tir*Y474F/Y454F S434/463A (referred as quad) is a p*tir* plasmid containing four substitutions at described residues. Strains carrying pACYC184 based plasmids were selected with chloramphenicol (25 µg/ml, final concentration). pSK-T7*map*HA [pBluescript (pSK) plasmid (Stratagene)] was selected with carbenicillin (100 µg/ml). All these DNA plasmids were obtained from Dr. Brendan Kenny (University of Newcastle. Newcastle-upon-Tyne. England).

3.5. Purification and elution of GST fusion proteins

A volume of 200 mL of LB medium was inoculated with 2 ml of an overnight culture of *E. coli* BL21 transformed with the expression vector pGEX-6P2/cortactin constructs, and grown at 37 °C with shaking till the O.D. 600 reached 0.6-0.7. GST-fusion protein expression was induced by the addition of isopropyl-β-D-thiogalactopyranoside (IPTG) to a final concentration of 1 mM. After 2 h of incubation, the culture was harvested by centrifugation at 5,000 × g for 10 min. The pellet was resuspended in 10 ml of 1X PBS (phosphate buffer saline, BD Bioscience) containing phenylmethylsulfonyl fluoride (PMSF) to a final concentration of 1 mM. Lysozyme was added to a final concentration of 0.1 mg/ml and incubated 5 min on ice. Triton X-100 was added to a final concentration of 1% and the sample was sonicated (3 × 30 s) on ice. The sample was then centrifuged for 20 min at 10,000 × g at 4 °C. The supernatant was filtered through a 0.45 µm filter and incubated with 200 µl of pre-washed Glutathione-Sepharose 4 Fast Flow beads (GSH, Amersham Bioscience) for 4 h at 4 °C with gentle rotation. After that, centrifugation for 5 min at 3,000 × g and 4 °C and the supernatant was discarded. The beads were washed three times with 1X PBS containing 0.1% Tween-20 and three times with 1X PBS. Finally, beads were stored at 4 ºC in 1 ml of 1X PBS. GST fusion proteins with GSH-Sepharose beads were used in pull down assays.

For actin polymerisation assays the bound GST-cortactin was eluted with elution buffer (16 mM glutathione, 100 mM NaCl [pH 7.6]). The eluates containing the protein were collected and further purified using a column with a cutt-off of 50 ± 10 KDa (Centricon YM-50, Millipore) and dialysed using Slide-A-Lyzer Dialysis Cassettes 10K MWCO (PIERCE) according to the manufacture's instruction.

When necessary, the GST was cleavaged from cortactin construct. The bound GST-cortactin was washed with PreScission Cleavage Buffer (50 mM Tris-HCl, 150 mM NaCl,

1 mM EDTA, 1 mM dithiothreitol [pH 7.0]) and the residual buffer was removed. The PreScission protease (GE Healthcare) was added to the fusion protein-bound matrix in Cleavage Buffer and the reaction proceeded at 4 °C for 16 h. The samples were dialysed using Slide-A-Lyzer Dialysis Cassettes (PIERCE) according to the manufacture's instruction.

4. Antibodies

All primary antibodies (Ab) used in western blotting (WB) and immunofluorescence (IF) are listed in Table 1. Antibodies for bacterial proteins are marked in grey. All secondary antibodies are listed in Table 2.

Table 1

Primary antibody	Species	Dilution used in WB	IF	Source
Anti-acetylated-lysine	Rabbit Poly Ab	1:300	-	Cell Signalling (#9441)
Anti-actin clone C4	Mouse Mo Ab	1:3000 (for ECL) 1:150,000 (for Odyssey)	_	MP Biomedicals (#69100)
Anti-cortactin (EP1922Y)	Rabbit Mo Ab	1:1500	-	Novus Biological NB110-55723
Anti-cortactin 4F11 1 mg/ml	Mouse Mo Ab	1:1,000	_	Millipore (#05-180)
Anti-Crk (clone 22) 250 µg/ml	Mouse Mo Ab	1:500	_	BD Biosciences Pharmingen (No. 610035)
Anti-CrkII H-53 200 µg/ml	Rabbit poly Ab	1:250	_	Santa Cruz Biotechnology (sc-9004)
Anti-CrKL (C-20) 200 µg/ml	Rabbit poly Ab	1:350	_	Santa Cruz Biotechnology (sc-319)
Anti-HA High Affinity (clone 3F10) 100 µg/ml	Rat Mo Ab	1:100	-	Roche (No. 11867423001)
Anti-Myc tag (clone 4A6) 1 mg/ml	Mouse Mo Ab	1:500	_	Millipore (#05-724)
Anti-Nck (clone 108) 250 µg/ml	Mouse Mo Ab	1:500	_	BD Biosciences Pharmingen (No. 610099)
Anti-N-WASP	Rabbit Poly Antiserum	1:2,000	_	(Miki et al., 1998)

Anti-p44/42 MAP Kinase	Rabbit Poly Ab	1:1,000	-	Cell Signalling (#9101)
Anti-phospho-p44/42 (T202/Y204) (clone E10)	Mouse Mo Ab	1:500	-	Cell Signalling (#9106)
Anti-phospho-tyrosine (p-tyr-100)	Mouse Mo Ab	1:750	-	Cell Signalling (#9411)
Anti-phosphoY207-CrkL	Rabbit poly Ab	1:250	_	Cell Signalling (#3181)
Anti-phosphoY221-CrkII	Rabbit poly Ab	1:200	_	Cell Signalling (#3491)
Anti-phosphoY416-Src	Rabbit poly Ab	1:1,000	_	Upstate
Anti-phosphoY466-cortactin 1 mg/ml	Rabbit Poly Ab	1:500	_	Abcam (ab51073)
Anti-phosphoY466-cortactin 100 µg/ml	Rabbit Poly Ab	1:1,000	_	Santa Cruz Biotechnology (sc-101661)
anti-Src (clone GD11) 1 mg/ml	Mouse Mo Ab	1:500	_	Millipore (#05-184)
Anti-tubulin alpha (clone YOL1/34) 1 mg/ml	Rat Mo Ab	1:15,000	_	AbD Serotec (No. MCA78G)
Mouse IgG1, Myeloma 1 mg/ml	Mouse Mo Ab	This Ab was used as a control for inmuno-precipitations.	_	Calbiochem (No. 401122)
Anti-*E.coli* DnaK (clone 8E2/2)	Mouse Mo Ab	1:2,000	-	Enzo Life Sciences (No. ADI-SPA-880)
Anti-*E.coli* LPS (clone 2D7/1) 0.5 mg/ml	Mouse Mo Ab	-	1:100	Abcam (ab35654)
Anti-EspB	Rabbit poly Ab	1:4,000	-	Laboratory of B. Kenny
Anti-EspF	Rabbit poly Ab	1:4,000	-	Laboratory of B. Kenny
Anti-EspF	Rabbit poly Ab	1:500	-	Laboratory of C. Sasakawa
Anti-Tir	Rabbit poly Ab	1:12,000	-	Laboratory of B. Kenny
Anti-Tir2A5 (N-terminal)	Mouse Mo Ab	1:1,000	1:100	Laboratory of B. Finlay
Anti-Tir2C3 (C-terminal)	Mouse Mo Ab	1:1,000	-	Laboratory of B. Finlay

Table 2

Secondary antibody	Species	Dilution used in WB	Dilution used in IF	Source
Alexa Fluor 405-labeled anti-mouse IgG (H+L) 2 mg/ml	Goat	-	1:750	Invitrogen (Molecular Probes)
Alexa Fluor 488-labeled anti-mouse IgG (H+L) 2 mg/ml	Goat	-	1:1,000	Invitrogen (Molecular Probes)
Alexa Fluor 488-labeled anti-rabbit IgG (H+L) 2 mg/ml	Goat Poly Ab	_	1:1,500	Invitrogen (Molecular Probes)
Alexa Fluor 680-labeled anti-mouse IgG (H+L) 2 mg/ml	Goat Poly Ab	1:7,000	_	Invitrogen (Molecular Probes)
Horseradish peroxidase-linked anti-mouse IgG	Sheep Poly Ab	1:3,000	_	Amersham Biosciences (GE Healthcare)
Horseradish peroxidase-linked anti-rabbit IgG	Donkey Poly Ab	1:2,000	_	Amersham Biosciences (GE Healthcare)
IRDye 800CW-labeled anti-mouse IgG (H+L) highly cross adsorbed. 1 mg/ml	Goat	1:5,000	_	Li-cor Biosciences (Fisher Scientific)
IRDye 800CW-labeled anti-rabbit IgG (H+L) highly cross adsorbed. 1 mg/ml	Goat Poly Ab	1:5,000	_	Li-cor Biosciences (Fisher Scientific)
IRDye 800CW-labeled anti-rat IgG (H+L) highly cross adsorbed. 1 mg/ml	Goat	1:5,000	_	Li-cor Biosciences (Fisher Scientific)

5. Cell transfection

Plasmid DNAs for cell transfection were purified with endotoxin-free, transfection-grade JetStart Maxi columns as per manufacturer´s instructions. Cell transfection was carried out using Lipofectamine™ 2000 reagent (Invitrogen). Cells were grown to 60-70% confluence in 6-well or 100 mm-plates and transfected with 5 µg or 24 µg, respectively, of the indicated plasmid. Transfected cells were incubated for approximately 16 hours in medium containing 10% FBS but no antibiotics. Western blotting was carried out on cells from a single well or from a 100 mm-plate. Cell monolayers were washed once with cold 1X D-PBS that contains calcium and

magnesium (Dulbecco's Phosphate-Buffered Saline, Invitrogen) and scraped into 200 µl of 2X Laemmli sample buffer (24 mM Tris-HCl pH 6.8, 10% Glycerol, 0.8% sodium dodecyl sulphate (SDS), 6 mM β-mercaptoethanol and 0.04% bromophenol blue) in the case of a single well. Samples were homogenised by six passages through a syringe with a 25-gauge needle, followed by centrifugation at 21,000 x g (14,000 r.p.m. in a standard table centrifuge) for 15 min at 4 ºC and boiled for 5 min.

6. SDS-PAGE and western immunoblot analysis

Twenty to thirty microliters of samples were resolved by 10% (or 12% when indicated) sodium dodecyl sulfate-polyacrylamide gel electrophoresis (SDS-PAGE). Molecular weight (MW) of the proteins was estimated by extrapolating from a commercial protein molecular weight marker (Invitrogen or BioRad). Electrophoresis was performed in running buffer (25 mM Tris, 192 mM Glycine and 0.1% SDS, pH 8.3) at a constant voltage (150V) for 80 min. After SDS-PAGE the proteins were transferred to nitrocellulose membranes (Amersham) using a Biorad transfer system at 300 mA for 90 min. The electrotransfer solution contained 25 mM Tris Base, 192 mM Glycine and 20% methanol (pH 8.3).

Membranes were developed using enhanced chemiluminiscence system (ECL, Amersham) or Odyssey Infrared System (LI-COR, Fisher Scientific) as follows.

6.1. Chemiluminiscence system

Blots were blocked for 1 hour at room temperature with 5% skim milk in Tris-buffered saline with Tween-20 (TBS-T; 150 mM NaCl and 10 mM Tris-HCl, 0.1% Tween-20 pH 7.5) and incubated overnight with the primary antibody diluted in TBS-T with 2% skim milk. Blots were washed three times for 10 min with TBS-T, and then incubated for 1 hour with the horseradish peroxidase (HRP)-conjugate secondary antibody (see Table 2). Blots were washed three times for 10 min with TBS-T and once with PBS and developed using ECL. When required, membranes were stripped for 30 min at 50 ºC in stripping buffer (100 mM β-mercaptoethanol, 2% SDS, 625 mM Tris-HCl pH 6.7) and reprobed with a different antibody. Quantification of bands was done by densitometry using NIH Image J software. Normalisation for each experiment was done by

normalising for actin or for the unphosphorylated form of the protein as indicated. Results were reported as the average from at least three independent experiments ± standard deviations (SD).

6.2. Odyssey Infrared system

Blots were blocked for 1 hour with Odyssey blocking buffer (Fisher Scientific) and incubated overnight with primary antibody diluted in blocking buffer containing 0.1% Tween-20. Blots were washed four times for 5 min with PBS containing 0.1% Tween-20 (PBS-T), then incubated for 1 hour with the appropriate secondary antibody. Membranes were washed four times for 5 min with PBS-T and scanned using the red (700nm) and green (800 nm) channels. When significantly different intensities were observed between the two colour signals, we performed sequential antibody incubations. Membranes were stripped using NewBlot Nitro Stripping buffer (LI-COR) during 20 min at room temperature (RT) and incubated first with secondary Ab alone, and scanned them to confirm the efficiency of the stripping process before incubating them with a different primary Ab. The protein molecular weight marker was detected using the red channel (700 nm); therefore the real bands were shown in certain figures. When not detected, the marker is represented by a short black line to the right of the panel. Quantification of the bands was performed on the scanned images with the Odyssey Scan band tool. Statistical analyses were carried out using the two-tailed Student's *t*-test and displayed graphically using GraphPad Prism software (version 5.0). Graphs represent mean ± SD.

7. EPEC infections

Cells were grown in 6-well-plate to 70-80% confluency. Overnight bacterial cultures were grown in LB broth at 37 ºC with shaking at 200 r.p.m. In initial infection experiments of HeLa cells, bacteria from overnight cultures were directly added to wells, as indicated. For preactivation experiments, overnight bacterial cultures were diluted 1:100 in IMDM medium containing 10% FBS but no antibiotics and grown at 37 ºC with 5% CO_2 to enhance type III-dependent secretion. After 2 hours of preactivation, the O.D. of the suspension was measured at 600 nm to adjust to 0.2 and 12.5 µl were

added to each well referred to as **X EPEC**. The Multiplicity of Infection (MOI) is the number of bacteria added per cell at the beginning of the infection. The MOI was calculated by colony forming assay of serial bacterial dilutions in triplicate and assuming that the number of cells is approximately $1x10^6$ cells per well of a 6-well plate at the confluence used. We determined that X EPEC is equivalent to a **MOI** of **3**. This result was corroborated considering that 1 O.D. 600 unit is equivalent to 10^9 bacteria per ml (Current Protocols in Molecular Biology. Vol. 1). When indicated, the cells were infected at higher MOIs referred to as 10X, 50X or 100X. Cells were infected for indicated times (1, 2 or 3 hours) in medium containing 10% FBS but no antibiotics at 37 ºC in a humidified atmosphere with 5% CO_2.

8. siRNA treatment

Inhibition of the expression of human cortactin and CrkI/II including a scrambled nucleotide was done using Santa Cruz siRNA kits, as per manufacture instructions. Briefly, HeLa cells were grown to 60% confluency in 6-well-plate and transfected with 4 to 8 µl of siRNA duplex and 1:1 siRNA Transfection Reagent (Santa Cruz) in 1 ml of serum-free medium. After the 6-h transfection period, 1 ml of 20% FBS medium was added to the cells to achieve a final serum concentration of 10%, and cells were further cultured for 16-20 hours prior to EPEC infection.

siRNA treatment for the inhibition of *Mus musculus* CrkL was carried out using Silencer Pre-designed siRNA (Ambion. Life Technologies). MEFs were grown to 50-60% confluency in 6-well-plate and transfected with 20 nM of siRNA plus 3 µl of lipofectamine™ RNAiMAX (Invitrogen) per well. Cells were incubated for 20 hours prior to EPEC infection.

siRNA treatment for the inhibition of Nck1/Nck2 in HeLa cells was carried out using Silencer Pre-designed siRNA (Ambion. Life Technologies). HeLa cells were grown to 50 - 60% confluency in 6-well-plate and transfected with 40 nM of siRNA plus 6 µl of lipofectamine™ RNAiMAX (Invitrogen) per well. Afterwards, the cells were incubated for 20 hours prior to EPEC infection.

9. Actin polymerisation assays

Tir and Tir D (explain latter) recombinant proteins from pcDNA3.1HisB-Tir and pcDNA3.1HisB-TirY474D respectively were generated by *in vitro* transcription coupled to translation (TNT translation kit, Promega) according to the manufacture's instruction. The following protocol and the Arp2/3 complex and actin protein were kindly provided by Marie-France Carlier and Christophe LeClainche (CNRS. Gif-sur-Yvette. France). Carboxilate microspheres (1 µm; Polysciences Inc.) were washed three times with Xb buffer (10 mM HEPES pH 7.8, 100 mM KCl, 0.1 mM $CaCl_2$, 1 mM $MgCl_2$, 1 mM ATP). A volume of 5 µl of microspheres was incubated with 500 nM of Tir/TirD proteins in Xb buffer for 1 hour at 4 ºC with gentle rotation. Control microspheres were incubated only with Xb buffer. The microspheres were washed once with Xb buffer and twice with Xb buffer containing 1% of bovine serum albumin (BSA) to block non-specific interactions. An eighth of the microspheres was then incubated with purified actin (2.5 µM) and Arp2/3 complex (300 nM), and with cortactin and its mutants (500 nM) to a final volume of 25 µl of Xb buffer. As a control the microspheres were incubated with actin and Arp in the absence of cortactin protein. After 1h-incubation at RT, TRITC-phalloidin was added to a final concentration of 3.3 µM. The solution containing the beads was placed on a slide and sealed with melted paraffin. Pictures were acquired at 600x magnification keeping all relevant parameters fixed (gain, exposure time) to allow for fluorescence intensity comparison. Experiments were performed at least three times. We briefly modified the above protocol to use it with GST-cortactin coupled to GSH beads. A volume of 15 µl of GSH beads (of a total of 1 ml of GSH beads resuspended in 1 ml of 1X PBS) was washed once with Xb buffer and twice with Xb buffer containing 1% BSA with Xb buffer. Then, a third of the beads were incubated with purified actin (2.5 µM), Arp2/3 complex (300 nM) and Tir/TirD proteins (500nM) to a final volume of 50 µl of Xb buffer and the same steps were followed as described above.

10. Membrane enrichment procedure

EPEC-infected MEFs were fractionated as previously described (Patel et al., 2006) with some modifications. MEFs were grown to 70-80% confluency in 150 mm-plates and infected with preactivated EPEC. After 3 hours of infection, cells were washed once with

ice-cold D-PBS and rapidly lysed at 4 ºC by overlaying the cell monolayer for 10 min with 1 ml of imidazole lysis buffer (3 mM imidazole pH 7.4, 250 mM sucrose, 1 mM sodium orthovanadate (Na_3OV_4), 1 mM sodium fluoride (NaF), one tablet of protease-phosphatase inhibitor cocktail [Complete^{TM}-mini EDTA-free, Roche] and a half of a tablet of phosphatase inhibitor [PhosStop, Amersham] per 50 ml of buffer). The cells were then collected using a cell scraper (Sarstedt) and disrupted by six passages through a syringe with a 25-gauge needle, followed by centrifugation at 3,000 x g for 15 min at 4 ºC to remove cellular debris, bacteria and nuclei. Clarified lysates were centrifuged again for 1 hour at 21,000 x g at 4 ºC to separate the membrane (pellet) from the cytoplasmic fraction (supernatant). Both of these final fractions were stored at -80 ºC until further use. The pellets (membrane fraction) were resuspended in 400 µl of imidazole lysis buffer containing 0.1% Triton X-100.

11. GST pull-down assays

For pull-down experiments equivalent amounts (10-25 µL) of GST fusion proteins estimated from Coomassie-stained SDS-PAGE were used for each sample. GST was used as a negative control. For pull-downs with GST fusion cortactin constructs, a volume of 100 µl of resuspended pellets (membrane fraction) was used for each pull-down assay. The sepharose bound GST proteins were incubated with the membrane fraction with tumbling for 3 hours at 4 ºC and were then washed three times with 100 µl of imidazole lysis buffer diluted 1:10 in PBS containing 0.05% Tween-20.

Pull-down assays with *in vitro* expressed Tir/TirD proteins were performed. A volume of 10 µl of resuspended sepharose bound GST fusion proteins was incubated with Tir or TirD (250 nM) in PBS containing 0.5% Tween-20 with tumbling for 4 h at 4 ºC. Pull-downs were washed three times with 100 µl of PBS containing 0.05% Tween-20 and eluted by boiling in 2X Laemmli buffer for 5 min. The samples were separated by SDS-PAGE and analysed by WB. In parallel, one fiftieth of each recombinant protein that was used in each pull down was loaded and the gel was stained with Coomassie blue staining solution (0.25% Coomassie Brilliant Blue R-250, 45% methanol and 10% glacial acetic acid) for 20 min at RT. The gel was then destained with Coomassie blue destaining solution (10% methanol and 10% glacial acetic acid).

12. Pervanadate treatment

Pervanadate treatment was carried out by mixing 1 mM of Na_3VO_4 with 1% hydrogen peroxide (H_2O_2) and diluting two-fold with IMDM medium for 30 min at 37 ºC in a humidified atmosphere with 5% CO_2. Due to the high intensity of the signal following pervanadate treatment, lysates of DMSO-treated and pervanadate-treated MEFs were diluted 1:500 in Laemmli sample buffer for WB analysis.

13. Immunoprecipitation of Tir

Cells were grown to 70-80% confluency on 150-mm plates, then washed once with D-PBS and scraped into 700 µl modified Ripa lysis buffer [50 mM Tris-HCl (pH 7.4), 150 mM NaCl, 15% glycerol, 2 mM EDTA, 0.1% SDS, 1% Triton X-100, 1 mM Na_3VO_4, 10 mM NaF, 1 mM PMSF, protease inhibitor cocktail (Amersham), phosphatase inhibitor (PhosSTOP, Roche)] and disrupted by three passages through a syringe with a 25-gauge needle, followed by centrifugation at 12,000 x g for 15 min. 25 µl of Magnetic Pan mouse Dynabeads (Invitrogen) were washed and blocked with PBS containing 0.1% BSA for 10 min, then incubated with tumbling for 2 h with 4 µl of Tir2A5 monoclonal Ab per IP. After three washes with PBS-0.1% BSA, the beads were added to 300 µl of cell lysate and incubated with tumbling at 4 ºC for 3 h. The beads were washed three times with the help of a magnet (Invitrogen) and 200 µl Ripa lysis buffer diluted 1:10 in PBS. The beads were resuspended in 40 µl 2X Laemmli buffer and boiled for 5 min before SDS-PAGE.

14. Immunofluorescence microscopy and quantification of pedestal formation

For immunofluorescence studies, cells were seeded and grown overnight in 6-well-plates with four pre-heated glass coverslips in each well. Cells were fixed with formalin buffered solution (containing 4% w/v formaldehyde, Sigma) for 20 min at RT and permeabilised with PBS containing 0.1% Triton X-100 for 5 min. After three washes for 5 min with PBS, cells were blocked with PBS containing 2% BSA for 10 min, stained with the appropriate primary Ab for 1 h at RT, washed three times with PBS, and finally incubated for 1 h with secondary Ab. Actin cytoskeleton was visualised by staining with

1 µg/ml tetramethyl-rhodamine-isothiocyanate (TRITC)-phalloidin (Sigma-Aldrich) for 15 min. After three washes with PBS, cells were stained with 4'-6-diamidino-2-phenylindole (DAPI, 300 nM) for 5 min to visualise bacteria and nuclei. When indicated, bacteria were staining with 5 µg/ml of anti-LPS antibody for 1 h at RT, washed three times with PBS, and incubated for 1 h with Alexa Fluor 405-labeled anti-mouse. After three washes with PBS the coverslips were allowed to dry at RT during 20 min and mounted using 5 µl of mounting medium (100 mM Tris-HCl pH 8.5, 10% Mowiol 4-88 (Calbiochem), 25% Glycerol with phenylnediamine (Sigma)). Quantification was done using a Nikon Eclipse TE 200-U fluorescence microscope equipped with a Hamamatsu camera. Images were processed with Adobe Photoshop. Confocal microscopy was performed at the "Parque Científico de Madrid" microscopy facility with a Leica Confocal SP2/DMEIR2, using Leica software (version 2.61). Quantification of pedestal formation was done by counting the numbers of pedestals of attached bacteria for a total of 100 cells in representative microscope fields. Experiments were performed at least three times. Statistical analyses were carried out using the two-tailed Student's *t*-test (or Mann Whitney test when the data cannot be assumed to follow a Gaussian distribution in each group) and displayed graphically using GraphPad Prism software. Graphs represent mean ± SD.

15. Treatment of cells with different inhibitors prior to EPEC infection

Table 3. Chemical inhibitors

Inhibitor and Usage	Product description
MG-132 (Calbiochem) 50 µM pre-treatment for 1 h	A potent, reversible, and cell-permeable proteasome inhibitor. Reduces the degradation of ubiquitin-conjugated proteins in mammalian cells and permeable strains of yeast by the 26S complex without affecting its ATPase or isopeptidase activities. Activates c-Jun N-terminal kinase (JNK1), which initiates apoptosis. Inhibits NF-κB activation (IC50 = 3 µM). Also reported to increases the survival rate of mesenchymal stem cells following their transplantation. Prevents β-secretase cleavage.

Protease Inhibitor Cocktail P8340 (Sigma-Aldrich) 1:1000 pre-treatment for 4 h (or 20 h)	This protease inhibitor cocktail has been optimized and tested for mammalian cell and tissue extracts. It contains broad-specificity inhibitors. The specific inhibitory properties of the components are: -AEBSF – [4-(2-Aminoethyl)benzenesulfonyl fluoride hydrochloride] – serine proteases, e.g.., trypsin, chymotrypsin, plasmin, kallikrein and thrombin. -Aprotinin – serine proteases, e.g., trypsin, chymotrypsin, plasmin, and kallikrein; human leukocyte elastase, but not pancreatic elastase. -Bestatin hydrochloride– aminopeptidases, e.g., leucine aminopeptidase and alanyl aminopeptidase. -E-64 – [N-(trans-Epoxysuccinyl)-L-leucine 4-guanidinobutylamide] – cysteine proteases, e.g.,calpain, papain, cathepsin B, and cathepsin L. -Leupeptin hemisulfate salt– both serine and cysteine proteases, e.g., plasmin, trypsin, papain,and cathepsin B. -Pepstatin A – acid proteases, e.g., pepsin, renin and cathepsin D, and many microbial aspartic proteases.
Trichostatin A (TSA) (Sigma-Aldrich) 5 µM pre-treatment for 16 h	Trichostatin A (TSA) is a Streptomyces metabolite, which specifically inhibits mammalian histone deacetylase at nanomolar concentrations and causes accumulation of highly acetylated histone molecules in mammalian cells. For that reason, TSA has been used as a tool to study the consequences of histone acetylation in vivo. TSA induces cell differentiation, cell cycle arrest, reversal of transformed cells morphology, and apoptosis and is able to modulate transcription. TSA was used to establish a new cloning technique, which increases the success rates for mouse cloning (product information).
U0186 (Calbiochem) 2.5 µM and 5 µM pre-treatment for 1 h	A potent and specific inhibitor of MEK1 and MEK2. The inhibition is non-competitive with respect to MEK substrate, ATP and ERK. U0126 also acts as an immunosuppressant by effectively blocking IL-2 synthesis and T cell proliferation without affecting the long-term outcomes of either T cell activation or tolerance.
Z-VAD-FMK (Promega) 50 µM pre-treatment for 2 h	A cell-permeable pan caspase inhibitor that irreversibly binds to the catalytic site of caspase proteases and can inhibit induction of apoptosis. For inhibition of apoptosis, Z-VAD-FMK should be added at the same time that apoptosis is induced.

15.1. Treatment of cells with the specific proteasome inhibitor MG-132

MEFs were grown in 100-mm plates to 70-80% confluency and pretreated for 1 h with proteasome inhibitor MG-132 (Calbiochem) at a final concentration of 50 µM (Ruchaud-Sparagano et al., 2007). Cells were then infected with preactivated EPEC for 3 h in the presence of the inhibitor. After infection, cells were washed three times with IMDM supplemented with 10% FBS and bactericidal levels of gentamicin (100 µg/ml, final concentration). Cells were incubated at 37 ºC 5% CO_2 with IMDM supplemented

with 10% FBS, gentamicin and MG-132 for various times post-infection. Then, cells were washed once with ice-cold D-PBS and collected at indicated times by scrapping the cells with 300 µl of imidazole buffer. Clarified lysates were obtained following the previously described protocol (see section 10; Membrane enrichment procedure).

15.2. Treatment of cells with caspase and protease inhibitors

The caspase inhibitor Z-VAD-FMK (Promega) was used at a final concentration of 50 µM for 2 h prior to infections (Ching et al., 2002). The protease inhibitor cocktail P8340 (SIGMA-ALDRICH), which contains inhibitors with a broad specificity (see Table 3), was used at a concentration of 1:1000 for 4 h or 20 h prior to infections. To test the effect of both inhibitors MEFs were grown in 6-well plates to 70-80% confluency and pretreated with the corresponding inhibitor for the indicated time prior to infection. Cells were then infected with preactivated EPEC for 3 h in the presence of the inhibitor. Then, cells were collected by directly adding 200 µl of 2X Laemmli sample buffer and processed as previously described in section 5.

15.3. Treatment of cells with Trichostatin A

MEFs cells were grown in 6-well-plates to 70-80% confluency and pretreated with the deacetylase inhibitor Trichostatin A (TSA) (from *Streptomyces sp*, SIGMA-ALDRICH) for 16 h prior to infections (Zhang et al., 2007) at a final concentration of 5 µM. After 3h-infection in the presence of the inhibitor cells were washed three times in cold D-PBS and lysed by adding 200 µl of 1% Triton X-100 lysis buffer, according to the protocol described in next section.

16. Protein extraction and quantification of attached bacteria

Cells were grown in 6-well-plate to 70-80% confluency and were infected with EPEC strains as described. The monolayers were washed three times in cold D-PBS, and the cells were lysed using the protocol that was kindly provided by Brendan Kenny (University of Newcastle. Newcastle-upon-Tyne. England) consisting of adding 200 µl of 1% Triton X-100 lysis buffer (PBS containing 0.4 mM Na_3VO_4, 1 mM NaF and 0.1 mM PMSF). After 5 min incubation on ice, the samples were centrifuged at 21,000 x g for 5

min at 4 ºC (as described previously (Kenny and Finlay, 1997). Triton X-100 was used to solubilise the membrane proteins from the remaining insoluble fraction, which contained adherent bacteria, host nuclei and cytoskeleton. The soluble supernatant containing the cytoplasmic and membrane fractions was removed and the insoluble pellet was washed in 200 µl of PBS. The insoluble pellet was resuspended in 200 µl of 1X Laemmli sample buffer by mixing with a vortex. Both fractions were boiled for 5 min and a volume of 30 µl of each fraction was subject to SDS-PAGE and WB as described above.

Quantification of attached bacteria was done by WB analysis of the insoluble fraction with a monoclonal antibody against DnaK, which is an abundant bacterial heat shock protein.

17. Inhibition of bacterial protein synthesis with chloramphenicol

MEFs cells were grown in 6-well-plates to 70-80% confluency. Cells were infected during 15 min with 100X preactivated EPEC (at an approximate MOI of 250). After 15 minutes of infection, chloramphenicol was added to a final concentration of 100 µg/ml (Rosenshine et al., 1996). As a vehicle control, a volume of 10 µl of 70% ethanol was added per well to the untreated cells as vehicle control. Cells were then incubated at 37 ºC 5% CO_2 for 1, 2 and 3 hours. Monolayers were then washed three times with ice-cold D-PBS and lysed by adding 200 µl of 1% Triton X-100 lysis buffer, according to the protocol previously described in section 16.

RESULTS

RESULTS

Part I: Role of cortactin in pedestal formation by EPEC

1. siRNA of cortactin impairs pedestal formation by EPEC

To investigate the functional role of cortactin in pedestal formation by EPEC we inhibited the expression of cortactin in HeLa cells (Fig. 11). For this purpose we used a commercially available siRNA against cortactin and a scrambled sequence nucleotide as negative control. As shown in Fig. 11A, 16 hours after transfection the levels of cortactin were reduced by 72% as quantified by western blotting. At that point the cells were infected with EPEC to allow the formation of pedestals. Treatment of cells with siRNA against cortactin results in a significantly reduced number of pedestals with respect to control cells. This reduction is clearly visible in images of immunofluorescence staining of polymerised actin using fluorescence phalloidin and bacteria using DAPI (Fig. 11B). Panel C of figure 11 shows that depletion of cortactin reduces the percentage of pedestal formation by 57% (29.0 ± 5.4 in control cells *vs* 12.4 ± 4.8 in cortactin siRNA cells). This result demonstrates that cortactin contributes to pedestal formation.

2. Role of cortactin motifs in pedestal formation by EPEC

Reduction of cortactin expression by siRNA (Fig. 11) or overexpression of its isolated SH3 domain, polyproline region or its α-helical region (Cantarelli et al., 2006) result in a dramatic decrease in actin-pedestal formation during infection by EPEC. We decided to investigate the contribution of the different motifs of cortactin to actin assembly on pedestals formation by EPEC. For that purpose, we performed infection experiments of HeLa cells transiently transfected with different constructs of cortactin fused to GFP (Fig. 12A). Since the constructs bear a GFP tag we were able to simultaneously assess the localisation of the different cortactin forms. Pedestals were visualised by immunofluorescence staining of actin using fluorescent phalloidin and bacteria with DAPI (Fig. 12B).

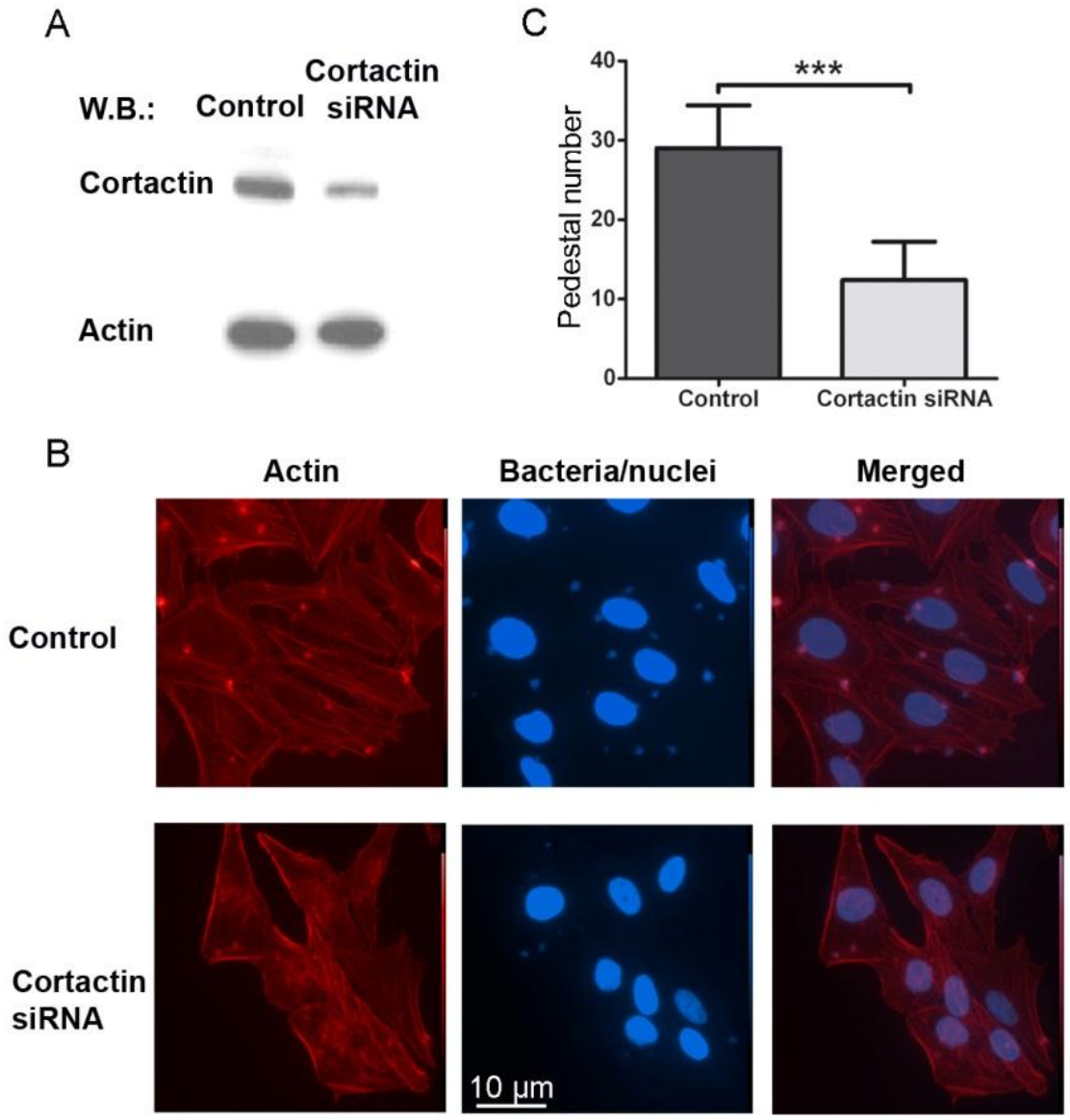

Figure 11. siRNA against cortactin blocks pedestal formation by EPEC. (A) Western-blot with anti-cortactin antibody showed a 72 % decrease of cortactin protein levels of cells treated with siRNA (average of four experiments after normalizing for actin), compared to control oligonucleotide treated cells (upper bands). Actin was used as a loading control (lower bands). **(B)** Immunofluorescence images of HeLa cells treated using siRNA with a nucleotide against cortactin compared to control treated cells were infected with 5 µl of an overnight EPEC culture for 3 hours. Red pictures showed actin staining. DAPI was used to stain EPEC microcolonies and nuclei of the cells. The merged images shown in last column were generated with Adobe Photoshop. Pictures are at 600X magnification. Scale bar represents 10 µm. **(C)** Quantification was done by counting the number of microcolonies of 100 cells in representative microscope fields. Graph represents mean ± SD. Statistical analysis using the Student´s *t*-test from three independent experiments. *, $p<0.05$; **, $p<0.01$; ***, $p<0.001$. The experiments in this figure were performed by Narcisa Martínez-Quiles.

The NTA domain of cortactin, that binds and activates the Arp2/3 complex, carries a 20DDW22 motif which mutation to 20DD**A**22, hereafter referred to as W22A, abolished this activity (Uruno et al., 2001). We transfected HeLa cells with GFP-W22A in order to determine whether this motif is necessary for pedestal formation. We used wild type cortactin (referred to as GFP-full length, GFP-FL) and GFP alone as controls. As shown in figure 12, overexpression of GFP-FL cortactin allows pedestal formation to levels similar to those in cells expressing GFP. Figure 12C (black bars) shows normalised percentages and standard deviations for GFP-FL. We observed GFP-FL cortactin to localise in 70% of pedestals, compared to 4% for GFP-transfected cells (open bars). Importantly, the number of pedestals in cells expressing GFP-W22A mutant was significantly lower than in GFP-FL transfected cells (51% *vs* 83%). This result indicates that cortactin W22A exerts a dominant negative effect, which may mean that cortactin binding and activation of the Arp2/3 complex is necessary for pedestal formation.

Cortactin has a C-terminal SH3 domain that binds several proteins. Mutation of a critical amino acid (W525K) in the SH3 domain abolishes its binding to known targets (Du et al., 1998) such as N-WASP (Martinez-Quiles et al., 2004). We used this mutant to assess the contribution of the cortactin SH3 domain to pedestal formation and found that its expression inhibits pedestal formation to an even greater extent than the W22A mutant (31% *vs* 51%). This indicates that cortactin W525K mutant exerts a dominant negative effect, corroborating previous results (Cantarelli et al., 2006).

N-WASP is one of the SH3 cortactin targets, that was shown essential for pedestal formation, as demonstrated by the fact that N-WASP-deficient cells do not form pedestals (Lommel et al., 2001). In previous work, the P.I of our group described that the cortactin SH3 domain is able to activate N-WASP and proposed a model for the regulation of N-WASP activation by cortactin. According to our model cortactin is switched on by Erk phosphorylation at serines 405 and 418, while it is switched off by Src phosphorylation at tyrosines 421, 466 and 482 (Martinez-Quiles et al., 2004). Hence, we repeated the pedestal formation assay with cells expressing the cortactin S405,418D doble mutant, which mimics Erk phosphorylation and activates N-WASP *in vitro*, as well as its non-phosphorylatable counterpart (S405,418A). The S405,418D mutant allows

pedestal formation to a similar extent as the WT cortactin (90%) and to a greater extent, although not significantly, than the GFP negative control (83%). The phosphoserine-mimicking cortactin mutant accumulates in only 21% of pedestals and shows a weak, diffuse pattern of localisation in the cytoplasm and pronounced staining in the nucleus. In contrast, the mutant that abolishes Erk phosphorylation (S405,418A) impairs pedestal formation (34%) and its own translocation to them (3%). These results suggest that Erk phosphorylation of cortactin contributes to pedestals formation.

Similarly, we wanted to address the role of Src-mediated phosphorylation of cortactin. We therefore used the phosphotyrosine-mimicking mutant (Y421,466,482D) and the phosphotyrosine deficient mutant (Y421,466,482F). In both cases, pedestal formation and location of these constructs on them are impaired (33%/7%; 28%/14%, Fig. 12B and C). These results indicate that Src-mediated phoshorylation of cortactin seems to inhibit pedestal formation.

3. EPEC induces N-WASP-dependent tyrosine phosphorylation of cortactin

A major regulatory mechanism of cortactin is its phosphorylation which is induced by different stimuli. As mentioned before, cortactin is phosphorylated on tyrosines 421, 466 and 482 by Src family kinases (Huang et al., 1998), which decreases cortactin affinity for N-WASP *in vitro* (Martinez-Quiles et al., 2004). It has been shown that EPEC infection of CH7 mouse fibroblasts induces tyrosine phosphorylation of cortactin (Cantarelli et al., 2007). In addition, both Nck and N-WASP are indispensable for pedestal formation as demonstrated using mouse embryonic fibroblast (MEFs) deficient in these proteins (Gruenheid et al., 2001, Lommel, 2001 #41). These observations prompted us to examine the phosphorylation status of cortactin in two different cell types: N-WASP and Nck1/2-deficient MEFs.

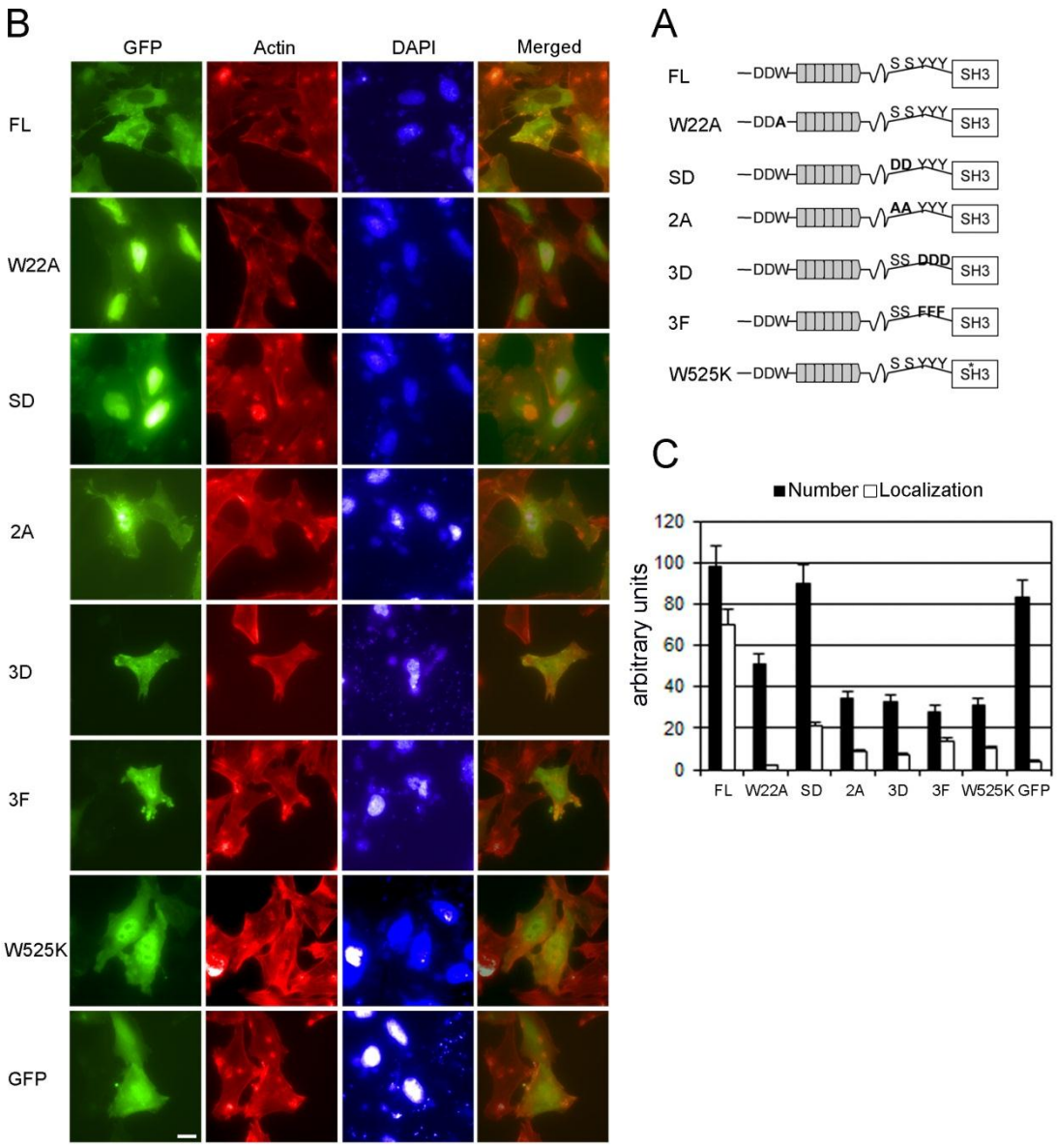

Figure 12. Effect of the overexpression of WT and cortactin mutants on pedestal formation. (**A)** Schematic of cortactin domains and mutants under investigation. **(B)** Immunofluorescence images of HeLa cells transfected with WT (FL) and cortactin mutants and infected for 3 h with 1 µl of overnight EPEC culture per well of a 6-well-plate. Mutants used are: Arp2/3 activation mutant (W22A), Erk-phosphorylation-mimicking mutant S405,418D (SD), Erk non-phosphorylatable mutant S405,418A (2A), Src-phosphorylation-mimicking mutant Y421,466,482D (3D), Src non-phosphorylatable mutant Y421,466,482F (3F) and SH3 domain mutant (W525K). GFP staining is shown in green, F-actin is in red, and bacteria and nuclei are in blue. The last column shows merged images of GFP and actin staining. Pictures are at 600× magnification. Scale bar 10 µm. **(C)** Quantification of pedestal number and cortactin localisation. Black bars represent percentages normalized to WT of pedestal formed after 3 hours of infection of HeLa cells expressing GFP-FL and cortactin mutants. White bars represent normalized percentages of localisation to pedestals. Results of three independent experiments were considered statistically significant ($p<0.01$ by Student's *t*-test).The experiments in this figure were performed by Narcisa Martínez-Quiles.

First, we performed Western blotting control experiments to assess the expression of N-WASP and Nck proteins in the different cell types. As loading control we blotted for cortactin and actin (Fig. 13A). Fig. 13A shows that EPEC induces phosphorylation of tyrosine 466 of cortactin at 3 hours of infection in WT MEFs, as detected using an antibody against phosphoY466-cortactin (pY466 Ab). This result was corroborated using a second phospho-specific antibody (pY421 Ab) (Fig. 13E). Unexpectedly, tyrosine phosphorylation of cortactin is not induced in N-WASP-deficient cells. This result suggests that tyrosine phosphorylation of cortactin during EPEC infection depends on the presence of N-WASP. To verify this, we infected N-WASP-deficient cells that were retrovirally reconstituted with N-WASP (hereafter referred to as N-WASP reconstituted cells, R) and examined the levels of phosphoY466-cortactin. Fig. 13A shows that N-WASP re-expression partially restored cortactin tyrosine phosphorylation levels. In three independent experiments the normalised average induction was 1 ± 0.2 for WT cells, 0 for N-WASP-deficient cells and 0.5 ± 0.1 for R cells. This supports the idea that EPEC-induced tyrosine phosphorylation of cortactin in cultured cells requires N-WASP.

On the other hand, Nck-deficient cells show a higher basal level of phosphoY466-cortactin that is maintained or slightly reduced after EPEC infection. This higher basal level of cortactin phosphorylation could be explained by the higher level of cortactin total protein consistently found in these cells (Fig. 13A and Fig. 13C).

Given the absence of induction of cortactin tyrosine phosphorylation in EPEC-infected N-WASP and Nck-deficient cells, we then checked Src activation, using a commercially available phospho-active Src antibody (pY416 Ab). Fig. 13B demonstrated that equal activation of Src is achieved during EPEC infection in all cell types studied, while, as expected, the levels of total Src remain constant during infection. This result shows that the lack of cortactin phosphorylation in N-WASP-deficient cells is not due to a block in Src activation. As a further control, we treated the cells with pervanadate and observed robust phosphorylation of cortactin tyrosine 466 (Fig. 13C, upper panel).

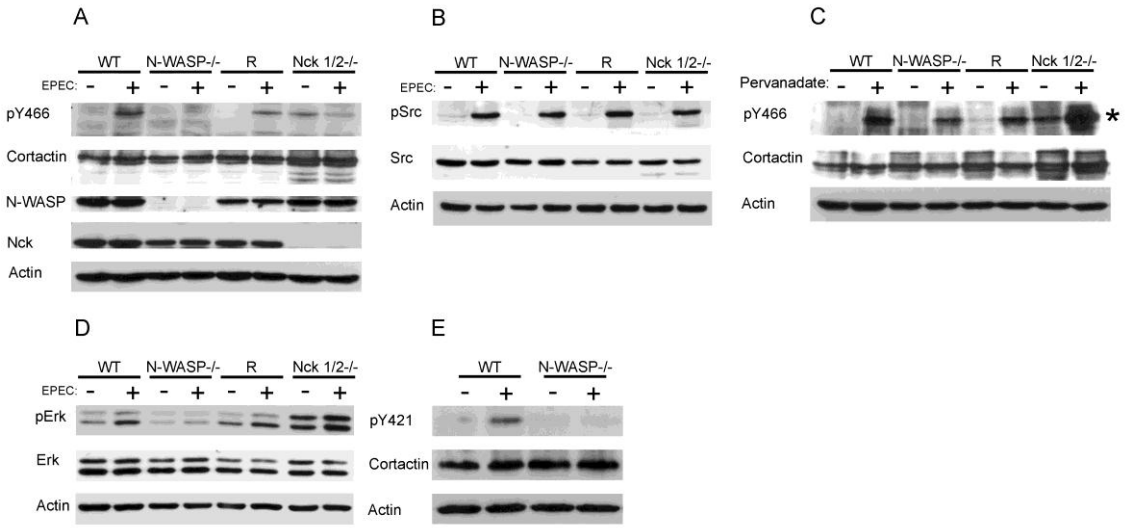

Figure 13. EPEC-induced tyrosine phosphorylation of cortactin depends on N-WASP. WT, N-WASP-deficient cells (N-WASP-/-), N-WASP reconstituted cells (R) as well as Nck-deficient cells (Nck1/2-/-) were infected with X preactivated EPEC for 3 h. **(A) Tyrosine phosphorylation of cortactin occurs in WT but not in N-WASP-deficient MEFs.** Cell lysates were subjected to SDS-PAGE and Western blotted with an antibody against phospho-Y466 cortactin (upper panel). The same membrane was stripped and reprobed with anti-cortactin monoclonal antibody 4F11. Anti-N-WASP and anti-Nck was performed to confirm the genotype of the MEFs. Actin was used as a loading control. **(B) EPEC infection activates Src to similar extends in all cell-types studied.** The activation of Src was analysed with anti-phospho-Y416 Src (upper panel). Medium and lower panels showed Src and actin blots, respectively. **(C) Pervanadate treatment induces a robust phosphorylation of cortactin on tyrosine 466 in all cell-types studied.** Lysates of vehicle DMSO-treated MEFs and pervanadate-treated MEFs (diluted 1/500 *) were examined by WB with antibody against phospho-Y466 cortactin. A second gel was loaded in parallel with the same amount of protein for both types of lysates and blotted for cortactin and actin for protein and loading controls, respectively. **(D) EPEC infection induces Erk1/2 activation in WT and Nck-deficient but not in N-WASP-deficient MEFs.** Cell lysates were examined by WB using a MoAb specific for activated Erk phosphorylated on Thr202 and Tyr204 (upper panel). Medium and lower panels show Erk and actin blots for Erk protein and loading control respectively. Similar results were obtained in at least three independent experiments. **(E) Tyrosine phosphorylation at Y421 cortactin occurs in WT but not in N-WASP-deficient MEFs.** Cell lysates were examined by WB with an antibody against phospho-Y421 cortactin (upper panel). The same membrane was stripped and reprobed with anti-cortactin MoAb 4F11. Actin was used as a loading control.

Then, we sought to establish the activation status of Erk in EPEC-infected cells. We used a phospho-specific monoclonal antibody that detects the activated form of Erk1/2 (anti pThr202/pTyr204). EPEC induces the activation of Erk in WT MEFs (Fig. 13D, first lane), in agreement with a previous report in T84 epithelial cells (Savkovic et al., 2001). However, infection of N-WASP-deficient cells showed reduced activation of Erk which

was recovered in R cells. On the contrary, Nck-deficient cells have a higher basal level of Erk and strong activation upon EPEC infection. These results imply that Erk is activated by EPEC and may phosphorylate cortactin in EPEC-infected cells. More importantly, N-WASP is absolutely required for the induction of Erk activation and for the induction of tyrosine phosphorylation of cortactin at 3 hours of infection, while Nck is dispensable.

In collaboration with Dr. Steffen Backert (School of Biomolecular and Biomedical Sciences, University College Dublin, Ireland) we explored the serine phosphorylation status of cortactin in MEFs at 3 hours of EPEC infection by using specific antibodies against phosphorylated serine residues 405 and 418 (Tegtmeyer et al., 2011). A preliminary result corresponding to a single experiment shows that EPEC induces at least the phosphorylation of serine residue 405 (Fig. 14, upper panel). As it occurred with tyrosine phosphorylation, the phosphorylation of serine residue 405 is not induced in N-WASP-deficient cells. However, N-WASP re-expression does not restore serine phosphorylation levels of cortactin. On the other hand, Nck-deficient cells show a higher basal level of phosphorylation of serine residues 405 and 418 that is increased after EPEC infection (Fig. 14).

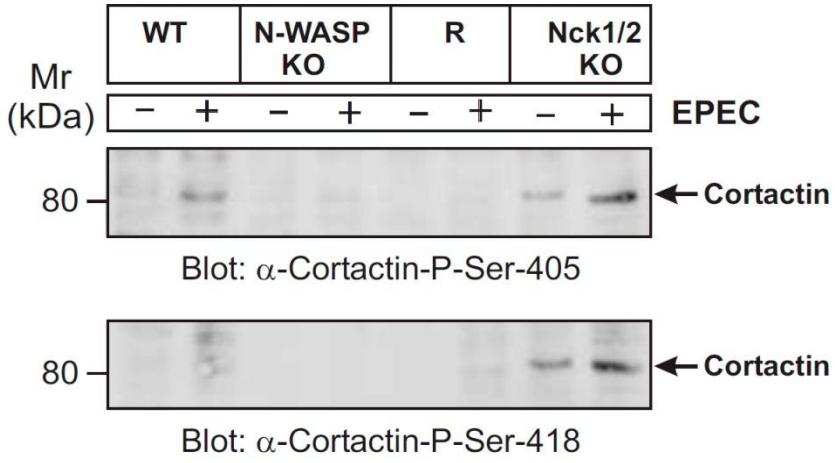

Figure 14. EPEC induces phosphorylation of cortactin in serine residues that depends on N-WASP. WT, N-WASP-deficient (N-WASP KO), N-WASP reconstituted cells (R) as well as Nck-deficient cells (Nck1/2 KO) were infected with X preactivated EPEC for 3 h. The level of serine phosphorylation of cortactin was assessed by Western blotting using phospho-specific antibodies against S405 (upper panel) and S418 (lower panel). This preliminary result was performed only once and was produced by Steffen Backert (University College Dublin, Ireland) using our cell lysates.

It has been described that the Src family inhibitor PP1 has no effect on actin polymerisation induced by EPEC (Cantarelli et al., 2000; Swimm et al., 2004a). However, it was not known whether chemical inhibition of Erk would block pedestal formation. To that extend, we treated WT MEFs with Erk inhibitor U0126 and found that there is no difference in the number of pedestal formed by EPEC (Figure 15). This result has also been corroborated by a complementary study (Cantarelli et al., 2006) .

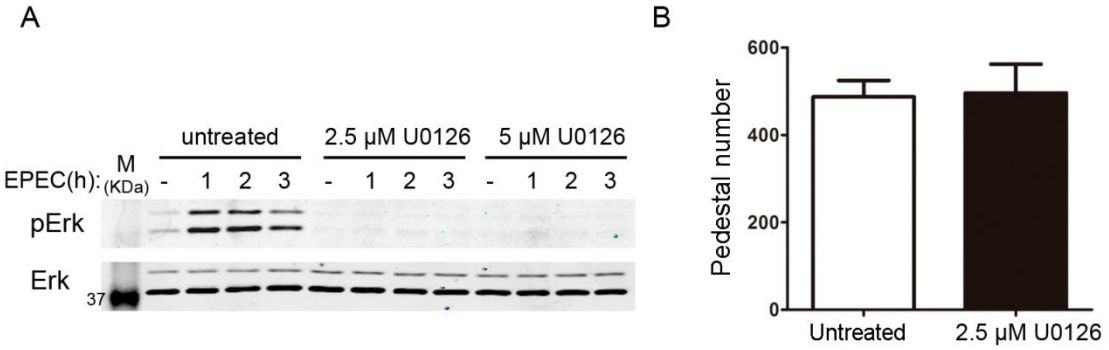

Figure 15. The number of pedestals is not affected by blocking Erk activation. (A) WT MEFs were treated with the Erk inhibitor U0126 at 2.5 µM or 5 µM for 1 hour prior to infection with X preactivated EPEC at indicated times. Cells were left untreated as a negative control. The levels of Erk activation were assessed by Western blotting with a MoAb against phospho-T202/T204 Erk (upper panel) and secondly with an Ab against Erk and visualised with the Odyssey system. **(B)** Quantification was done by counting the number of pedestals in untreated WT MEFs (white bar) and in U0126-treated WT MEFs at 2.5 µM (black bar) of 100 cells. Non-statistical difference was found for the analysis of two independent experiments as shown.

4. Tir binds cortactin and induces the latter to nucleate actin *in vitro* through an Arp2/3 complex-mediated pathway

The bacterial effector Tir initiates what is considered to be the principal signalling pathway for actin assembly in a manner dependent on phosphorylation of tyrosine 474 (Kenny, 1999) by host cell kinases. This modification serves to recruit Nck (Gruenheid et al., 2001) that presumably binds N-WASP to initiate Arp2/3 complex-mediated actin polymerisation. We wanted to gain insights into how cortactin functions in pedestal signalling. Our initial hypothesis was that cortactin and Tir interact directly. Therefore we used the Scansite database (Yaffe et al., 2001) to search for motifs in the Tir sequence to which cortactin SH3 domain could bind. We found a consensus motif (NNS**I**PPA**P**PL**P**SOTD) centered on proline 20 of Tir.

We first performed *in vitro* pull-down experiments with cortactin recombinant proteins and with purified Tir (Fig. 16A). We produced WT GST-Tir that was purified using GSH beads and treated with PreScission enzyme, which excised Tir and at the same time removed the GST tag (Fig. 16A, Coomassie gel). Tir protein was used as the input in pull-down experiments with WT and mutants GST-cortactin fusion protein. The first line of figure 16A shows that cortactin binds Tir *in vitro*.

To map the domains involved in the interaction, we performed pull-down experiments using cortactin mutants as follows: full-length W525K (mutated SH3 domain), full-length W22A (mutated Arp2/3 binding domain), the N-terminus (NH2, residues 1-333), and the isolated SH3 domain (SH3, residues 458-546). GST was used as a negative control. In agreement with our initial hypothesis, the isolated SH3 domain of cortactin binds Tir. However, the N-terminal domain of cortactin also binds Tir (Fig. 16A, third line). This unforeseen interaction was confirmed in experiments with cortactin carrying the point mutations W525K and W22A (Fig. 16A). Next we tested the cortactin S405,418D (SD) and Y421,482,486D (3D) mutants which are similar to the WT form in their ability to bind Tir (Fig. 16A). These results demonstrate that cortactin and Tir interact directly *in vitro*, that this interaction involves both the N-terminal part and the SH3 domain, and that it appears to be independent of cortactin phosphorylation.

Given the direct interaction between Tir and cortactin, we wondered whether Tir can activate the ability of cortactin to promote Arp2/3-mediated actin polymerisation. We coupled recombinant Tir protein to carboxilate beads. Next we incubated them with purified Arp and actin in Xb buffer containing WT and cortactin mutants. Column 2 of figure 16B shows that Tir activated WT cortactin as well as the SD and 3D mutants. The W525K mutant was also activated, although weakly. As expected, W22A cortactin was not activated, indicating that the effect was mediated by cortactin activation of the Arp2/3 complex. As a negative control we used naked beads that showed no activation (Fig. 16B; column 1). In addition, we also coupled recombinant Tir phospho-mimicking mutant TirY474D to carboxilate beads (Fig. 16B; column 3) and we obtained similar results. Collectively these results indicate that Tir activates the ability of cortactin to

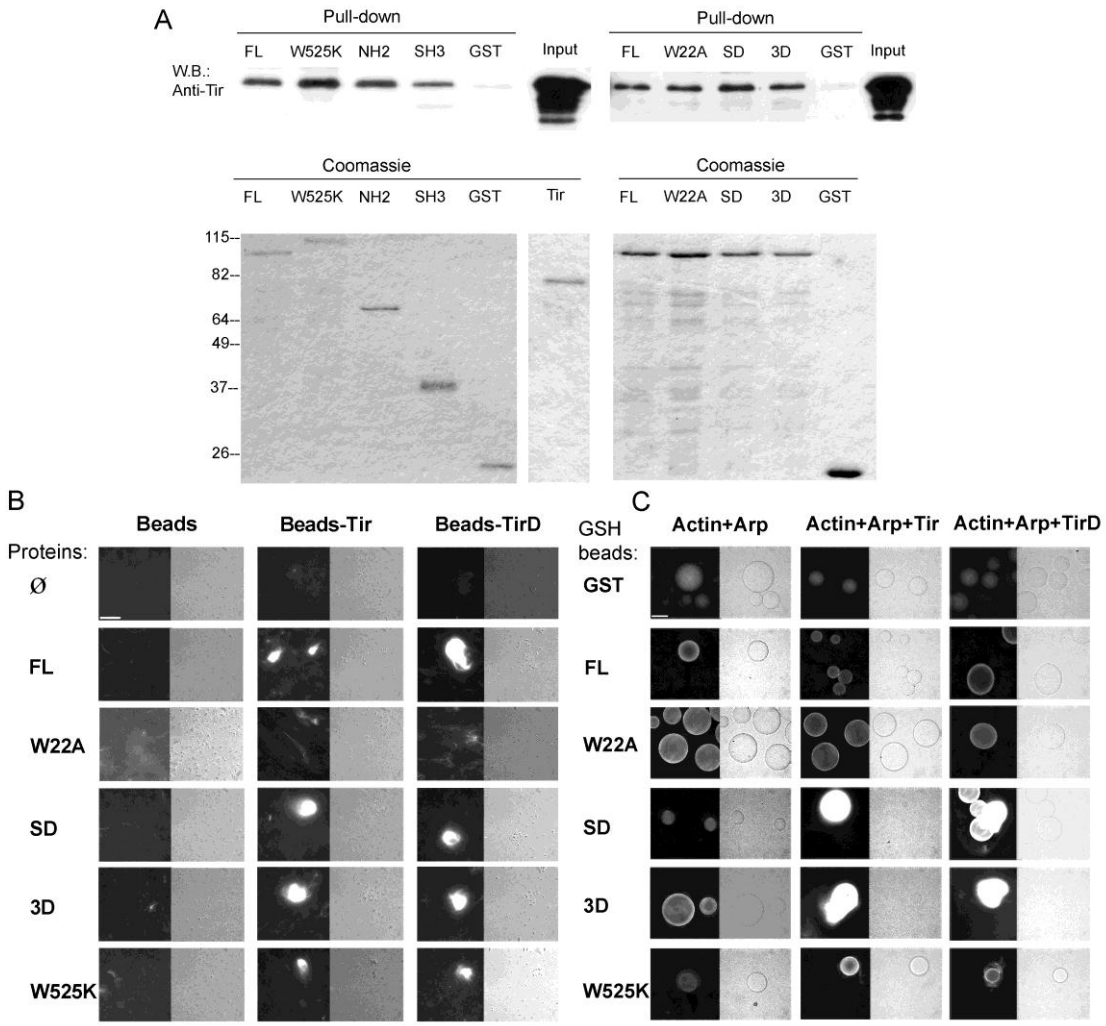

Figure 16. Tir binds cortactin and promotes its activation of Arp2/3-mediated actin polymerisation. (A) Cortactin binds Tir through its N-terminal and SH3 domain and independently of cortactin phosphorylation *in vitro*. Recombinant Tir was incubated with WT cortactin (FL) and with the GST-tagged mutants: the SH3 domain mutant (W525K), the N-terminal (NH2) domain, the SH3 domain (SH3), Arp2/3 domain mutant (W22A), Erk-phosphorylation-mimicking mutant (SD) and Src-phosphorylation-mimicking mutant (3D). GST served as a negative control. The pull-downs were subjected to SDS PAGE and blotted with anti-Tir MoAb. In the last line, one-fifth of the total amount of Tir that was used as input per pull-down sample (upper panel). Coomassie staining of proteins is also shown (lower panels). **(B) Tir induces cortactin to nucleate actin *in vitro* through an Arp2/3 complex-mediated pathway.** Immunofluorescence images of Tir-coupled beads incubated with actin, Arp2/3 and cortactin/mutants. Uncoupled carboxilate beads (left panels) or coupled to Tir or TirD proteins were incubated with a solution of 500 nM WT cortactin or cortactin mutants proteins for 1 h. Actin and Arp were then added and incubated to allow actin polymerisation. After 1 h TRITC-phalloidin was added, and the samples were observed immediately on a fluorescence microscope. Pictures were taken at 600X magnification. Scale bar represents 40 µm. **(C)** Immunofluorescence images of GSH beads coupled to GST, WT or cortactin mutants incubated with actin, Arp2/3 and Tir/TirD. GSH beads coupled to the proteins were incubated with a solution of 500 nM Tir or TirD proteins or buffer alone as a control (left panels) for 1 h. Then actin and Arp was added and incubated for 1 h to allow actin polymerisation. To end TRITC-phalloidin was added, and the samples were observed immediately on a microscope. Pictures were taken at 200X magnification. Scale bar represents 40 µm.

promote Arp2/3-mediated actin polymerisation *in vitro* independently of cortactin phosphorylation status.

Conversely, experiments in which GST-cortactin and its mutants were coupled to Glutathione Sepharose (GSH) beads and incubated in solution with Tir or TirD were performed (Fig. 16C). Although WT cortactin is not activated, we obtained similar results with all the other mutants.

5. Cortactin binding to Tir in Nck and N-WASP-deficient cells infected by EPEC

Because cortactin binds directly Tir (Fig. 16), N-WASP (Martinez-Quiles et al., 2004) and Nck (Okamura and Resh, 1995), we analysed cortactin-Tir interaction in N-WASP and Nck-deficient cells. Keeping in mind that Nck-deficient cells allow the formation of a small percentage of pedestals compared to WT cells ((Campellone et al., 2004a) and further analysed in (Figure 28B)), while N-WASP-deficient cells are even more resistant to pedestal formation (Lommel et al., 2004), we wanted to analyse the possible complexes formed between Tir, Nck, N-WASP and cortactin in cells infected by EPEC.

To address this question, we adapted a previously described fractionation protocol that enriches in Tir-containing membranes ((Patel et al., 2006) and Materials and Methods). As expected, Tir is enriched in the pellets compared to supernatants, as detected by western-blotting with a monoclonal antibody against Tir (Fig. 17A). We observed that a band with slower electrophoretic motility is the predominant form of Tir in the pellets, which represents fully-modified Tir (Kenny and Warawa, 2001). Unexpectedly, we found that the Nck-deficient cells present a drastic reduction of fully-modified Tir, while N-WASP-deficient cells present detectable amounts of this Tir form.

With the limitation that Nck-deficient cells do contain reduced levels of Tir, we performed pull-downs assays with cortactin construct. As full-length cortactin has a closed conformation (Cowieson et al., 2008; Martinez-Quiles et al., 2004), we decided to use N-terminal cortactin (NH2) and the isolated SH3 domain (SH3) to perform pull-

down experiments with the membrane-enrich fraction of EPEC infected and uninfected WT, N-WASP-deficient and N-WASP reconstituted cells (N-WASP R), as well as Nck-deficient cells. GST was used as a negative control.

Western blotting analysis with an anti-Tir MoAb shows that NH2 binds Tir in EPEC infected but not uninfected cells (negative control) with no appreciable differences between WT, N-WASP and N-WASP reconstituted cells (Fig. 17B). No binding was detected using Nck-deficient cell lysates which could be attributed to the reported low amount of Tir protein initially present on the lysate. In contrast, neither the isolated SH3 domain nor the GST negative control bind Tir in any of the cells type used. Similar results were obtained performing pull down experiments with clarified total cell lysates although longer exposure times where necessary to detect Tir (Fig. 17C).

In view of these results, we can conclude that in cultured cells cortactin binds Tir primarily through its N-terminal region. It has been described that cortactin interact with N-WASP thought its SH3 domain (Martinez-Quiles et al., 2004). To test whether the SH3 domain of cortactin prefers to bind N-WASP over Tir, we performed pull-downs experiments with clarified total lysates, and we then stripped and reprobed the blots with anti-N-WASP antibody. As shown in figure 17C the SH3 domain of cortactin is able to pull-down N-WASP in EPEC-infected WT cells but not N-WASP-deficient cells. However, in N-WASP reconstituted cells the SH3 domain of cortactin does not pull-down N-WASP. On the other hand, the SH3 domain of cortactin binds N-WASP in Nck-deficient cells. The same results were obtained in uninfected cells (Fig. 17C; -EPEC). This observation argues in favour of the conclusion that the N-terminal region of cortactin is involved in binding Tir, while the SH3 domain is involved in binding N-WASP.

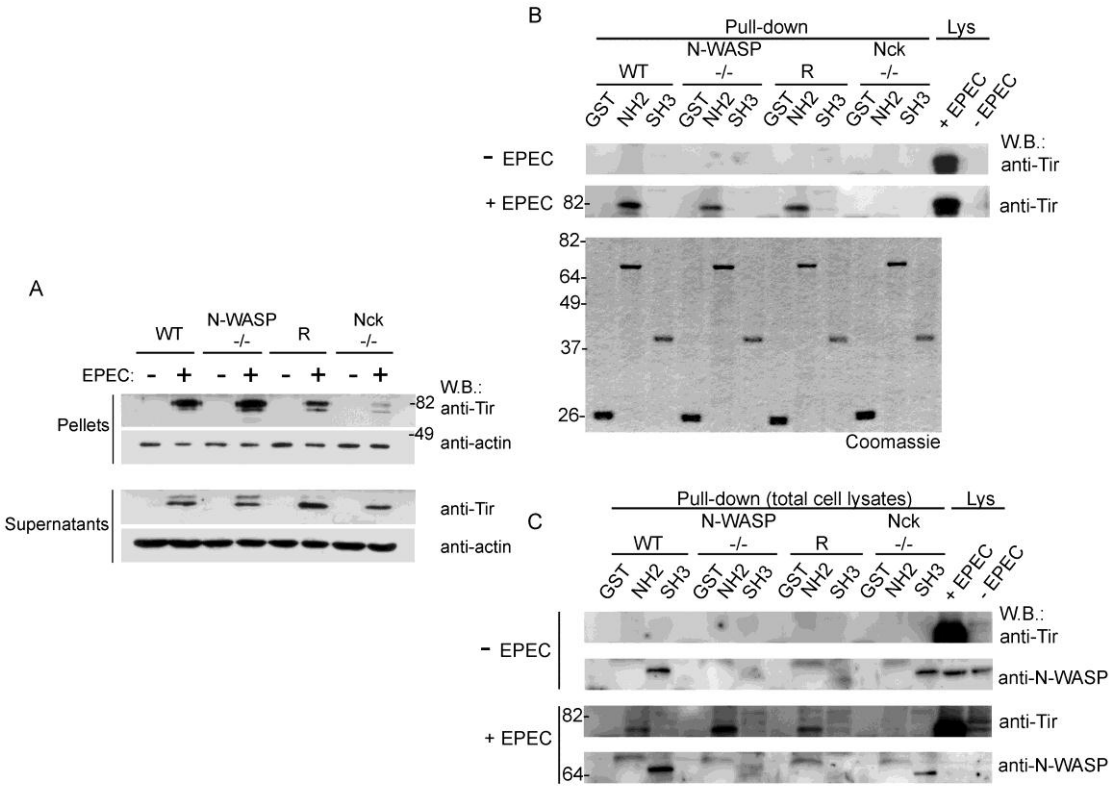

Figure 17. Cortactin binds Tir in the absence of N-WASP and Nck1/2. (A) Tir is abundant in membrane-enriched fractions, except in Nck-deficient cells. WT, N-WASP-deficient (N-WASP-/-), N-WASP reconstituted cells (R) and Nck-deficient cells (Nck-/-) were infected with X preactivated EPEC. Cell monolayers were lysed in imidazole buffer, fractionated, subjected to SDS-PAGE and blotted with anti-Tir MoAb. As previously described, Tir appears as a doublet whose upper band is enriched in the membrane fractions (pellets). Actin is shown as a loading control. **(B)(C) Cortactin binds Tir in cells through its N terminal domain and N-WASP through its SH3 domain.** The membrane fraction (B) or clarified total cell lysates (C) of uninfected and EPEC-infected WT, N-WASP-/-, N-WASP reconstituted cells (R) and Nck-/- were used for pull-down experiments with GST fusion proteins as follows: cortactin N-terminal truncation mutant (NH2), the isolated SH3 domain (SH3) and GST alone. Pull-down experiments were analysed by WB with indicated antibodies. In the last two lines, one-sixth of the total amount of cell lysate used for each PD assay was loaded (lysate from WT cells in control blots (-EPEC) and from NWASP-deficient cells in +EPEC blots). Coomassie staining of proteins is also shown. These experiments were performed at least three times.

Part II. Role of the adaptor Crk in pedestal formation by EPEC

1. The inhibition of CrkII expression has no effect on pedestal formation

The Crk family of adaptor proteins (CrkI, Crk II and CrkL) assembles protein complexes and transmits signals downstream of tyrosine kinases participating in many signalling pathways. Crk localises to EPEC pedestals (Goosney et al., 2001) and was shown to cooperate with tyrosine phosphorylated cortactin to promote actin polymerisation during *Shigella* invasion (Bougneres et al., 2004). These data prompted us to investigate the role of Crk isoforms in pedestal formation by EPEC. In figure 18A western blot analysis shows the expression of the three isoforms in HeLa cells. Endogenous levels of CrkII and CrkL are readily detected whereas CrkI isoform is only expressed at almost non-detectable levels (Fig 18A and (Dokainish et al., 2007)).

First, we silenced CrkI/II expression with siRNA oligonucleotide specific for CrkI and CrkII. Western blot analysis indicates a 76% decrease in CrkII levels in cells after 16 hours of transfection with siRNA, compared with control samples (average of three experiments after normalising for actin) (Fig. 18B). At that point we infected the cells with EPEC to allow the formation of pedestals. Figure 18C shows immunofluorescence staining of polymerised actin and bacteria. The number of pedestals does not differ between siRNA-treated cells and control cells in three different experiments (Fig. 18D). This result indicates that a reduction in the levels of expression of CrkI/II by siRNA has no effect in the number of pedestal formed by EPEC.

2. Expression of a Crk dominant negative mutant does not affect the efficiency of pedestal formation

To confirm the siRNA result, we used a complementary approach and performed transfection experiments of HeLa cells with a myc-tagged Crk dominant negative mutant (R38V), which is mutated in the SH2 domain (Fig. 19). The arginine residue R38 is conserved in all SH2 domains and is essential for recognition of phosphotyrosine

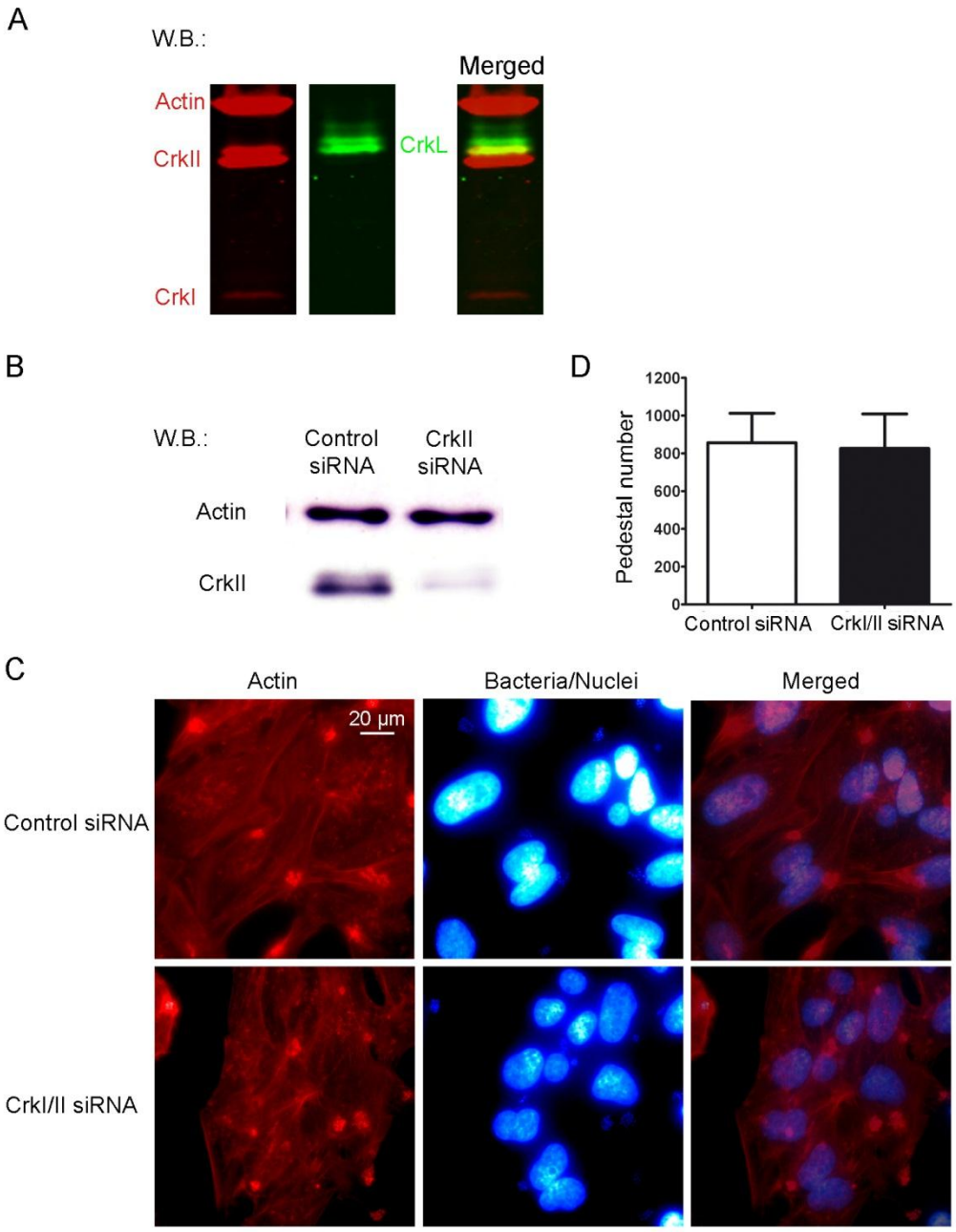

Figure 18. Pedestal formation is not affected by siRNA depletion of CrkI and CrkII in HeLa cells. (A) Levels of expression of CrkI, CrkII and CrkL in HeLa cells by western blotting analysis with the Odyssey Scan System. **(B)** Western blotting analysis using chemiluminiscence shows the decrease of CrkII protein levels of cells treated using siRNA oligonucleotide against CrkI/II compared to control oligonucleotide treated cells (lower bands). Actin was used as a loading control (upper bands). **(C)** Immunofluorescence images of HeLa cells treated using siRNA oligonucleotide against CrkI/II compared to control oligonucleotide treated cells and infected with X preactivated EPEC for 2 hours. Red pictures show actin staining with TRITC-Phalloidin. DAPI was used to stain EPEC. The merged images shown in last column were generated with Adobe Photoshop. Pictures are at 600X magnification. Scale bar represents 20 µm. **(D)** Quantification was done by counting the number of pedestals from 100 cells in representative microscope fields. Graph represents mean ± SD. Non-statistical difference was found for the analysis of three independent experiments.

groups. More importantly, its mutation abolished the interaction of Crk with its binding partners (Kiyokawa et al., 1998) and blocked *Shigella* invasion (Bougneres et al., 2004).

Western analysis with an anti-myc monoclonal antibody shows that the level of expression of wild type CrkII and R38V mutant is similar. Cells were treated with the transfection reagent (mock) as a negative control (Fig. 19A). Fig. 19B shows the immunofluorescence staining of HeLa cells transfected with WT CrkII or R38V mutant constructs and infected with EPEC. As shown in Fig. 19C the number of pedestal formed in cells transfected with the dominant negative R38V does not differ from cells transfected with WT CrkII or mock cells. Together our results indicate that the overexpression of neither the WT CrkII nor the Crk dominant negative mutant has any effect on pedestal formation.

3. Inhibition of the three Crk isoforms is associated with enhanced formation of actin pedestals

With the aim to test the effect of the total absence of CrkI and CrkII on the formation of pedestals by EPEC, we next used CrkI/II-deficient mouse embryonic fibroblasts to perform EPEC infection experiments. To distinguish between CrkI and CrkII contributions, we transfected CrkI/II-deficient cells with myc-CrkII (referred to as Rescued Crk, R CrkII) (Fig. 20). We quantified the number of pedestals and found no difference in the number of pedestals between WT, CrkI/II-deficient MEFs or CrkII reconstituted MEFs (Fig20C), which confirm the result obtained with HeLa cells (Fig. 18).

At this point we favoured the hypothesis that CrkL could be compensating for the lack of CrkI/II. Therefore we inhibited the expression of CrkL in CrkI/II-deficient cells using siRNA and cells were then infected with EPEC. The expression levels of CrkL are reduced by 60% as quantified by WB analysis (Fig. 21A). Figure 21B shows immunofluorescence staining of polymerised actin with TRITC-phalloidin (in red). In this experiment we used a monoclonal antibody against *E. coli* LPS (in blue) to avoid the overexposure of the cell nuclei necessary to visualise the bacteria. The quantification of the results showed a significant increase in the number of pedestals in CrkI/II-deficient cells depleted for

CrkL with respect to WT cells (Fig. 21C). Thus, cells expressing none of the three isoforms formed significantly more pedestals, indicating a potential inhibitory role of Crk family adaptor proteins in the formation of pedestals.

To further confirm this result, we expressed the R38V dominant negative Crk mutant in WT and CrkI/II-deficient MEFs (Fig. 22A). We observed a significant increase in the number of pedestals in cells transfected with the dominant negative R38V when compared to WT or CrkI/II-deficient cells (Fig. 22B). These results point towards a redundancy and a possible inhibitory role in the contribution to pedestal formation by Crk proteins.

4. CrkL-deficient cells present no differences in the number of pedestals formed by EPEC

To test whether CrkL could have a more relevant role than CrkII/I in pedestal formation we next used CrkL-deficient mouse embryonic fibroblasts to perform EPEC infection experiments. We quantified the number of pedestals and found no difference in the number of pedestals between WT, CrkL-deficient MEFs or CrkL reconstituted MEFs (Fig23A).

Collectively these results indicate that CrkII or CrkL expression is sufficient to compensate for the absence of the other, confirming that Crk isoforms act redundantly to inhibit pedestal formation.

To further corroborate the redundancy function, we followed the same approach and expressed the R38V dominant negative Crk mutant in WT and CrkL-deficient MEFs. Although the differences do not reach statistical significance with five experiments, an increase in the number of pedestals was observed in cells transfected with the dominant negative mutant (R38V) when compared to WT or CrkL-deficient cells (Fig. 23B).

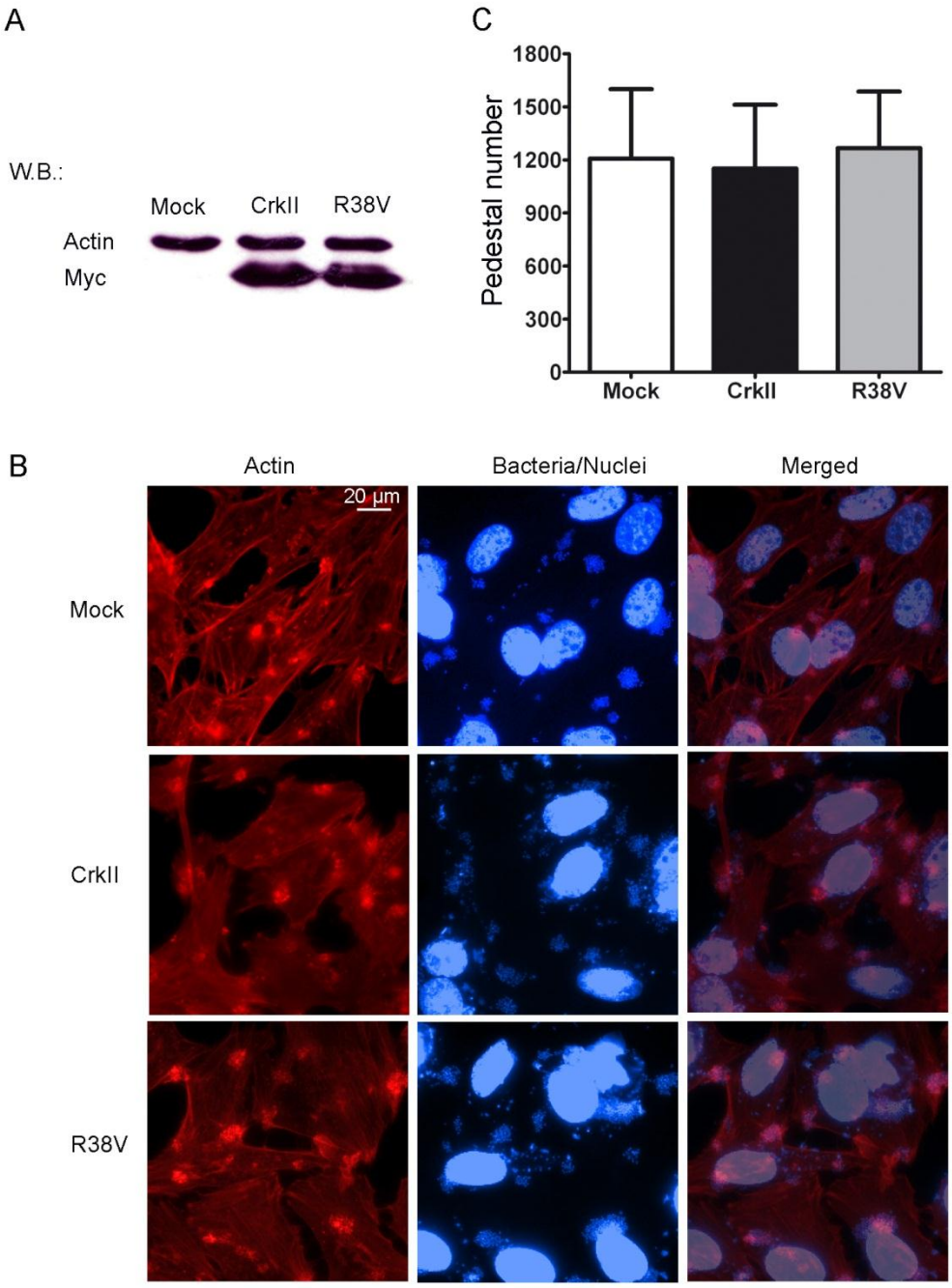

Figure 19. Pedestal formation is not affected in HeLa cells expressing a Crk dominant negative R38V mutant form. (A) The expression of transfectants was assessed by western blotting with anti-myc MoAb (lower bands). Actin was used as a loading control (upper bands). **(B)** Immunofluorescence images of HeLa cells transfected with WT CrkII or a dominant negative mutant (R38V) or treated with the vehicle (mock) and infected with X preactivated EPEC for 2 hours. Red pictures show actin staining; DAPI was used to stain EPEC (blue). The merged images shown in last column were generated with Adobe Photoshop. Pictures are at 600X magnification. Scale bar represents 20 µm. **(C)** Quantification of pedestals was done by counting the number of pedestals from 100 cells. Graph represents mean ± SD. Non-statistical difference was found for the analysis of three independent experiments.

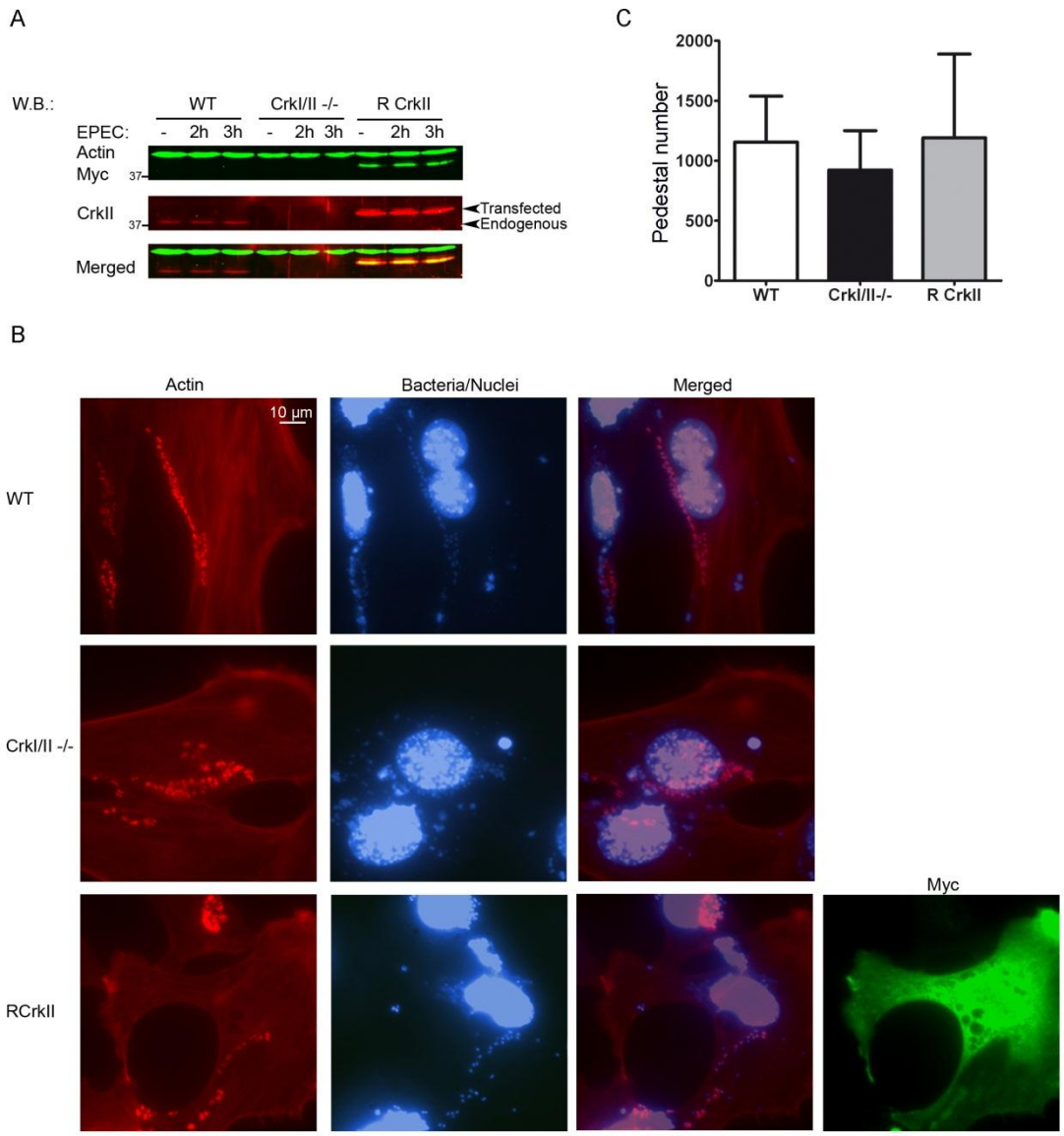

Figure 20. Pedestal formation is not affected in CrkI/II-deficient mouse embryonic fibroblasts. (A) Western-blot using the Odyssey scan system with anti-CrkII antibody in wild type and CrkI/II-deficient MEFS to show the endogenous levels of expression and the reconstitution with transfected myc-CrkII (R CrkII). Actin was used as a loading control. The merge of both images is shown. **(B)** Immunofluorescence images of MEFs infected with X preactivated EPEC for 3 hours. Red pictures show actin staining. DAPI was used to stain EPEC. The merged images shown were generated using Adobe Photoshop. Transfected cells were stained with anti-myc MoAb followed by Alexa-488 conjugated goat anti-mouse secondary Ab. Pictures are at 1000X magnification. Scale bar represents 10 µm. **(C)** Quantification of the number of pedestals of WT MEFs (white bar), CrkI/II-deficient MEFs (black bar) and Rescued CrkII cells (R CrkII, grey bar). Quantification was done by counting the number of pedestals from 100 cells. Graph represents mean ± SD. Non-statistical difference was found for the analysis of three independent experiments as shown.

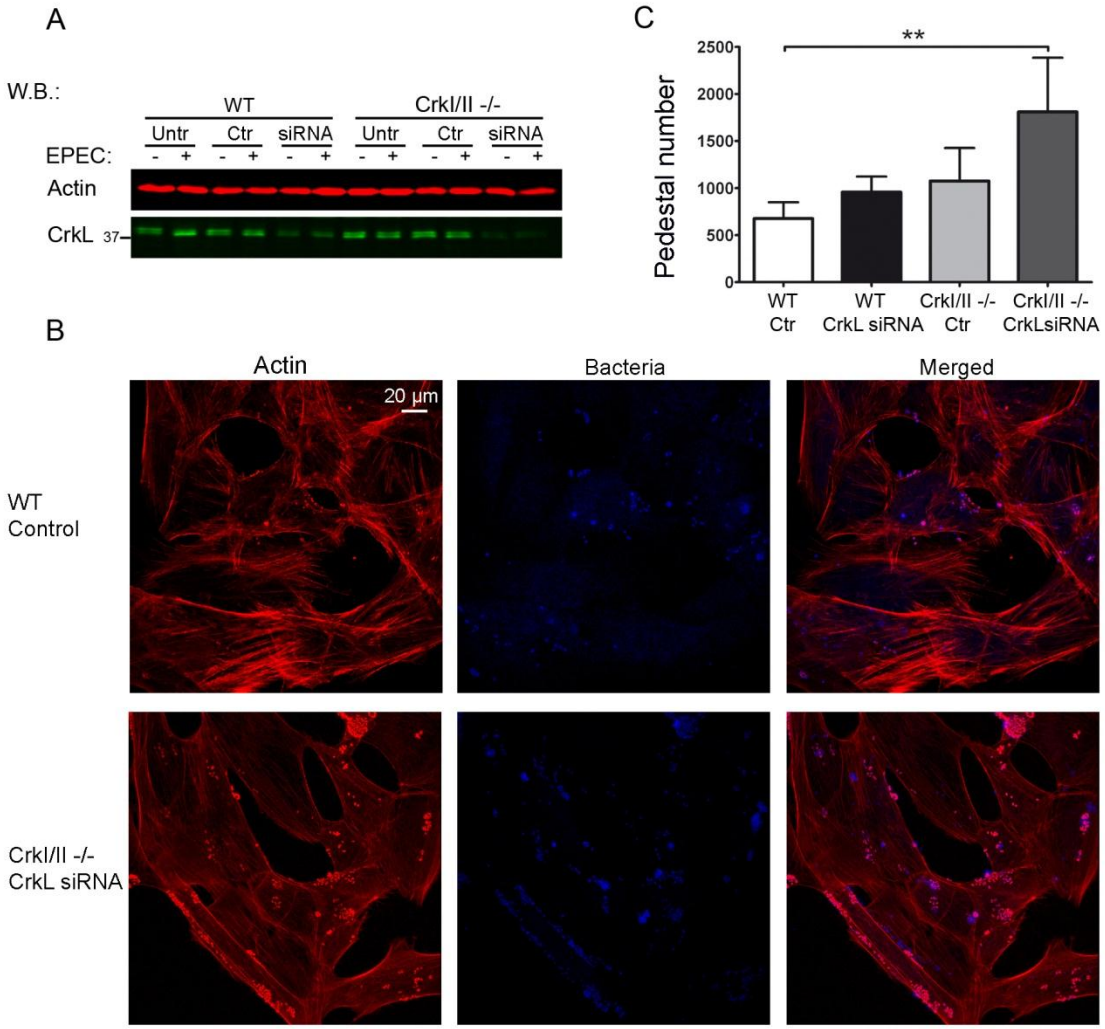

Figure 21. Pedestal formation is enhanced in CrkI/II-deficient mouse embryonic fibroblasts with CrkL expression inhibited by siRNA. (A) Western-blot with anti-CrkL antibody in WT and CrkI/II-deficient MEFS treated using the siRNA oligonucleotide against CrkL compared to control oligonucleotide treated cells (lower bands). As a loading control the blots were probed with anti-actin antibody (upper bands). **(B)** Immunofluorescence images of WT MEFs and CrkI/II-deficient cells with CrkL expression inhibited by siRNA and infected with X preactivated EPEC for 3 hours. Red pictures show actin staining with TRITC-Phalloidin. Anti-LPS MoAb followed by Alexa-405 conjugated goat anti-mouse secondary Ab was used to stain EPEC (in blue). The merge of both images was generated using Leica software. Confocal pictures are at 600X magnification. Scale bar represents 20 µm. **(C)** Quantification of pedestals of wild type (WT) and CrkI/II-deficient cells treated with a control oligonucleotide (white and grey bars respectively) and depleted of CrkL by siRNA (black and dark-grey bars respectively). Quantification was done by counting the number of pedestals from 100 cells. Graph represents mean ± SD. Statistical analysis was performed using the Student´s t-test from three independent experiments. *, $p<0.05$; **, $p<0.01$; ***, $p<0.001$.

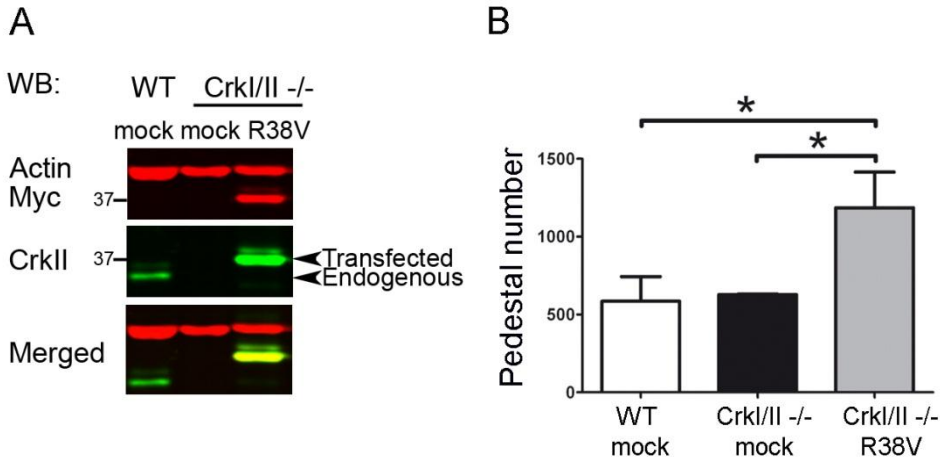

Figure 22. Increased pedestal formation in CrkI/II-deficient cells expressing a Crk dominant negative R38V mutant form. (A) The expression of transfectants was assessed by western blotting with anti-myc MoAb. The blot was also probed with anti-CrkII Ab to show the endogenous levels of expression of CrkII and the transfected Crk dominant negative mutant (arrows). Actin was used as a loading control. The merge of both images is shown. **(B)** Quantification of pedestals of mock treated wild type cells (white bar) and mock treated CrkI/II-deficient cells (black bar) or CrkI/II-deficient cells transfected with the dominant negative R38V mutant (grey bar) and infected with X preactivated EPEC for 3 hours. Quantification was done by counting the number of pedestals from 100 cells. Graph represents mean ± SD. Statistical analysis were performed using the Student´s t-test from three independent experiments is shown. *, p<0.05; **, p<0.01; ***, p<0.001.

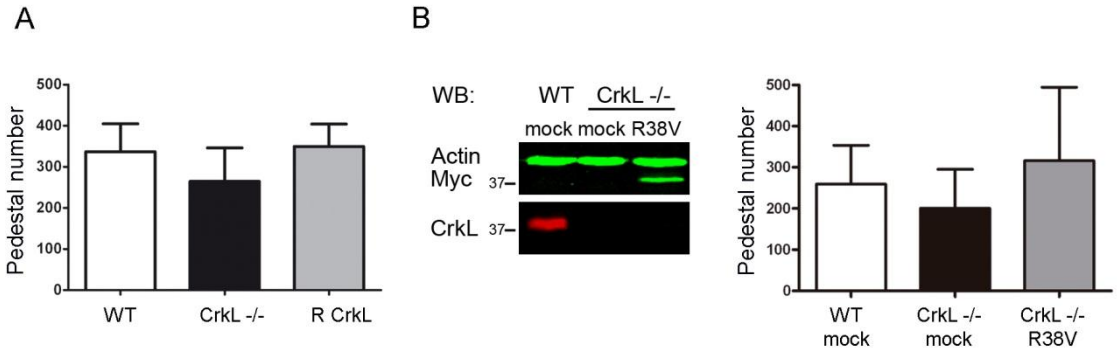

Figure 23. (A) Pedestal formation is not affected in CrkL-deficient mouse embryonic fibroblasts. Quantification of pedestals of WT MEFs (white bar), CrkL-deficient MEFs (black bar) and CrkL reconstituted cells (R CrkL, grey bar). Quantification was done by counting the number of pedestals from 100 cells. Graph represents mean ± SD. Non-statistical difference was found for the analysis of three independent experiments as shown. **(B) Increased pedestal formation in CrkL-deficient cells expressing a Crk dominant negative mutant form.** The expression of transfectants was assessed by western blotting with anti-myc MoAb. Actin was used as a loading control. The merge of both images is shown. Graph represents the quantification of number of pedestals of mock treated wild type cells (white bar) and mock treated CrkL-deficient cells (black bar) or CrkL-deficient cells transfected with the R38V dominant negative mutant (R38V, grey bar) and infected with X preactivated EPEC for 3 hours. Quantification was done by counting pedestal number of 20 transfected cells in five independent experiments. Graph represents mean ± SD. The experiments in part B were performed by Eugenia Meiler.

Part III. Role of the adaptor protein Nck in pedestal formation by EPEC

1. Levels of Tir are reduced in Nck-deficient MEFs infected by EPEC

It is well established that in the absence of Nck in cultured mammalian cells pedestals are not formed by EPEC (Campellone et al., 2002; Campellone and Leong, 2005; Campellone et al., 2004a; Gruenheid et al., 2001). The rationale for this requirement is that Nck recruits and is thought to activate N-WASP promoting Arp2/3 dependent-actin polymerisation. As shown previously in figure 17, Nck1/2-deficient MEFs (designated hereafter as Nck-deficient cells) present a reduced amount of Tir protein upon EPEC infection when compared to WT MEFs. To corroborate this initial observation we infected Nck-deficient cells that were retrovirally reconstituted with EGFP and myc-tagged Nck1 (Nck reconstituted cells, RNck). We used uninfected cells as a negative control.

Western blot analysis from total cell lysates with a MoAb against Tir after 1, 2 and 3 hours of EPEC infection (Fig. 24A) indicated that the levels of Tir are reduced by 88% (average of six experiments after normalising for actin) in Nck-deficient cells infected with X EPEC when compared to WT control cells. Moreover, Nck reconstituted cells present normal levels of Tir protein (Fig. 24A).

To confirm this result we next used the fractionation protocol (Fig. 17) to enrich in Tir-containing membranes (pellet) with respect to the cytoplasmic fraction that remains in the supernatant (Fig. 24B). As previously described (Fig. 17) the fully modified form is the predominant form of Tir in the membrane fraction. As shown in Figure 24B, WB analysis with anti-Tir MoAb corroborated that the membrane enriched fraction present a reduced amount of Tir.

We next wondered whether the reduction of Tir in Nck-deficient cells would also affect other TTSS-secreted EPEC effectors. Therefore, we reprobed the membranes for detection of EspF. In contrast to Tir levels, we found equal amounts of EspF protein in

all cell types analysed (Fig. 24A and B). This result demonstrated that Nck-deficient cells present normal levels of injected EspF effector protein.

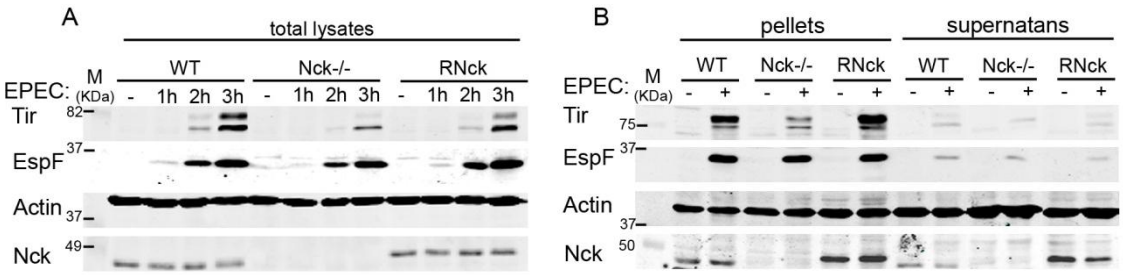

Figure 24. EPEC-infected Nck-deficient cells have lower levels of Tir, but not of EspF, when compared with WT cells. (A) WT, Nck-deficient cells (Nck-/-) and Nck reconstituted cells (RNck) were infected with X preactivated EPEC for 1, 2 or 3 hours or left uninfected as a negative control. Cell monolayers from single wells of 6-well-plate was collected by directly adding Laemmli sample buffer and processed. Lysates were blotted with anti-Tir MoAb and secondly with anti-EspF. **(B)** WT, Nck-/- and RNck were infected with X preactivated EPEC for 3 hours or left uninfected as a negative control. Cell monolayers were lysed in imidazole buffer and fractionated. The membrane fraction was resuspended in Laemmli sample buffer. One third of the pellet (membrane fraction) and one fiftieth of the supernatant (cytoplasmic fraction) were blotted with anti-Tir MoAb and anti-EspF Ab. In both (A) and (B) blots were visualised with the Odyssey Scan system. Actin was used as a loading control and anti-Nck blotting was performed to confirm the genotype of the MEFs used.

2. Depletion of Nck by siRNA in HeLa cells results in a decrease of Tir levels and pedestal formation

To corroborate our phenotype in a different cell line we next analysed the levels of Tir in the absence of Nck in human epithelial HeLa cells infected by EPEC. For that purpose we used commercially available oligonucleotides against human Nck1 and Nck2 to inhibit their expression in HeLa cells and a scrambled sequence nucleotide as negative control (Fig. 25).

Western blot analysis of the Triton X-100-soluble fraction, that contains the host cytoplasmic and membrane fraction (see Materials and Methods), with a MoAb against Nck revealed that 16 hours after transfection with the siRNAs the levels of Nck were reduced by 85% (average of three experiments after normalising for actin) (Fig. 25A). At that point the cells were infected with preactivated EPEC to allow the formation of pedestals. Treatment of cells with the siRNAs against Nck1/2 resulted in a statistically

significant decrease of Tir levels that is more obvious in the fully-modified Tir band (Fig. 25B). Moreover, we quantified the number of pedestals and there is a significant reduced number of pedestals between siRNA-treated cells and control cells (Fig. 25D). These results seem to indicate that a reduction of the levels of the expression of human Nck in HeLa cells affects the levels of Tir and the number of pedestals formed.

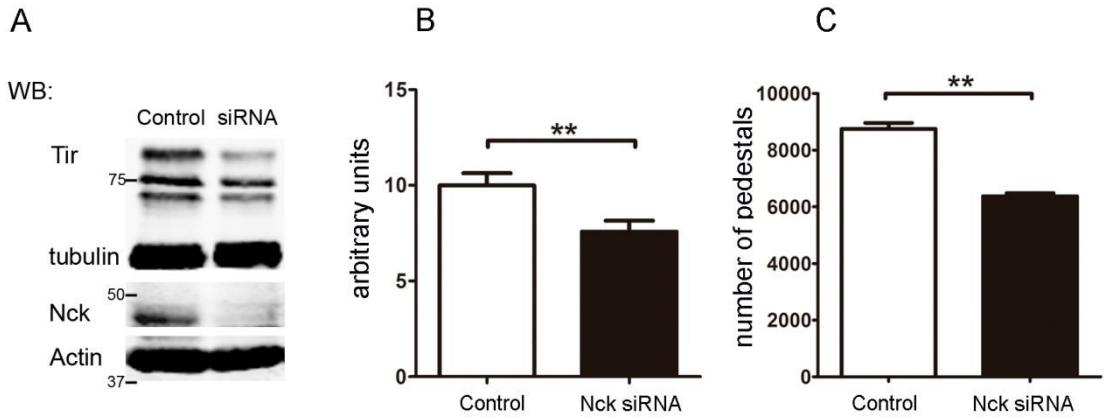

Figure 25. Tir levels are diminished in HeLa cells when the expression of Nck1/2 is inhibited by siRNA treatment. (A) HeLa cells were treated with siRNAs for Nck1/2 and infected with 5X preactivated EPEC strains for 3 hours. Monolayers were lysed in 1% Triton X-100 lysis buffer. The soluble supernatants were analysed by WB with anti-Tir polyclonal Ab and visualised with the Odyssey Scan system. The levels of Nck were analysed by blotting with anti-Nck MoAb. Actin and tubulin were used as a loading control. **(B)** The quantification of the intensity of the three WB bands was performed with the Odyssey Scan band tool. Graph represents mean ± SD. Statistical analysis using the Student´s *t*-test from three independent experiments. **(C)** Quantification was done by counting the number of pedestals from 100 cells. Graph represents mean ± SD. Statistical analysis using the Student´s *t*-test from two independent experiments. *, $p<0.05$; **, $p<0.01$; ***, $p<0.001$.

3. Levels of Tir are not reduced in N-WASP-deficient MEFs infected by EPEC

In order to analysed the levels of Tir in a cell type also resistant to EPEC pedestal formation we infected the previously used N-WASP-deficient MEFs (NW-/-) (see Fig. 17). EPEC infected cells were fractionated into Triton X-100-soluble fraction, that contains the host cytoplasmic and membrane fraction, and therefore injected EPEC effectors, and Triton X-100-insoluble fraction that contains the host cytoskeleton, the nuclei and adherent EPEC (see Materials and Methods and (Kenny et al., 1997)).

As noticeable in the soluble fraction of figure 26A the levels of Tir are not diminished in N-WASP-deficient cells when compared to WT cells. The translocated effector EspB, which forms the translocation pore, and EspF were analysed as controls. Actin was used as a loading control. Blotting with anti-N-WASP antibody was performed to confirm the genotype of the MEFs. This result implicates that the low levels of Tir found in Nck-deficient cells cannot be attributed exclusively to the absent of pedestals since both cell types lack them.

We next analysed the adhesion of EPEC to this cell line. In addition to indirect detection by fluorescence microscopy, another technique that has been described to semiquantitative attached bacteria to the cell surface is the Western blot analysis of the insoluble fraction with a MoAb against DnaK-an abundant bacterial heat-shock protein. Moreover, the levels of Tir and that of other effectors detected in the insoluble fraction are also an indicator of the bacterial attachment (Wolff et al., 1998). We observed similar levels of DnaK, Tir and EspF in N-WASP-deficient cells and N-WASP reconstituted cells, and these levels are even higher than in WT cells (Fig. 26B; fourth panel). However, contrary to the expected result EspB was not found in the insoluble fraction. These results seem to indicate that the bacterial attachment to N-WASP-deficient cells is not compromised.

4. Levels of Tir in Nck-deficient cells infected at higher MOIs and bacterial attachment to these cells

As mentioned in Material and Methods, Multiplicity of infection (MOI) is the number of bacteria added per cell at the beginning of the infection. It has been demonstrated that increasing the MOI accelerates the attachment rate as well as the translocation efficiency of EPEC (Mills et al., 2008). Thus, we examined whether the infection at higher MOIs results in an increase in the levels of Tir in Nck-deficient cells. In addition, we wondered whether the attachment of EPEC to Nck-deficient cells is compromised and whether it is improved by increasing the MOI.

Hence, MEFs were infected at MOIs ranging from 25 (referred as 10X) to 250 (referred as 100X) bacteria per cell and Triton X-100-soluble fraction was subjected to WB analysis along with the corresponding Triton X-100-insoluble fractions.

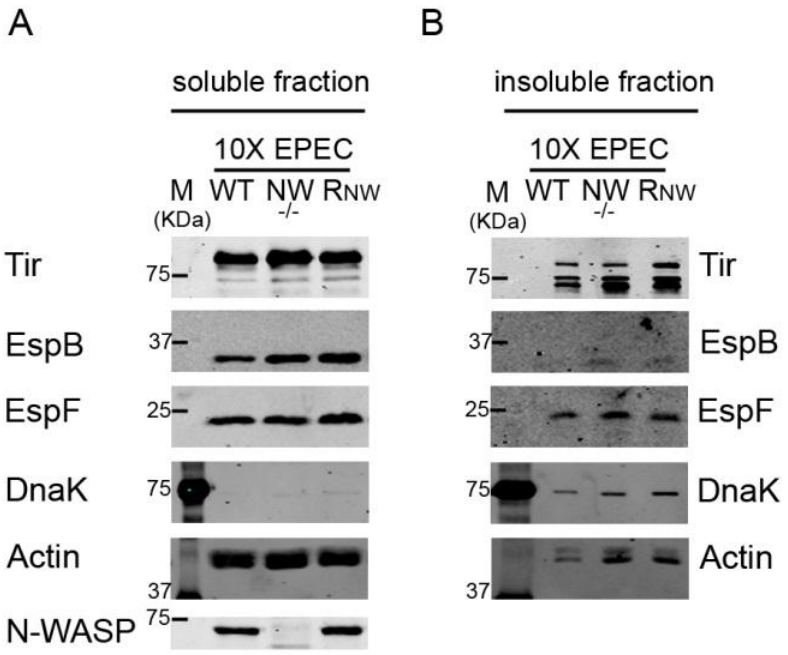

Figure 26. EPEC-infected N-WASP-deficient cells have equal levels of Tir when compared to WT cells. WT, N-WASP-deficient cells (NW-/-) and N-WASP reconstituted cells (RNW) were infected with 10X of preactivated EPEC for 3 hours. Monolayers were lysed in 1% Triton X-100 lysis buffer. The soluble supernatant containing the cytoplasmic and membrane fractions **(A)** and the insoluble pellet containing the attached bacteria **(B)** were subjected to 12 % SDS-PAGE, blotted with anti-Tir, anti-EspB and anti-EspF polyclonal Abs and with anti-Dnak MoAb and visualised with the Odyssey Scan system. Anti-actin was used as a loading control and anti-N-WASP were performed to confirm the genotype of the MEFs.

Western blot analysis of the soluble fraction with a polyclonal Ab against Tir shows that a remarkable increase in the number of bacteria per cell, results only in a slight increase in the levels of Tir in Nck-deficient cells, and the levels remain significantly lower in Nck-deficient cells than in WT cells in all MOIs tested (Fig. 27A; upper panel). Actin was used as a loading control and blotting with anti-Nck antibody was performed to confirm the genotype of the MEFs used.

As shown in figure 27B, we found that the adhesion of EPEC to Nck-deficient cells is decreased with respect to WT cells or Nck reconstituted cells (see the red asterisk in

figure 27). As noticeable in figure 27B, the levels of Tir and other EPEC effectors, EspB and EspF, in the insoluble fraction are also reduced with respect to WT cells, which could be the consequence of an adhesion defect to Nck-deficient cells.

To determine whether the defect in EPEC adhesion to Nck-deficient cells is affecting the injection of EspB, we analyse in the soluble fraction by WB the levels of this effector. As shown in the second panel of figure 27A, the levels of EspB were not diminished in Nck-deficient cells, as occurred with the levels of EspF that were analysed in parallel in the same blot.

On the other side, it can be noticed that an increase in the MOI results in a higher number of cell-associated bacteria, but the levels of Tir in these cells are always lower when compared to WT cells (Fig. 27B). In summary, we can conclude that Nck-deficient cells have not the same levels of Tir than WT cells or Nck1-expressing cells and that they have an EPEC adhesion defect.

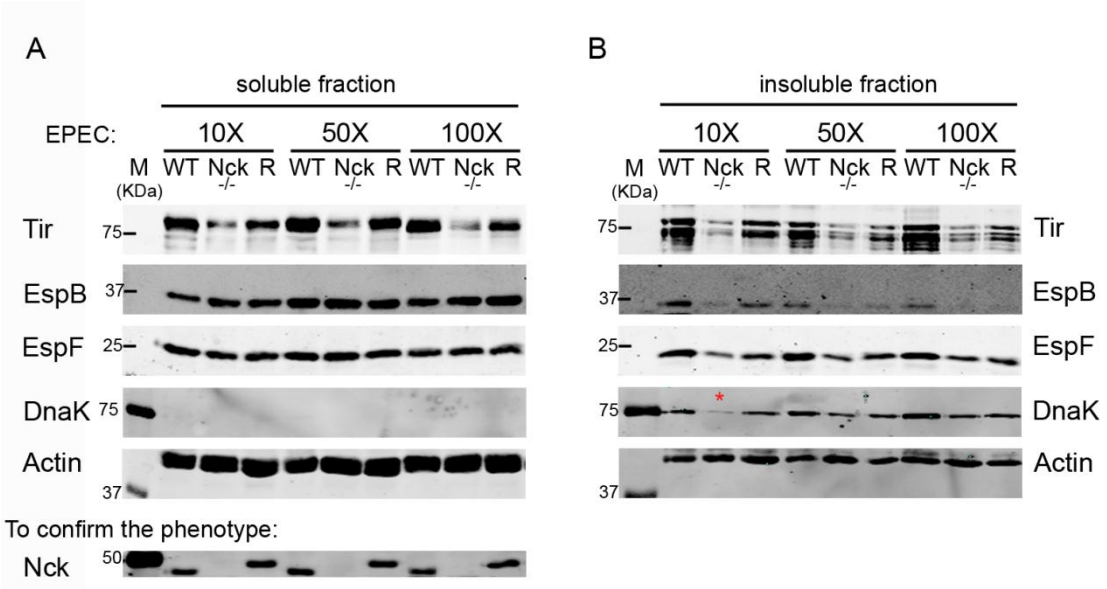

Figure 27. EPEC-infected Nck-deficient cells have slight higher levels of Tir when the MOI is increased. Adhesion of EPEC to these cells is affected. WT, Nck-deficient cells (Nck-/-) and Nck reconstituted cells (R) were infected with 10X, 50X or 100X preactivated EPEC for 3 hours. Monolayers were lysed in 1% Triton X-100 lysis buffer. The soluble supernatant containing the cytoplasmic and membrane fractions **(A)** and the insoluble pellet containing the attached bacteria **(B)** were subjected to 12 % SDS-PAGE, blotted with indicated antibodies and visualised with the Odyssey Scan system. Actin was used as a loading control and blotting with anti-Nck was performed to confirm the genotype of the MEFs used.

5. Immunofluorescence staining corroborates the low levels of pedestal formation and bacterial adhesion to Nck-deficient cells

In order to confirm the bacterial adhesion defect found in Nck-deficient cells (Fig. 27B), semiquantitative assessment was made by counting the number of attached bacteria in 100 cells in representative microscope fields. For that purpose, immunofluorescence staining of cell-associated bacteria using DAPI in WT, Nck-deficient and Nck reconstituted cells after EPEC infection was performed. The actin cytoskeleton was visualised with fluorescent phalloidin. As shown in figure 28B the number of bacteria attached to Nck-deficient cells is significantly lower compared to the bacteria attached to WT or Nck reconstituted cells (46,9% in Nck-/- vs 90,8% in RNck, considering that the attached bacteria to WT cells is 100%). Hence, immunofluorescence staining corroborates the western blot results (Fig. 27B) where we detected lower levels of bacterial attachment to Nck-deficient cells.

In addition, quantification of pedestal formation in Nck-deficient cells was also assessed. It has been described that Nck-deficient cells are still capable of generating actin pedestals, although at fourfold less efficiency compared to Nck-expressing cells (Campellone et al., 2004b). Our results show a 20-fold decrease in the efficiency of pedestal formation in Nck-deficient cells with respect to WT cells (6% in Nck-/- vs 73% in RNck, considering that the pedestals formed in WT cells is 100%) (Fig. 28B; right graph). The disagreement cannot be attributed to differences in cell types because the cells used in both cases were obtained from the same Nck mutant mouse embryos (Bladt et al., 2003).

Collectively, these results seem to indicate that the decrease in EPEC attachment to Nck-deficient MEFs is related to the low levels of Tir protein found in these cells.
Collectively, these results seem to indicate that there is a decrease in EPEC attachment to Nck-deficient MEFs and that these cells present low levels of Tir protein and diminished pedestal formation.

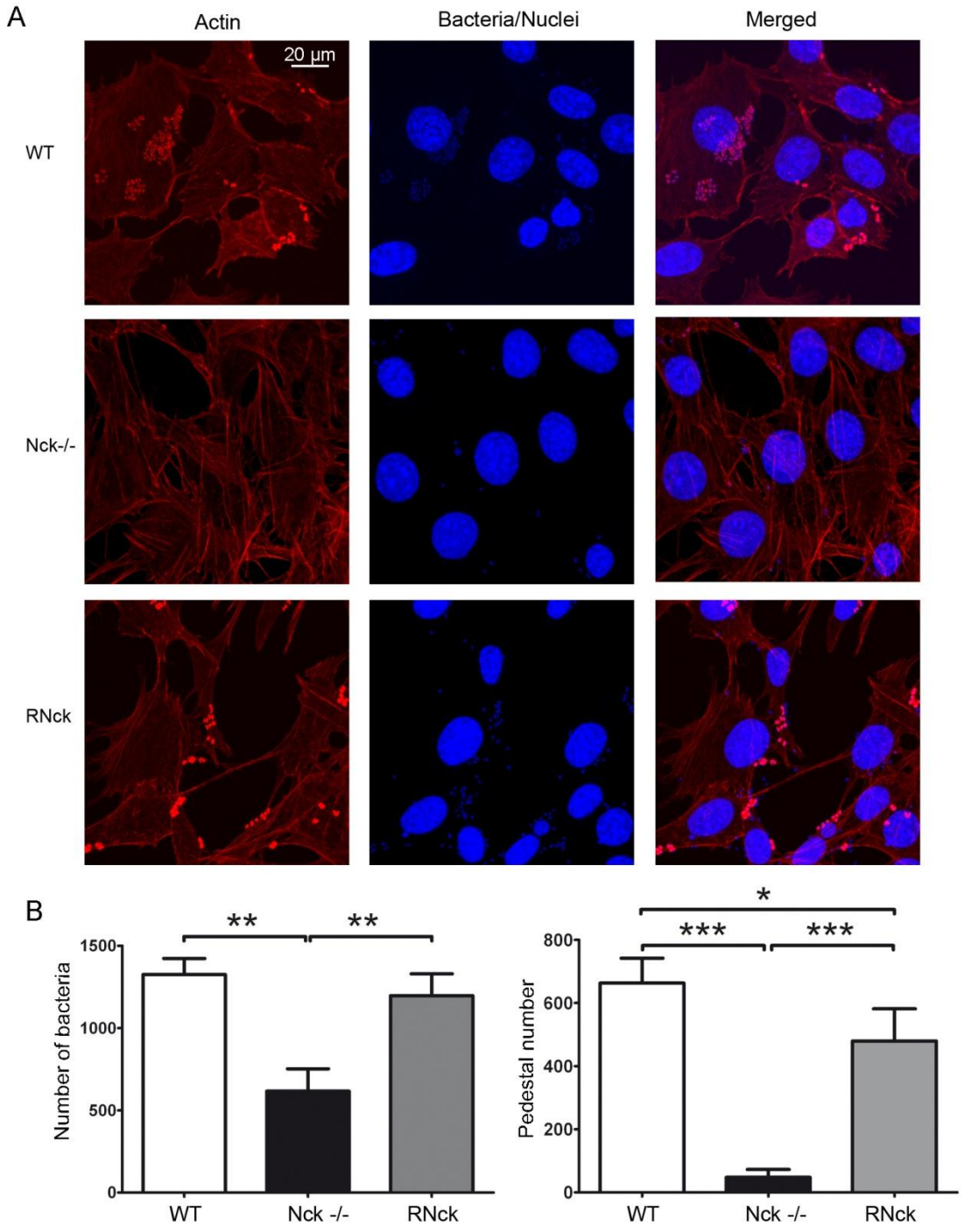

Figure 28. Pedestal formation and bacterial adhesion are compromised in EPEC-infected Nck-deficient cells. (A) Immunofluorescence images of WT, Nck-deficient cells and Nck reconstituted cells (RNck) infected with X preactivated EPEC for 3 hours. Red pictures show actin staining with TRITC-Phalloidin. DAPI was used to stain EPEC and host cell nuclei. The merge of both images was generated using Leica software and is shown in the last column. Pictures were taken in a confocal microscope at 600X magnification. Scale bar represents 20 µm. **(B)** The number of attached bacteria and pedestals of a total of 100 cells was quantified from immunofluorescence images. Graph represents mean ± SD. Statistical analysis were performed using the Student´s *t*-test from at least three independent experiments is shown. *, $p<0.05$; **, $p<0.01$; ***, $p<0.001$.

6. EPEC adhesion to murine cells has a higher dependence on intimin-Tir interaction than in the case of HeLa cells.

As mentioned in the introduction, the final step of EPEC adhesion to cells involves an intimate adherence that is mediated by the interaction between intimin and the translocated effector Tir (Kenny et al., 1997).

With the aim to study the role of the interaction between intimin and Tir in EPEC adhesion to mouse embryonic fibroblast (MEFs), we performed infection experiments of MEFs with an EPEC strain lacking intimin (Δ*eae* mutant) and with a strain lacking Tir (Δ*tir* mutant). As a control we used the strain lacking Tir complemented with Tir expressed on a low-copy-number plasmid (Δ*tir*+p*tir*). In order to compare EPEC adhesion to murine cells with the adhesion to human cells we also infected HeLa cells in parallel. We analysed by WB the Triton X-100-soluble supernatant containing the cytoplasmic and membrane fractions along with the Triton X-100-insoluble pellet containing the host cell nuclear and cytoskeletal proteins and adherent EPEC.

Western blot analysis of the soluble fraction (Fig. 29A) of Δ*eae* mutant-infected cells shows that the levels of Tir in murine cells are really low with respect to human cells (Fig. 29A, upper panel), in contrast to the levels of EspB and EspF effectors that were clearly comparable. In the upper panel of figure 29A, although the intensity of the bands is low, it is also noticeable that the levels of Tir in Nck-deficient cells infected with Δ*eae* mutant are lower than the levels of Tir in WT MEFs. Actin was used as a loading control and blotting with anti-Nck antibody was performed to confirm the genotype of the MEFs used.

To examine the amount of attached bacteria to MEFs with respect to HeLa cells we analysed by WB the Triton X-100-insoluble fraction with Dnak MoAb. As shown in figure 29B, we found that the adhesion of Δ*eae* mutant to murine fibroblasts (MEFs) is clearly reduced with respect to Hela cells. As detectable in figure 29B, the levels of the effectors Tir, EspB and EspF also indicate the lower adhesion of Δ*eae* mutant to MEFs with respect to HeLa cells. We then infected MEFs and HeLa cells with a strain lacking

Tir (Δ*tir* mutant) and obtained similar results. Western blot analysis with the antibody against Tir corroborated the absence of Tir in this strain (Fig. 29A and B).

When Δ*tir* mutant was complemented with p*tir*, the levels of Tir in murine WT and Nck reconstituted cells are almost restored at the level observed in HeLa cells (Fig. 29A). It is very remarkable that the level of Tir in Nck-deficient cells is higher than previously detected in these cells.

Moreover, the adhesion of Δ*tir*+p*tir* strain to MEFs is increased with respect to Δ*eae* or Δ*tir* mutants, as shown by western blot analysis of the insoluble fraction when probed with Dnak MoAb (Fig. 29B). As occurred with WT EPEC strain (Fig. 29), the adhesion of Δ*tir*+p*tir* strain to Nck-deficient cells is lower when compared to WT MEFs or Nck reconstituted cells (see the red asterisk, Fig. 29B).

Collectively, these results show that the adhesion of EPEC to murine cells in the absence of intimin or Tir is clearly diminished with respect to HeLa cells. Hence, the adhesion of EPEC to murine cells has a higher dependence on intimin-Tir interaction than in the case of HeLa cells.

7. The small fraction of Tir protein present in Nck-deficient MEFs is tyrosine-phosphorylated and stable up to 6 hours postinfection

Next we wanted to analyse certain characteristics of the small but detectable fraction of Tir present in Nck-deficient cells. Clustering of Tir apparently unleash signal transduction events including its phosphorylation at tyrosine residue 474 (Y474) within the C-terminal cytoplasmic domain (Kenny, 1999) by several mammalian tyrosine kinases including c-Fyn, a Src family kinase (Phillips et al., 2004), Abl, Arg and Etk (Bommarius et al., 2007; Swimm et al., 2004a). This phosphotyrosine is the binding site for Nck (Gruenheid et al., 2001).

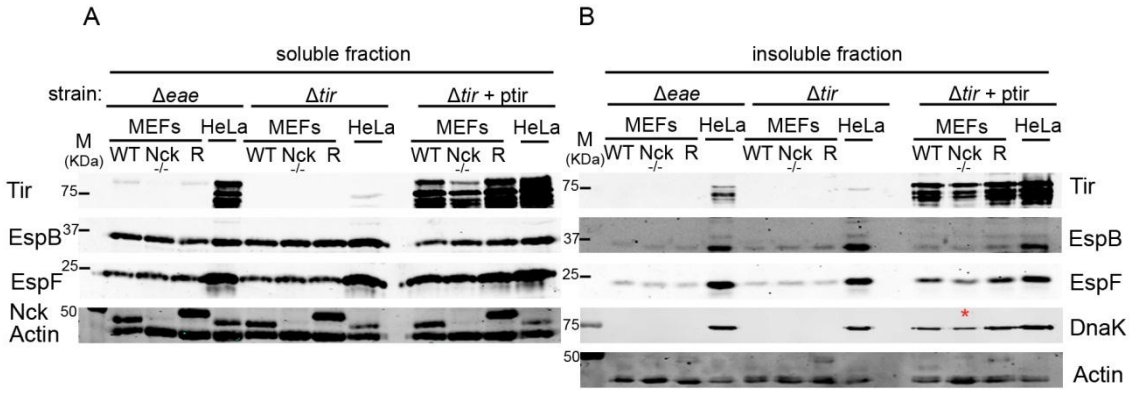

Figure 29. Higher dependence on intimin-Tir interaction of EPEC to adhere to mouse embryonic fibroblasts (MEFs). WT, Nck-deficient cells (Nck-/-) and Nck reconstituted cells (R) were infected with 20X preactivated EPEC strains for 3 hours. EPEC strains used were Δ*eae* mutant (strain lacking intimin), Δ*tir* mutant (strain lacking Tir) and Δ*tir*+p*tir* (Δ*tir* mutant complemented with Tir). Cell monolayers were lysed in 1% Triton X-100 lysis buffer. The soluble supernatant containing the cytoplasmic and membrane fractions **(A)** and the insoluble pellet containing the attached bacteria **(B)** were subjected to 12 % SDS-PAGE, blotted with indicated antibodies and visualised with the Odyssey Scan system. Actin was used as a loading control and blotting with anti-NWASP was performed to confirm the genotype of the MEFs.

In order to examine the phosphorylation status of injected Tir in Nck-deficient cells, we performed immunoprecipitation experiments using an anti-Tir MoAb, followed by WB with a generic phospho-tyrosine MoAb. As shown in figure 30A, the small fraction of Tir present in Nck-deficient cells is tyrosine phosphorylated as visualised in the merge of both images.

Subsequently, we examined the stability of Tir present in MEFs treating the cells with bactericidal levels of gentamicin, which is a broad spectrum antibiotic that inhibits bacterial protein synthesis by binding to the 30S subunit of the ribosome. It is established that gentamicin stops the infection process and the injection of effectors by EPEC by killing extra-cellular bacteria (Ruchaud-Sparagano et al., 2007). After three hours of infection we treated the cells with gentamicin and incubated the cells during six hours post-infection. We detected the fully-modified Tir band (Kenny and Warawa, 2001) even six hours after infection in WT and Nck-deficient cells (Fig. 30B). It is also noticeable in figure 30B that the band with faster electrophoretic motility, that represents the partially modified Tir form (Kenny and Warawa, 2001), seem to be converted to the fully modified form over time. As it has been mentioned in the

introduction, the increase in apparent molecular mass of Tir molecule observed in cells is not due to tyrosine phosphorylation (Kenny, 1999). Although Tir levels in Nck-deficient cells are decreased with respect to WT cells in all conditions, we could conclude that the fraction of Tir is stable and inserted into the membrane even six hours after infection in both cell types (Fig. 30B).

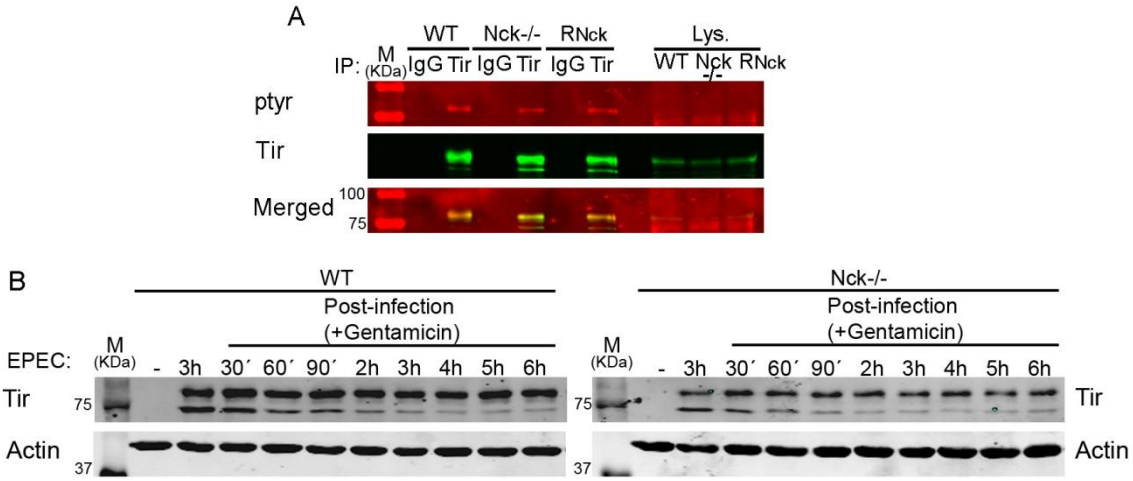

Figure 30. Phosphorylation and stability of the small fraction of Tir protein present in Nck-deficient MEFs. (A) Tir is tyrosine phosphorylated in Nck-deficient cells. WT, Nck-deficient cells (Nck-/-) and Nck reconstituted cells (RNck) were infected with 10X preactivated EPEC for 3 hours. Cell monolayers were lysed in Ripa buffer and the lysates were used to perform IPs using a Tir MoAb that were examined by WB first with a generic phospho-tyrosine MoAb (in red) and second with Tir Ab (in green) and visualised with the Odyssey system. The merge of both images is shown. The isotype control IP (IgG) and the cell lysates loaded in the same gel are shown. **(B) Fully modified Tir is stable even 6 hours after infection in Nck-deficient cells.** WT and Nck-/- cells were infected with 5X preactivated EPEC for 3 hours or left uninfected as a negative control. After 3 hours of infection, the cells were treated with gentamicin (100 µg/ml) and incubated for 6 hours post-infection. Cell monolayers from a single well of a 6-well-plate were collected at indicated times by directly adding Laemmli sample buffer. Lysates were blotted with anti-Tir MoAb and visualised with the Odyssey system. Actin was used as a loading control.

8. Levels of Tir are also diminished in Nck-deficient cells infected with Tir phosphorylation-deficient mutants of EPEC

Phosphorylation of Tir in tyrosine residue 474 (Y474) generates a docking site for the host cell adaptor protein Nck. However, Tir also nucleates actin inefficiently through a second phosphorylated-tyrosine (Y454). In addition, it has been identified two serine residues in Tir (S434 and S463) that are phosphorylated by PKA. Serine phosphorylation

has been shown to be responsible for Tir molecular mass shift and it has been proposed that these modifications may induce changes in the three-dimensional structure of Tir that may promote its insertion into the host plasma membrane (Kenny, 1999) (Warawa and Kenny, 2001). Taking into consideration the former data, we wanted to analyse the levels of Tir protein in Nck-deficient cells infected by Tir phosphorylation-deficient mutants of EPEC.

For that purpose we infected MEFs with strains lacking *tir* and complemented with a low-copy number plasmid expressing non-phosphorylatable forms of Tir. The strain referred as dY (Δ*tir*+p*tir*Y474F/Y454F) expresses Tir with substitutions in tyrosine phosphorylation sites 474 and 454, the strain referred as dS (Δ*tir*+ p*tir*S434/463A) expresses Tir with substitutions in serine phosphorylation sites 434 and 463, and the strain referred as quad (Δ*tir*+p*tir*Y474F/Y454F S434/463A) expresses Tir with substitutions in the two tyrosine and the two serine sites. Infection with Δ*tir*+p*tir* strain (Δ*tir* mutant complemented with a low-copy number plasmid expressing Tir) was used as a control.

Western blot analysis of the Triton X-100-soluble fraction revealed lower levels of Tir in Nck-deficient cells infected with all EPEC strains used with respect to WT cells (Fig. 31A). The analysis of DnaK protein in the Triton X-100-insoluble fraction also indicates that the adhesion of the different strains to Nck-deficient cells is diminished when compared to WT cells (Fig. 31B).

These results show that Nck-deficient cells infected with Tir phosphorylation-deficient mutants also have low levels of Tir and that the adhesion of these mutants to Nck-deficient cells is also diminished, as occurred in infection experiments using WT EPEC. Thus, the mutation in the tyrosine and serine relevant residues of the Tir molecule does not impact on the low levels of Tir in Nck-deficient cells.

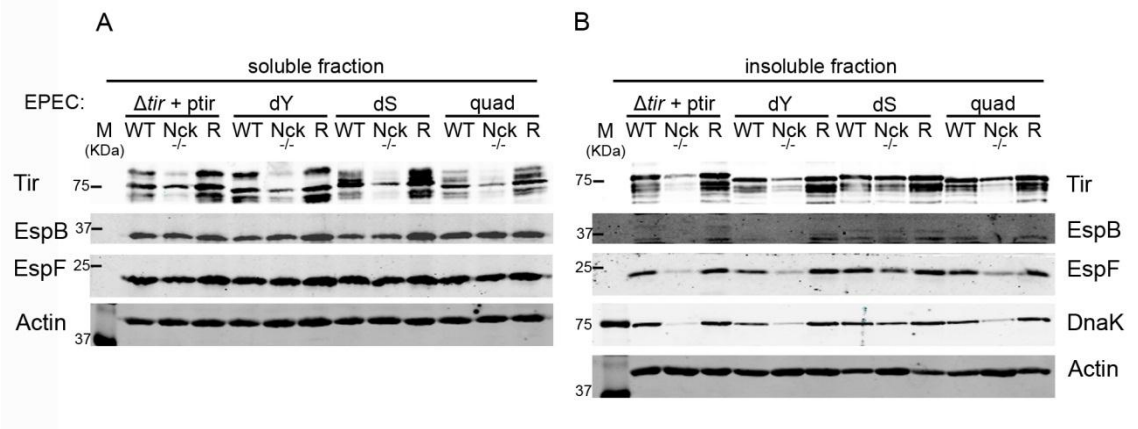

Figure 31. Nck-deficient cells infected with Tir phosphorylation-deficient mutants also have lower levels of Tir when compared with WT cells . WT, Nck-deficient cells (Nck-/-) and Nck reconstituted cells (R) were infected with 20X preactivated EPEC strains for 3 hours. EPEC strains used were Δ*tir*+p*tir*Y474F/Y454F strain (referred as dY), Δ*tir*+p*tir*S434/463A strain (referred as dS) and Δ*tir*+p*tir*Y474F/Y454F S434/463A strain (referred as quad). Infection with Δ*tir* mutant complemented with Tir was used as a control. Monolayers were lysed in 1% Triton X-100 lysis buffer. The soluble supernatant containing the cytoplasmic and membrane fractions **(A)** and the insoluble pellet containing the attached bacteria **(B)** were subjected to 12 % SDS-PAGE, blotted with indicated antibodies and visualised with the Odyssey Scan system. Actin was used as a loading control.

9. Tir does not undergo full modification in Nck-deficient MEFs when bacterial protein synthesis is inhibited

It has been described that the induction of pedestal formation and tyrosine phosphorylation of Tir by preactivated EPEC is dependent on *de novo* bacterial protein synthesis during the few first minutes of the encounter between the bacteria and the host cell (Rosenshine, 1996). Accordingly, 15 to 20 minutes of infection at a high MOI is sufficient for EPEC to trigger the process of pedestal formation and tyrosine phosphorylation of injected Tir which continued during the treatment with an antibiotic that inhibits protein synthesis, chloramphenicol.

The phosphorylation of Tir on non-tyrosine residues is linked to shifts in apparent molecular mass converting the unmodified Tir population to the modified Tir form. Moreover, this modified form undergoes modifications leading to the fully-modified form, detected as the band that has the slowest electrophoretic motility (represented with the upper arrow in figure 37) (Kenny and Warawa, 2001). These shifts in Tir are

thought to reflect phosphorylation-induced conformational changes facilitating the insertion into the plasma membrane (Kenny, 1999).

Taken the previous findings into account, we ought to analyse the distinct forms of Tir at early time points following infection at a high MOI and after inhibiting protein synthesis. For that purpose, WT and Nck-deficient cells were infected for 15 minutes at a MOI of 250 with preactivated EPEC and bacterial protein synthesis was then inhibited by adding chloramphenicol. The cells were incubated for 1, 2 and 3 hours, and then proteins were extracted in 1% Triton X-100-lysis buffer and used for WB with a polyclonal antibody against Tir. WB analysis of the Triton X-100-soluble fraction with anti-Tir Ab after 3 hours in the presence of chloramphenicol, revealed the shift from the band which represent the partially modified Tir form to the slower electrophoretic motility band of Tir, which represents fully-modified Tir form in WT cells (Fig. 32, left panel).

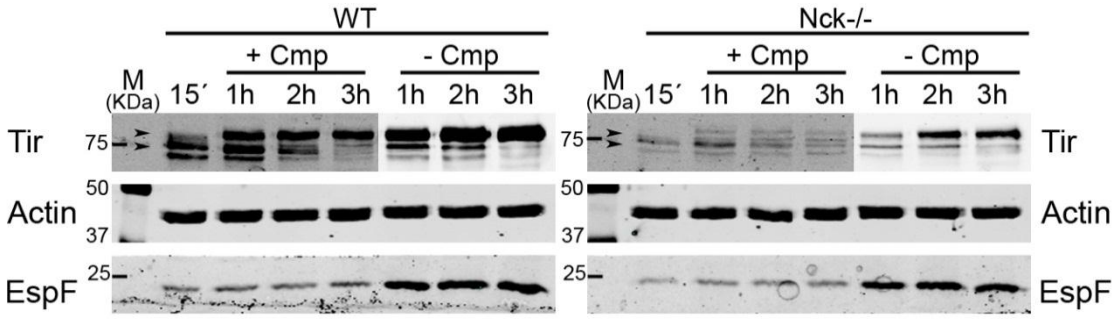

Figure 32. The inhibiton of bacterial protein synthesis results only in partial modification of Tir protein in MEFs lacking Nck. WT and Nck-deficient cells were infected with 100X (equivalent to a MOI of 250) of preactivated EPEC for 15 minutes. Cells were then treated with chloramphenicol (+Cmp, 100 µg/ml) or vehicle-treated as a control (-Cmp) and incubated for 1, 2 and 3 h. Monolayers were lysed in 1% Triton X-100 lysis buffer. The soluble supernatant containing the cytoplasmic and membrane fractions were used for WB with anti-Tir Ab and anti-EspF and visualised with the Odyssey Scan system. Actin was used as a loading control. The image of Tir Ab in the part of the gel that corresponds to the untreated infected-cells was adjusted at lower intensity for better visualisation of the different bands of Tir. Arrows indicate the partially modified and the fully-modified Tir forms.

On the contrary, we could not detect the fully-modified Tir form in Nck-deficient cells at any time (Fig. 32, right panel). Moreover, after 180 minutes of treatment with chloramphenicol we were not able to detect the band of partially modified Tir form in Nck-deficient cells. In summary, these results suggest that *de novo* protein synthesis in

EPEC is necessary for the conversion of the partially modified to fully modified Tir form in the absence of Nck. In addition, the results seemed to indicate that the non fully-modified Tir can be degraded in the absence of Nck.

10. Map, another CesT-dependent EPEC effector, is also diminished in infected-Nck-deficient cells

The efficiency of bacterial attachment to the host cell and the interaction of the effectors with chaperones are important parameters that regulate translocation efficiencies (Mills et al., 2008). Because of the tight regulation of the process of secretion and translocation, some proteins are stored in the bacterial cytoplasm before they are secreted. In some cases, these proteins require the presence of a dedicated family of TTS chaperones. Certain TTS chaperones are thought to bind a single effector (class IA), whereas others have been demonstrated to bind more than one effector (class IB) (Parsot et al., 2003). The class IB chaperone CesT binds and enhances the translocation of Tir and Map (Creasey et al., 2003), and probably also influences the translocation of EspH, EspZ, and some non-LEE efectors (Thomas et al., 2005). With the aim of analysing the levels of other CesT-dependent effector, we infected Nck-deficient cells with a modified EPEC strain that expresses a haemagglutinin (HA)-tagged Map effector.

Western blot analysis of Triton X-100-soluble fraction with a monoclonal antibody against HA shows a reduction in the levels of Map in Nck-deficient cells when compared with WT cells (Fig. 33). This result indicates that in addition to Tir, another EPEC effector is diminished in Nck-deficient cells. A possible interpretation considering this result is an Nck-dependent translocation defect of CesT-dependent effectors, such as Tir and Map, or alternatively, a specific degradation process dependent on the CesT chaperone. In any case these defects do not impact on EspF or EspB (Fig. 33), which use a different chaperone for their delivery process.

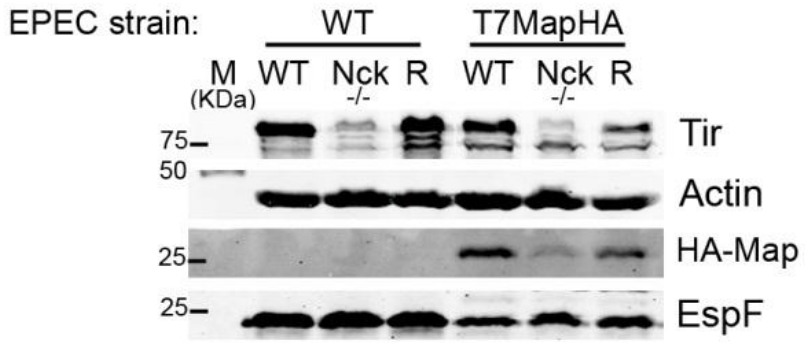

Figure 33. The levels of Map effector protein in infected-Nck-deficient cells are lower than in WT cells. WT, Nck-deficient cells and Nck reconstituted MEFs (R) were infected with 20X of preactivated WT EPEC or EPEC strain that expresses tagged-Map (T7MapHA) for 3 hours. Monolayers were lysed in 1% Triton X-100 lysis buffer. The soluble supernatant containing the cytoplasmic and membrane fractions were analyse for WB with anti-Tir Ab, anti-HA and with anti-EspF and visualised with the Odyssey Scan system. Actin was used as a loading control.

11. Analysis of the possible degradation of bacterial Tir

11.1. Ectopic expression of Tir is not reduced in Nck-deficient MEFs

A possible explanation for the reduction of Tir levels in Nck-deficient cells could be that the rate of Tir degradation is increased during infection in the host cell. Hence, to determine whether the expression of ectopically expressed EPEC Tir was compromised, we transfected Nck-deficient cells with a mammalian expression plasmid encoding His-tagged full length Tir. We found that transfected Tir is not reduced in Nck-deficient cells when compared to WT cells (Fig. 34A). Parallel transfections of GFP-tagged cortactin served as a control for the transfection efficiency (Fig. 34A). This result seems to indicate that transfected Tir is not being degraded within Nck-deficient cells.

However, the EPEC-infection of transfected WT MEFs showed that both bands of transfected Tir display smaller apparent molecular masses than the EPEC-delivered Tir (Fig. 34B). This result demonstrates that ectopically expressed Tir only undergoes partial modification within host cell as it has been published (Kenny and Warawa, 2001). Moreover, the studies of Kenny and Warawa indicate that transfected Tir does not get inserted into the membrane for intimin interaction and predict that EPEC encodes additional factors that have to be coexpressed or codelivered with Tir to enable its full

modification (Kenny and Warawa, 2001). The former data represent a limitation for the use of the ectopic expression of Tir in our study.

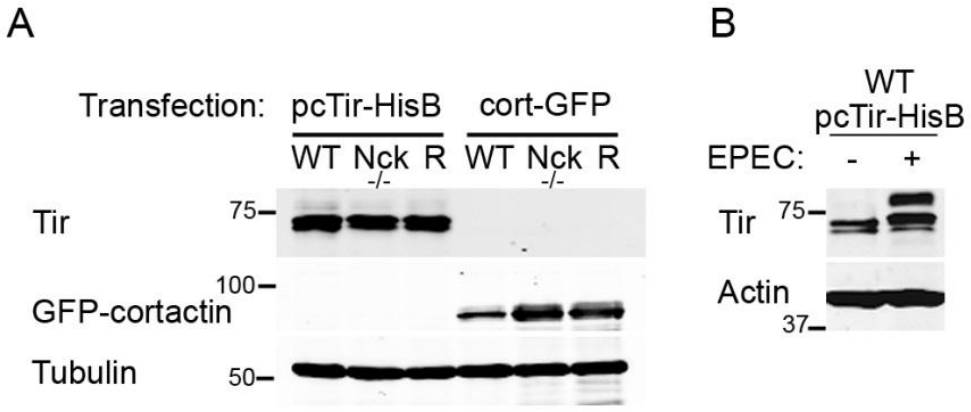

Figure 34. The levels of ectopically expressed Tir are neither reduced nor modified in Nck-deficient cells. (A) WT, Nck-deficient cells (Nck-/-) and Nck reconstituted cells (R) were transfected with pcDNA3.1HisB-Tir or pC2-EGFP-cortactin. Cell monolayers from a single well of 6-well-plates were collected after 20 h of transfection by directly adding Laemmli sample buffer. Lysates were blotted with anti-Tir MoAb and anti-cortactin MoAb and visualised with the Odyssey Scan system. Tubulin was used as a loading control. **(B)** WT MEFs were transfected with pcDNA3.1HisB-Tir and infected with X preactivated EPEC for 3 hours. Cell monolayers from a single well of 6-well-plates were collected by directly adding Laemmli sample buffer. Lysates were blotted with anti-Tir MoAb and visualised with the Odyssey Scan system. Actin was used as a loading control.

11.2. Proteasome inhibitor and two distinct protease inhibitors failed to recover the levels of Tir in Nck-deficient cells

Ubiquitination followed by proteasomal degradation (Kubori and Galan, 2003) or degradation by cytoplasmic proteases (Thomas et al., 2005) are two mechanisms by which bacterial pathogens control the intracellular effector protein activity in the host cell. Hence, we tested the effect of chemical inhibitors in order to block a possible degradation of Tir.

To this end we treated the cells prior to infection with a specific proteasome inhibitor, MG-132, at a concentration of 50 μM for 1 hour known to prevent EPEC-induced protein degradation in infected cells (Ruchaud-Sparagano et al., 2007; Savkovic et al., 2001). Untreated cells were used as a control. EPEC infections were stopped by

gentamicin treatment and cellular extracts were collected at indicated times after infection. As shown in figure 35A western blot analysis of the cellular extracts with a monoclonal antibody against Tir revealed that the levels of Tir do not differ between treated or untreated Nck-deficient cells.

On the other hand, it has been proposed that caspase-1, which belongs to a family of cysteine proteases implicated in apoptosis and inflammation, might be subverted by several enteropathogenic bacteria. The activation of RhoGTPases might represent a novel type of signalling input that can activate caspase-1 signalling (Muller et al., 2010). Hence, caspases could be activated in EPEC infection and implicated in degradation of EPEC effectors. We treated WT and Nck-deficient MEFs with a general cell-permeable caspase inhibitor (Z-VAD-FMK) for 2 hours prior infection or cells were left untreated as a control. As shown in Figure 35B (left panel) the treatment with Z-VAD-FMK does not increase the levels of Tir in WT cells or in Nck-deficient cells.

Finally, considering the possible role of host proteases in degradation of bacterial effectors we analysed the levels of Tir after inhibiting a broad spectrum of cellular proteases. For that purpose, we treated WT and Nck-deficient cells with protease inhibitor cocktail P8340 for 4 hours prior infection or cells were left untreated as a control. As shown in Figure 35B (right panel) the treatment does not increase the levels of Tir in any of the cell types studied. We also treated the cells with P8340 for 20 hours pre-infection with similar results (data not shown). Collectively, these results seem to indicate that Tir is not being degraded by proteasome, caspases or proteases in EPEC-infected Nck-deficient cells.

11.3. The lack of calpain 1 and calpain 2 does not increase the levels of Tir in Nck-deficient cells

The calpains are a family of cysteine proteases that are found in many tissue types and cleave a large number of host proteins. Calpain 4 is a small regulatory subunit required for expression and activity of the ubiquitously expressed calpains 1 and 2. Moreover, EPEC infection leads to the activation of host calpains (Dean et al., 2010).

In order to test the effect of the absence of calpains in the levels of Tir we infected WT and calpain 4-deficient MEFs with EPEC. As a control we infected MEFs that were retrovirally reconstituted with calpain 4. As shown in figure 35C we did not detect any variation in the levels of Tir in cells that lack calpain 1 and calpain 2. This result seems to indicate that calpains are not involved in Tir degradation.

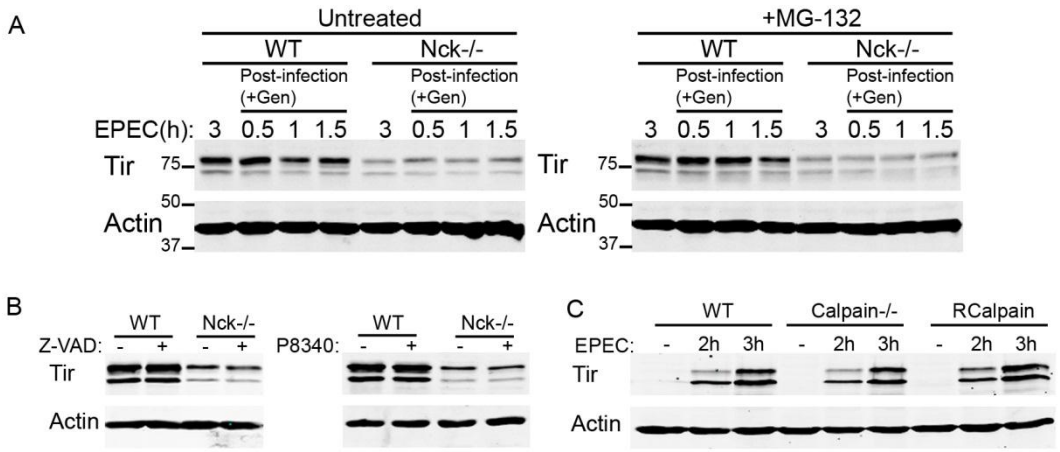

Figure 35. Tir levels are not recovered in Nck-deficient cells after the treatment with different inhibitors. The absence of calpain1 and calpain2 does not promote an increase in Tir levels. (A) Treatment with proteasome inhibitor failed to recover Tir protein levels. WT and Nck-deficient cells were treated with the proteasome inhibitor MG132 (50 μM) for 1 h prior to 3h-infection with 5X preactivated EPEC. Cells were left untreated as a control. After infection, cells were treated with gentamicin (100 μg/ml) and incubated for 1.5 h post-infection. Monolayers were collected at indicated times and lysed in imidazole buffer. Clarified lysates were obtained by centrifugation, were analysed by WB with anti-Tir MoAb. The numbers to the left of the blots indicate the molecular mass in KDa. **(B) Treatment with caspase inhibitor and general protease inhibitor failed to recover Tir protein levels.** WT and Nck-/- cells were treated with caspase inhibitor Z-VAD-FMK (50 μM) for 2 h prior to infection or with protease inhibitor cocktail P8340 (1:1000) for 4 h prior to 3h-infection with 5X preactivated EPEC. **(C) In the absence of calpain 1/2 the levels of Tir do not increase.** WT, calpain-deficient cells and calpain reconstituted cells (Rcalpain) were infected with X preactivated EPEC for 1, 2 and 3 hours. In both (B) and (C) cell monolayers from a single well of 6-well-plates were collected by directly adding Laemmli sample buffer and analysed by WB with anti-Tir MoAb. The blots were visualised with the Odyssey Scan system. Actin was used as a loading control.

11.4. The treatment with Trichostatin A increases the levels of Tir and improves EPEC attachment

Trichostatin A (TSA) was isolated from the metabolites of strains of *Streptomyces hygroscopicus* and originally characterised as an anti-fungal antibiotic (Tsuji et al., 1976) and later identified as specific histone deacetylase inhibitor (HDACi). TSA specifically inhibits class I and II histone deacetylases (Matsuyama et al., 2002), such as HDAC6 which acts as a tubulin and cortactin deacetylase. HDACis have shown promise in inhibiting tumorigenesis and metastasis due to their potent anti-proliferative and apoptotic effects in malignant cells (reviewed in (Barneda-Zahonero and Parra, 2012)). HDAC inhibitors have been shown to exhibit anti-inflammatory activity. Thus, recently it has been demonstrated that TSA directly inhibits nuclear factor kB (NF-kB) induced transcription and the induction of inflammatory genes by tumour necrosis factor-α (TNF- α) (Furumai et al., 2011). Interestingly, it has been also reported that HDAC6 controls autophagosome maturation essential for the autophagy independent of nutrient status named quality-control autophagy (Lee et al., 2010). Hence, the prototypical HDAC inhibitor TSA could suppress autophagy, as has been recently described in pathological cardiac remodelling (Cao et al., 2011).

In order to test the effect of the treatment with TSA in the levels of Tir we treated Nck-deficient cells and their WT counterparts for 16 h prior to infection, or left them untreated as a control. Nck reconstituted cells were used as a control. Western blotting analysis of the Triton X-100-soluble fraction with a polyclonal antibody against Tir revealed that the levels of Tir are increased in TSA-treated Nck-deficient cells with respect to untreated Nck-deficient cells. Moreover, the treatment with TSA also increases Tir levels in WT and Nck reconstituted cells (Fig. 36A, upper panel). It is noticeable that the levels of EspB and EspF are also increased with TSA treatment (Fig. 36A). These results seem to indicate that the treatment with TSA has a general effect on TTSS-dependent effectors.

To determine whether TSA treatment affects the attachment of EPEC to MEFs we analyse by WB the levels of DnaK in the Triton X-100-insoluble fraction. As shown in figure 36B, we found a general increment in the levels of EPEC adhesion after TSA

treatment. Thus, we can conclude that TSA treatment increases the levels of Tir and the adhesion of EPEC to mouse embryonic fibroblast.

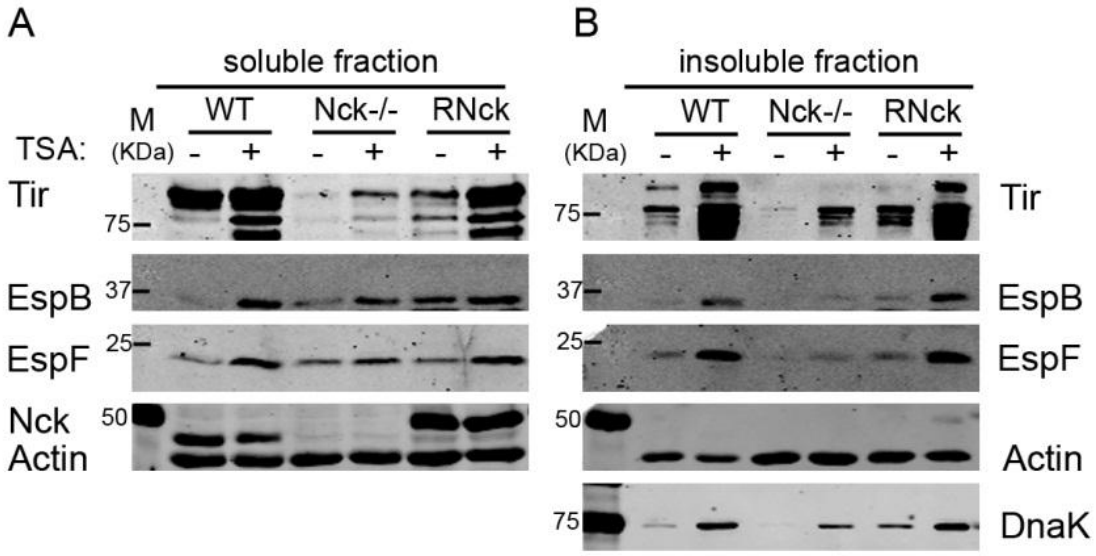

Figure 36. TSA treatments increase the levels of Tir in EPEC-infected MEFs and also increase bacterial attachment. WT, Nck-deficient cells (Nck-/-) and Nck reconstituted cells (RNck) were treated with the Trichostatin A (TSA, 5 μM) for 16 hours prior to 3h-infection with 5X preactivated EPEC. Cell monolayers were lysed in 1% Triton X-100 lysis buffer. The soluble supernatant containing the cytoplasmic and membrane fractions **(A)** and the insoluble pellet containing the attached bacteria **(B)** were subjected to 12 % SDS-PAGE, blotted with indicated antibodies and visualised with the Odyssey Scan system. Actin was used as a loading control and blotting with anti-Nck was performed to confirm the genotype of the MEFs.

11.5. The treatment with Trichostatin A increases the efficiency of pedestal formation

In order to study if the increased levels of Tir after TSA treatments correlate with an increment in the number of pedestal formed in Nck-deficient cells we quantified the number of pedestals formed in TSA treated and untreated cells. The immunofluorescence staining for actin in figure 37A shows that the treatment with TSA increases significantly the efficiency of pedestal formation with respect to untreated MEFs.

As shown in the graph, the number of pedestals formed in TSA-treated-Nck-deficient cells increases four fold with respect to untreated Nck-deficient cells (Fig. 37B). This result implicates that a recovery in Tir levels induced by TSA corresponds with higher pedestal formation efficiency. In addition, it can be noticed that TSA treatments also result in an increase in EPEC attachment to cells (Fig 37B, bottom graph).

The levels of Tir were further supported by immunofluorescence staining using a monoclonal antibody against Tir in TSA-treated or untreated MEFs. As shown in figure 38 the staining of Tir in Nck-deficient cells is remarkably fainter than in WT cells. This observation corroborates previous results obtained by WB analysis of Tir levels in Nck-deficient MEFs (Fig. 24). Importantly, TSA-treated Nck-deficient cells exhibited higher staining levels of Tir. In summary, the results obtained with WB and immunofluorescence assays demonstrate that treatments with Trichostatin A increase the levels of Tir, the number of pedestals and the adhesion of EPEC to mouse embryonic fibroblasts.

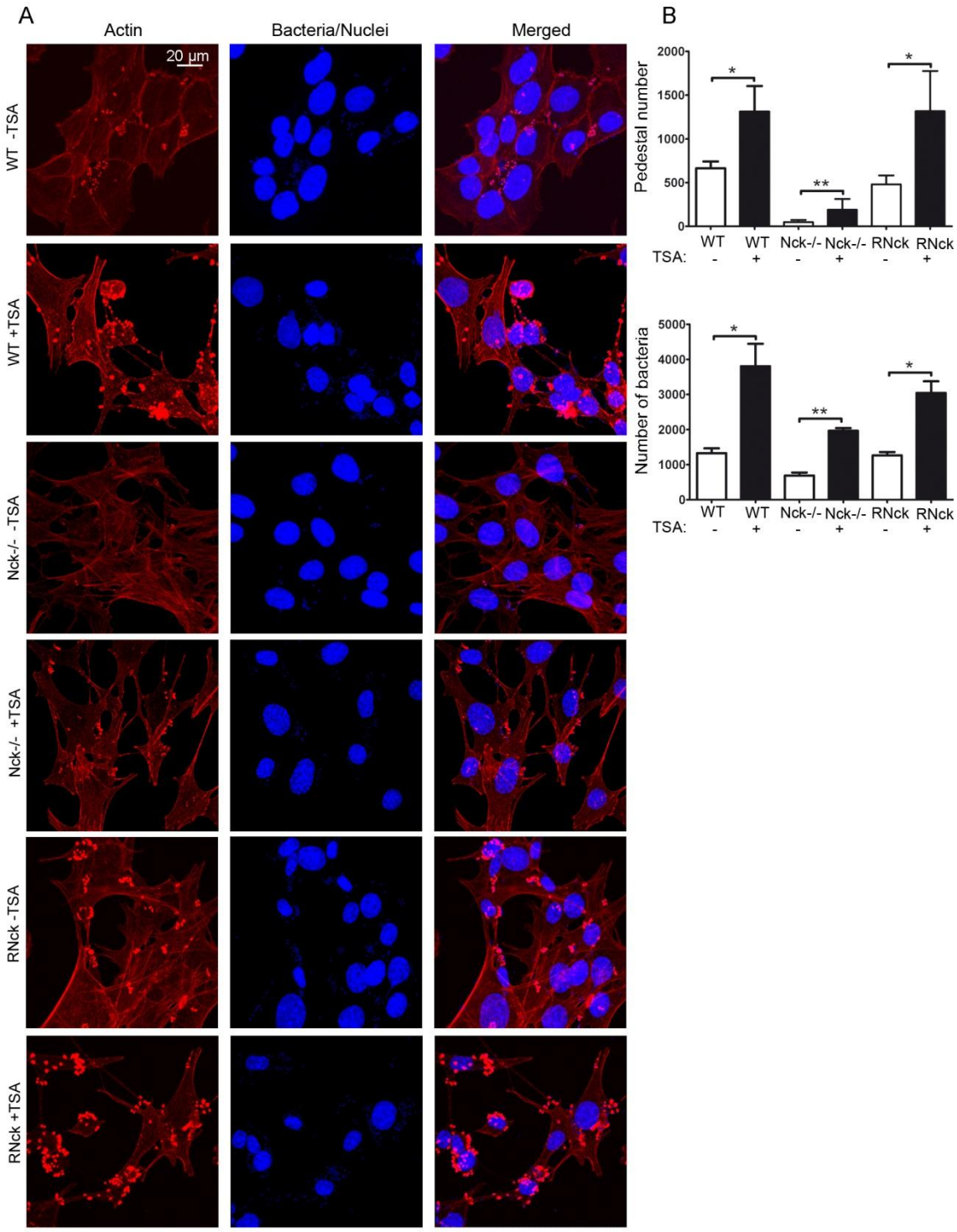

Figure 37. TSA treatments increase the formation of pedestals and the bacterial attachment to MEFs. (A) WT, Nck-deficient cells (Nck-/-) and Nck reconstituted cells (RNck) were treated with Trichostatin A for 16 h and infected with X preactivated EPEC for 3 hours. Red pictures show actin staining with TRITC-Phalloidin. DAPI was used to stain EPEC. The merge of both images was generated with Leica software and is shown in the last column. Pictures were taken in a confocal microscope at 600X magnification. Scale bar represents 20 µm. **(B)** The number of attached bacteria and pedestals of a total of 100 cells were quantified from immunofluorescence images. Graph represents mean ± SD. Statistical analysis using Mann Whitney test from two independent experiments for the number of bacteria or four independent experiments for the number of pedestals is shown. *, $p<0.05$; **, $p<0.01$

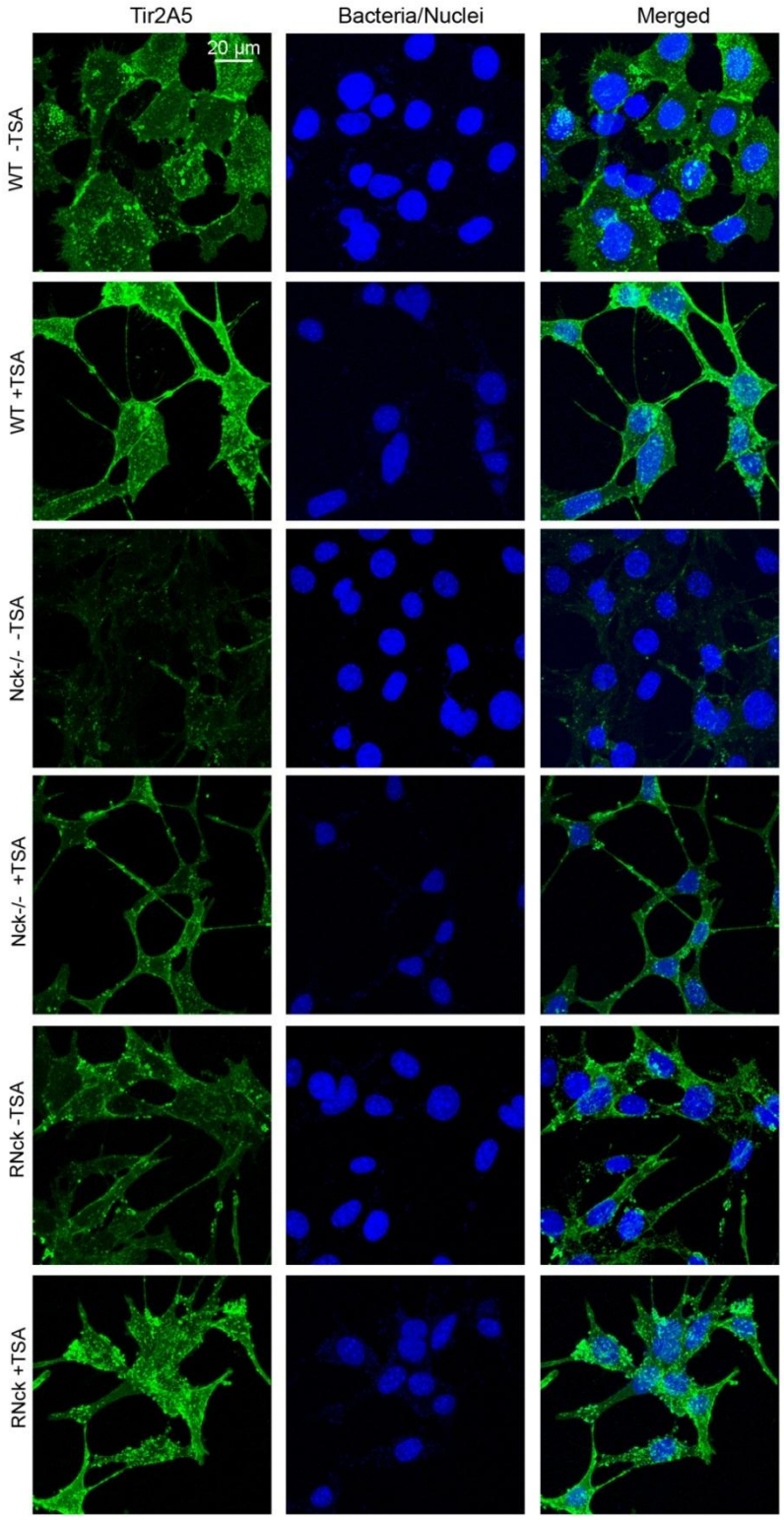

Figure 38. Tir staining by immunofluorescence in MEFs treated with TSA. Immunofluorescence images of WT, Nck-deficient cells (Nck-/-) and Nck reconstituted cells (RNck) treated with Trichostatin A for 16 h (or left untreated as a control) and infected with X preactivated EPEC for 3 hours. Immunofluorescence staining was done using Tir 2A5 MoAb (in green) and DAPI was used to stain EPEC (in blue). The merge of both images was generated with Leica software and is shown in the last column. Pictures were taken in a confocal microscope at 600X magnification. Scale bar represents 20 µm.

DISCUSSION

DISCUSSION

Numerous pathogens have evolved mechanisms to subvert for their own benefit the cellular regulatory complexes that control actin polymerisation. Enteropathogenic *Escherichia coli* (EPEC) manipulates the host actin cytoskeleton from an extracellular position providing a potent model system to study eukaryotic signalling events in response to external stimuli (Hayward et al., 2006).

Diverse host cell proteins implicated in cytoskeletal remodelling, and normally localised as part of focal adhesions, are recruited to the site of EPEC attachment including α-actinin, talin, vinculin (Goosney et al., 2001) as well as actin regulatory proteins such as cortactin (Cantarelli et al., 2000), linking the extracellular bacterium to the host cell cytoskeleton. Besides those proteins, several adaptor proteins are also recruited to the pedestal such as p130Cas, Grb2 and Crk (Goosney et al., 2001). Although over 10 years have passed since this study, the precise role of most of these proteins in pedestal formation remains to be elucidated.

EPEC initiates localised actin assembly to generate pedestals by injecting its translocated intimin receptor (Tir) into the host cell. Once Tir is inserted into the host plasma membrane, its extracellular domain is available to bind the bacterial adhesin intimin. The clustering of Tir in the host cell membrane upon intimin binding appears to trigger downstream signalling cascade leading to the formation of actin pedestals (Kenny et al., 1997). The formation of pedestals is dependent on phosphorylation of Tir in tyrosine residue 474 which is a docking site for the host adaptor protein Nck (Gruenheid et al., 2001). Nck recruits and activate N-WASP, leading to Arp2/3 complex activation promoting actin polymerisation. Cortactin, which is required for pedestal formation ((Cantarelli et al., 2002) and this study), is an additional activator of N-WASP protein. In addition to binding and activating N-WASP (Martinez-Quiles et al., 2004), cortactin can promote actin nucleation by activating the Arp2/3 complex (Uruno et al., 2001). Furthermore, cortactin can bind Nck (Okamura and Resh, 1995) and WIP (Kinley

et al., 2003), which makes cortactin a potential candidate protein for participating in the complex scenario of Tir-mediated signalling to actin polymerisation.

In the present study we tried to gain further insight into the contribution of cortactin and the adapter Crk to pedestal formation. Moreover, we investigated the reduced amount of Tir protein we found in mouse embryonic fibroblast lacking Nck. This issue might have important consequences on the current model for pedestal formation since the Tir:Nck:N-WASP signalling pathway has been the principal one considered both necessary and sufficient for actin polymerisation. Tir is the first effector injected into the cell and has the highest steady-state levels (Mills et al., 2008). Indeed, Tir is a major translocated effector shown to be essential for disease development (Deng et al., 2003; Marches et al., 2000). Moreover, *in vitro* cultured cells appear to be a selective pressure for the preservation of the Tir Y474 or Y454 signalling pathways responsible for actin polymerisation leading pedestal formation. Collectively, the former data highlight the importance of studying a possible regulation of Tir in the absence of Nck.

Cortactin contributes to Tir:Nck:N-WASP signalling pathway

Although it was described that cortactin localises to EPEC pedestals (Cantarelli *et al.*, 2000) and its NTA domain truncated form exerts a dominant negative effect (Cantarelli et al., 2002), its role in pedestal formation was uncertain. The inhibition of the expression of cortactin with specific siRNA oligonucleotides resulted in a drastic reduction in the number of pedestals formed by EPEC. This result has been corroborated by a complementary study (Cantarelli et al., 2006) and it further supports an essential role for cortactin in actin assembly induced by EPEC.

Overexpression of wild type cortactin in HeLa cells has no effect on pedestal formation when compared with mock cells. However, overexpression of W22A cortactin mutant, that fails to bind the Arp2/3 complex, and that of the W525K, that abrogates the binding to SH3-binding targets, inhibit pedestal formation (Fig. 12). These results indicate that both constructs exerts a dominant negative effect, which may mean that cortactin binding and activation of the Arp2/3 complex through the NTA domain, and N-WASP or any other SH3-binding partner, is necessary for pedestal formation.

Collectively, these results demonstrate that cortactin indeed contributes to efficient actin polymerisation. In addition, the study of Cantarelli and colleagues corroborated our results regarding WT cortactin and the W525K mutant, although the W22A mutant was not studied in their work (Cantarelli et al., 2006).

With the aim to address the role of Erk and Src phosphorylation of cortactin, we next used both phosphorylation-mimicking and non-phosphorylatable mutants. The mutant that mimics phosphorylation by Erk has a 'neutral' effect on pedestal formation, while the Erk non-phosphorylatable form blocked pedestal formation (Fig. 12). These results prompted us to conclude that **phosphorylation of cortactin by Erk may positively regulate pedestal formation**. The presence of endogenous cortactin could explain why the phosphoserine-mimicking mutant did not lead to significantly more pedestals than WT cortactin, although an increase was detectable. Otherwise, this mutant accumulates in only one-fourth of pedestals and shows weak diffuse staining in the cytoplasm and a strong nuclear staining. The role of this distribution needs further investigation. In contrast, Cantarelli and colleagues did not use the phosphoserine-mimicking mutant concluding that this phosphorylation is not necessary for pedestal formation (Cantarelli et al., 2006).

To continue, we overexpressed the mutant that mimics phosphorylation by Src and the corresponding non-phosphorylatable mutant. In both cases pedestal formation is impaired, as well as the accumulation of the mutant proteins to the EPEC-induced pedestals (Fig. 12). These results seem to indicate that tyrosine phosphorylation of cortactin inhibits pedestal formation. The same conclusion was reached using the double Y421,466D mutant which partially mimics Src phosphorylation (Cantarelli et al., 2006). However, the fact that both Src mimicking and non-phosphorylatable cortactin forms inhibited the formation of pedestals might indicate that a **dynamic tyrosine phosphorylation** play a role in the formation of pedestals.

We next analysed the phosphorylation status of cortactin following EPEC infection concluding that the presence of N-WASP is required for EPEC-induced tyrosine phosphorylation of cortactin in mouse embryonic fibroblast (MEFs) (Fig. 13). Moreover,

we showed that EPEC induces at least the phosphorylation of cortactin at serine residue 405 which, as occurred with tyrosine-phosphorylation, is not up-regulated in EPEC infected N-WASP-deficient cells (Fig. 14). On the other hand, MEFs depleted for Nck show higher basal levels of phosphotyrosine cortactin that were maintained or slightly reduced after EPEC infection (Fig. 13). These cells also show a higher basal level of phosphorylation at S405 and S418 that was increased after EPEC infection (Fig. 14). The higher levels of total cortactin protein consistently found on Nck-deficient MEFs could explain the higher basal levels of cortactin phosphorylation. Together these findings suggest that tyrosine/serine phosphorylation of cortactin induced by EPEC infection could require the presence of N-WASP, while Nck is not required at least for the serine phosphorylation of cortactin.

We reported a robust phosphorylation of Y466 of cortactin after pervanadate treatment, thus the signalling cascade leading to cortactin phosphorylation was not impaired in any of the cell types used (Fig. 13). Importantly, we also concluded that EPEC-induced Src activation is not affected by the absence of N-WASP, whereas Erk activation is seriously compromised. Hence, the lack of cortactin tyrosine phosphorylation found in N-WASP-deficient cells is not due to a defect on Src activation, whereas the lack of serine phosphorylation could be due to a defect on Erk activation (Figs. 13 and 14). The former result implicates that Erk could potentially phosphorylate cortactin during the process of pedestal formation by EPEC, while other tyrosine kinase distinct of Src could phosphorylate cortactin.

It was shown that EPEC is still capable of forming pedestals on cells lacking Abl-1 and Abl-2 or those lacking Src, Yes and Fyn (SYF cells) and that the Src family inhibitor PP1 has no effect on actin polymerisation induced by EPEC (Cantarelli et al., 2000; Swimm et al., 2004a). Likewise, we observed that treatments with the Erk inhibitor U0126 do not affect the number of pedestals formed by EPEC (Fig. 15). Knowing that EPEC uses any of several functionally redundant tyrosine kinases to ensure Tir phosphorylation (Swimm et al., 2004a), it might be possible that in the presence of inhibitors other redundant kinases would lead to pedestal formation.

Collectively, the results obtained with the overexpression of the cortactin mutants seem to indicate that serine phosphorylation of cortactin contributes to pedestal formation, whereas tyrosine phosphorylation inhibits it. On the other hand, we reported that the infection with EPEC induces the N-WASP-dependent phosphorylation of cortactin in tyrosine and serine residues. These findings strongly suggest a coordinated action of cortactin and N-WASP during pedestal formation, consistent with the on/off switching mechanism by which cortactin activates N-WASP *in vitro* (Martinez-Quiles et al., 2004). In like manner, the serine phosphorylation of cortactin would positively regulate pedestal formation by allowing the interaction of cortactin with N-WASP.

Recently it has been shown in a commentary that cortactin can be simultaneously phosphorylated in serine and tyrosine residues as evidence opposing the 'S-Y Switch' model (Kelley et al., 2011). However, the 'S-Y Switch' model only proposes that the tyrosine phosphorylation of cortactin abrogates the effect of the serine phosphorylation with respect to the activation of N-WASP, and it does not assume that cortactin cannot be phosphorylated in serine and tyrosine residues simultaneously. A remaining question is whether cortactin is phosphorylated sequentially, e.g. serine followed by tyrosine phosphorylation. Future studies will clarify the still controversial regulation of this protein.

A crucial finding of this study is that cortactin and Tir bind each other directly *in vitro*, as demonstrated using purified recombinant proteins (Fig. 16A). Since Tir possesses a consensus motif for binding to cortactin, centered on proline residue P20, our initial hypothesis was that they would interact directly through the SH3 domain of cortactin. Indeed, the SH3 domain of cortactin is able to bind Tir, but unexpectedly, the NH2 domain is also found to bind Tir. In addition, we did not detect differences in the affinity binding of cortactin mutants that mimic phosphorylation by Erk and Src (Fig. 16A). These results contrast the previous binding studies of Martinez-Quiles and colleagues in which a mutant that mimics phosphorylation by Erk was found to bind preferentially to N-WASP (Martinez-Quiles et al., 2004). In summary, cortactin binds Tir through both its N-terminal region and the SH3 domain, and this interaction seems to occur independently of cortactin phosphorylation.

In agreement with this conclusion, experiments using a two-hybrid system show that both the N-terminal region and the SH3 domain of cortactin bind Tir of the related pathogen EHEC (Cantarelli et al., 2007). Moreover, Cantarelli and colleagues also corroborate the induction of cortactin tyrosine phosphorylation after EPEC infection (Cantarelli et al., 2007). Contrary to these findings, the authors show that EHEC induces dephosphorylation of cortactin that occurs concomitantly with a transient interaction between the N-terminal part of Tir_{EHEC} and the N-terminal domain of cortactin. These results highlight the fine-tuned nature of cortactin regulation during EPEC and EHEC infections.

Cortactin can directly binds to and activate the Arp2/3 complex through its NTA domain (Uruno et al., 2001). We report here that Tir-coated beads activate cortactin *in vitro* leading to Arp2/3 complex-dependent actin polymerisation. Furthermore, the activation of cortactin by Tir is not affected by the phosphorylation status of cortactin, as occurred for the binding (Fig. 16B). These results further support the idea that Tir binds and activates cortactin independently of the latter's phosphorylation status in EPEC signalling. The fact that the phosphorylation mimicking Tir mutant (Y474D) did not show significant differences from WT Tir in both binding and activation experiments may means: (I) the mutant does not behave like the phosphorylated form or (II) the binding and activation of cortactin is independent of Tir phosphorylation on residue 474. Further experiments are needed to address this question.

Considering all the data we hypothesised that the relevant contribution underlying cortactin-Tir binding occurs through the N-terminal moiety of cortactin, since our previous studies indicated that phosphorylation of cortactin affects mainly its interaction with partners through the SH3 domain.

To test this hypothesis, we used lysates from cultured MEFs that represent a more restrictive scenario. Consistent with our reasoning, cortactin binds Tir primarily through its N-terminal region, while the contribution of the SH3 domain seems to be irrelevant. Furthermore, this interaction does not require N-WASP (Fig. 17). Alternatively, the SH3

domain of cortactin may be occupied by other SH3 domain-containing proteins such as tyrosine kinases (Swimm et al., 2004a) or may have a preference for binding N-WASP. We were not able to detect the binding of cortactin to Tir in Nck-deficient cells. Notably, the dramatic reduction of Tir found in those cells infected by EPEC could explain why we failed to detect such interaction. Alternatively, it is possible that the interaction between Tir and cortactin requires Nck. Further experiments will be required to determine if cortactin and Tir interact in the absence of Nck in MEFs.

Finally, in an attempt to understand what kind of complexes could be formed *in vivo*, we considered all available *in vitro* data concerning the interaction of Tir, Nck, N-WASP and cortactin. Thus, Nck binds cortactin only when phosphorylated by Src (Tehrani et al., 2007). Therefore since Tir and Nck interact through the single SH2 domain of Nck, formation of a Tir-Nck-cortactin complex appears to be impossible. Cortactin phosphorylated by Src is not able to interact with N-WASP, as shown with recombinant proteins (Martinez-Quiles et al., 2004) and further corroborated in the yeast two-hybrid assay (Cantarelli et al., 2007). That adds to the evidence against the possibility that cortactin bridges both proteins, i.e. Nck-cortactin-N-WASP.

The previous data leave three possible types of complexes: (I) Tir-Nck-N-WASP-cortactin, (II) Tir-cortactin-N-WASP and (III) Tir-cortactin. Given the fact that cortactin depletion by siRNA inhibits pedestal formation ((Cantarelli et al., 2006) and this study), that EPEC infection induces cortactin phosphorylation in an N-WASP-dependent fashion (Fig. 13), and that Tir binds and activates cortactin (Fig. 16) we hypothesise that cortactin contributes to the Tir:Nck:N-WASP pathway, possibly by regulating N-WASP activity. The fact that the SH3 domain of cortactin pulls down N-WASP ((Martinez-Quiles et al., 2004) and Fig. 17) supports the hypothesis that cortactin binds Tir through the N terminus and N-WASP through the SH3 domain. In other words, cortactin and N-WASP would act in a complex in this scenario.

If we envision pedestals as a dynamic actin structure, and in fact pedestal motility has been shown (Sanger et al., 1996), then it is reasonable to think that proteins promoting actin polymerisation would act in a cyclic manner. We speculate that cortactin is a

cycling switch for N-WASP in pedestals. In this case, phosphorylation switch should affect only the binding of cortactin to N-WASP, hence, cortactin phosphorylated on serine would bind both Tir and N-WASP whereas cortactin phosphorylated on tyrosine would bind only Tir (Model).

Notably, it has been shown that in the case of EHEC infection, cortactin is recruited by different mechanisms in cultured cells than in human *in vitro* organ cultures (IVOC). Thus, the recruitment of cortactin via an EspFu- and N-WASP-independent pathway in IVOC contrasts with the EspFu dependent recruitment of cortactin in cells (Mousnier et al., 2008). Therefore, cortactin seems to have a more influential role during EHEC infection of mucosal surfaces than of cultured cells *in vitro*.

Crepin and colleagues have recently shown that Tir:Nck signalling pathway is not necessary for A/E lesion formation or N-WASP recruitment during *Citrobacter rodentium* infection of mice (Crepin et al., 2010) or EPEC infection of human intestinal IVOC (Crepin et al., 2010; Schuller et al., 2007). These studies prove that the A/E lesions induced *in vivo* and *ex vivo* are not strictly comparable to studies in cultured cells *in vitro*. Finally we speculate that cortactin could have an important role in mediating A/E lesion formation *in vivo* although this assumption needs further investigation.

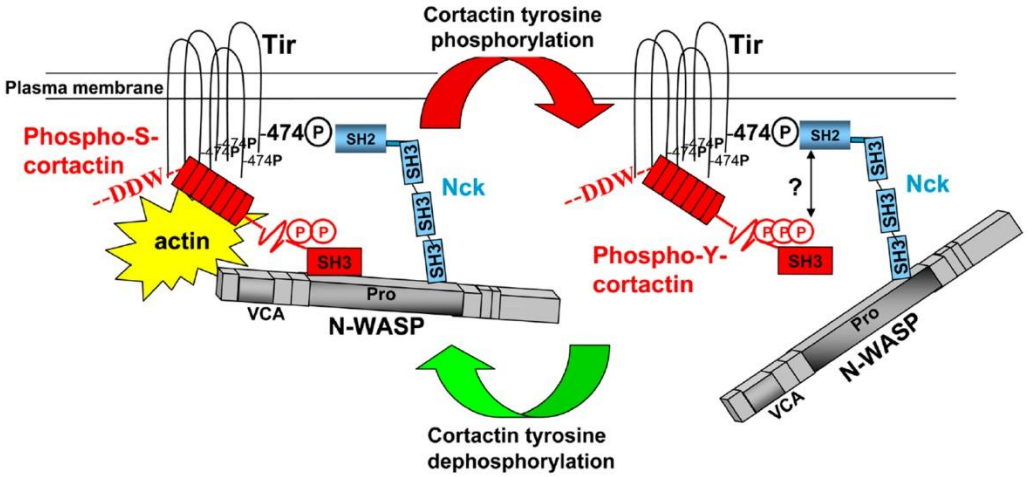

Model of coordinated action by cortactin and N-WASP on EPEC pedestals. In theory, cortactin may bind Tir and N-WASP simultaneously, via its N-terminal and SH3 domain interaction respectively. EPEC-induced tyrosine phosphorylation of cortactin would terminate cortactin interaction with N-WASP but not with Tir. This could constitute a cyclical regulatory mechanism of actin polymerisation on EPEC pedestals. Phosphotyrosine-cortactin might as well compete for the SH2 domain of Nck, thus uncoupling Tir from the Nck/N-WASP complex.

Crk negatively regulates actin polymerisation in EPEC pedestals

Crk proteins are a ubiquitously expressed family of adaptors that assembles protein complexes playing an important role in intracellular signal transduction integrating signals from a wide variety of sources, including bacterial pathogens. The observation by Goosney *et al.* that Crk adaptors, named in general Crk by the authors, localise to pedestals formed by EPEC (Goosney et al., 2001) raises the possibility that Tir signalling may involve these host adaptors. Hence, we investigated the role of CrkI, CrkII, and the paralog Crk-like (CrkL) in EPEC pedestal formation.

We observed that the inhibition of the expression of CrkI/II by siRNA or the overexpression of the dominant negative mutant of Crk (R38V) in HeLa cells has no effect on EPEC-induced pedestal formation (Figs. 18 and 19). Moreover, EPEC infection of MEFs lacking both CrkI and CrkII allowed us to corroborate the previous results, since pedestal formation is not affected in this cell line (Fig. 20). Considering that CrkI isoform is only expressed at almost non-detectable levels in HeLa cells (Fig. 18A), and

that CrkL shares high sequence identity with CrkII and have overlapping functions in certain cases, our results might indicate that Crk adaptors could be compensating for each other in pedestal formation.

Interestingly, depletion of CrkL by siRNA in MEFs cells that lack both CrkI and CrkII allowed us to determine that the absence of all major isoforms of Crk adaptors significant increases the number of pedestals formed by EPEC (Fig. 21). We corroborated this unexpected result overexpressing the dominant negative mutant of Crk in this cell line (Fig. 22).

The redundant function of the proteins was further confirmed with CrkL-deficient MEFs. As occurred with CrkI/II, the absence of CrkL does not affect the formation of pedestals induced by EPEC, indicating that CrkII and CrkL adaptors could be compensating for each other. In addition, the expression of a dominant negative mutant of Crk in CrkL-deficient cells elicits an increase in the number of pedestals formed (Fig. 23). It seems that the effect of the dominant negative mutant is obvious only when the expression of at least one isoform (CrkI/II or alternatively CrkL) is previously knock-down.

Finally, we inhibited the expression of CrkL by siRNA in HeLa cells and observed that the number of pedestals remains unchanged (data not shown) pointing again to a functional redundancy of Crk family proteins. Although the study of knock-out mice of CrkI/II and CrkL and other observations show independent roles for these proteins, a number of recent studies suggest that CrkI/II and CrkL can compensate to each other in different signalling pathways. Thus, Crk adaptors show overlapping functions in promoting cell migration stimulated by PDGF and in the formation of focal adhesions (Antoku and Mayer, 2009).

Collectively, the results seem to indicate a redundant inhibitory role of Crk family adaptors during actin polymerisation in pedestals formed by EPEC, although the mechanism requires further investigations.

The fact that tyrosine phosphorylated cortactin cooperates with Crk to trigger actin polymerisation during *Shigella* invasion of epithelial cells (Bougneres et al., 2004) prompted us to investigate a possible interaction between cortactin and Crk after EPEC infection. Moreover, the uptake of *Yersinia* involves the tyrosine phosphorylation of p130Cas and the subsequent formation of p130Cas-Crk complexes (Weidow et al., 2000). Hence, we also analysed the interaction of Crk with other partners, such as p130Cas. Based on immunoprecipitation assays, we could not detect an interaction between Crk and cortactin in uninfected or EPEC-infected HeLa cells (data not shown). Likewise, we could not detect an interaction between Crk and p130Cas (data not shown). Although further experiments, such as *in vitro* pull down assays, will be required to discard a possible interaction of these proteins following EPEC infection, presumably cortactin and p130Cas are not interacting with Crk in the process of pedestal formation.

As mentioned, Crk family adaptors are required for the remodelling of actin cytoskeleton and for the formation and turnover of focal adhesions (Antoku and Mayer, 2009). Crk has also been implicated in the regulation of migration, proliferation and cellular adhesion (Feller, 2001). Therefore, we could contemplate that the inhibition of Crk expression affects cytoskeleton-related proteins that could favour the formation of pedestals. The implication of Crk family adaptor in regulating the formation of finger-like protrusive structures that contain actin bundles called filopodia (Antoku et al., 2008), could be also be related to the formation of pedestals. The effector Map induces the formation of transient filopodia at the bacterial attachment sites (Kenny et al., 2002; Kenny and Jepson, 2000). The retraction that occurs at early times post-infection is dependent on Tir (Kenny et al., 2002). The model proposed by Berger and colleagues suggests that the rapid withdraw of Map-induced filopodia leads to widespread pedestals. The authors also showed that eliminating Nck blocked pedestal formation and promoted a long-term presence of filopodia (Berger et al., 2009). In like manner, depletion of Crk could interfere in the formation of filopodia leading to increased number of pedestals. However, the fact that the cells with knockdown of Crk family proteins increased filopodium formation (Antoku et al., 2008) does not point in favour of this hypothesis.

In addition, CrkII and CrkL are phosphorylated by Abl, and in fact the Abl-family kinases Abl and Arg have also been shown to phosphorylate Tir and associate with an N-terminal proline-rich peptide of Tir using their SH3 domain (Bommarius, Maxwell et al. 2007). One possible hypothesis is that the binding of Crk proteins to Abl could compete for the binding to Tir. Thus, depletion of Crk proteins would liberate Abl resulting in the enhancement of pedestal formation.

Another possibility could be that Crk participates in the Tir:Nck:N-WASP signalling pathway for pedestal formation. It will be very interesting to determine if Crk interacts with bacterial Tir through its SH2 domain and moreover if this interaction is directly or mediated by others proteins, such as N-WASP. The phosphorylation of Tir in tyrosine residue 474 generates the binding site for the SH2 domain of Nck. In addition, the second tyrosine residue phosphorylated (Y454) is responsible for the low actin polymerisation that occurs independently of Nck (Campellone and Leong, 2005). Likewise, it is possible that Y454 recruits other phosphotyrosine-binding molecule that can promote actin assembly. It has been described that the adaptor Grb2, although localised to pedestals formed by EPEC (Goosney et al., 2001), does not interact with any of two tyrosine residues. It is tempting to speculate that Crk adaptor proteins could bind to tyrosine residue Y474 or Y454 playing an inhibitory role in EPEC signalling.

These and others intriguing hypotheses are currently under investigation by our group. In summary, the major finding of this part of the study is the inhibitory role of Crk family adaptors during actin polymerisation in pedestals. Future experimentation will clarified the underlying mechanism of the role of Crk family proteins.

Depletion of Nck affects the levels of bacterial protein Tir

Mouse embryonic fibroblast lacking Nck produced by the group of Dr. Tony Pawson (Bladt et al., 2003) are routinely used to study EPEC-induced pedestal formation. Our experimental results based on this cell line demonstrated an unforeseen reduced amount of the bacterial effector Tir. The reduction observed in both total cell lysates and Tir-enriched cell fractions of EPEC-infected Nck-deficient cells is recovered when Nck1 expression was restored (Fig. 24).

In order to corroborate that the observed phenotype was not linked to the cell line used, Nck1/2 expression was inhibited in human epithelial Hela cells. Similarly, our results demonstrated that the depletion of Nck1/2 by siRNA in HeLa results in a decrease of Tir levels (Fig. 25). This reduction is not as high as the one observed in infected Nck-deficient cells. This difference could be explained because the inhibition of the expression of Nck by siRNA is only partial and not complete as in Nck-deficient cells. Furthermore, Nck-depleted Hela cells present a reduction in the number of pedestals formed by EPEC, although not as drastic as in Nck deficient cells. In view of these results we decided that the initial observation deserved further investigations.

We report here a 20-fold reduction in the efficiency of pedestal formation by EPEC. Furthermore, we describe an 88% of decrease in Tir levels in Nck-deficient MEFs with respect to WT MEFs by WB analysis (Figs. 24 and 28). This dramatic decrease in Tir levels was also corroborated by immunofluorescence with a monoclonal antibody against Tir (Fig. 38). These results contrast with the 4-fold decrease in the efficiency of pedestal formation (Campellone et al., 2004b), and with the 25% decrease of Tir translocated into Nck-deficient cells with respect to Nck1 reconstituted cells as measured by HA staining by Campellone´s group (Campellone and Leong, 2005). Campellone and colleagues used in their experiments an EPEC strain that lacks a chromosomal copy of *tir* and that is complemented with a plasmid expressing HA-tagged Tir (pHA-*tir*). However, in our opinion the usage of this strain does not justify the reported differences since it regained the ability to cause A/E lesions in IVOC (Schuller et al., 2007). We speculate that the authors would have found more

pronounced differences if they had compared cells lacking Nck isoforms with cells expressing both Nck1 and Nck2 isoforms like in our study.

Moreover, another major conclusion of our study is that Nck might be required for efficient intimin-Tir mediated bacterial attachment to murine cells (Fig. 28). To our knowledge, this is the first reported decrease in bacterial attachment to MEFs lacking Nck. As mentioned, the intimate adherence of EPEC to HeLa cells requires the interaction between intimin and Tir (Kenny et al., 1997). We concluded that there exist a higher dependence of the presence of intimin and Tir for EPEC binding to MEFs than in the case of EPEC binding to human HeLa cells (Fig. 29), which could have implications for the use of these cells as a model system.

In this line of reasoning, the diminished adhesion of EPEC to Nck-deficient cells might be a consequence of the low levels of Tir found in these cells, which is supported by the fact that tir-intimin interaction is needed for the adhesion of EPEC to murine cells.

Interestingly, in N-WASP-deficient cells, which are also resistant to EPEC pedestal formation, Tir and bacterial attachment levels are equal to the ones observed in WT cells (Fig. 26). Accordingly, it has been shown that EPEC translocates Tir into N-WASP deficient cells at wild type levels (Vingadassalom et al., 2010). These results prompted us to conclude that the low levels of Tir and bacterial attachment found in Nck-deficient cells cannot be due exclusively to the absence of pedestals.

Two **hypotheses** to explain the reduced Tir levels found in MEFs lacking Nck were formulated:

(I) A defect in the delivery of Tir effector into the host cells

(II) An increased rate of degradation of Tir in the host cells

In an attempt to test the hypothesis of a defective delivery process, we examined by western blotting the protein levels of another two TTSS-secreted EPEC effectors, EspF and EspB. EspB is especially interesting as it is inserted into the host membrane forming

the translocation pore (Wolff et al., 1998). We observed normal levels of EspF and EspB in Nck-deficient cells concluding that the reduction of Tir is not affecting the delivery process or the degradation of these effectors. We next tried to improve EPEC translocation efficiency by increasing the MOI (Mills et al., 2008), however higher number of bacteria per cell does not result in increased levels of Tir in Nck-deficient cells (Fig. 27).

Our results contrast with the current injection model that proposes that Tir is one of the EPEC effectors that has high translocation efficiency (Mills et al., 2008). Furthermore, it was proposed that the injection of EPEC effectors follows a hierarchical order and that Tir is required for the efficient injection of other effectors, including EspF (Thomas et al., 2007). However, this idea is questioned by others studies where *tir* deficient strains have EPEC capacities to induce effector-driven cellular alterations in macrophages, HeLa cells and polarised epithelial models (Dean et al., 2006). In addition, our findings do not indicate a requirement of Tir for the efficient delivery of other effectors, such as EspB or EspF.

Interestingly, Vingadassalom and colleagues have recently described the requirement of N-WASP and actin assembly for the translocation of Tir_{EHEC} and EspFu into mammalian cells by EHEC. They also reported that N-WASP is required for efficient EHEC attachment to the cell surface. An interesting approach used in this study is the induction of the formation of pedestals in N-WASP-deficient cells, which normally do not form them, using an EPEC-derived strain to enhance the translocation of Tir_{EHEC} and EspFu. They hypothesised that EspFu can signal to the Arp2/3 complex by recruiting an alternative host factor. However, the authors use the same bacterial strain in a different N-WASP-deficient cell line (Lommel et al., 2001) and pedestals were not formed. The authors tried to reconcile these different results assuming that Lommel´s cells may lack the alternative actin promoting factor (Vingadassalom et al., 2010). Considering these results with the related pathogen EHEC, we could point in favour of the hypothesis that Nck is required for the translocation of Tir by EPEC.

Trying to gain some insight on the degradation hypothesis we analysed the tyrosine-phosphorylation status of the low but detectable fraction of Tir in Nck-deficient cells. We concluded that the underlying process is not dependent on the lack of Tir phosphorylation, since Tir is tyrosine phosphorylated and stably inserted into the membrane even six hours after EPEC infection (Fig. 30). The stability of Tir in HeLa cells 90 minutes after infection was already known (Mills et al., 2008).

We also analysed the levels of non-phosphorylatable Tir mutants in Nck-deficient cells using EPEC strains lacking *tir* that are complemented with a plasmid expressing Tir. We use the WT form of Tir and Tir with point mutations in the relevant residues sites susceptible for tyrosine and serine phosphorylation. The results seem to indicate that the levels of Tir are not affected by a different conformation of the protein due to mutations in serine residues, since low levels of Tir in Nck-deficient cells were also observed with serine/tyrosine mutated Tir (Fig. 31).

Once the process of pedestal formation is triggered in infected HeLa cells, *de novo* bacterial protein synthesis is not needed for the tyrosine phosphorylation of Tir (Rosenshine et al., 1996). Chloramphenicol is an antibiotic long known to inhibit bacterial protein synthesis (Rendi and Ochoa, 1962). Accordingly, a period of 15 minutes of infection with preactivated EPEC prior to chloramphenicol treatment is sufficient to detect the "upper" band of Tir that represents fully-modified Tir (Fig. 32, WT cells treated with chloramphenicol). This result indicates that once Tir is inserted in the plasma membrane, it is stable for at least 20 hours (data not shown). Interestingly, although the fully-modified Tir form was detected in WT cells treated for 180 minutes with chloramphenicol, we could not detect fully-modified Tir in chloramphenicol-treated Nck-deficient cells at any time.

Moreover, after 180 minutes of chloramphenicol treatment the band of partially modified Tir observed after 1 hour of treatment in Nck-deficient cells was not detected by WB. These results seem to indicate that, in the absence of Nck, *de novo* bacterial protein synthesis is required to maintain steady-state levels of the fully modified Tir

form. Notably, the form of Tir that is not fully modified seems to be degraded in Nck-deficient cells. Considering that the shifts in Tir are thought to reflect phosphorylation-induced conformational changes facilitating the insertion into the plasma membrane (Kenny, 1999), it is tempting to speculate that the non-fully modified Tir could be more susceptible for degradation.

We next tested the infection with a modified EPEC strain that expresses HA-tagged Map and determined that the levels of Map in Nck-deficient cells are also reduced when compared to WT cells (Fig. 33). Unfortunately, we could not corroborate this result infecting with WT EPEC due to the lack of a specific antibody to detect Map. In view of this result we could consider that the reduction in Tir and Map levels relates to an Nck-dependent translocation defect of CesT-dependent effectors, or alternatively, to a specific degradation process of these effectors. Then, it would be wise to analyse the levels of other CesT-dependent effectors such as NleA, NleF, NleH1 and NleH2 (Creasey et al., 2003; Thomas et al., 2007).

In order to test the hypothesis of a possible degradation of Tir, we thought of using ectopically expressed Tir as a model system to determine the effect of various chemical inhibitors. Therefore we determined Tir expression by transfecting the cells with a mammalian expression plasmid encoding Tir. The transfections of Nck-deficient cells allowed us to conclude that ectopically expressed Tir is not reduced in these cells with respect to WT cells (Fig. 34), consequently we discarded this line of study.

For the purpose of blocking a possible degradation of Tir in Nck-deficient cells we tested the effect of several protease inhibitors. Treatments of 1 hour prior to EPEC infection with proteasome inhibitor (MG-132) failed to recover the levels of Tir in Nck-deficient cells. In agreement with this result it has been described in an elegant study that the translocation rate of the six EPEC effectors EspF, EspG, EspH, EspZ, Map and Tir in HeLa cells is not affected by proteasome inhibition (Mills et al., 2008). In this line, neither a general caspase inhibitor (Z-VAD-FMK) nor a broad spectrum protease inhibitor cocktail (P8340) recovered the levels of Tir in Nck-deficient cells. Moreover, we observed that the lack of calpains in MEFs does not affect the levels of Tir. Collectively,

these results indicate that Tir is not being degraded by proteasome, caspases or proteases.

Finally, treatments with Trichostatin A (TSA), a known deacetylase and autophagy inhibitor (Lee et al., 2010; Matsuyama et al., 2002), resulted in a significant increment of the levels of Tir in Nck-deficient cells. Moreover, TSA treatments significantly increased the bacterial attachment and the number of pedestals formed in these cells, as visualised by immunofluorescence staining. We might think that the increase in the efficiency of pedestal formation is a consequence of the higher levels of Tir after TSA treatment. This unforeseen result indicates that the absence of pedestals found in these cells could be due to the dramatic decrease of Tir levels, and not merely due to a lack of N-WASP activation as a result of the absence of Nck, as it is currently assumed. Thus, when the levels of Tir are restored the number of pedestals increases concomitantly. Consequently, in TSA-treated Nck-deficient cells another host adaptor could recruit N-WASP to promote pedestal formation. This assumption allows us to speculate that cortactin could bridge Tir and N-WASP promoting actin polimerisation that leads to pedestal formation in the absence of Nck.

It is difficult to comprehend the mechanism by which TSA increases the levels of Tir protein in MEFs lacking Nck, because this inhibitor can affect many cellular processes. It is thought that TSA specifically inhibits class Ⅰ and Ⅱ histone deacetylases such as HDAC6 (known as class Ⅱ), which acts as a tubulin and cortactin deacetylase. Indeed, HDAC6 and cortactin are implicated in quality-control autophagy, which is independent of nutrient status. HDAC6 is recruited to ubiquitinated substrates where it stimulates the fusion of the autophagosome with the lysosome by promoting F-actin remodeling in a cortactin-dependent manner (Lee et al., 2010). Autophagy is an ubiquitous degradation pathway recently reported to play an important role in host defense against *Citrobacter rodentium* infection in intestinal epithelial cells (Inoue et al., 2012). However, the sole inhibition of the expression of HDAC6 by siRNA treatment does not increase the levels of Tir in Nck-deficient cells (data not shown) which could indicate that another TSA sensitive deacetylase it is responsible for the phenotype.

On the other hand, we have to consider that the drug is having a general effect on cell cytoskeleton, since the general morphology of cells dramatically changes during treatments with TSA ((Hoshikawa et al., 1994) and our observation). It has been described that the effect of TSA is related to histone deacetylase inhibition activity and to the enhancement of expression of an actin-regulatory protein, gelsolin (Hoshikawa et al., 1994). It is tempting to speculate that the TSA-induced rearrangement of the cytoskeleton could favor the translocation of EPEC effectors. Likewise, there are evidences indicating that F-actin assembly promotes type III translocation of effectors by others pathogens such as *Yersinia* and *Shigella* (Mejia et al., 2008; Mounier et al., 2009) and the related EHEC (Vingadassalom et al., 2010).

It has to be noticed that we found variability in TSA treatments and the increase in the levels of Tir following TSA treatment was not observed by WB analysis in all the experiments performed. Interestingly, the number of pedestals does not increase in TSA-treated Nck-deficient cells when the levels of Tir are not restored (data not shown). This result discards the possibility that the effect of the treatment on the cells could be influencing on pedestal formation and seems to indicate that the increment in pedestal formation is due to an increase in the levels of Tir.

Finally, considering that the lysosome is a common intracellular destination for endocytic, autophagic, and secretory molecules targeted for degradation (Knecht et al., 2009), it will be worthy to test lysosomal degradation inhibitors.

To summarise, our results partially point to a defective delivery of Tir, however we cannot discard the initial alternative hypotheses of a possible degradation of Tir protein inside the host cell. It is tempting to speculate that both processes could be occurring simultaneously. In any case, it seems that the process affects CesT-dependent effectors since levels of both Tir and Map are reduced in Nck-deficient cells, while levels of EspF and EspB, which use different chaperones for their delivery process, are not affected.

The experiments to definitively discern whether the drastic reduction of Tir levels in the absence of Nck is due to degradation, to a defective delivery process or even to both

simultaneously, is the real-time measurement of the translocation kinetics of EPEC effectors in Nck-deficient cells. The failure to obtain funding to perform the experiments using "the real-time, high-throughput translocation assay" in the laboratory of Dr. Rosenshine in Israel (Mills et al., 2008) did not allow us to obtain the quantitative data required to determine the underlying mechanism.

The importance of the results obtained in this study is highlighted by the fact that the mouse embryonic fibroblast lacking Nck has been widely used since Gruenheid *et al.* described the binding of Nck to Tir leading pedestal formation (Gruenheid et al., 2001). The finding that infected Nck-deficient cells have reduced amount of Tir levels and reduced bacterial attachment could have consequences in the results obtained and in future experiments that will be performed with these cells.

CONCLUSIONS

CONCLUSIONS

Part I

1. Cortactin is necessary for pedestal formation by enteropathogenic *Escherichia coli* (EPEC). Moreover, the integrity of the Arp2/3 complex binding domain and the SH3 domain of cortactin is required for pedestal formation by EPEC.
2. Serine phosphorylation of cortactin, probably by the kinase Erk positively regulates EPEC pedestal formation while dynamic cycles of tyrosine phosphorylation and dephosphorylation of cortactin are required for the process.
3. N-WASP is required for EPEC-induction of serine and tyrosine phosphorylation of cortactin. Moreover, Src activation following EPEC infection is independent of N-WASP presence, whereas the activation of Erk is N-WASP dependent.
4. Serine phosphorylation of cortactin is independent of Nck presence and both Src and Erk kinases are induced by EPEC infection in mouse embryonic fibroblast that lack Nck.
5. Cortactin and Tir protein bind each other directly *in vitro*. This interaction promotes Arp2/3 complex-mediated actin polymerisation *in vitro* independently of the phosphorylation status of cortactin.
6. Cortactin binds Tir in EPEC-infected cells in the absence of N-WASP.

Part II

1. Crk family adaptor proteins have a redundant inhibitory role in regulating actin polymerisation in pedestals formed by EPEC.

Part III

1. The absence of Nck in EPEC-infected mouse embryonic fibroblasts results in a reduction of bacterial Tir levels, in contrast ectopically expressed Tir is not reduced. The levels of EspF or EspB effectors are not altered in Nck-deficient cell, whereas the levels of Map effector are also reduced in these cells.
2. Nck depletion in the human cell line HeLa results in the reduction of Tir levels, although less remarkable than in mouse embryonic fibroblasts.
3. The levels of Tir are not reduced in N-WASP-deficient cells infected by EPEC.
4. The number of bacteria per cell is not the limiting factor for the reduced levels of Tir in cells that lack Nck.
5. The adhesion of EPEC to murine cells is affected by the absence of Nck and is more dependent on Tir-intimin interaction than that of HeLa cells.
6. The tyrosine phosphorylation of the small fraction of Tir found in Nck-deficient cells is not impaired and Tir is stably inserted in the membrane up to six hours.
7. The reduction in the levels of Tir in Nck-deficient cells is not dependent of the phosphorylation status of Tir.
8. *De novo* protein synthesis in EPEC is necessary for the conversion of the modified to fully modified form of Tir in Nck-deficient cells.
9. Neither the inhibition of proteasome, nor of caspases or proteases was accompanied by an increase in the levels of Tir in Nck-deficient cells. The absence of calpain1/2 does not promote an increase in the levels of Tir.
10. The treatment of Nck-deficient cells with Trichostatin A increases the levels of Tir, EspF and EspB, the efficiency of pedestal formation and the adhesion of EPEC to these cells.

SPANISH SUMMARY

SPANISH SUMMARY
(Resumen en Español)

Escherichia coli enteropatógena (EPEC) es un patógeno entérico que causa inflamación intestinal y diarrea aguda, constituyendo una de las principales causas de mortalidad infantil en los países en vías de desarrollo. EPEC es capaz de adherirse a las células del epitelio intestinal formando una lesión histopatológica conocida como de adherencia y destrucción (A/E) (del inglés *attaching and effacing*) caracterizada por la destrucción local de las microvellosidades, la adherencia íntima de la bacteria a la membrana plasmática de la célula hospedadora y la formación de una estructura rica en filamentos de actina denominada pedestal. De esta forma la bacteria induce la reorganización del citoesqueleto de actina permaneciendo en la superficie extracelular y constituye un modelo útil para el estudio de las rutas de señalización celular en respuesta a estímulos externos.

Una de las proteínas bacterianas esenciales para la formación del pedestal es Tir (del inglés *translocated intimin receptor*) que es translocada por la bacteria a través de la membrana plasmática gracias a un sistema de secreción tipo III. Una vez en el interior de la célula, Tir se inserta en la membrana plasmática siendo susceptible de fosforilación por proteínas quinasas celulares. Numerosas proteínas celulares, incluidas N-WASP, cortactina y el complejo Arp2/3, son atraídas a los sitios de adhesión de la bacteria para estimular la polimerización de actina dando lugar a la formación del pedestal. El reclutamiento de N-WASP es inducido principalmente por la interacción de la proteína adaptadora Nck con la proteína Tir fosforilada en el residuo de tirosina Y474. Hasta el momento la ruta de señalización Tir:Nck:N-WASP es considerada la vía principal para la polimerización de actina en los pedestales formados por la bacteria. Sin embargo, también se produce la polimerización de actina inducida por Tir de manera independiente de la proteína Nck en menor grado.

Cortactina es una proteína de unión a filamentos de actina que fue inicialmente identificada como un sustrato de la tirosina quinasa v-Src. Hoy en día se sabe que

cortactina es una oncoproteína implicada en migración, invasión y metástasis tumoral. Esta proteína está involucrada además en muchos otros procesos relacionados con la dinámica de membrana y la reorganización del citoesqueleto, incluyendo fenómenos de motilidad celular, endocitosis, formación de uniones intracelulares e invasión bacteriana.

Existen numerosos patógenos bacterianos como EPEC, *Shigella* y *Helicobacter pylory*, capaces de manipular en su propio beneficio el citoesqueleto de actina de las células eucariotas. Muchos de estos patógenos tienen como diana la oncoproteína cortactina. El primer objetivo de la tesis doctoral ha sido el estudio de la contribución de la proteína cortactina en el proceso de polimerización de actina durante la formación del pedestal por EPEC. Este objetivo se enmarca dentro del modelo propuesto de regulación de la interacción de cortactina y N-WASP denominado "interruptor de encendido-apagado" (del inglés *S-Y switch model*), según el cual la activación de N-WASP por cortactina es promovida por la fosforilación por la serina treonina quinasa Erk e inhibida por la fosforilación por la tirosina quinasa Src (Martinez-Quiles et al., 2004).

En el momento de inicio de este trabajo existían dos publicaciones del mismo grupo acerca de la contribución de cortactina en la formación del pedestal. En primer lugar el grupo de Cantarelli demostró mediante técnicas de microscopia confocal que cortactina se acumula en los sitios de adhesión de EPEC en células HeLa (Cantarelli et al., 2000). En el año 2002 el mismo grupo describió que la sobreexpresión de formas truncadas de la proteína que carecen del extremo amino terminal inhibe la formación de pedestales en células HeLa infectadas por EPEC. Estos datos sugerían un papel esencial de cortactina en la formación del pedestal por EPEC. Además, en este trabajo observaron mediante técnicas de inmunoprecipitación que los complejos de Tir contienen cortactina (Cantarelli et al., 2002). Basándose en los datos expuestos, la hipótesis inicial era la participación de cortactina en la ruta principal de señalización Tir:Nck:N-WASP para la polimerización de actina en la formación de pedestales por EPEC.

La infección por EPEC provoca el reclutamiento de otras muchas proteínas de la célula eucariota, algunas de ellas implicadas en la regulación de adhesiones focales, como talina y vinculina, y también diversas proteínas adaptadoras como p130Cas y Crk. La función de muchas de estas proteínas es desconocida, tal es el caso de la proteína adaptadora Crk cuya localización en los pedestales formados por EPEC en células HeLa se describió en el año 2001 (Goosney et al., 2001). Además la proteína Crk había sido implicada en la internalización de *Shigella* en células epiteliales mediante la interacción con cortactina fosforilada en residuos de tirosina. La interacción entre Crk y cortactina se describió como necesaria para la polimerización de actina requerida para la entrada de la bacteria en la célula hospedadora. Teniendo en cuenta estos datos, en la segunda parte de la tesis nos propusimos investigar el papel de Crk durante la formación de los pedestales por EPEC.

Durante la consecución del primero de los objetivos se realizaron experimentos usando como herramienta la línea celular de fibroblastos embrionarios de ratón que carecen de la proteína Nck. Los resultados obtenidos demostraron que las células deficientes en Nck infectadas por EPEC presentaban una drástica reducción de los niveles de la proteína bacteriana Tir. Debido a la importancia de esta proteína en el proceso de formación de pedestales por EPEC, contribuyendo a la ruta de señalización principal, decidimos estudiar este fenómeno en profundidad.

Así mismo los **objetivos** de esta tesis se han dividido en tres partes:

<u>Parte I</u>

1. Estudio del papel de cortactina en la formación del pedestal por *Escherichia coli* enteropatógena (EPEC) y de la implicación del modelo "interruptor de encendido-apagado" propuesto para la regulación de cortactina por fosforilación por las quinasas Erk y Src.
2. Estudio de contribución de cortactina a la activación de la polimerización de actina mediada por complejo Arp2/3 en los pedestales formados por EPEC.

Parte II

1. Estudio del papel de la proteína adaptadora Crk en la formación del pedestal por EPEC.

Parte III

1. Papel de la proteína adaptadora Nck en la regulación de la translocación y/o degradación de la proteína bacteriana Tir.

Las principales **conclusiones** obtenidas del trabajo son:

Parte I

1. La proteína cortactina es necesaria para la formación del pedestal por EPEC. Asimismo, tanto el dominio NTA de cortactina, mediante el cual se une al complejo Arp2/3, como el dominio SH3 tienen un papel importante en la formación del pedestal.
2. La fosforilación en serinas de cortactina, presumiblemente por la serina treonina quinasa Erk, regula positivamente la formación del pedestal. Por otro lado, es necesaria la existencia de fosforilación en tirosinas de manera cíclica para la formación del pedestal por EPEC.
3. EPEC induce la fosforilación de cortactina tanto en residuos de tirosina como en residuos de serina. Además, esta fosforilación es dependiente de la proteína N-WASP. Así mismo se demuestra que la activación de la tirosina quinasa Src es independiente de la ausencia de la proteína N-WASP, mientras que la activación de Erk si depende de N-WASP.
4. La fosforilación en serinas de cortactina es independiente de la presencia de Nck. Además, tanto Src como Erk se activan en las células murinas embrionarias que carecen de Nck tras la infección con EPEC.
5. La interacción directa entre cortactina y la proteína bacteriana Tir *in vitro* promueve la polimerización de actina mediada por el complejo Arp2/3, de manera además independiente del estado de fosforilación de cortactina.
6. La interacción entre cortactina y Tir ocurre en ausencia de la proteína N-WASP.

Parte II

1. Las proteínas adaptadoras de la familia Crk tienen un papel redundante e inhibitorio en la formación del pedestal por EPEC.

Parte III

1. Las células murinas embrionarias que carecen de Nck infectadas por EPEC presentan una notable reducción de los niveles de la proteína bacteriana Tir. Por el contrario, los niveles de expresión de Tir transfectado en estas células no se ven disminuidos. Los niveles de otros dos efectores de EPEC, EspF y EspB no se han visto alterados en ausencia de Nck, sin embargo los niveles del efector Map también aparecen reducidos en las células murinas deficientes en Nck.
2. La inhibición de la expresión de Nck mediante ARN de interferencia en la línea de células humana HeLa también conlleva una reducción en los niveles de Tir en células infectadas con EPEC, sin embargo esta reducción no es tan drástica como se observa en la línea celular carente de Nck.
3. Los niveles de Tir detectados en las células deficientes en N-WASP infectadas por EPEC no se han visto alterados.
4. El número de bacterias por célula (multiplicidad de infección o MOI) no es el factor limitante en la reducción de los niveles de Tir en las células deficientes en Nck.
5. La adhesión de EPEC a las células murinas deficientes en Nck requiere la presencia de Nck y tiene mayor grado de dependencia de la presencia de intimina y Tir que a las células humanas HeLa.
6. La fracción de Tir detectable en las células murinas deficientes en Nck está fosforilada en tirosinas y establemente insertada en la membrana de la célula hospedadora después de seis horas de infección por EPEC.
7. La reducción de Tir observada en las células murinas deficientes en Nck no es dependiente del estado de fosforilación de Tir.
8. La síntesis proteica bacteriana *de novo* es necesaria para la correcta conversión de la forma parcialmente modificada de Tir a la forma completamente modificada de Tir en las células murinas deficientes en Nck.

9. La inhibición del proteasoma, de proteínas caspasas, proteasas o la ausencia de las calpainas1/2 no afecta a los niveles de Tir en las células murinas deficientes en Nck.
10. El tratamiento con el inhibidor Trichostatin A (TSA) en células murinas deficientes en Nck conlleva un aumento en los niveles de Tir, de EspF y de EspB. Asimismo dicho tratamiento aumenta tanto la eficiencia de formación de pedestales como la adhesión de EPEC a dichas células.

REFERENCES

REFERENCES

Abe, A., M. de Grado, R.A. Pfuetzner, C. Sanchez-Sanmartin, R. Devinney, J.L. Puente, N.C. Strynadka, and B.B. Finlay. 1999. Enteropathogenic *Escherichia coli* translocated intimin receptor, Tir, requires a specific chaperone for stable secretion. *Molecular microbiology*. 33:1162-1175.

Alto, N.M., A.W. Weflen, M.J. Rardin, D. Yarar, C.S. Lazar, R. Tonikian, A. Koller, S.S. Taylor, C. Boone, S.S. Sidhu, S.L. Schmid, G.A. Hecht, and J.E. Dixon. 2007. The type III effector EspF coordinates membrane trafficking by the spatiotemporal activation of two eukaryotic signaling pathways. *The Journal of cell biology*. 178:1265-1278.

Ammer, A.G., and S.A. Weed. 2008. Cortactin branches out: roles in regulating protrusive actin dynamics. *Cell motility and the cytoskeleton*. 65:687-707.

Antoku, S., and B.J. Mayer. 2009. Distinct roles for Crk adaptor isoforms in actin reorganization induced by extracellular signals. *Journal of cell science*. 122:4228-4238.

Antoku, S., K. Saksela, G.M. Rivera, and B.J. Mayer. 2008. A crucial role in cell spreading for the interaction of Abl PxxP motifs with Crk and Nck adaptors. *Journal of cell science*. 121:3071-3082.

Anton, I.M., W. Lu, B.J. Mayer, N. Ramesh, and R.S. Geha. 1998. The Wiskott-Aldrich syndrome protein-interacting protein (WIP) binds to the adaptor protein Nck. *The Journal of biological chemistry*. 273:20992-20995.

Balkovetz, D.F., and J. Katz. 2003. Bacterial invasion by a paracellular route: divide and conquer. *Microbes Infect*. 5:613-619.

Barneda-Zahonero, B., and M. Parra. 2012. Histone deacetylases and cancer. *Mol Oncol*.

Batchelor, M., S. Prasannan, S. Daniell, S. Reece, I. Connerton, G. Bloomberg, G. Dougan, G. Frankel, and S. Matthews. 2000. Structural basis for recognition of the translocated intimin receptor (Tir) by intimin from enteropathogenic *Escherichia coli*. *The EMBO journal*. 19:2452-2464.

Berger, C.N., V.F. Crepin, M.A. Jepson, A. Arbeloa, and G. Frankel. 2009. The mechanisms used by enteropathogenic *Escherichia coli* to control filopodia dynamics. *Cellular microbiology*. 11:309-322.

Birge, R.B., J.E. Fajardo, C. Reichman, S.E. Shoelson, Z. Songyang, L.C. Cantley, and H. Hanafusa. 1993. Identification and characterization of a high-affinity interaction between v-Crk and tyrosine-phosphorylated paxillin in CT10-transformed fibroblasts. *Molecular and cellular biology*. 13:4648-4656.

Birge, R.B., C. Kalodimos, F. Inagaki, and S. Tanaka. 2009. Crk and CrkL adaptor proteins: networks for physiological and pathological signaling. *Cell Commun Signal*. 7:13.

Bladt, F., E. Aippersbach, S. Gelkop, G.A. Strasser, P. Nash, A. Tafuri, F.B. Gertler, and T. Pawson. 2003. The murine Nck SH2/SH3 adaptors are important for the development of mesoderm-derived embryonic structures and for regulating the cellular actin network. *Molecular and cellular biology*. 23:4586-4597.

Bommarius, B., D. Maxwell, A. Swimm, S. Leung, A. Corbett, W. Bornmann, and D. Kalman. 2007. Enteropathogenic *Escherichia coli* Tir is an SH2/3 ligand that

recruits and activates tyrosine kinases required for pedestal formation. *Molecular microbiology*. 63:1748-1768.

Bougneres, L., S.E. Girardin, S.A. Weed, A.V. Karginov, J.C. Olivo-Marin, J.T. Parsons, P.J. Sansonetti, and G.T. Van Nhieu. 2004. Cortactin and Crk cooperate to trigger actin polymerization during *Shigella* invasion of epithelial cells. *The Journal of cell biology*. 166:225-235.

Bowden, E.T., M. Barth, D. Thomas, R.I. Glazer, and S.C. Mueller. 1999. An invasion-related complex of cortactin, paxillin and PKCmu associates with invadopodia at sites of extracellular matrix degradation. *Oncogene*. 18:4440-4449.

Boyle, S.N., G.A. Michaud, B. Schweitzer, P.F. Predki, and A.J. Koleske. 2007. A critical role for cortactin phosphorylation by Abl-family kinases in PDGF-induced dorsal-wave formation. *Curr Biol*. 17:445-451.

Brandt, S., B. Kenny, M. Rohde, N. Martinez-Quiles, and S. Backert. 2009. Dual infection system identifies a crucial role for PKA-mediated serine phosphorylation of the EPEC-Tir-injected effector protein in regulating Rac1 function. *Cellular microbiology*. 11:1254-1271.

Bray, H.A. 1945. Strict bed rest in pulmonary tuberculosis; an appraisal. *Am Rev Tuberc*. 52:483-489.

Bryce, J., C. Boschi-Pinto, K. Shibuya, and R.E. Black. 2005. WHO estimates of the causes of death in children. *Lancet*. 365:1147-1152.

Buday, L., L. Wunderlich, and P. Tamas. 2002. The Nck family of adapter proteins: regulators of actin cytoskeleton. *Cellular signalling*. 14:723-731.

Burton, E.A., R. Plattner, and A.M. Pendergast. 2003. Abl tyrosine kinases are required for infection by *Shigella flexneri*. *The EMBO journal*. 22:5471-5479.

Caldieri, G., I. Ayala, F. Attanasio, and R. Buccione. 2009. Cell and molecular biology of invadopodia. *Int Rev Cell Mol Biol*. 275:1-34.

Campbell, D.H., R.L. Sutherland, and R.J. Daly. 1999. Signaling pathways and structural domains required for phosphorylation of EMS1/cortactin. *Cancer research*. 59:5376-5385.

Campellone, K.G., A. Giese, D.J. Tipper, and J.M. Leong. 2002. A tyrosine-phosphorylated 12-amino-acid sequence of enteropathogenic *Escherichia coli* Tir binds the host adaptor protein Nck and is required for Nck localization to actin pedestals. *Molecular microbiology*. 43:1227-1241.

Campellone, K.G., and J.M. Leong. 2005. Nck-independent actin assembly is mediated by two phosphorylated tyrosines within enteropathogenic *Escherichia coli* Tir. *Molecular microbiology*. 56:416-432.

Campellone, K.G., S. Rankin, T. Pawson, M.W. Kirschner, D.J. Tipper, and J.M. Leong. 2004a. Clustering of Nck by a 12-residue Tir phosphopeptide is sufficient to trigger localized actin assembly. *The Journal of cell biology*. 164:407-416.

Campellone, K.G., D. Robbins, and J.M. Leong. 2004b. EspFU is a translocated EHEC effector that interacts with Tir and N-WASP and promotes Nck-independent actin assembly. *Developmental cell*. 7:217-228.

Campellone, K.G., and M.D. Welch. 2010. A nucleator arms race: cellular control of actin assembly. *Nat Rev Mol Cell Biol*. 11:237-251.

Cantarelli, V.V., T. Kodama, N. Nijstad, S.K. Abolghait, T. Iida, and T. Honda. 2006. Cortactin is essential for F-actin assembly in enteropathogenic *Escherichia coli* (EPEC)- and enterohaemorrhagic *E. coli* (EHEC)-induced pedestals and the

alpha-helical region is involved in the localization of cortactin to bacterial attachment sites. *Cellular microbiology*. 8:769-780.

Cantarelli, V.V., T. Kodama, N. Nijstad, S.K. Abolghait, S. Nada, M. Okada, T. Iida, and T. Honda. 2007. Tyrosine phosphorylation controls cortactin binding to two enterohaemorrhagic *Escherichia coli* effectors: Tir and EspFu/TccP. *Cellular microbiology*.

Cantarelli, V.V., A. Takahashi, Y. Akeda, K. Nagayama, and T. Honda. 2000. Interaction of enteropathogenic or enterohemorrhagic *Escherichia coli* with HeLa cells results in translocation of cortactin to the bacterial adherence site. *Infection and immunity*. 68:382-386.

Cantarelli, V.V., A. Takahashi, I. Yanagihara, Y. Akeda, K. Imura, T. Kodama, G. Kono, Y. Sato, T. Iida, and T. Honda. 2002. Cortactin is necessary for F-actin accumulation in pedestal structures induced by enteropathogenic *Escherichia coli* infection. *Infection and immunity*. 70:2206-2209.

Cao, D.J., Z.V. Wang, P.K. Battiprolu, N. Jiang, C.R. Morales, Y. Kong, B.A. Rothermel, T.G. Gillette, and J.A. Hill. 2011. Histone deacetylase (HDAC) inhibitors attenuate cardiac hypertrophy by suppressing autophagy. *Proceedings of the National Academy of Sciences of the United States of America*. 108:4123-4128.

Caron, E., V.F. Crepin, N. Simpson, S. Knutton, J. Garmendia, and G. Frankel. 2006. Subversion of actin dynamics by EPEC and EHEC. *Current opinion in microbiology*. 9:40-45.

Cicchetti, P., B.J. Mayer, G. Thiel, and D. Baltimore. 1992. Identification of a protein that binds to the SH3 region of Abl and is similar to Bcr and GAP-rho. *Science (New York, N.Y.* 257:803-806.

Clark, E.S., A.S. Whigham, W.G. Yarbrough, and A.M. Weaver. 2007. Cortactin is an essential regulator of matrix metalloproteinase secretion and extracellular matrix degradation in invadopodia. *Cancer research*. 67:4227-4235.

Colicelli, J. 2010. ABL tyrosine kinases: evolution of function, regulation, and specificity. *Sci Signal*. 3:re6.

Cornelis, G.R. 2006. The type III secretion injectisome. *Nature reviews*. 4:811-825.

Cosen-Binker, L.I., and A. Kapus. 2006. Cortactin: the gray eminence of the cytoskeleton. *Physiology (Bethesda, Md*. 21:352-361.

Cowieson, N.P., G. King, D. Cookson, I. Ross, T. Huber, D.A. Hume, B. Kobe, and J.L. Martin. 2008. Cortactin adopts a globular conformation and bundles actin into sheets. *The Journal of biological chemistry*. 283:16187-16193.

Creasey, E.A., R.M. Delahay, A.A. Bishop, R.K. Shaw, B. Kenny, S. Knutton, and G. Frankel. 2003. CesT is a bivalent enteropathogenic *Escherichia coli* chaperone required for translocation of both Tir and Map. *Molecular microbiology*. 47:209-221.

Crepin, V.F., F. Girard, S. Schuller, A.D. Phillips, A. Mousnier, and G. Frankel. 2010. Dissecting the role of the Tir:Nck and Tir:IRTKS signaling pathways *in vivo*. *Molecular microbiology*.

Croxen, M.A., and B.B. Finlay. 2010. Molecular mechanisms of *Escherichia coli* pathogenicity. *Nature reviews*. 8:26-38.

Cheng, H.C., B.M. Skehan, K.G. Campellone, J.M. Leong, and M.K. Rosen. 2008. Structural mechanism of WASP activation by the enterohaemorrhagic *E. coli* effector EspF(U). *Nature*. 454:1009-1013.

Ching, J.C., N.L. Jones, P.J. Ceponis, M.A. Karmali, and P.M. Sherman. 2002. *Escherichia coli* shiga-like toxins induce apoptosis and cleavage of poly(ADP-ribose) polymerase via *in vitro* activation of caspases. *Infection and immunity*. 70:4669-4677.

Daly, R.J. 2004. Cortactin signalling and dynamic actin networks. *The Biochemical journal*. 382:13-25.

Darkoh, C., and H.L. Dupont. 2011. Unraveling the Role of Host Endocytic Proteins in Pedestal Formation During Enteropathogenic *Escherichia coli* Infection. *The Journal of infectious diseases*. 204:667-668.

de Jong, R., J. ten Hoeve, N. Heisterkamp, and J. Groffen. 1997. Tyrosine 207 in CRKL is the BCR/ABL phosphorylation site. *Oncogene*. 14:507-513.

Dean, P., and B. Kenny. 2004. Intestinal barrier dysfunction by enteropathogenic *Escherichia coli* is mediated by two effector molecules and a bacterial surface protein. *Molecular microbiology*. 54:665-675.

Dean, P., M. Maresca, S. Schuller, A.D. Phillips, and B. Kenny. 2006. Potent diarrheagenic mechanism mediated by the cooperative action of three enteropathogenic *Escherichia coli*-injected effector proteins. *Proceedings of the National Academy of Sciences of the United States of America*. 103:1876-1881.

Dean, P., S. Muhlen, S. Quitard, and B. Kenny. 2010. The bacterial effectors EspG and EspG2 induce a destructive calpain activity that is kept in check by the co-delivered Tir effector. *Cellular microbiology*.

Dehio, C., M.C. Prevost, and P.J. Sansonetti. 1995. Invasion of epithelial cells by *Shigella flexneri* induces tyrosine phosphorylation of cortactin by a pp60c-src-mediated signalling pathway. *The EMBO journal*. 14:2471-2482.

Deibel, C., S. Kramer, T. Chakraborty, and F. Ebel. 1998. EspE, a novel secreted protein of attaching and effacing bacteria, is directly translocated into infected host cells, where it appears as a tyrosine-phosphorylated 90 kDa protein. *Molecular microbiology*. 28:463-474.

Delahay, R.M., and G. Frankel. 2002. Coiled-coil proteins associated with type III secretion systems: a versatile domain revisited. *Molecular microbiology*. 45:905-916.

Deng, W., J.L. Puente, S. Gruenheid, Y. Li, B.A. Vallance, A. Vazquez, J. Barba, J.A. Ibarra, P. O'Donnell, P. Metalnikov, K. Ashman, S. Lee, D. Goode, T. Pawson, and B.B. Finlay. 2004. Dissecting virulence: systematic and functional analyses of a pathogenicity island. *Proceedings of the National Academy of Sciences of the United States of America*. 101:3597-3602.

Deng, W., B.A. Vallance, Y. Li, J.L. Puente, and B.B. Finlay. 2003. *Citrobacter rodentium* translocated intimin receptor (Tir) is an essential virulence factor needed for actin condensation, intestinal colonization and colonic hyperplasia in mice. *Molecular microbiology*. 48:95-115.

Derry, J.M., H.D. Ochs, and U. Francke. 1994. Isolation of a novel gene mutated in Wiskott-Aldrich syndrome. *Cell*. 78:635-644.

DeVinney, R., M. Stein, D. Reinscheid, A. Abe, S. Ruschkowski, and B.B. Finlay. 1999. Enterohemorrhagic *Escherichia coli* O157:H7 produces Tir, which is translocated to the host cell membrane but is not tyrosine phosphorylated. *Infection and immunity*. 67:2389-2398.

Dokainish, H., B. Gavicherla, Y. Shen, and K. Ireton. 2007. The carboxyl-terminal SH3 domain of the mammalian adaptor CrkII promotes internalization of *Listeria monocytogenes* through activation of host phosphoinositide 3-kinase. *Cellular microbiology*. 9:2497-2516.

Dong, N., L. Liu, and F. Shao. 2010. A bacterial effector targets host DH-PH domain RhoGEFs and antagonizes macrophage phagocytosis. *The EMBO journal*. 29:1363-1376.

Donnenberg, M.S., and J.B. Kaper. 1991. Construction of an eae deletion mutant of enteropathogenic *Escherichia coli* by using a positive-selection suicide vector. *Infection and immunity*. 59:4310-4317.

Donnenberg, M.S., J.B. Kaper, and B.B. Finlay. 1997. Interactions between enteropathogenic *Escherichia coli* and host epithelial cells. *Trends in microbiology*. 5:109-114.

Donnenberg, M.S., C.O. Tacket, S.P. James, G. Losonsky, J.P. Nataro, S.S. Wasserman, J.B. Kaper, and M.M. Levine. 1993a. Role of the eaeA gene in experimental enteropathogenic *Escherichia coli* infection. *The Journal of clinical investigation*. 92:1412-1417.

Donnenberg, M.S., S. Tzipori, M.L. McKee, A.D. O'Brien, J. Alroy, and J.B. Kaper. 1993b. The role of the eae gene of enterohemorrhagic *Escherichia coli* in intimate attachment *in vitro* and in a porcine model. *The Journal of clinical investigation*. 92:1418-1424.

Du, Y., S.A. Weed, W.C. Xiong, T.D. Marshall, and J.T. Parsons. 1998. Identification of a novel cortactin SH3 domain-binding protein and its localization to growth cones of cultured neurons. *Molecular and cellular biology*. 18:5838-5851.

Elliott, S.J., S.W. Hutcheson, M.S. Dubois, J.L. Mellies, L.A. Wainwright, M. Batchelor, G. Frankel, S. Knutton, and J.B. Kaper. 1999. Identification of CesT, a chaperone for the type III secretion of Tir in enteropathogenic *Escherichia coli*. *Molecular microbiology*. 33:1176-1189.

Elliott, S.J., C.B. O'Connell, A. Koutsouris, C. Brinkley, M.S. Donnenberg, G. Hecht, and J.B. Kaper. 2002. A gene from the locus of enterocyte effacement that is required for enteropathogenic *Escherichia coli* to increase tight-junction permeability encodes a chaperone for EspF. *Infection and immunity*. 70:2271-2277.

Elliott, S.J., V. Sperandio, J.A. Giron, S. Shin, J.L. Mellies, L. Wainwright, S.W. Hutcheson, T.K. McDaniel, and J.B. Kaper. 2000. The locus of enterocyte effacement (LEE)-encoded regulator controls expression of both LEE- and non-LEE-encoded virulence factors in enteropathogenic and enterohemorrhagic *Escherichia coli*. *Infection and immunity*. 68:6115-6126.

Feller, S.M. 2001. Crk family adaptors-signalling complex formation and biological roles. *Oncogene*. 20:6348-6371.

Feller, S.M., B. Knudsen, and H. Hanafusa. 1994. c-Abl kinase regulates the protein binding activity of c-Crk. *The EMBO journal*. 13:2341-2351.

Finlay, B.B., and P. Cossart. 1997. Exploitation of mammalian host cell functions by bacterial pathogens. *Science (New York, N.Y.*. 276:718-725.

Fioretos, T., N. Heisterkamp, J. Groffen, S. Benjes, and C. Morris. 1993. CRK proto-oncogene maps to human chromosome band 17p13. *Oncogene*. 8:2853-2855.

Frankel, G., D.C. Candy, E. Fabiani, J. Adu-Bobie, S. Gil, M. Novakova, A.D. Phillips, and G. Dougan. 1995. Molecular characterization of a carboxy-terminal eukaryotic-cell-

binding domain of intimin from enteropathogenic *Escherichia coli*. *Infection and immunity*. 63:4323-4328.

Frankel, G., A.D. Phillips, I. Rosenshine, G. Dougan, J.B. Kaper, and S. Knutton. 1998. Enteropathogenic and enterohaemorrhagic *Escherichia coli*: more subversive elements. *Molecular microbiology*. 30:911-921.

Frischknecht, F., V. Moreau, S. Rottger, S. Gonfloni, I. Reckmann, G. Superti-Furga, and M. Way. 1999. Actin-based motility of *vaccinia virus* mimics receptor tyrosine kinase signalling. *Nature*. 401:926-929.

Frischknecht, F., and M. Way. 2001. Surfing pathogens and the lessons learned for actin polymerization. *Trends in cell biology*. 11:30-38.

Furumai, R., A. Ito, K. Ogawa, S. Maeda, A. Saito, N. Nishino, S. Horinouchi, and M. Yoshida. 2011. Histone deacetylase inhibitors block nuclear factor-kappaB-dependent transcription by interfering with RNA polymerase II recruitment. *Cancer Sci*. 102:1081-1087.

Garmendia, J., G. Frankel, and V.F. Crepin. 2005. Enteropathogenic and enterohemorrhagic *Escherichia coli* infections: translocation, translocation, translocation. *Infection and immunity*. 73:2573-2585.

Garmendia, J., A.D. Phillips, M.F. Carlier, Y. Chong, S. Schuller, O. Marches, S. Dahan, E. Oswald, R.K. Shaw, S. Knutton, and G. Frankel. 2004. TccP is an enterohaemorrhagic *Escherichia coli* O157:H7 type III effector protein that couples Tir to the actin-cytoskeleton. *Cellular microbiology*. 6:1167-1183.

Germane, K.L., and B.W. Spiller. 2011. Structural and functional studies indicate that the EPEC effector, EspG, directly binds p21-activated kinase. *Biochemistry*. 50:917-919.

Ghosh, P. 2004. Process of protein transport by the type III secretion system. *Microbiol Mol Biol Rev*. 68:771-795.

Goosney, D.L., R. DeVinney, and B.B. Finlay. 2001. Recruitment of cytoskeletal and signaling proteins to enteropathogenic and enterohemorrhagic *Escherichia coli* pedestals. *Infection and immunity*. 69:3315-3322.

Grassart, A., V. Meas-Yedid, A. Dufour, J.C. Olivo-Marin, A. Dautry-Varsat, and N. Sauvonnet. 2010. Pak1 phosphorylation enhances cortactin-N-WASP interaction in clathrin-caveolin-independent endocytosis. *Traffic*. 11:1079-1091.

Gruenheid, S., R. DeVinney, F. Bladt, D. Goosney, S. Gelkop, G.D. Gish, T. Pawson, and B.B. Finlay. 2001. Enteropathogenic *E. coli* Tir binds Nck to initiate actin pedestal formation in host cells. *Nature cell biology*. 3:856-859.

Guris, D.L., J. Fantes, D. Tara, B.J. Druker, and A. Imamoto. 2001. Mice lacking the homologue of the human 22q11.2 gene CRKL phenocopy neurocristopathies of DiGeorge syndrome. *Nat Genet*. 27:293-298.

Hardwidge, P.R., W. Deng, B.A. Vallance, I. Rodriguez-Escudero, V.J. Cid, M. Molina, and B.B. Finlay. 2005. Modulation of host cytoskeleton function by the enteropathogenic *Escherichia coli* and *Citrobacter rodentium* effector protein EspG. *Infection and immunity*. 73:2586-2594.

Hashimoto, Y., H. Katayama, E. Kiyokawa, S. Ota, T. Kurata, N. Gotoh, N. Otsuka, M. Shibata, and M. Matsuda. 1998. Phosphorylation of CrkII adaptor protein at tyrosine 221 by epidermal growth factor receptor. *The Journal of biological chemistry*. 273:17186-17191.

Hayward, R.D., J.M. Leong, V. Koronakis, and K.G. Campellone. 2006. Exploiting pathogenic *Escherichia coli* to model transmembrane receptor signalling. *Nature reviews*. 4:358-370.

Hecht, G. 1999. Innate mechanisms of epithelial host defense: spotlight on intestine. *Am J Physiol*. 277:C351-358.

Hemrajani, C., C.N. Berger, K.S. Robinson, O. Marches, A. Mousnier, and G. Frankel. 2010. NleH effectors interact with Bax inhibitor-1 to block apoptosis during enteropathogenic *Escherichia coli* infection. *Proceedings of the National Academy of Sciences of the United States of America*. 107:3129-3134.

Hemrajani, C., O. Marches, S. Wiles, F. Girard, A. Dennis, F. Dziva, A. Best, A.D. Phillips, C.N. Berger, A. Mousnier, V.F. Crepin, L. Kruidenier, M.J. Woodward, M.P. Stevens, R.M. La Ragione, T.T. MacDonald, and G. Frankel. 2008. Role of NleH, a type III secreted effector from attaching and effacing pathogens, in colonization of the bovine, ovine, and murine gut. *Infection and immunity*. 76:4804-4813.

Hoffmann, I., E. Eugene, X. Nassif, P.O. Couraud, and S. Bourdoulous. 2001. Activation of ErbB2 receptor tyrosine kinase supports invasion of endothelial cells by *Neisseria meningitidis*. *The Journal of cell biology*. 155:133-143.

Holmes, A., S. Muhlen, A.J. Roe, and P. Dean. 2010. The EspF effector, a bacterial pathogen's Swiss army knife. *Infection and immunity*. 78:4445-4453.

Hoshikawa, Y., H.J. Kwon, M. Yoshida, S. Horinouchi, and T. Beppu. 1994. Trichostatin A induces morphological changes and gelsolin expression by inhibiting histone deacetylase in human carcinoma cell lines. *Exp Cell Res*. 214:189-197.

Huang, C., J. Liu, C.C. Haudenschild, and X. Zhan. 1998. The role of tyrosine phosphorylation of cortactin in the locomotion of endothelial cells. *The Journal of biological chemistry*. 273:25770-25776.

Huang, C., Y. Ni, T. Wang, Y. Gao, C.C. Haudenschild, and X. Zhan. 1997. Down-regulation of the filamentous actin cross-linking activity of cortactin by Src-mediated tyrosine phosphorylation. *The Journal of biological chemistry*. 272:13911-13915.

Hueck, C.J. 1998. Type III protein secretion systems in bacterial pathogens of animals and plants. *Microbiol Mol Biol Rev*. 62:379-433.

Hughes, D.T., and V. Sperandio. 2008. Inter-kingdom signalling: communication between bacteria and their hosts. *Nature reviews*. 6:111-120.

Humphries, R.M., and G.D. Armstrong. 2010. Sticky situation: localized adherence of enteropathogenic *Escherichia coli* to the small intestine epithelium. *Future microbiology*. 5:1645-1661.

Iguchi, A., N.R. Thomson, Y. Ogura, D. Saunders, T. Ooka, I.R. Henderson, D. Harris, M. Asadulghani, K. Kurokawa, P. Dean, B. Kenny, M.A. Quail, S. Thurston, G. Dougan, T. Hayashi, J. Parkhill, and G. Frankel. 2009. Complete genome sequence and comparative genome analysis of enteropathogenic *Escherichia coli* O127:H6 strain E2348/69. *Journal of bacteriology*. 191:347-354.

Iizumi, Y., H. Sagara, Y. Kabe, M. Azuma, K. Kume, M. Ogawa, T. Nagai, P.G. Gillespie, C. Sasakawa, and H. Handa. 2007. The enteropathogenic *E. coli* effector EspB facilitates microvillus effacing and antiphagocytosis by inhibiting myosin function. *Cell host & microbe*. 2:383-392.

Inoue, J., S. Nishiumi, Y. Fujishima, A. Masuda, H. Shiomi, K. Yamamoto, M. Nishida, T. Azuma, and M. Yoshida. 2012. Autophagy in the intestinal epithelium regulates *Citrobacter rodentium* infection. *Arch Biochem Biophys*. 521:95-101.

Jankowski, W., T. Saleh, M.T. Pai, G. Sriram, R.B. Birge, and C.G. Kalodimos. 2012. Domain organization differences explain Bcr-Abl's preference for CrkL over CrkII. *Nat Chem Biol*.

Jarvis, K.G., J.A. Giron, A.E. Jerse, T.K. McDaniel, M.S. Donnenberg, and J.B. Kaper. 1995. Enteropathogenic *Escherichia coli* contains a putative type III secretion system necessary for the export of proteins involved in attaching and effacing lesion formation. *Proceedings of the National Academy of Sciences of the United States of America*. 92:7996-8000.

Jerse, A.E., J. Yu, B.D. Tall, and J.B. Kaper. 1990. A genetic locus of enteropathogenic *Escherichia coli* necessary for the production of attaching and effacing lesions on tissue culture cells. *Proceedings of the National Academy of Sciences of the United States of America*. 87:7839-7843.

Jones, N., I.M. Blasutig, V. Eremina, J.M. Ruston, F. Bladt, H. Li, H. Huang, L. Larose, S.S. Li, T. Takano, S.E. Quaggin, and T. Pawson. 2006. Nck adaptor proteins link nephrin to the actin cytoskeleton of kidney podocytes. *Nature*. 440:818-823.

Kalman, D., O.D. Weiner, D.L. Goosney, J.W. Sedat, B.B. Finlay, A. Abo, and J.M. Bishop. 1999. Enteropathogenic *E. coli* acts through WASP and Arp2/3 complex to form actin pedestals. *Nature cell biology*. 1:389-391.

Kanack, K.J., J.A. Crawford, I. Tatsuno, M.A. Karmali, and J.B. Kaper. 2005. SepZ/EspZ is secreted and translocated into HeLa cells by the enteropathogenic *Escherichia coli* type III secretion system. *Infection and immunity*. 73:4327-4337.

Kaper, J.B., J.P. Nataro, and H.L. Mobley. 2004. Pathogenic *Escherichia coli*. *Nature reviews*. 2:123-140.

Kelley, L.C., K.E. Hayes, A.G. Ammer, K.H. Martin, and S.A. Weed. 2010. Cortactin Phosphorylated by ERK1/2 Localizes to Sites of Dynamic Actin Regulation and Is Required for Carcinoma Lamellipodia Persistence. *PloS one*. 5:e13847.

Kelley, L.C., K.E. Hayes, A.G. Ammer, K.H. Martin, and S.A. Weed. 2011. Revisiting the ERK/Src cortactin switch. *Commun Integr Biol*. 4:205-207.

Kenny, B. 1999. Phosphorylation of tyrosine 474 of the enteropathogenic *Escherichia coli* (EPEC) Tir receptor molecule is essential for actin nucleating activity and is preceded by additional host modifications. *Molecular microbiology*. 31:1229-1241.

Kenny, B. 2001. The enterohaemorrhagic *Escherichia coli* (serotype O157:H7) Tir molecule is not functionally interchangeable for its enteropathogenic E. coli (serotype O127:H6) homologue. *Cellular microbiology*. 3:499-510.

Kenny, B., R. DeVinney, M. Stein, D.J. Reinscheid, E.A. Frey, and B.B. Finlay. 1997. Enteropathogenic *E. coli* (EPEC) transfers its receptor for intimate adherence into mammalian cells. *Cell*. 91:511-520.

Kenny, B., S. Ellis, A.D. Leard, J. Warawa, H. Mellor, and M.A. Jepson. 2002. Co-ordinate regulation of distinct host cell signalling pathways by multifunctional enteropathogenic *Escherichia coli* effector molecules. *Molecular microbiology*. 44:1095-1107.

Kenny, B., and B.B. Finlay. 1997. Intimin-dependent binding of enteropathogenic *Escherichia coli* to host cells triggers novel signaling events, including tyrosine

phosphorylation of phospholipase C-gamma1. *Infection and immunity*. 65:2528-2536.

Kenny, B., and M. Jepson. 2000. Targeting of an enteropathogenic *Escherichia coli* (EPEC) effector protein to host mitochondria. *Cellular microbiology*. 2:579-590.

Kenny, B., and J. Warawa. 2001. Enteropathogenic *Escherichia coli* (EPEC) Tir receptor molecule does not undergo full modification when introduced into host cells by EPEC-independent mechanisms. *Infection and immunity*. 69:1444-1453.

Kim, A.S., L.T. Kakalis, N. Abdul-Manan, G.A. Liu, and M.K. Rosen. 2000. Autoinhibition and activation mechanisms of the Wiskott-Aldrich syndrome protein. *Nature*. 404:151-158.

Kim, J., A. Thanabalasuriar, T. Chaworth-Musters, J.C. Fromme, E.A. Frey, P.I. Lario, P. Metalnikov, K. Rizg, N.A. Thomas, S.F. Lee, E.L. Hartland, P.R. Hardwidge, T. Pawson, N.C. Strynadka, B.B. Finlay, R. Schekman, and S. Gruenheid. 2007. The bacterial virulence factor NleA inhibits cellular protein secretion by disrupting mammalian COPII function. *Cell host & microbe*. 2:160-171.

Kinley, A.W., S.A. Weed, A.M. Weaver, A.V. Karginov, E. Bissonette, J.A. Cooper, and J.T. Parsons. 2003. Cortactin interacts with WIP in regulating Arp2/3 activation and membrane protrusion. *Curr Biol*. 13:384-393.

Kirkbride, K.C., B.H. Sung, S. Sinha, and A.M. Weaver. 2011. Cortactin: a multifunctional regulator of cellular invasiveness. *Cell Adh Migr*. 5:187-198.

Kiyokawa, E., Y. Hashimoto, T. Kurata, H. Sugimura, and M. Matsuda. 1998. Evidence that DOCK180 up-regulates signals from the CrkII-p130(Cas) complex. *The Journal of biological chemistry*. 273:24479-24484.

Knecht, E., C. Aguado, J. Carcel, I. Esteban, J.M. Esteve, G. Ghislat, J.F. Moruno, J.M. Vidal, and R. Saez. 2009. Intracellular protein degradation in mammalian cells: recent developments. *Cell Mol Life Sci*. 66:2427-2443.

Knutton, S., T. Baldwin, P.H. Williams, and A.S. McNeish. 1989. Actin accumulation at sites of bacterial adhesion to tissue culture cells: basis of a new diagnostic test for enteropathogenic and enterohemorrhagic *Escherichia coli*. *Infection and immunity*. 57:1290-1298.

Knutton, S., I. Rosenshine, M.J. Pallen, I. Nisan, B.C. Neves, C. Bain, C. Wolff, G. Dougan, and G. Frankel. 1998. A novel EspA-associated surface organelle of enteropathogenic *Escherichia coli* involved in protein translocation into epithelial cells. *The EMBO journal*. 17:2166-2176.

Kobashigawa, Y., and F. Inagaki. 2012. Structural biology: CrkL is not Crk-like. *Nat Chem Biol*. 8:504-505.

Kobashigawa, Y., M. Sakai, M. Naito, M. Yokochi, H. Kumeta, Y. Makino, K. Ogura, S. Tanaka, and F. Inagaki. 2007. Structural basis for the transforming activity of human cancer-related signaling adaptor protein CRK. *Nature structural & molecular biology*. 14:503-510.

Kruchten, A.E., E.W. Krueger, Y. Wang, and M.A. McNiven. 2008. Distinct phospho-forms of cortactin differentially regulate actin polymerization and focal adhesions. *Am J Physiol Cell Physiol*.

Kubori, T., and J.E. Galan. 2003. Temporal regulation of *salmonella* virulence effector function by proteasome-dependent protein degradation. *Cell*. 115:333-342.

Kurisu, S., and T. Takenawa. 2009. The WASP and WAVE family proteins. *Genome Biol*. 10:226.

Lee, J.Y., H. Koga, Y. Kawaguchi, W. Tang, E. Wong, Y.S. Gao, U.B. Pandey, S. Kaushik, E. Tresse, J. Lu, J.P. Taylor, A.M. Cuervo, and T.P. Yao. 2010. HDAC6 controls autophagosome maturation essential for ubiquitin-selective quality-control autophagy. *The EMBO journal*. 29:969-980.

Lettau, M., J. Pieper, and O. Janssen. 2009. Nck adapter proteins: functional versatility in T cells. *Cell Commun Signal*. 7:1.

Levine, M.M., E.J. Bergquist, D.R. Nalin, D.H. Waterman, R.B. Hornick, C.R. Young, and S. Sotman. 1978. *Escherichia coli* strains that cause diarrhoea but do not produce heat-labile or heat-stable enterotoxins and are non-invasive. *Lancet*. 1:1119-1122.

Li, Y., M. Tondravi, J. Liu, E. Smith, C.C. Haudenschild, M. Kaczmarek, and X. Zhan. 2001. Cortactin potentiates bone metastasis of breast cancer cells. *Cancer research*. 61:6906-6911.

Lin, A.E., A. Benmerah, and J.A. Guttman. 2011. Eps15 and Epsin1 are crucial for enteropathogenic *Escherichia coli* pedestal formation despite the absence of adaptor protein 2. *The Journal of infectious diseases*. 204:695-703.

Lommel, S., S. Benesch, M. Rohde, J. Wehland, and K. Rottner. 2004. Enterohaemorrhagic and enteropathogenic *Escherichia coli* use different mechanisms for actin pedestal formation that converge on N-WASP. *Cellular microbiology*. 6:243-254.

Lommel, S., S. Benesch, K. Rottner, T. Franz, J. Wehland, and R. Kuhn. 2001. Actin pedestal formation by enteropathogenic *Escherichia coli* and intracellular motility of *Shigella flexneri* are abolished in N-WASP-defective cells. *EMBO reports*. 2:850-857.

Lua, B.L., and B.C. Low. 2005. Cortactin phosphorylation as a switch for actin cytoskeletal network and cell dynamics control. *FEBS letters*. 579:577-585.

Luo, Y., E.A. Frey, R.A. Pfuetzner, A.L. Creagh, D.G. Knoechel, C.A. Haynes, B.B. Finlay, and N.C. Strynadka. 2000. Crystal structure of enteropathogenic *Escherichia coli* intimin-receptor complex. *Nature*. 405:1073-1077.

Machesky, L.M., and R.H. Insall. 1998. Scar1 and the related Wiskott-Aldrich syndrome protein, WASP, regulate the actin cytoskeleton through the Arp2/3 complex. *Curr Biol*. 8:1347-1356.

Mader, C.C., M. Oser, M.A. Magalhaes, J.J. Bravo-Cordero, J. Condeelis, A.J. Koleske, and H. Gil-Henn. 2011. An EGFR-Src-Arg-cortactin pathway mediates functional maturation of invadopodia and breast cancer cell invasion. *Cancer research*. 71:1730-1741.

Marchand, J.B., D.A. Kaiser, T.D. Pollard, and H.N. Higgs. 2001. Interaction of WASP/Scar proteins with actin and vertebrate Arp2/3 complex. *Nature cell biology*. 3:76-82.

Marches, O., V. Covarelli, S. Dahan, C. Cougoule, P. Bhatta, G. Frankel, and E. Caron. 2008. EspJ of enteropathogenic and enterohaemorrhagic *Escherichia coli* inhibits opsono-phagocytosis. *Cellular microbiology*. 10:1104-1115.

Marches, O., J.P. Nougayrede, S. Boullier, J. Mainil, G. Charlier, I. Raymond, P. Pohl, M. Boury, J. De Rycke, A. Milon, and E. Oswald. 2000. Role of tir and intimin in the virulence of rabbit enteropathogenic *Escherichia coli* serotype O103:H2. *Infection and immunity*. 68:2171-2182.

Martin, K.H., E.D. Jeffery, P.R. Grigera, J. Shabanowitz, D.F. Hunt, and J.T. Parsons. 2006. Cortactin phosphorylation sites mapped by mass spectrometry. *Journal of cell science*. 119:2851-2853.

Martinez-Quiles, N., H.Y. Ho, M.W. Kirschner, N. Ramesh, and R.S. Geha. 2004. Erk/Src phosphorylation of cortactin acts as a switch on-switch off mechanism that controls its ability to activate N-WASP. *Molecular and cellular biology*. 24:5269-5280.

Martinez-Quiles, N., R. Rohatgi, I.M. Anton, M. Medina, S.P. Saville, H. Miki, H. Yamaguchi, T. Takenawa, J.H. Hartwig, R.S. Geha, and N. Ramesh. 2001. WIP regulates N-WASP-mediated actin polymerization and filopodium formation. *Nature cell biology*. 3:484-491.

Martinez, J.J., and P. Cossart. 2004. Early signaling events involved in the entry of Rickettsia conorii into mammalian cells. *Journal of cell science*. 117:5097-5106.

Matsuda, M., B.J. Mayer, and H. Hanafusa. 1991. Identification of domains of the v-crk oncogene product sufficient for association with phosphotyrosine-containing proteins. *Molecular and cellular biology*. 11:1607-1613.

Matsuda, M., S. Tanaka, S. Nagata, A. Kojima, T. Kurata, and M. Shibuya. 1992. Two species of human CRK cDNA encode proteins with distinct biological activities. *Molecular and cellular biology*. 12:3482-3489.

Matsuyama, A., T. Shimazu, Y. Sumida, A. Saito, Y. Yoshimatsu, D. Seigneurin-Berny, H. Osada, Y. Komatsu, N. Nishino, S. Khochbin, S. Horinouchi, and M. Yoshida. 2002. *In vivo* destabilization of dynamic microtubules by HDAC6-mediated deacetylation. *The EMBO journal*. 21:6820-6831.

Matsuzawa, T., A. Kuwae, S. Yoshida, C. Sasakawa, and A. Abe. 2004. Enteropathogenic *Escherichia coli* activates the RhoA signaling pathway via the stimulation of GEF-H1. *The EMBO journal*. 23:3570-3582.

Mayer, B.J., M. Hamaguchi, and H. Hanafusa. 1988a. Characterization of p47gag-crk, a novel oncogene product with sequence similarity to a putative modulatory domain of protein-tyrosine kinases and phospholipase C. *Cold Spring Harb Symp Quant Biol*. 53 Pt 2:907-914.

Mayer, B.J., M. Hamaguchi, and H. Hanafusa. 1988b. A novel viral oncogene with structural similarity to phospholipase C. *Nature*. 332:272-275.

McDaniel, T.K., K.G. Jarvis, M.S. Donnenberg, and J.B. Kaper. 1995. A genetic locus of enterocyte effacement conserved among diverse enterobacterial pathogens. *Proceedings of the National Academy of Sciences of the United States of America*. 92:1664-1668.

McNamara, B.P., A. Koutsouris, C.B. O'Connell, J.P. Nougayrede, M.S. Donnenberg, and G. Hecht. 2001. Translocated EspF protein from enteropathogenic *Escherichia coli* disrupts host intestinal barrier function. *The Journal of clinical investigation*. 107:621-629.

Meiler, E., E. Nieto-Pelegrin, and N. Martinez-Quiles. 2012. Cortactin tyrosine phosphorylation promotes its deacetylation and inhibits cell spreading. *PloS one*. 7:e33662.

Mejia, E., J.B. Bliska, and G.I. Viboud. 2008. Yersinia controls type III effector delivery into host cells by modulating Rho activity. *PLoS pathogens*. 4:e3.

Mertins, P., H.C. Eberl, J. Renkawitz, J.V. Olsen, M.L. Tremblay, M. Mann, A. Ullrich, and H. Daub. 2008. Investigation of protein-tyrosine phosphatase 1B function by quantitative proteomics. *Mol Cell Proteomics*. 7:1763-1777.

Miki, H., K. Miura, and T. Takenawa. 1996. N-WASP, a novel actin-depolymerizing protein, regulates the cortical cytoskeletal rearrangement in a PIP2-dependent manner downstream of tyrosine kinases. *The EMBO journal*. 15:5326-5335.

Miki, H., T. Sasaki, Y. Takai, and T. Takenawa. 1998. Induction of filopodium formation by a WASP-related actin-depolymerizing protein N-WASP. *Nature*. 391:93-96.

Mills, E., K. Baruch, X. Charpentier, S. Kobi, and I. Rosenshine. 2008. Real-time analysis of effector translocation by the type III secretion system of enteropathogenic *Escherichia coli*. *Cell host & microbe*. 3:104-113.

Mizutani, K., H. Miki, H. He, H. Maruta, and T. Takenawa. 2002. Essential role of neural Wiskott-Aldrich syndrome protein in podosome formation and degradation of extracellular matrix in src-transformed fibroblasts. *Cancer research*. 62:669-674.

Mounier, J., M.R. Popoff, J. Enninga, M.C. Frame, P.J. Sansonetti, and G.T. Van Nhieu. 2009. The IpaC carboxyterminal effector domain mediates Src-dependent actin polymerization during *Shigella* invasion of epithelial cells. *PLoS pathogens*. 5:e1000271.

Mousnier, A., A.D. Whale, S. Schuller, J.M. Leong, A.D. Phillips, and G. Frankel. 2008. Cortactin recruitment by enterohemorrhagic *Escherichia coli* O157:H7 during infection *in vitro* and *ex vivo*. *Infection and immunity*.

Muller, A.J., C. Hoffmann, and W.D. Hardt. 2010. Caspase-1 activation via Rho GTPases: a common theme in mucosal infections? *PLoS pathogens*. 6:e1000795.

Muralidharan, V., K. Dutta, J. Cho, M. Vila-Perello, D.P. Raleigh, D. Cowburn, and T.W. Muir. 2006. Solution structure and folding characteristics of the C-terminal SH3 domain of c-Crk-II. *Biochemistry*. 45:8874-8884.

Nataro, J.P., and J.B. Kaper. 1998. Diarrheagenic *Escherichia coli*. *Clinical microbiology reviews*. 11:142-201.

Neter, E. 1955. *Escherichia coli* diarrhea: an outbreak among infants on a surgical ward. *AMA Am J Dis Child*. 89:564-566.

Nieto-Pelegrin, E., E. Meiler, and N. Martinez-Quiles. 2010. Cortactin, an oncoprotein targeted by pathogens during infection. *In* Current Research, Technology and Education Topics in Applied Microbiology and Microbial Biotechnology. Microbiology book series - Number 2. Vol. Vol. 1. Formatex, editor. 607-614.

Nougayrede, J.P., and M.S. Donnenberg. 2004. Enteropathogenic *Escherichia coli* EspF is targeted to mitochondria and is required to initiate the mitochondrial death pathway. *Cellular microbiology*. 6:1097-1111.

Nougayrede, J.P., P.J. Fernandes, and M.S. Donnenberg. 2003. Adhesion of enteropathogenic *Escherichia coli* to host cells. *Cellular microbiology*. 5:359-372.

Noy, E., S. Fried, O. Matalon, and M. Barda-Saad. 2012. WIP Remodeling Actin behind the Scenes: How WIP Reshapes Immune and Other Functions. *Int J Mol Sci*. 13:7629-7647.

Okamura, H., and M.D. Resh. 1995. p80/85 cortactin associates with the Src SH2 domain and colocalizes with v-Src in transformed cells. *The Journal of biological chemistry*. 270:26613-26618.

Oser, M., H. Yamaguchi, C.C. Mader, J.J. Bravo-Cordero, M. Arias, X. Chen, V. Desmarais, J. van Rheenen, A.J. Koleske, and J. Condeelis. 2009. Cortactin regulates cofilin

and N-WASp activities to control the stages of invadopodium assembly and maturation. *The Journal of cell biology*. 186:571-587.

Padrick, S.B., and M.K. Rosen. 2010. Physical mechanisms of signal integration by WASP family proteins. *Annual review of biochemistry*. 79:707-735.

Pantaloni, D., C. Le Clainche, and M.F. Carlier. 2001. Mechanism of actin-based motility. *Science (New York, N.Y*. 292:1502-1506.

Park, T.J., K. Boyd, and T. Curran. 2006. Cardiovascular and craniofacial defects in Crk-null mice. *Molecular and cellular biology*. 26:6272-6282.

Parsot, C., C. Hamiaux, and A.L. Page. 2003. The various and varying roles of specific chaperones in type III secretion systems. *Current opinion in microbiology*. 6:7-14.

Patel, A., N. Cummings, M. Batchelor, P.J. Hill, T. Dubois, K.H. Mellits, G. Frankel, and I. Connerton. 2006. Host protein interactions with enteropathogenic *Escherichia coli* (EPEC): 14-3-3tau binds Tir and has a role in EPEC-induced actin polymerization. *Cellular microbiology*. 8:55-71.

Phillips, N., R.D. Hayward, and V. Koronakis. 2004. Phosphorylation of the enteropathogenic E. coli receptor by the Src-family kinase c-Fyn triggers actin pedestal formation. *Nature cell biology*. 6:618-625.

Pollard, T.D., and J.A. Cooper. 2009. Actin, a central player in cell shape and movement. *Science (New York, N.Y*. 326:1208-1212.

Race, P.R., A.S. Solovyova, and M.J. Banfield. 2007. Conformation of the EPEC Tir protein in solution: investigating the impact of serine phosphorylation at positions 434/463. *Biophysical journal*. 93:586-596.

Ren, G., M.S. Crampton, and A.S. Yap. 2009. Cortactin: Coordinating adhesion and the actin cytoskeleton at cellular protrusions. *Cell motility and the cytoskeleton*. 66:865-873.

Rendi, R., and S. Ochoa. 1962. Effect of chloramphenicol on protein synthesis in cell-free preparations of *Escherichia coli*. *The Journal of biological chemistry*. 237:3711-3713.

Ritchie, J.M., C.M. Thorpe, A.B. Rogers, and M.K. Waldor. 2003. Critical roles for *stx2*, *eae*, and *tir* in enterohemorrhagic *Escherichia coli*-induced diarrhea and intestinal inflammation in infant rabbits. *Infection and immunity*. 71:7129-7139.

Rivera, G.M., C.A. Briceno, F. Takeshima, S.B. Snapper, and B.J. Mayer. 2004. Inducible clustering of membrane-targeted SH3 domains of the adaptor protein Nck triggers localized actin polymerization. *Curr Biol*. 14:11-22.

Rivero-Lezcano, O.M., A. Marcilla, J.H. Sameshima, and K.C. Robbins. 1995. Wiskott-Aldrich syndrome protein physically associates with Nck through Src homology 3 domains. *Molecular and cellular biology*. 15:5725-5731.

Rohatgi, R., P. Nollau, H.Y. Ho, M.W. Kirschner, and B.J. Mayer. 2001. Nck and phosphatidylinositol 4,5-bisphosphate synergistically activate actin polymerization through the N-WASP-Arp2/3 pathway. *The Journal of biological chemistry*. 276:26448-26452.

Rosen, M.K., T. Yamazaki, G.D. Gish, C.M. Kay, T. Pawson, and L.E. Kay. 1995. Direct demonstration of an intramolecular SH2-phosphotyrosine interaction in the Crk protein. *Nature*. 374:477-479.

Rosenshine, I., S. Ruschkowski, and B.B. Finlay. 1996. Expression of attaching/effacing activity by enteropathogenic *Escherichia coli* depends on growth phase,

temperature, and protein synthesis upon contact with epithelial cells. *Infection and immunity*. 64:966-973.

Ruchaud-Sparagano, M.H., M. Maresca, and B. Kenny. 2007. Enteropathogenic *Escherichia coli* (EPEC) inactivate innate immune responses prior to compromising epithelial barrier function. *Cellular microbiology*. 9:1909-1921.

Ruchaud-Sparagano, M.H., S. Muhlen, P. Dean, and B. Kenny. 2011. The enteropathogenic E. coli (EPEC) Tir effector inhibits NF-kappaB activity by targeting TNFalpha receptor-associated factors. *PLoS pathogens*. 7:e1002414.

Sakai, R., A. Iwamatsu, N. Hirano, S. Ogawa, T. Tanaka, H. Mano, Y. Yazaki, and H. Hirai. 1994. A novel signaling molecule, p130, forms stable complexes *in vivo* with v-Crk and v-Src in a tyrosine phosphorylation-dependent manner. *The EMBO journal*. 13:3748-3756.

Sallee, N.A., G.M. Rivera, J.E. Dueber, D. Vasilescu, R.D. Mullins, B.J. Mayer, and W.A. Lim. 2008. The pathogen protein EspF(U) hijacks actin polymerization using mimicry and multivalency. *Nature*. 454:1005-1008.

Sanger, J.M., R. Chang, F. Ashton, J.B. Kaper, and J.W. Sanger. 1996. Novel form of actin-based motility transports bacteria on the surfaces of infected cells. *Cell motility and the cytoskeleton*. 34:279-287.

Sangrar, W., Y. Gao, M. Scott, P. Truesdell, and P.A. Greer. 2007. Fer-mediated cortactin phosphorylation is associated with efficient fibroblast migration and is dependent on reactive oxygen species generation during integrin-mediated cell adhesion. *Molecular and cellular biology*. 27:6140-6152.

Sason, H., M. Milgrom, A.M. Weiss, N. Melamed-Book, T. Balla, S. Grinstein, S. Backert, I. Rosenshine, and B. Aroeti. 2009. Enteropathogenic *Escherichia coli* subverts phosphatidylinositol 4,5-bisphosphate and phosphatidylinositol 3,4,5-trisphosphate upon epithelial cell infection. *Molecular biology of the cell*. 20:544-555.

Savkovic, S.D., A. Ramaswamy, A. Koutsouris, and G. Hecht. 2001. EPEC-activated ERK1/2 participate in inflammatory response but not tight junction barrier disruption. *American journal of physiology*. 281:G890-898.

Scita, G., S. Confalonieri, P. Lappalainen, and S. Suetsugu. 2008. IRSp53: crossing the road of membrane and actin dynamics in the formation of membrane protrusions. *Trends in cell biology*. 18:52-60.

Schauer, D.B., and S. Falkow. 1993. The *eae* gene of *Citrobacter freundii* biotype 4280 is necessary for colonization in transmissible murine colonic hyperplasia. *Infection and immunity*. 61:4654-4661.

Schuller, S., Y. Chong, J. Lewin, B. Kenny, G. Frankel, and A.D. Phillips. 2007. Tir phosphorylation and Nck/N-WASP recruitment by enteropathogenic and enterohaemorrhagic *Escherichia coli* during ex vivo colonization of human intestinal mucosa is different to cell culture models. *Cellular microbiology*. 9:1352-1364.

Schuuring, E., E. Verhoeven, S. Litvinov, and R.J. Michalides. 1993. The product of the EMS1 gene, amplified and overexpressed in human carcinomas, is homologous to a v-src substrate and is located in cell-substratum contact sites. *Molecular and cellular biology*. 13:2891-2898.

Selbach, M., and S. Backert. 2005. Cortactin: an Achilles' heel of the actin cytoskeleton targeted by pathogens. *Trends in microbiology*. 13:181-189.

Selbach, M., S. Moese, R. Hurwitz, C.R. Hauck, T.F. Meyer, and S. Backert. 2003. The *Helicobacter pylori* CagA protein induces cortactin dephosphorylation and actin rearrangement by c-Src inactivation. *The EMBO journal*. 22:515-528.

Selbach, M., F.E. Paul, S. Brandt, P. Guye, O. Daumke, S. Backert, C. Dehio, and M. Mann. 2009. Host cell interactome of tyrosine-phosphorylated bacterial proteins. *Cell host & microbe*. 5:397-403.

Selyunin, A.S., S.E. Sutton, B.A. Weigele, L.E. Reddick, R.C. Orchard, S.M. Bresson, D.R. Tomchick, and N.M. Alto. 2011. The assembly of a GTPase-kinase signalling complex by a bacterial catalytic scaffold. *Nature*. 469:107-111.

Shames, S.R., W. Deng, J.A. Guttman, C.L. de Hoog, Y. Li, P.R. Hardwidge, H.P. Sham, B.A. Vallance, L.J. Foster, and B.B. Finlay. 2010. The pathogenic E. coli type III effector EspZ interacts with host CD98 and facilitates host cell prosurvival signalling. *Cellular microbiology*. 12:1322-1339.

She, H.Y., S. Rockow, J. Tang, R. Nishimura, E.Y. Skolnik, M. Chen, B. Margolis, and W. Li. 1997. Wiskott-Aldrich syndrome protein is associated with the adapter protein Grb2 and the epidermal growth factor receptor in living cells. *Molecular biology of the cell*. 8:1709-1721.

Small, J.V., T. Stradal, E. Vignal, and K. Rottner. 2002. The lamellipodium: where motility begins. *Trends in cell biology*. 12:112-120.

Snapper, S.B., F. Takeshima, I. Anton, C.H. Liu, S.M. Thomas, D. Nguyen, D. Dudley, H. Fraser, D. Purich, M. Lopez-Ilasaca, C. Klein, L. Davidson, R. Bronson, R.C. Mulligan, F. Southwick, R. Geha, M.B. Goldberg, F.S. Rosen, J.H. Hartwig, and F.W. Alt. 2001. N-WASP deficiency reveals distinct pathways for cell surface projections and microbial actin-based motility. *Nature cell biology*. 3:897-904.

Songyang, Z., S.E. Shoelson, M. Chaudhuri, G. Gish, T. Pawson, W.G. Haser, F. King, T. Roberts, S. Ratnofsky, R.J. Lechleider, and et al. 1993. SH2 domains recognize specific phosphopeptide sequences. *Cell*. 72:767-778.

Sriram, G., and R.B. Birge. 2010. Emerging roles for crk in human cancer. *Genes Cancer*. 1:1132-1139.

Stuible, M., N. Dube, and M.L. Tremblay. 2008. PTP1B regulates cortactin tyrosine phosphorylation by targeting Tyr446. *The Journal of biological chemistry*. 283:15740-15746.

Suzuki, M., H. Mimuro, T. Suzuki, M. Park, T. Yamamoto, and C. Sasakawa. 2005. Interaction of CagA with Crk plays an important role in *Helicobacter pylori*-induced loss of gastric epithelial cell adhesion. *J Exp Med*. 202:1235-1247.

Swimm, A., B. Bommarius, Y. Li, D. Cheng, P. Reeves, M. Sherman, D. Veach, W. Bornmann, and D. Kalman. 2004a. Enteropathogenic *Escherichia coli* use redundant tyrosine kinases to form actin pedestals. *Molecular biology of the cell*. 15:3520-3529.

Swimm, A., B. Bommarius, P. Reeves, M. Sherman, and D. Kalman. 2004b. Complex kinase requirements for EPEC pedestal formation. *Nature cell biology*. 6:795; author reply 795-796.

Tan, Y., N. Dourdin, C. Wu, T. De Veyra, J.S. Elce, and P.A. Greer. 2006. Ubiquitous calpains promote caspase-12 and JNK activation during endoplasmic reticulum stress-induced apoptosis. *The Journal of biological chemistry*. 281:16016-16024.

Taylor, K.A., P.W. Luther, and M.S. Donnenberg. 1999. Expression of the EspB protein of enteropathogenic *Escherichia coli* within HeLa cells affects stress fibers and cellular morphology. *Infection and immunity*. 67:120-125.

Taylor, K.A., C.B. O'Connell, P.W. Luther, and M.S. Donnenberg. 1998. The EspB protein of enteropathogenic *Escherichia coli* is targeted to the cytoplasm of infected HeLa cells. *Infection and immunity*. 66:5501-5507.

Tegtmeyer, N., R. Wittelsberger, R. Hartig, S. Wessler, N. Martinez-Quiles, and S. Backert. 2011. Serine phosphorylation of cortactin controls focal adhesion kinase activity and cell scattering induced by *Helicobacter pylori*. *Cell host & microbe*. 9:520-531.

Tehrani, S., N. Tomasevic, S. Weed, R. Sakowicz, and J.A. Cooper. 2007. Src phosphorylation of cortactin enhances actin assembly. *Proceedings of the National Academy of Sciences of the United States of America*.

ten Hoeve, J., C. Morris, N. Heisterkamp, and J. Groffen. 1993. Isolation and chromosomal localization of CRKL, a human crk-like gene. *Oncogene*. 8:2469-2474.

Thanabalasuriar, A., A. Koutsouris, A. Weflen, M. Mimee, G. Hecht, and S. Gruenheid. 2010. The bacterial virulence factor NleA is required for the disruption of intestinal tight junctions by enteropathogenic *Escherichia coli*. *Cellular microbiology*. 12:31-41.

Thomas, N.A., W. Deng, N. Baker, J. Puente, and B.B. Finlay. 2007. Hierarchical delivery of an essential host colonization factor in enteropathogenic *Escherichia coli*. *The Journal of biological chemistry*. 282:29634-29645.

Thomas, N.A., W. Deng, J.L. Puente, E.A. Frey, C.K. Yip, N.C. Strynadka, and B.B. Finlay. 2005. CesT is a multi-effector chaperone and recruitment factor required for the efficient type III secretion of both LEE- and non-LEE-encoded effectors of enteropathogenic *Escherichia coli*. *Molecular microbiology*. 57:1762-1779.

Tomar, A., C. Lawson, M. Ghassemian, and D.D. Schlaepfer. 2012. Cortactin as a Target for FAK in the Regulation of Focal Adhesion Dynamics. *PloS one*. 7:e44041.

Touze, T., R.D. Hayward, J. Eswaran, J.M. Leong, and V. Koronakis. 2004. Self-association of EPEC intimin mediated by the beta-barrel-containing anchor domain: a role in clustering of the Tir receptor. *Molecular microbiology*. 51:73-87.

Tsuji, N., M. Kobayashi, K. Nagashima, Y. Wakisaka, and K. Koizumi. 1976. A new antifungal antibiotic, trichostatin. *J Antibiot (Tokyo)*. 29:1-6.

Tu, X., I. Nisan, C. Yona, E. Hanski, and I. Rosenshine. 2003. EspH, a new cytoskeleton-modulating effector of enterohaemorrhagic and enteropathogenic *Escherichia coli*. *Molecular microbiology*. 47:595-606.

Tzipori, S., F. Gunzer, M.S. Donnenberg, L. de Montigny, J.B. Kaper, and A. Donohue-Rolfe. 1995. The role of the *eae*A gene in diarrhea and neurological complications in a gnotobiotic piglet model of enterohemorrhagic *Escherichia coli* infection. *Infection and immunity*. 63:3621-3627.

Uruno, T., J. Liu, P. Zhang, Y. Fan, C. Egile, R. Li, S.C. Mueller, and X. Zhan. 2001. Activation of Arp2/3 complex-mediated actin polymerization by cortactin. *Nature cell biology*. 3:259-266.

Vingadassalom, D., K.G. Campellone, M.J. Brady, B. Skehan, S.E. Battle, D. Robbins, A. Kapoor, G. Hecht, S.B. Snapper, and J.M. Leong. 2010. Enterohemorrhagic *E. coli*

requires N-WASP for efficient type III translocation but not for EspFU-mediated actin pedestal formation. *PLoS pathogens*. 6.

Vingadassalom, D., A. Kazlauskas, B. Skehan, H.C. Cheng, L. Magoun, D. Robbins, M.K. Rosen, K. Saksela, and J.M. Leong. 2009. Insulin receptor tyrosine kinase substrate links the *E. coli* O157:H7 actin assembly effectors Tir and EspFU during pedestal formation. *Proceedings of the National Academy of Sciences of the United States of America*.

Warawa, J., and B. Kenny. 2001. Phosphoserine modification of the enteropathogenic *Escherichia coli* Tir molecule is required to trigger conformational changes in Tir and efficient pedestal elongation. *Molecular microbiology*. 42:1269-1280.

Wattiau, P., S. Woestyn, and G.R. Cornelis. 1996. Customized secretion chaperones in pathogenic bacteria. *Molecular microbiology*. 20:255-262.

Weaver, A.M. 2008. Cortactin in tumor invasiveness. *Cancer Lett*. 265:157-166.

Weaver, A.M., J.E. Heuser, A.V. Karginov, W.L. Lee, J.T. Parsons, and J.A. Cooper. 2002. Interaction of cortactin and N-WASp with Arp2/3 complex. *Curr Biol*. 12:1270-1278.

Weaver, A.M., A.V. Karginov, A.W. Kinley, S.A. Weed, Y. Li, J.T. Parsons, and J.A. Cooper. 2001. Cortactin promotes and stabilizes Arp2/3-induced actin filament network formation. *Curr Biol*. 11:370-374.

Webb, B.A., S. Zhou, R. Eves, L. Shen, L. Jia, and A.S. Mak. 2006. Phosphorylation of cortactin by p21-activated kinase. *Arch Biochem Biophys*. 456:183-193.

Weed, S.A., and J.T. Parsons. 2001. Cortactin: coupling membrane dynamics to cortical actin assembly. *Oncogene*. 20:6418-6434.

Weidow, C.L., D.S. Black, J.B. Bliska, and A.H. Bouton. 2000. CAS/Crk signalling mediates uptake of *Yersinia* into human epithelial cells. *Cellular microbiology*. 2:549-560.

Weiss, S.M., M. Ladwein, D. Schmidt, J. Ehinger, S. Lommel, K. Stading, U. Beutling, A. Disanza, R. Frank, L. Jansch, G. Scita, F. Gunzer, K. Rottner, and T.E. Stradal. 2009. IRSp53 links the enterohemorrhagic *E. coli* effectors Tir and EspFU for actin pedestal formation. *Cell host & microbe*. 5:244-258.

Wolff, C., I. Nisan, E. Hanski, G. Frankel, and I. Rosenshine. 1998. Protein translocation into host epithelial cells by infecting enteropathogenic *Escherichia coli*. *Molecular microbiology*. 28:143-155.

Wong, A.R., J.S. Pearson, M.D. Bright, D. Munera, K.S. Robinson, S.F. Lee, G. Frankel, and E.L. Hartland. 2011. Enteropathogenic and enterohaemorrhagic *Escherichia coli*: even more subversive elements. *Molecular microbiology*.

Wong, A.R., B. Raymond, J.W. Collins, V.F. Crepin, and G. Frankel. 2012. The enteropathogenic *E. coli* effector EspH promotes actin pedestal formation and elongation via WASP-interacting protein (WIP). *Cellular microbiology*.

Wu, H., A.B. Reynolds, S.B. Kanner, R.R. Vines, and J.T. Parsons. 1991. Identification and characterization of a novel cytoskeleton-associated pp60src substrate. *Molecular and cellular biology*. 11:5113-5124.

Wu, X., B. Knudsen, S.M. Feller, J. Zheng, A. Sali, D. Cowburn, H. Hanafusa, and J. Kuriyan. 1995. Structural basis for the specific interaction of lysine-containing proline-rich peptides with the N-terminal SH3 domain of c-Crk. *Structure*. 3:215-226.

Wunderlich, L., A. Goher, A. Farago, J. Downward, and L. Buday. 1999. Requirement of multiple SH3 domains of Nck for ligand binding. *Cellular signalling*. 11:253-262.

Yaffe, M.B., G.G. Leparc, J. Lai, T. Obata, S. Volinia, and L.C. Cantley. 2001. A motif-based profile scanning approach for genome-wide prediction of signaling pathways. *Nat Biotechnol*. 19:348-353.

Yu, H., J.K. Chen, S. Feng, D.C. Dalgarno, A.W. Brauer, and S.L. Schreiber. 1994. Structural basis for the binding of proline-rich peptides to SH3 domains. *Cell*. 76:933-945.

Zhang, X., Z. Yuan, Y. Zhang, S. Yong, A. Salas-Burgos, J. Koomen, N. Olashaw, J.T. Parsons, X.J. Yang, S.R. Dent, T.P. Yao, W.S. Lane, and E. Seto. 2007. HDAC6 modulates cell motility by altering the acetylation level of cortactin. *Molecular cell*. 27:197-213.

Zhang, Y., M. Zhang, H. Dong, S. Yong, X. Li, N. Olashaw, P.A. Kruk, J.Q. Cheng, W. Bai, J. Chen, S.V. Nicosia, and X. Zhang. 2009. Deacetylation of cortactin by SIRT1 promotes cell migration. *Oncogene*. 28:445-460.

Zurawski, D.V., K.L. Mumy, L. Badea, J.A. Prentice, E.L. Hartland, B.A. McCormick, and A.T. Maurelli. 2008. The NleE/OspZ family of effector proteins is required for polymorphonuclear transepithelial migration, a characteristic shared by enteropathogenic *Escherichia coli* and *Shigella flexneri* infections. *Infection and immunity*. 76:369-379.

APPENDIX

Cell Communication and Signaling BioMed Central

Research

Open Access

Distinct phosphorylation requirements regulate cortactin activation by Tir_{EPEC} and its binding to N-WASP

Elvira Nieto-Pelegrin and Narcisa Martinez-Quiles*

Address: Microbiología II, Facultad de Farmacia, Universidad Complutense de Madrid, Madrid, Spain

Email: Elvira Nieto-Pelegrin - enieto@farm.ucm.es; Narcisa Martinez-Quiles* - narcisaquiles@farm.ucm.es

* Corresponding author

Published: 6 May 2009

Cell Communication and Signaling 2009, **7**:11 doi:10.1186/1478-811X-7-11

Received: 10 February 2009
Accepted: 6 May 2009

This article is available from: http://www.biosignaling.com/content/7/1/11

Abstract

Background: Cortactin activates the actin-related 2/3 (Arp2/3) complex promoting actin polymerization to remodel cell architecture in multiple processes (e.g. cell migration, membrane trafficking, invadopodia formation etc.). Moreover, it was called the Achilles' heel of the actin cytoskeleton because many pathogens hijack signals that converge on this oncogenic scaffolding protein. Cortactin is able to modulate N-WASP activation *in vitro* in a phosphorylation-dependent fashion. Thus Erk-phosphorylated cortactin is efficient in activating N-WASP through its SH3 domain, while Src-phosphorylated cortactin is not. This could represent a switch on/off mechanism controlling the coordinated action of both nucleator promoting factors (NPFs). Pedestal formation by enteropathogenic *Escherichia coli* (EPEC) requires N-WASP activation. N-WASP is recruited by the cell adapter Nck which binds a major tyrosine-phosphorylated site of a bacterial injected effector, Tir (translocated intimin receptor). Tir-Nck-N-WASP axis defines the current major pathway to actin polymerization on pedestals. In addition, it was recently reported that EPEC induces tyrosine phosphorylation of cortactin.

Results: Here we demonstrate that cortactin phosphorylation is absent on N-WASP deficient cells, but is recovered by re-expression of N-WASP. We used purified recombinant cortactin and Tir proteins to demonstrate a direct interaction of both that promoted Arp2/3 complex-mediated actin polymerization *in vitro*, independently of cortactin phosphorylation.

Conclusion: We propose that cortactin binds Tir through its N-terminal part in a tyrosine and serine phosphorylation independent manner while SH3 domain binding and activation of N-WASP is regulated by tyrosine and serine mediated phosphorylation of cortactin. Therefore cortactin could act on Tir-Nck-N-WASP pathway and control a possible cycling activity of N-WASP underlying pedestal formation.

Background

Enteropathogenic *Escherichia coli* (EPEC) are an important cause of infantile diarrhea, especially in developing countries. EPEC adhere, and cause the local effacement of the microvilli of intestinal epithelial cells, giving raise to so-called attaching and effacing (A/E) lesions. *In vitro*, EPEC attach to infected cells by forming pedestal-like structures enriched in polymerized actin and other host cell proteins [1]. The type III secretion system delivers into host cells the translocated intimin receptor (Tir), which is inserted into the cell plasma membrane such that a loop is exposed on the cell surface that binds to another bacterial

protein, the adhesin intimin [2]. This binding induces the clustering of Tir, followed by its phosphorylation on tyrosine residue 474 in the cytoplasmic C-terminal domain. The phosphotyrosine moiety recruits the host cell adaptor protein Nck [3], which binds and presumably activates N-WASP, leading to actin polymerization mediated by the Arp2/3 complex [4]. Although this pathway is recognized as the principal one operating in EPEC, another Nck-independent pathway has also been described in these bacteria [5]. Furthermore, the complexity of EPEC signal transduction is not fully understood [6].

Tir is inserted in the cell membrane, where it adopts a hairpin-loop structure, with both N and C termini projecting into the host cytoplasm [2]. Pedestals are dynamic structures that undergo constant remodeling by cycles of actin polymerization/depolymerization [7]. It is important to understand the contribution of other signals to pedestal formation, not only for EPEC but also for other actin-based processes. For instance, it has been postulated that Tir-Nck signaling mimics the nephrin-Nck-actin pathway [8].

Cortactin is a key regulator of the actin cytoskeleton which plays a crucial role in cell invasion [9] and actin-based motility during the infection of many microbial pathogens [10]. Cortactin possesses an N-terminal acidic domain (NTA) which harbors a DDW motif that activates, albeit weakly, the Arp2/3 complex at branching points [11,12]. The NTA domain is followed by a series of repeat domains that bind filamentous actin (F-actin). The C-terminal SH3 domain of cortactin [13] binds various proteins, such as N-WASP [14], which is a ubiquitously expressed member of the WASP (Wiskott-Aldrich Syndrome) family of proteins. Cortactin can be phosphorylated by tyrosine kinases (Src, Fer, Syk and Abl) and serine/threonine kinases (Erk and Pak) [15]. Src kinase targets tyrosine residues 421, 466 and 482 while Erk phosphorylates serines 405 and 418 [16] which lie in a proline-rich area. Interestingly, a Src family member (Fyn) [17] and Abl kinases phosphorylate Tir [18].

The Arp2/3 complex can be independently activated to initiate actin polymerization by the VCA (Verprolin Cofilin Acidic) domain of WASP members and by both the NTA and F-actin-binding repeats of cortactin. Theoretically N-WASP, cortactin and the Arp2/3 complex can form ternary complexes [19]. Cortactin has been shown *in vitro* to bind and activate N-WASP via an SH3 proline-rich domain interaction [14]. This activation is regulated positively and negatively when cortactin is phosphorylated by Erk and Src respectively. Erk phosphorylation of cortactin or the double mutation S405,418D in cortactin that mimics this phosphorylation enhance the protein's binding to and activation of N-WASP. Conversely, Src phosphorylation inhibits the ability of both Erk-phosphorylated cortactin, and that doubly mutated S405,418D cortactin, to activate N-WASP. Furthermore, phospho-mimetic mutation of the three tyrosine residues targeted by Src (Y421, Y466, and Y482) inhibited the ability of S405,418D cortactin to activate N-WASP. These results led us to hypothesize that Erk phosphorylation liberates the SH3 domain of cortactin from intramolecular interactions, allowing it to synergize with N-WASP in activating the Arp2/3 complex, and that Src phosphorylation terminates cortactin activation of N-WASP. This proposed on/off switching mechanism suggests that phosphorylation of cortactin regulates the accessibility and/or affinity of its SH3 domain towards its targets. 'S/Y model' may be relevant for actin dynamics in multiple cell processes [15] and it may partially explain the coordinated action of cortactin and N-WASP proteins, therefore connecting the two major families of Arp2/3 complex activators. Consistent with this model, recent structural data showed that cortactin adopts a 'closed' globular conformation in which its SH3 domain interacts with the actin-binding repeats [20].

This model has opened up new directions for studies in many cell systems. For example, serine phosphorylation of cortactin has been proposed to be relevant for actin polymerization, while tyrosine phosphorylation have been shown to selectively control adhesion turnover [21]. This suggests that different phosphocortactin forms participate in distinct signaling pathways.

Although it is clear that cortactin participates in pedestal actin dynamics, the underlying mechanism is not well understood. Previous studies have shown that cortactin translocates to EPEC pedestals. Over-expression of truncated forms of cortactin blocks pedestal formation [22]. A follow-up study to this work focused on the role of cortactin domains and Erk/Src phosphorylation, and it confirmed that truncated forms of cortactin exert a dominant negative effect in pedestal formation by EPEC and EHEC (Enterohemorrhagic Escherichia coli). This study suggests that cortactin is recruited through its α-helical region, and the authors conclude that tyrosine phosphorylation is relevant to pedestal formation, whereas serine phosphorylation seems to have no effect on actin assembly underneath the bacteria [23]. However, this conclusion is based exclusively on experiments with phosphorylation-mimicking mutants, without any comparison with the corresponding non-phosphorylatable counterparts.

Nck is not involved in N-WASP recruitment by EHEC. Instead, the $EspF_u$/Tccp effector activates N-WASP, thereby mimicking Cdc42 signaling [24,25]. Cantarelli *et al*. have proposed cortactin as the 'missing link' connecting Tir_{EHEC} and $EspF_u$/Tccp [26]. They showed that EHEC initially induces tyrosine phosphorylation of cortactin

and then induces its dephosphorylation, similarly to the transient cortactin phosphorylation during *Helicobacter pylori* infection [27]. However, using the two-hybrid system, they reported that tyrosine-phosphorylated cortactin binds both Tir_{EHEC} and $EspF_u$/Tccp, and consistent with previously described binding assays using recombinant purified proteins [14], only Erk-phosphorylated cortactin binds N-WASP. Recent *in vitro* studies using cells deficient in N-WASP suggest that cortactin recruitment to EHEC pedestals occurs downstream of $EspF_u$/Tccp and N-WASP [28]. It is therefore necessary to gain further insights into cortactin function in both systems. Major unresolved questions include whether cortactin and Tir_{EPEC} interact directly, whether cortactin participates in the Tir-Nck-N-WASP pathway, and how cortactin binding partners modulate its nucleating activity on pedestals. Thus, deepening our understanding of the involvement of cortactin on pedestals dynamics is relevant for many reasons.

Results

Role of cortactin motifs in pedestal formation

Reduction of cortactin expression by siRNA or over-expression of its isolated SH3 domain, polyproline region or its α-helical region resulted in a drastic decrease in actin-pedestal formation during infection with EPEC [23]. However the role of cortactin's Arp2/3 binding and activating region has not been addressed [23]. Therefore, we investigated its contribution to actin assembly on pedestals using EPEC to infect HeLa cells transiently transfected with GFP-cortactin. Pedestals were visualized by immunofluorescent staining of actin using fluorescent phalloidin and bacteria with DAPI. As previously reported [23], no differences on the number of attached bacteria were observed for the transfectants used (data not shown).

The cortactin NTA domain carries a 20DDW22 motif that binds and activates the Arp2/3 complex. Mutation of this motif to 20DDA22, hereafter referred to as W22A, abolished this activity [11]. To determine whether this motif is necessary for pedestal formation we transfected HeLa cells with GFP-W22A. We used wild-type (WT) cortactin (GFP-FL) and GFP alone as controls. As shown in Fig. 1, over-expression of GFP-FL cortactin allowed pedestal formation to levels similar to those in cells expressing GFP. Fig. 1C (black bars) shows normalized percentages and standard deviations for GFP-FL. Results of three independent experiments were considered statistically significant ($p < 0.01$ by Student's t-test). Since the constructs bear a GFP-tag we were able to simultaneously assess the localization of different cortactin forms (Fig. 1A, B and 1C). We observed GFP-FL cortactin to localize in 70% of pedestals, compared to 4% for GFP-transfected cells (open bars). Importantly, the number of pedestals in cells expressing GFP-W22A mutant was significantly lower than in GFP-FL transfected cells (51% *vs* 83%). This result indicates that cortactin W22A exerts a dominant negative effect, which may mean that cortactin binding and activation of the Arp2/3 complex is necessary for pedestal formation.

Cortactin has a C-terminal SH3 domain that binds several proteins. Mutation of a critical amino acid (W525K) abolishes its binding to known targets [29] such as N-WASP [14]. We used this mutant to assess the contribution of the cortactin SH3 domain to pedestal formation; we found that its expression inhibits pedestal formation to an even greater extent than the W22A mutant (31% *vs* 51%). This indicates that cortactin W525K mutant exerts a dominant-negative effect, corroborating previous results [23]. In previous work, we described that the cortactin SH3 domain is able to activate N-WASP and we proposed a model for the regulation of N-WASP activation by cortactin, in which cortactin is switched on by Erk phosphorylation of serines 405 and 418, while it is switched off by Src phosphorylation of tyrosines 421, 466 and 482 [14]. Next we repeated the pedestal formation assay with cells expressing the cortactin S405,418D double mutant, which mimics Erk phosphorylation and activates N-WASP *in vitro*, as well as its non-phosphorylatable counterpart (S405,418A). The S405,418D mutant allowed pedestal formation to a similar extent as the WT cortactin (90%) and to a greater extent, although not significantly greater, than the GFP negative control (83%). The phosphoserine-mimicking cortactin mutant accumulated in only 21% of pedestals and showed a weak, diffuse pattern of localization in the cytoplasm and pronounced staining in the nucleus. In contrast, the mutant that abolished Erk phosphorylation (S405,418A) impaired pedestal formation (34%) and its own translocation to them (3%). These results suggest that Erk phosphorylation of cortactin contributes to pedestals formation.

Similarly, we wanted to address the role of Src-mediated phosphorylation of cortactin. We therefore used the phosphotyrosine-mimicking mutant (Y421,466,482D) and the phosphotyrosine deficient mutant (Y421,466,482F). In both cases pedestal formation and location of these constructs on them were impaired (33%/7%; 28%/14%, Fig. 1B and 1C). These results indicate that Src-mediated phoshorylation of cortactin seems to inhibit pedestal formation and that a dynamic phosphorylation of these tyrosine residues play a role in the formation of pedestals.

Total F-actin content of cells transfected with different cortactin mutants

Although no appreciable changes in the cellular architecture were observed, we wanted to exclude the possibility that over-expression of cortactin mutants induces a general alteration of the actin cytoskeleton. We therefore used flow cytometry to assess the total basal F-actin content of the different transfectants. Fig. 1C (grey bars) and 1D

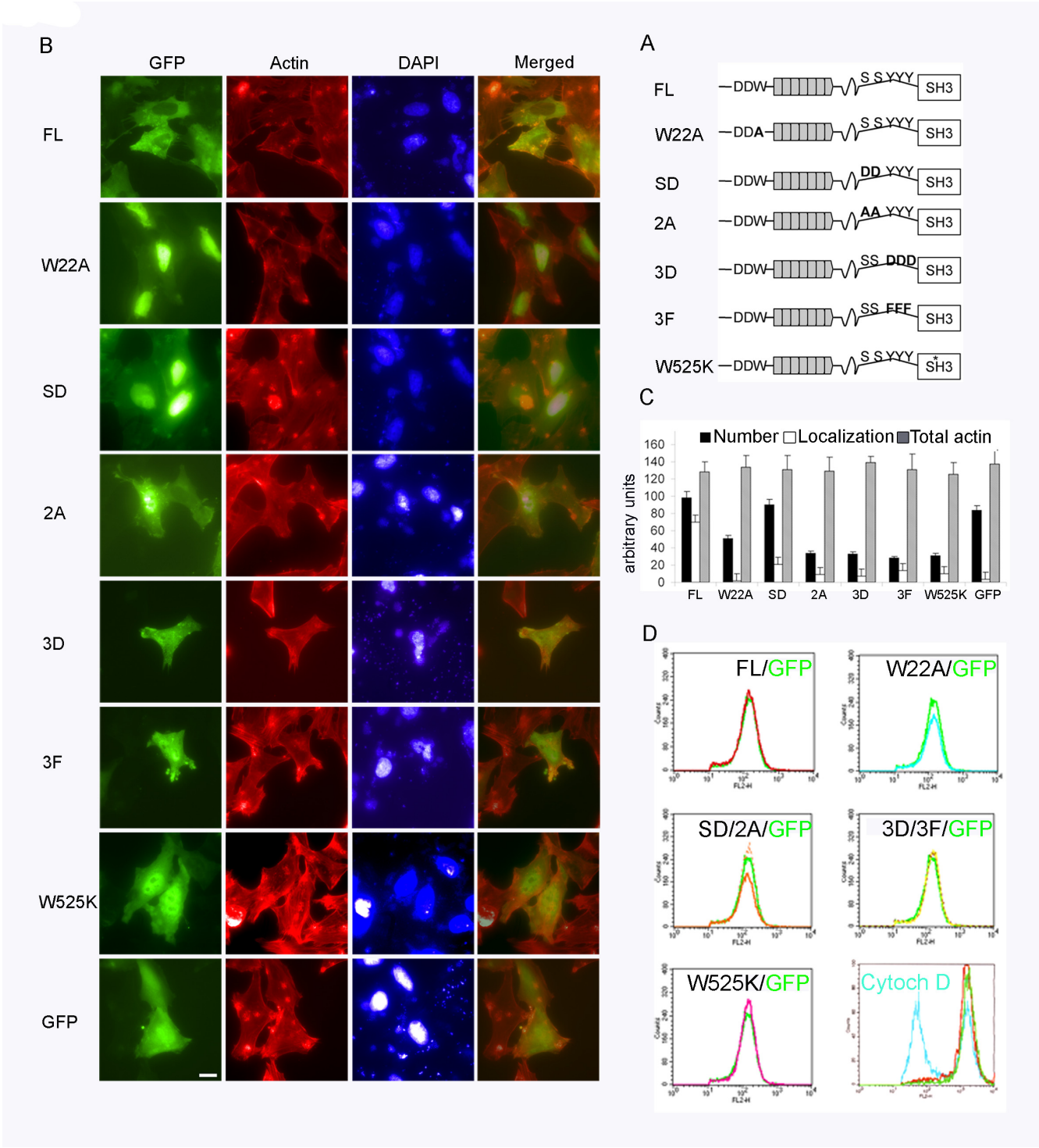

Figure 1 *(see legend on next page)*

Figure 1 *(see previous page)*
Effect of the overexpression of WT and cortactin mutants on pedestal formation and total actin content. (A) Schematic of cortactin domains and mutants under investigation. (B) Cortactin mutants block pedestal formation. Immunofluorescence images of HeLa cells transfected with WT (FL) and cortactin mutants and infected with EPEC for three hours. Mutants used are: Arp2/3 activation mutant (W22A), Erk-phosphorylation-mimicking mutant S405,418D (SD), Erk non-phosphorylatable mutant S405,418A (2A), Src-phosphorylation-mimicking mutant Y421,466,482D (3D), Src non-phosphorylatable mutant Y421,466,482F (3F) and SH3 domain mutant (W525K). GFP staining is shown in green, F-actin is in red, and bacteria and nuclei are in blue. The last column shows merged images of GFP and actin staining. Pictures are at 600× magnification. Scale bar 10 μm. (C) Quantification of pedestal number, cortactin localization and total F-actin content of transfectants. Black bars represent percentages normalized to WT of pedestal formed after 3 hours of infection of HeLa cells expressing GFP-FL and cortactin mutants. White bars represent normalized percentages of localization to pedestals. Grey bars represent the mean fluorescence of total actin content determined by flow cytometry. Experiments were performed at least three times with similar results. (D) Total actin content of HeLa cells transfected with WT and cortactin mutants. Histogram charts of HeLa cells expressing WT and cortactin mutants. Cells were permeabilized and stained with TRITC-phalloidin and total F-actin content was analyzed by flow cytometry. Overlaid histograms show the actin content of cortactin/mutants with respect to GFP transfected control cells (green curve). Pretreatment with cytochalasin D (blue curve) of cells expressing WT cortactin is shown as a control.

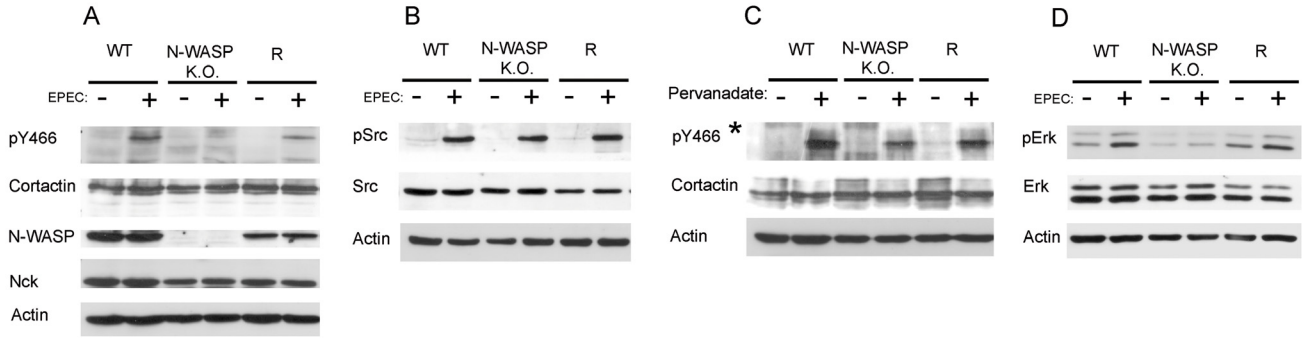

Figure 2
EPEC-induced tyrosine phosphorylation of cortactin depends on N-WASP. (A) Tyrosine phosphorylation of cortactin occurs in WT but not in N-WASP-deficient MEFs. WT, N-WASP-deficient and N-WASP reconstituted cells were infected with EPEC for three hours. The level of tyrosine phosphorylation of cortactin was assessed by Western blotting using an antibody against phospho-Y466 cortactin (upper panel). The same membrane was stripped and reprobed with anti-cortactin monoclonal antibody 4F11. N-WASP Western blotting was also performed to confirm the genotype of the MEFs. Actin was used as a loading control. Similar results were obtained in at least three independent experiments. (B) EPEC infection activates Src to similar extends in WT, N-WASP-deficient and R cells. WT, N-WASP-deficient and N-WASP reconstituted cells were infected with EPEC for three hours and analyzed for Src activation (phospho-Y416 Src) (upper panel). Medium and lower panels showed Src and actin blots, respectively. (C) Pervanadate treatment induces a robust phosphorylation of cortactin on tyrosine 466 in WT, N-WASP-deficient and R cells. Lysates of vehicle (DMSO)-treated MEFs and lysates of pervanadate-treated MEFs (diluted 1/500 *) were subjected to SDS-PAGE and Western blotted with antibody against phospho-Y466 cortactin. A second gel was loaded in parallel with the same amount of protein for both types of lysates and blotted for cortactin and actin for protein and loading controls, respectively (medium and lower panels). (D) EPEC infection induces Erk1/2 activation in WT but not N-WASP-deficient MEFs. WT, N-WASP-deficient and R cells were infected with EPEC for three hours. The level of Erk activation was assessed by Western blotting using a mAb specific for activated Erk phosphorylated on Thr202 and Tyr204 (upper panel). Medium and lower panels show Erk and actin blots for Erk protein and loading control respectively. Experiments were performed at least three times.

show the mean fluorescence of GFP transfectants, which did not significantly differ based on Student's t-test. As a control, transfected cell were pretreated with Cytochalasin D, a drug known to inhibit actin polymerization (Fig. 1D, bottom right panel). In addition, this experiment allowed us to calculate the transfection efficiency, which was estimated as 60–70%, based on the analysis of the expression of GFP constructs (data not shown).

EPEC induces N-WASP-dependent tyrosine phosphorylation of cortactin

Contrary to the transient phosphorylation induced by EHEC, EPEC infection of CH7 mouse fibroblasts induces tyrosine phosphorylation of cortactin [26]. Src has been shown to phosphorylate cortactin on tyrosines Y421, 466 and 482 [30], which decreases cortactin affinity for N-WASP *in vitro* [14]. In addition, N-WASP-deficient cells do not form pedestals [31]. These observations prompted us to examine the phosphorylation status of cortactin in WT mouse embryonic fibroblasts (MEFs), MEFs deficient in N-WASP and MEFs deficient in N-WASP in which the protein was later restored through retroviral transduction (rescued, R). First, we performed Western blotting control experiments to assess the expression of N-WASP, cortactin and actin (Fig. 2A).

Fig. 2A shows that EPEC induces phosphorylation of tyrosine 466 at 3 hours of infection in WT MEFs, as detected using an antibody against phospho-Y466-cortactin. This result was corroborated using a second phospho-specific antibody (pY421, data not shown). Unexpectedly, phosphorylation of tyrosine residue 466 was not induced in N-WASP-deficient cells. This result suggests that tyrosine phosphorylation of cortactin during EPEC infection depends on the presence of N-WASP. To verify this, we infected R cells with EPEC and examined levels of phosphoY466-cortactin. Fig. 2A shows that N-WASP re-expression partially restored cortactin tyrosine phosphorylation levels. In three independent experiments the normalized average induction was 1 ± 0.2 for WT cells, 0 for N-WASP-deficient cells and 0.5 ± 0.1 for R cells. This supports the idea that EPEC-induced tyrosine phosphorylation of cortactin in cells requires N-WASP.

Given the absence of cortactin tyrosine phosphorylation in EPEC-infected N-WASP-deficient cells, we then checked Src activation, using a commercially available phospho-active Src antibody (pY416). Fig. 2B demonstrated that equal activation of Src was achieved during EPEC infection in all cell types studied, while, as expected, the levels of total Src remained constant during infection. This result showed that the lack of cortactin phosphorylation in N-WASP-deficient cells was not due to a block in Src activation. As a further control, we treated the cells with pervanadate and observed robust phosphorylation of cortactin tyrosine 466 (Fig. 2C, upper panel).

Similarly we sought to establish the activation status of Erk in EPEC-infected cells. We used a phospho-specific monoclonal antibody that detects the activated form of Erk1/2 (anti pThr202-pTyr204). EPEC induced the activation of Erk on WT MEFs (Fig. 2D first lane), in agreement with a previous report on T84 epithelial cells [32]. However, infection of N-WASP-deficient cells showed reduced activation of Erk which was recovered in R cells. This result implies that Erk is activated by EPEC and may phosphorylate cortactin *in vivo*. More importantly, N-WASP is absolutely required for the induction of Erk activation at 3 hours of infection. However, WT MEFs treated with ERK inhibitors PD98056 or U0126 showed no difference in the number of pedestals formed ([23] and data not shown).

Tir binds cortactin and induces the latter to nucleate actin in vitro through an Arp2/3 complex-mediated pathway

The bacterial protein called Tir initiates what is considered to be the principal signaling cascade, which consists of Tir clustering and concomitant phosphorylation on its tyrosine 474, which then recruits Nck. The latter presumably binds N-WASP to initiate Arp2/3 complex-mediated actin polymerization [1]. We wanted to gain insights into how cortactin functions in pedestal signaling. Our initial hypothesis was that cortactin and Tir interact directly. Therefore we used the Scansite database [33] to search for motifs in the Tir sequence to which cortactin SH3 domain could bind. We found a consensus motif (NNS**I**PPA**P**PL**P**-SOTD) centered on proline 20 of Tir.

We first performed pull-down experiments with purified recombinant Tir [34] and cortactin proteins (Fig. 3). We produced WT GST-Tir that was purified using GSH beads and treated with PreScission enzyme, which excised Tir and at the same time removed the GST tag (Fig. 3, Coomassie gel). This Tir protein was used as the input in pull-down experiments with GST-cortactin. The first line of Fig. 3A shows that cortactin binds Tir *in vitro*.

To map the domains involved in the interaction, we performed pull-down experiments using cortactin mutants as follows: full-length W525K (mutated SH3 domain), the N-terminus (NH2, residues 1–333), and the isolated SH3 domain (SH3, residues 458–546). GST was used as a negative control. In agreement with our initial hypothesis, the isolated SH3 domain of cortactin bound Tir. However, the N-terminal domain of cortactin also bound Tir (Fig. 3A, third line). This unforeseen interaction was confirmed in experiments with cortactin carrying the point mutation, W525K in the SH3 domain (Fig. 3A). We obtained similar results using as input the Tir phospho-mimicking mutant

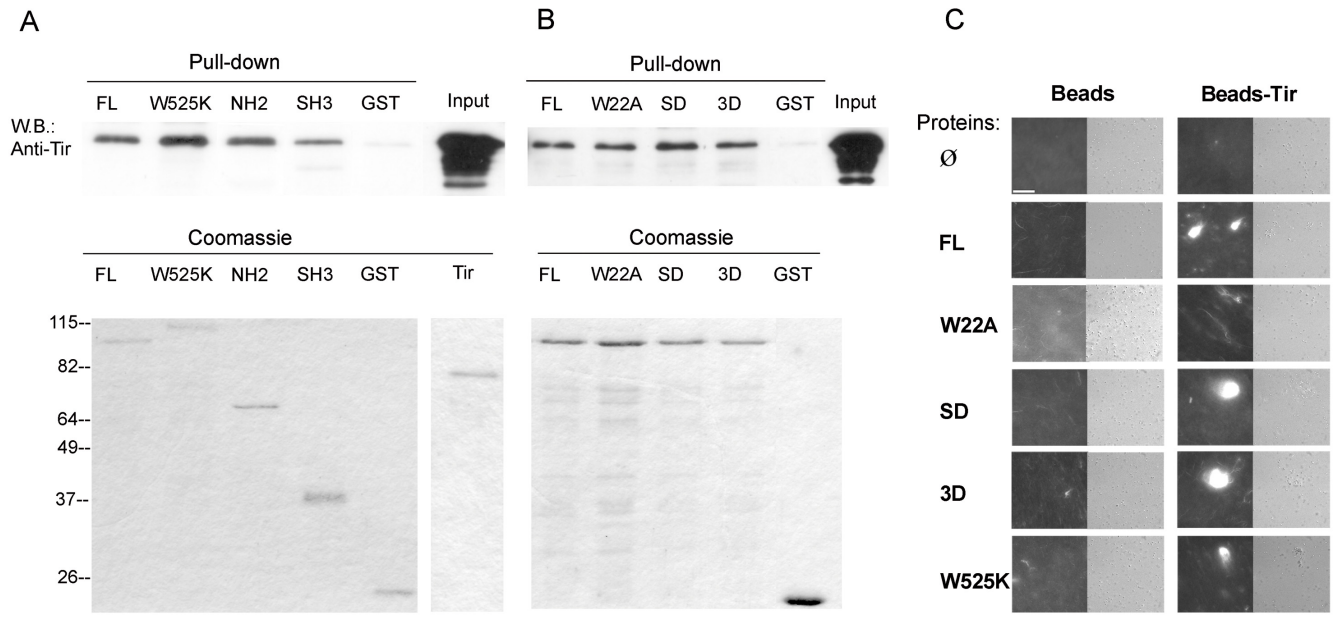

Figure 3

Tir binds cortactin and promotes its activation of Arp2/3-mediated actin polymerization. (A) Cortactin binds Tir through the N-terminal and the SH3 domains *in vitro*. Recombinant Tir was incubated with WT cortactin (FL) and with the three mutants expressed as GST fusion proteins: the SH3 domain mutant (W525K), the N-terminal (NH2) domain and the SH3 domain (SH3). GST alone served as a negative control. The pull-downs were subjected to SDS-PAGE and blotted with anti-Tir monoclonal antibody. In the last line, one-fifth of the total amount of Tir that was used as input per pull-down sample (upper left panel). Coomassie staining of proteins is also shown (lower panels). Half of the GST-proteins and on-fifth of Tir that was used in the pull-downs was stained with Coomassie blue. (B) Cortactin binds Tir independently of phosphorylation *in vitro*. Recombinant Tir was incubated with WT cortactin (FL) and with the three mutants expressed as GST fusion proteins: Arp2/3 domain mutant (W22A), Erk-phosphorylation-mimicking mutant (SD) and Src-phosphorylation- mimicking mutant (3D). GST alone served as a negative control (right upper panel). Coomassie staining of proteins is also shown (lower panels). Half of the GST-proteins and one-fifth of Tir that were used in the pull-downs were stained with Coomassie blue (shown in A). (C) Immunofluorescence images of Tir-coupled beads incubated with actin, Arp2/3 and cortactin/mutants. Carboxilate beads (diameter 1 μm) uncoupled (left panels) or coupled to Tir protein (right panels) were incubated with a solution of 500 nM WT cortactin or cortactin mutants proteins for 1 hour. Then, actin and Arp were added and incubated at RT to allow actin polymerization. After 1 hour TRITC-phalloidin was added, and the samples were observed immediately on a microscope. Pictures were taken at 600× magnification. Scale bar 40 μm.

TirY474D (TirD, data not shown). Next we tested the cortactin S405,418D (SD) and Y421,466,482D (3D) mutants which were similar to the WT form in their ability to bind both Tir (Fig. 3B) and TirD (data not shown). These results demonstrate that cortactin and Tir interact directly *in vitro*, that this interaction involves both the N-terminal part and the SH3 domain, and that it appears to be independent of cortactin phosphorylation.

Given the direct interaction between Tir and cortactin, we wondered whether Tir can activate the ability of cortactin to promote Arp2/3-mediated actin polymerization. We coupled recombinant Tir protein (or TirD, data not shown) to 1 μm beads, and then we washed the beads with Xb buffer and blocked them in Xb buffer containing 1% BSA. Next we incubated them with purified Arp and actin in Xb buffer containing WT and cortactin mutants. Fig. 3C shows that Tir activated WT cortactin and both SD and 3D mutants. Similar results were obtained for TirD (data not shown). The W525K mutant was also activated, although weakly. As expected, W22A cortactin was not activated, indicating that the effect was mediated by cortactin activation of the Arp2/3 complex. As a negative control we used naked beads that showed no activation. Conversely, experiments in which cortactin and its mutants were coupled to GSH beads showed similar results (data not shown). These results indicate that Tir activates the ability of cortactin to promote Arp2/3-mediated actin polymerization *in vitro*.

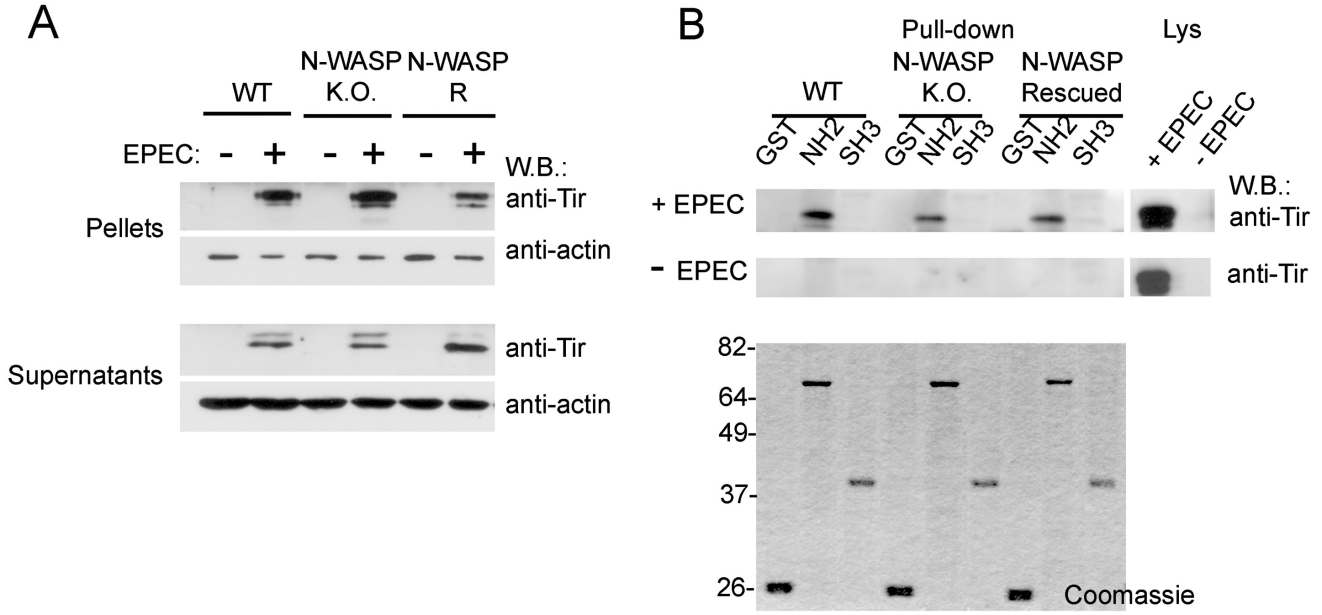

Figure 4

Cortactin binding to Tir in N-WASP-deficient cells infected by EPEC. (A) Tir is abundant in membrane-enriched fractions. EPEC-infected and uninfected P100 monolayers of WT, N-WASP-deficient, and R MEFs were lysed in imidazole buffer, fractionated, subjected to SDS-PAGE and blotted with anti-Tir mAb. As previously described, Tir appears as a doublet whose upper band is enriched in the membrane fractions (pellets). The signal from the anti-actin antibody is shown as a loading control. (B) Cortactin binds Tir in cells through its N-terminal domain. Cell lysates of uninfected and EPEC- infected WT, N-WASP-deficient, and R (R) MEFs were analyzed in pull-down experiments using GST fusion proteins as follows: cortactin N-terminal truncation mutant (NH2), the isolated SH3 domain (SH3), and GST alone. Western blotting with anti-Tir monoclonal antibody revealed a unique band corresponding to the slower-moving band. This band was present only in the NH2 pull-down conducted on all three types of lysates. These experiments were performed at least three times.

Cortactin binding to Tir in N-WASP-deficient cells infected by EPEC

Because cortactin binds directly both Tir (Fig. 3) and N-WASP [14], we analyze cortactin-Tir interaction in N-WASP-deficient cells. Since those cells do not form pedestals [35], we wondered if Tir would be present at similar levels to WT cells. To address this question, we used a previously described fractionation protocol that enriches in Tir-containing membranes ([36] and Materials and Methods). As shown in Fig. 4A, as expected Tir was enriched in the pellets compared to supernatants, as detected by western-blotting with anti-Tir mAb. We observed that a band with slower electrophoretic motility was the predominant form of Tir in the pellets, which represents fully-modified Tir [37]. WT and N-WASP-deficient cells presented detectable amounts of mature Tir that was slightly reduced on R cells.

FL cortactin has a closed conformation [14,20]. Therefore, we decided to use N-terminal cortactin (NH_2), the SH3 domain (SH3) and GST as a negative control to perform pull-down experiments with lysates of EPEC infected and uninfected WT, N-WASP-deficient and R cells. Western blotting in Fig. 4B shows that NH_2 bound Tir in EPEC infected but not uninfected cells, with no appreciable differences between WT, N-WASP and R cells. Similar results were obtained with total cell lysates although longer exposure times where necessary to detect Tir (data not shown).

In contrast, neither the isolated SH3 domain nor the GST negative control bound Tir in any of the cells types used. In view of these results, we can conclude that in cells, cortactin binds Tir primarily through its N-terminal region. To test whether the SH3 domain of cortactin prefers to bind N-WASP over Tir, we performed pull-downs with clarified total lysates, and we then stripped and reprobed the blots with anti-N-WASP antibody. This approach was necessary because the pellets did not contain easily detectable levels of N-WASP (data not shown). As previously described [14], the SH3 domain of cortactin was able to pull-down N-WASP in WT cells but not N-WASP-deficient cells (data not shown). This argues in favor of the conclusion that the N-terminal region of cortactin is involved in binding Tir, while the SH3 domain is involved in binding N-WASP.

Discussion

Cortactin is a scaffold protein implicated in many cellular processes since it directly contributes to cytoskeleton remodeling. Cortactin also has oncogenic properties due to its role in controlling invadopodia formation and cell migration. Moreover, cortactin has emerged as an important target of numerous pathogens, including enteropathogenic *E. coli* that manipulate the actin cytoskeleton in order to invade the host and propagate there [10]. EPEC cause severe diarrheal disease in humans by colonizing the gut mucosa and producing A/E lesions. EPEC attach to mammalian intestinal cells and induce reorganization of the actin cytoskeleton into 'pedestal-like' structures underneath the bacteria. A crucial event for pedestal formation is the insertion into the host-cell membranes of the EPEC effector Tir, which is initially injected into the cell by a type III secretion system. Tir mimics signaling pathways of the infected cell. Thus it can serve as a powerful model system to study eukaryotic transmembrane signaling [38]. In fact, the Tir-Nck-N-WASP pathway is the principal one through which actin polymerizes in EPEC pedestals. Those reasons prompted us to study cortactin signaling during EPEC infection using N-WASP-deficient cells. Although cortactin localizes to pedestals and its truncated forms exert a dominant negative effect, its function is not clear. For example, does cortactin on its own contribute to actin polymerization in pedestals? Our transfection experiments with the GFP-W22A cortactin point mutant demonstrate that cortactin binding and activation of the Arp2/3 complex is necessary for pedestal formation, which suggests that cortactin indeed contributes to efficient actin polymerization. A complementary study used a similar approach to examine the role of cortactin domains on pedestal formation [23]. It reported identical results to ours regarding WT cortactin and the mutant W525K. However, the W22A mutant was not studied in that work.

To address the role of Erk and Src phosphorylation of cortactin, we used both phosphorylation-mimicking and non-phosphorylatable mutants; previous studies have used only the former [23]. Therefore, we were able to detect a 'neutral' effect on pedestal formation of mutant that mimics phosphorylation by Erk, while the Erk non-phosphorylatable form blocked pedestal formation. Thus, we conclude that phosphorylation of cortactin by Erk may positively regulate pedestal formation. Our conclusion is also supported by other studies: over-expression of a mutant of cortactin mimicking phosphorylation on serine enhanced invadopodia formation in cells in which endogenous cortactin expression had previously been reduced by siRNA [39]. We could not use a similar approach in the present study because the cells detached and died upon EPEC infection (data not shown). The presence of endogenous cortactin may explain why the SD mutant did not lead to significantly more pedestals than WT, although an increase was detectable. Experiments with cortactin-deficient cells may provide the definitive answer to this question. In contrast, phosphoserine-mimicking cortactin accumulated in only one-fourth of pedestals and showed weak diffuse staining in the cytoplasm and a strong nuclear staining. We do not understand this distribution, and we are currently investigating it.

Src phosphorylates cortactin on positions Y421, 466, and 482 [30]. Therefore we used phosphorylation-mimicking and non-phosphorylatable triple mutants. In both cases pedestal formation was impaired, as well as the accumulation of the mutant proteins to the pedestals that did form. These results indicate that phoshorylation of cortactin by Src inhibits pedestal formation. The same conclusion was reached using the double Y421,466D mutant which partially mimics Src phosphorylation [23], which further supports the idea that cortactin phosphorylated on tyrosine inhibits pedestal formation. The fact that both Src mimicking and non-phosphorylatable cortactin forms inhibited the formation of pedestals might indicate that a dynamic phosphorylation of these tyrosine residues play a role in the formation of pedestals (Fig. 5). Finally, we can exclude that the effects on pedestals were due to changes in the total actin content of the transfectants, because the content was similar for all transfectants examined (Fig. 1). This argues that our results on pedestal formation reflect the specific effects of phosphorylation or lack of phosphorylation.

A crucial finding of this study is that tyrosine phosphorylation of cortactin is abrogated in N-WASP-deficient cells but recovered by N-WASP re-expression (Fig. 2). In agreement with these results, preliminary data using an antibody against cortactin phosphorylated on serine 405 show that EPEC induces serine phosphorylation of cortactin, which is not up-regulated in EPEC infected N-WASP-deficient cells (Narcisa Martínez-Quiles and Steffen Backert, unpublished results). Importantly, the lack of cortactin tyrosine phosphorylation was not due to a defect on Src activation. We think that only the fraction of cortactin that has translocated to the pedestals is available for serine and tyrosine phosphorylation. These findings strongly suggest a coordinated action of cortactin and N-WASP during pedestal formation, consistent with the on/off switching mechanism by which cortactin activates N-WASP *in vitro* [14]. A remaining question is whether cortactin is phosphorylated sequentially, e.g. serine followed by tyrosine phosphorylation. The lack of induction of cortactin phosphorylation in N-WASP-deficient cells should prove to be examined in many signaling transduction studies.

On the other hand, most studies have used inhibitors to establish the role of kinases on pedestal signaling and

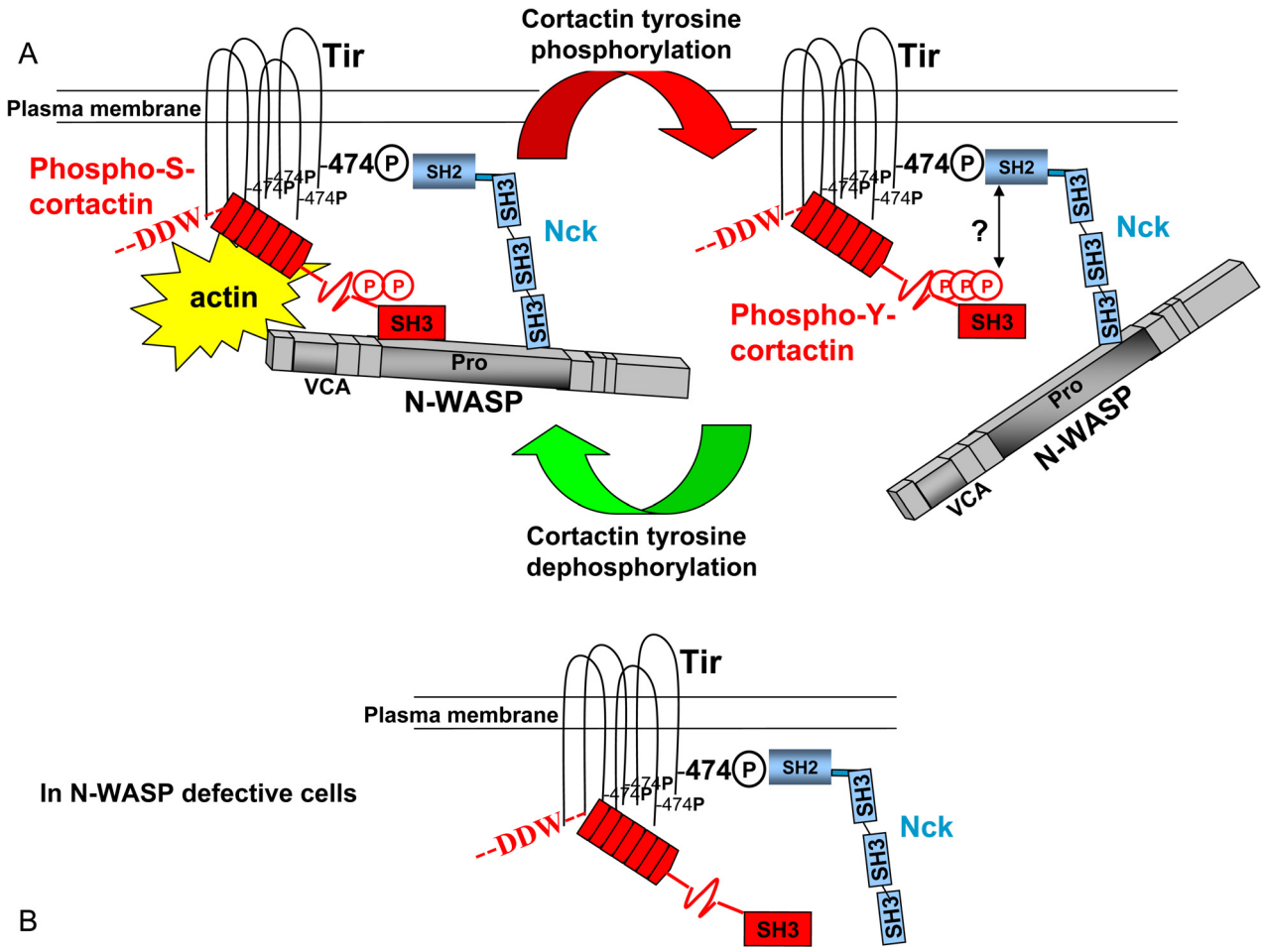

Figure 5

Model of cortactin action on EPEC pedestals. (A) Model of coordinated action by cortactin and N-WASP on EPEC pedestals. In theory, cortactin may bind Tir and N-WASP simultaneously, via its N-terminal and SH3 domain interaction respectively. EPEC-induced tyrosine phosphorylation of cortactin would terminate cortactin interaction with N-WASP but not with Tir. This could constitute a cyclical regulatory mechanism of actin polymerization on EPEC pedestals. Phosphotyrosine-cortactin might as well compete for the SH2 domain of Nck, thus uncoupling Tir from the Nck/N-WASP complex. (B) In the absence of N-WASP protein, cortactin would only interact with Tir, which would not be sufficient for pedestal formation.

have mainly focused on Tir phosphorylation [25]. To our knowledge this is the first report that establishes the status of Src activity during pedestal formation on N-WASP-deficient cells. Another conclusion that can be drawn is that Erk and Src kinases become activated in response to different signals. Thus Src is not affected by ablation of N-WASP whereas Erk activity is seriously compromised (Fig. 2). Erk activation is shut off sooner in N-WASP-deficient cells than in WT cells as seen in timing experiments. In contrast, the basal level of cortactin phosphorylated on serine was higher in Nck-deficient cells than in WT cells, and it was increased upon EPEC infection (data not shown). Thus we can be confident that the lack of cortactin phosphorylation is not merely due to the lack of pedestals, since cells deficient in either N-WASP or Nck do not form pedestals [3,31].

We report here that cortactin and Tir bind each other directly *in vitro* (Fig. 3A). Our initial hypothesis was that they would interact directly through the SH3 domain cortactin, because Tir possess a consensus motif centered on proline P20. Indeed, the SH3 domain was able to bind Tir, but unexpectedly, the NH2 domain was also found to bind Tir (Fig. 3). In addition, we did not detect differences in the affinity binding of mutants that mimic phosphorylation by Erk and Src, which contrast our previous binding studies in which a mutant that mimics phosphorylation by Erk was found to bind preferentially

to N-WASP [14]. These results demonstrated that cortactin and Tir interact directly *in vitro*, through both the N-terminal region and the SH3 domain of cortactin, and this interaction seems to occur independently of cortactin phosphorylation. In agreement with this conclusion, experiments using a two-hybrid system show that both the N-terminal region and the SH3 domain of cortactin bind Tir_{EHEC}. However, a major difference with our results is that only tyrosine-phosphorylated cortactin bind Tir_{EHEC}, which contrasts with the transient phosphorylation of cortactin induced by EHEC. Both findings were reconciled by suggesting cortactin and Tir initially bind transiently coincident with the tyrosine phosphorylation of cortactin [26]. In our system, EPEC-infected cells still showed high levels of N-WASP-dependent cortactin phosphorylation three hours after infection. These results highlight the fine-tuned nature of cortactin regulation during EPEC and EHEC infections.

Cortactin can activate the Arp2/3 complex directly through its NTA domain [11,12], and indirectly by using its SH3 domain to activate N-WASP [14]. We wondered whether the binding of Tir to cortactin would activate the latter and promote Arp2/3 complex-dependent actin polymerization. As shown in Fig. 3B, Tir-coated beads activated cortactin. Furthermore, as for the binding, the activation of cortactin by Tir was not affected by the phosphorylation status of cortactin, which further supports the idea that in EPEC signaling, Tir binds and activates cortactin independently of the latter's phosphorylation status. At this point, we favored the conclusion that the relevant contribution underlying cortactin-Tir binding occurs through the N-terminal moiety of cortactin, since our previous studies indicated that phosphorylation of cortactin affects mainly its interaction with partners through the SH3 domain [14]. To test this hypothesis, we used cell lysates that represent a more restrictive scenario with greater similarity to binding conditions *in vivo*. Consistent with our reasoning, the N-terminal region of cortactin bound Tir, whereas the isolated SH3 domain did not in any of the cells type tested. In view of these results, we can conclude that in cells cortactin binds Tir primarily through its N-terminal region, while the contribution of the SH3 domain seems to be irrelevant. Furthermore, the interaction between Tir and cortactin is independent of phosphorylation and does not require N-WASP, since we detected similar levels of interaction in WT, N-WASP-deficient and R cells.

Alternatively, the cortactin SH3 consensus site on Tir may be occupied by other SH3 domains such as tyrosine kinases [40] or the cortactin SH3-domain may have a preference for binding N-WASP. As previously described [14], the SH3 domain of cortactin pulls down N-WASP. This supports the idea that cortactin binds Tir through the N-terminus and N-WASP through the SH3 domain. In this case, phosphorylation should affect only the binding of cortactin to N-WASP; in other words, cortactin phosphorylated on serine would bind both Tir and N-WASP whereas cortactin phosphorylated on tyrosine would bind only Tir.

Both binding and activation experiments were also performed with the Tir phosphorylation mimicking Y474D mutant of Tir (data not shown). The fact that we did not observe significant differences from WT Tir may means: (i) the mutant does not behave like the phosphorylated form or (ii) the binding and activation of cortactin is independent of Tir phosphorylation on residue 474. Further experiments are needed to address this question.

Finally, in our effort to understand what kind of complexes form *in vivo*, we considered all available *in vitro* data concerning the interaction of Tir, Nck, N-WASP and cortactin. Thus Nck binds cortactin only when phosphorylated by Src [41], through an interaction between the phosphotyrosine and the SH2 domain [42]. Therefore since Tir and Nck interact through the single SH2 domain of Nck, formation of a Tir-Nck-cortactin complex appears to be impossible. Cortactin phosphorylated by Src is not able to interact with N-WASP, as shown with recombinant proteins [14] and further corroborated in the two-hybrid assay [26]. That adds to the evidence against the possibility that cortactin bridges both proteins, i.e. Nck-cortactin-N-WASP. This leaves three possible types of complexes: (i) Tir-Nck-N-WASP-cortactin, (ii) Tir-cortactin-N-WASP and (iii) Tir-cortactin. Given the fact that reducing of cortactin expression with siRNA inhibits pedestal formation ([23] and our unpublished results), that EPEC infection induces cortactin phosphorylation in an N-WASP-dependent fashion (Fig. 2), and that Tir binds and activates cortactin (Fig. 3) we conclude that cortactin contributes to the Tir-Nck-N-WASP pathway, possibly by regulating N-WASP activity. In other words, cortactin and N-WASP would act in a complex in this scenario. If we envision pedestals as a dynamic actin structure, and in fact pedestal motility has been shown [7], then it is reasonable to think that proteins promoting actin polymerization would act in a cyclic manner. We speculate that cortactin is a cycling switch for N-WASP in pedestals (Model in Fig. 5).

Deletion of Tir abrogates pedestal formation by EPEC [24] implying that Tir mediates the major but not only pathway for actin assembly in pedestals. Indeed, elegant work has shown that the EPEC effector protein EspF directly activates N-WASP [43]. We can not exclude that cortactin participates in this pathway.

Conclusion

The function of cortactin in pedestals, and how its function is regulated, seems to differ between EPEC and EHEC. EHEC induces tyrosine dephosphorylation of cortactin [26] whereas EPEC induces its tyrosine phophorylation ([26] and this study). During EHEC infection, the Tir-cortactin interaction was mapped to the N-terminal region of both molecules, but only cortactin phosphorylated by Src bound to Tir_{EHEC}.

In our study, cortactin bound directly to Tir_{EPEC} independently of phosphorylation since cortactin mutants mimicking phosphorylation by Erk and Src interacted with Tir, and were activated to a similar extent *in vitro*. This finding further supports our results using EPEC-infected cells that show that the interaction between Tir and cortactin is mediated through the N-terminal part of the cortactin molecule. Our results are compatible with the formation of complexes in which cortactin may interact with Tir via its N-terminal domain and with N-WASP via its SH3 domain. The later interaction would be terminated upon tyrosine phosphorylation of cortactin (Model in Fig. 5).

Methods

Cells, bacteria, reagents and antibodies

HeLa human epithelial cells were obtained from ATCC and grown in Iscove's Modified Dulbecco's Media (IMDM) supplemented with 10% FBS (fetal bovine serum). N-WASP-deficient and R mouse embryonic fibroblasts (MEFs) were obtained from Dr. Scott Snapper (Massachusetts General Hospital, Boston, USA) and Nck1/2-deficient MEFs from Dr. Tony Pawson (Samuel Lunenfeld Research Institute, Mount Sinai Hospital, Toronto, Canada). Enteropathogenic *Escherichia coli* (EPEC) E2348/69, as well as monoclonal antibodies against the N- and C-termini Tir (2A5 and 2C3, respectively) were provided by Dr. Brett B. Finlay (University of British Columbia, Vancouver, Canada). Anti-N-WASP antibody was previously described [44]. Commercial antibodies used were: anti-cortactin 4F11 monoclonal antibody, anti-Src GD11 monoclonal and polyclonal anti-phosphoY416 (activated Src) antibodies (Millipore), and anti-actin C4 monoclonal antibody (MP Biomedical). Anti-phospho-cortactin Y466 polyclonal antibody was from Abcam (Cambridge, UK). Polyclonal anti-Erk1/2 (p44/42) and monoclonal anti-phospho-Erk (Thr202/Tyr204, clone E10) antibodies were from Cell Signaling. Anti-rabbit and anti-mouse horseradish peroxidase (HRP) antibodies were from Amersham Pharmacia Biotech.

Cortactin and Tir constructs

Wild-type cortactin and selected mutants [14] were subcloned in frame with GFP at the N-terminus in the plasmid pC2-EGFP (Invitrogen) and verified by sequencing. The constructs used were full-length wild-type cortactin (FL), and the following derivatives: the single point mutants W22A and W525K; the double mutant S405,418D; the triple mutant Y421,466,482D; an N-terminal fragment of cortactin (NH2) containing residues 1–333, and a cortactin fragment (residues 458–546) containing the SH3 domain (SH3) aas. Two new mutants: S405,418A and Y421,466,482F, were generated using PCR and GST-FL as the template with the QuikChange site-directed mutagenesis kit (Stratagene). The Tir Y474D mutant was produced using the QuikChange kit.

Cell transfection, Western blotting and pedestal formation by EPEC

Cell transfection was carried out using Lipofectamine 2000 (Invitrogen). Briefly, HeLa cells were grown to 60–70% confluence in 6-well plates. Transfections were incubated for 16 hours in medium containing 10% FBS but no antibiotics. Western blotting was done on cells from a single well by directly adding 300 μl of 2× Laemmli buffer and scraping the cells. Samples were homogenized by six passages through a syringe with a 25-gauge needle, followed by centrifugation at 21,000 g for 15 min at 4°C. Samples were resolved by 10% SDS-PAGE and analyzed by Western blotting and developed with ECL (Amersham). Band densitometry was carried out using NIH ImageJ software. Normalization for each experiment was done by first, normalizing actin and next, the protein. The average difference was calculated from three independent experiments and reported as ± standard deviations.

EPEC infections were carried out as follows. Overnight bacterial culture were grown at 37°C with shaking at 200 r.p.m., and 1 μl of culture was added per well of a 6-well-plate. Pedestals were allowed to form for 3 hours in medium containing 10% FBS and no antibiotics at 37°C and 5% CO_2. When indicated, EPEC was preactivated by incubating a 1/100 dilution of the O/N culture for 2 hours in medium containing 10% FBS and no antibiotics at 37°C and 5% CO_2; the amount of bacteria from this preactivated culture that was added to wells was 1/8 that of non-preactivated bacteria. Quantification was done by counting the numbers of pedestals of attached bacteria for a total of 100 cells. Experiments were performed at least three times. Statistical analysis was carried out using Student's t-test in Microsoft Excel.

Immunofluorescence microscopy and determination of total content of F-actin

Cells were fixed with 4% formalin solution (Sigma) at room temperature and permeabilized with 0.1% Triton X-100 for 5 min. After two washes with PBS, cells were blocked with 2% BSA in PBS for 10 min and then sequentially stained with 1 μg/ml tetramethyl rhodamine isotiocianate (TRITC)-phalloidin (Sigma) and DAPI (300 nM). Photographs were taken using a Nikon Eclipse TE 200-U

fluorescence microscope equipped with a Hamamatsu camera. Images were processed with Adobe Phothoshop. For determination of total content of F-actin, TRITC-phalloidin was used at 5 μg/ml. As a control, cells were pretreated 15 min with cytochalasin D at 2 μg/ml. Samples were sorted by fluorescence using a FACS Scalibur station. Experiments were performed at least three times. Statistical analysis was carried out using Student's t-test in Microsoft Excel.

Actin polymerization assays

GST recombinant proteins were produced, purified and, when necessary, treated with PreScission protease according to the manufacturer's recommendations (GE Healthcare) to remove GST. Carboxilate microspheres (1 μm; Polysciences Inc.) were coupled to Tir/TirD in solution (500 nM) and washed once with Xb buffer (10 mM HEPES pH 7.8, 100 mM KCl, 0.1 mM $CaCl_2$, 1 mM $MgCl_2$, 1 mM ATP) and twice with Xb buffer-1% BSA to block nonspecific interactions. Purified actin (2.5 μM) and Arp (300 nM) were used. Cortactin and its mutants (500 nM) were added to a final volume of 25 μl of Xb buffer. After 1 hour TRITC-phalloidin was added to a final concentration of 3.3 μM. The solution containing the beads was placed on a slide and sealed with paraffin. Pictures were acquired while keeping all relevant parameters fixed (gain, exposure time) to allow for fluorescence intensity comparison. Experiments were performed at least three times.

Membrane enrichment procedure, pull-down experiments, and pervanadate treatment

After EPEC infection, MEFs were fractionated as described [36] with some modifications. Briefly, MEFs were grown to 70–80% confluence in 150-mm plates and infected with preactivated EPEC. After 3 hours of infection, cells were washed once with ice-cold PBS and rapidly lysed at 4°C by overlaying the cell monolayer for 10 min with 1 ml of buffer containing imidazole (pH 7.4), 250 mM sucrose, protease-phosphatase inhibitor cocktail (Complete™) and phosphatase inhibitor (PhosStop, Amersham). Then the cells were collected using a cell scraper (Sarstedt) and disrupted by six passages through a syringe with a 25-gauge needle, followed by 15 min centrifugation at 3,000 g to remove cellular debris, bacteria and nuclei. Clarified lysates were centrifuged again for 1 hour at 21,000 g to separate the membrane (pellet) from the cytoplasmic fraction (supernatant). Both of these final fractions were stored at -70°C until further use.

For pull-down experiments pellets were resuspended in 400 μl of lysis buffer containing 0.1% Triton-X100, and a fourth was used for each pull-down. GST, the GST-N terminal (NH2) cortactin fragment and the GST-SH3 cortactin domain were produced in BL21 *E. coli*, purified and coupled to GSH-beads. Pull-downs were washed three times with 100 μl of lysis buffer diluted 1:10 in PBS containing 0.05% Tween 20.

Pull-down experiments with recombinant proteins were performed as previously described [14]. When necessary the GST was removed by Precission enzyme treatment (Amersham).

Pervanadate treatment was carried out by mixing 1 mM of $NaVO_4$ with 1% H_2O_2 and diluting two-fold with IMDM medium for 30 min at 37°C and 5% CO_2.

Competing interests

The authors declare that they have no competing interests.

Authors' contributions

ENP and NMQ performed and designed the experiments. NMQ, the Senior/corresponding author, supervise the experiments and prepare the manuscript with the help of ENP.

Acknowledgements

We are very grateful to Marie-France Carlier for providing support, to members of her laboratory Dominique Didry and Diep Lê for Arp2/3 and actin purification and to Christophe Le Clainche for support and helpful discussions. We are very grateful to Dr. Finlay (University of British Columbia, Vancouver, Canada) for E2348/69 EPEC strain and anti-Tir moAbs, to Dr. Scott Snapper (Massachusetts General Hospital, Boston, USA) for N-WASP K.O. and Rescued cells, and to Dr. Phillip Hardwidge (University of Kansas Medical Center) for reading the manuscript. We express our appreciation to Dr. César Nombela, Dr. María Molina and Dr. Rafael Rotger for support and laboratory space, Dr Isabel Rodriguez-Escudero and Dr. Victor Cid for Tir DNA, and María Moreno Coca for help with experiments in Figure 2.

This work was funded by a Marie Curie International Reintegration grant (IRG 028995-cortactinNMQ) and a FIS grant (PI 060004) to NMQ. ENP was supported by the IRG grant. NMQ is a 'Ramón y Cajal' MEC-UCM researcher, partially funded by the European Social Fund (ESF).

References

1. Caron E, Crepin VF, Simpson N, Knutton S, Garmendia J, Frankel G: **Subversion of actin dynamics by EPEC and EHEC.** *Current opinion in microbiology* 2006, **9(1):**40-45.
2. Kenny B, DeVinney R, Stein M, Reinscheid DJ, Frey EA, Finlay BB: **Enteropathogenic E. coli (EPEC) transfers its receptor for intimate adherence into mammalian cells.** *Cell* 1997, **91(4):**511-520.
3. Gruenheid S, DeVinney R, Bladt F, Goosney D, Gelkop S, Gish GD, Pawson T, Finlay BB: **Enteropathogenic E. coli Tir binds Nck to initiate actin pedestal formation in host cells.** *Nature cell biology* 2001, **3(9):**856-859.
4. Kalman D, Weiner OD, Goosney DL, Sedat JW, Finlay BB, Abo A, Bishop JM: **Enteropathogenic E. coli acts through WASP and Arp2/3 complex to form actin pedestals.** *Nature cell biology* 1999, **1(6):**389-391.
5. Campellone KG, Leong JM: **Nck-independent actin assembly is mediated by two phosphorylated tyrosines within enteropathogenic Escherichia coli Tir.** *Molecular microbiology* 2005, **56(2):**416-432.
6. Hardwidge PR, Rodriguez-Escudero I, Goode D, Donohoe S, Eng J, Goodlett DR, Aebersold R, Finlay BB: **Proteomic analysis of the intestinal epithelial cell response to enteropathogenic**

Escherichia coli. *The Journal of biological chemistry* 2004, **279(19):**20127-20136.
7. Sanger JM, Chang R, Ashton F, Kaper JB, Sanger JW: **Novel form of actin-based motility transports bacteria on the surfaces of infected cells.** *Cell Motil Cytoskeleton* 1996, **34(4):**279-287.
8. Blasutig IM, New LA, Thanabalasuriar A, Dayarathna TK, Goudreault M, Quaggin SE, Li SS, Gruenheid S, Jones N, Pawson T: **Phosphorylated YDXV motifs and Nck SH2/SH3 adaptors act cooperatively to induce actin reorganization.** *Mol Cell Biol* 2008, **28(6):**2035-2046.
9. Weaver AM: **Cortactin in tumor invasiveness.** *Cancer letters* 2008, **265(2):**157-166.
10. Selbach M, Backert S: **Cortactin: an Achilles' heel of the actin cytoskeleton targeted by pathogens.** *Trends in microbiology* 2005, **13(4):**181-189.
11. Uruno T, Liu J, Zhang P, Fan Y, Egile C, Li R, Mueller SC, Zhan X: **Activation of Arp2/3 complex-mediated actin polymerization by cortactin.** *Nature cell biology* 2001, **3(3):**259-266.
12. Weaver AM, Karginov AV, Kinley AW, Weed SA, Li Y, Parsons JT, Cooper JA: **Cortactin promotes and stabilizes Arp2/3-induced actin filament network formation.** *Curr Biol* 2001, **11(5):**370-374.
13. Wu H, Parsons JT: **Cortactin, an 80/85-kilodalton pp60src substrate, is a filamentous actin-binding protein enriched in the cell cortex.** *The Journal of cell biology* 1993, **120(6):**1417-1426.
14. Martinez-Quiles N, Ho HY, Kirschner MW, Ramesh N, Geha RS: **Erk/Src phosphorylation of cortactin acts as a switch on-switch off mechanism that controls its ability to activate N-WASP.** *Nat Cell Biol* 2001, **3(5):**484-491.
15. Lua BL, Low BC: **Cortactin phosphorylation as a switch for actin cytoskeletal network and cell dynamics control.** *FEBS letters* 2005, **579(3):**577-585.
16. Cosen-Binker LI, Kapus A: **Cortactin: the gray eminence of the cytoskeleton.** *Physiology (Bethesda, Md)* 2006, **21:**352-361.
17. Phillips N, Hayward RD, Koronakis V: **Phosphorylation of the enteropathogenic E. coli receptor by the Src-family kinase c-Fyn triggers actin pedestal formation.** *Nature cell biology* 2004, **6(7):**618-625.
18. Swimm A, Bommarius B, Li Y, Cheng D, Reeves P, Sherman M, Veach D, Bornmann W, Kalman D: **Enteropathogenic Escherichia coli use redundant tyrosine kinases to form actin pedestals.** *Molecular biology of the cell* 2004, **15(8):**3520-3529.
19. Weaver AM, Heuser JE, Karginov AV, Lee WL, Parsons JT, Cooper JA: **Interaction of cortactin and N-WASp with Arp2/3 complex.** *Curr Biol* 2002, **12(15):**1270-1278.
20. Cowieson NP, King G, Cookson D, Ross I, Huber T, Hume DA, Kobe B, Martin JL: **Cortactin adopts a globular conformation and bundles actin into sheets.** *The Journal of biological chemistry* 2008, **283(23):**16187-16193.
21. Kruchten AE, Krueger EW, Wang Y, McNiven MA: **Distinct phospho-forms of cortactin differentially regulate actin polymerization and focal adhesions.** *Am J Physiol Cell Physiol* 2008.
22. Cantarelli VV, Takahashi A, Yanagihara I, Akeda Y, Imura K, Kodama T, Kono G, Sato Y, Iida T, Honda T: **Cortactin is necessary for F-actin accumulation in pedestal structures induced by enteropathogenic Escherichia coli infection.** *Infect Immun* 2002, **70(4):**2206-2209.
23. Cantarelli VV, Kodama T, Nijstad N, Abolghait SK, Iida T, Honda T: **Cortactin is essential for F-actin assembly in enteropathogenic Escherichia coli (EPEC)- and enterohaemorrhagic E. coli (EHEC)-induced pedestals and the alpha-helical region is involved in the localization of cortactin to bacterial attachment sites.** *Cellular microbiology* 2006, **8(5):**769-780.
24. Campellone KG, Rankin S, Pawson T, Kirschner MW, Tipper DJ, Leong JM: **Clustering of Nck by a 12-residue Tir phosphopeptide is sufficient to trigger localized actin assembly.** *The Journal of cell biology* 2004, **164(3):**407-416.
25. Garmendia J, Phillips AD, Carlier MF, Chong Y, Schuller S, Marches O, Dahan S, Oswald E, Shaw RK, Knutton S, *et al.*: **TccP is an enterohaemorrhagic Escherichia coli O157:H7 type III effector protein that couples Tir to the actin-cytoskeleton.** *Cellular microbiology* 2004, **6(12):**1167-1183.
26. Cantarelli VV, Kodama T, Nijstad N, Abolghait SK, Nada S, Okada M, Iida T, Honda T: **Tyrosine phosphorylation controls cortactin binding to two enterohaemorrhagic Escherichia coli effectors: Tir and EspFu/TccP.** *Cellular microbiology* 2007, **9(7):**1782-1795.
27. Selbach M, Moese S, Hurwitz R, Hauck CR, Meyer TF, Backert S: **The Helicobacter pylori CagA protein induces cortactin dephosphorylation and actin rearrangement by c-Src inactivation.** *The EMBO journal* 2003, **22(3):**515-528.
28. Mousnier A, Whale AD, Schuller S, Leong JM, Phillips AD, Frankel G: **Cortactin recruitment by enterohemorrhagic Escherichia coli O157:H7 during infection in vitro and ex vivo.** *Mol Cell Biol* 1998, **18(10):**5838-5851.
29. Du Y, Weed SA, Xiong WC, Marshall TD, Parsons JT: **Identification of a novel cortactin SH3 domain-binding protein and its localization to growth cones of cultured neurons.** *Mol Cell Biol.* 1998, **18(10):**5838-5851.
30. Huang C, Liu J, Haudenschild CC, Zhan X: **The role of tyrosine phosphorylation of cortactin in the locomotion of endothelial cells.** *The Journal of biological chemistry* 1998, **273(40):**25770-25776.
31. Lommel S, Benesch S, Rottner K, Franz T, Wehland J, Kuhn R: **Actin pedestal formation by enteropathogenic Escherichia coli and intracellular motility of Shigella flexneri are abolished in N-WASP-defective cells.** *EMBO reports* 2001, **2(9):**850-857.
32. Savkovic SD, Ramaswamy A, Koutsouris A, Hecht G: **EPEC-activated ERK1/2 participate in inflammatory response but not tight junction barrier disruption.** *American journal of physiology* 2001, **281(4):**G890-898.
33. Yaffe MB, Leparc GG, Lai J, Obata T, Volinia S, Cantley LC: **A motif-based profile scanning approach for genome-wide prediction of signaling pathways.** *Nature biotechnology* 2001, **19(4):**348-353.
34. Race PR, Solovyova AS, Banfield MJ: **Conformation of the EPEC Tir protein in solution: investigating the impact of serine phosphorylation at positions 434/463.** *Biophysical journal* 2007, **93(2):**586-596.
35. Lommel S, Benesch S, Rohde M, Wehland J, Rottner K: **Enterohaemorrhagic and enteropathogenic Escherichia coli use different mechanisms for actin pedestal formation that converge on N-WASP.** *Cellular microbiology* 2004, **6(3):**243-254.
36. Patel A, Cummings N, Batchelor M, Hill PJ, Dubois T, Mellits KH, Frankel G, Connerton I: **Host protein interactions with enteropathogenic Escherichia coli (EPEC): 14-3-3tau binds Tir and has a role in EPEC-induced actin polymerization.** *Cellular microbiology* 2006, **8(1):**55-71.
37. Kenny B, Warawa J: **Enteropathogenic Escherichia coli (EPEC) Tir receptor molecule does not undergo full modification when introduced into host cells by EPEC-independent mechanisms.** *Infect Immun* 2001, **69(3):**1444-1453.
38. Hayward RD, Leong JM, Koronakis V, Campellone KG: **Exploiting pathogenic Escherichia coli to model transmembrane receptor signalling.** *Nature reviews* 2006, **4(5):**358-370.
39. Ayala I, Baldassarre M, Giacchetti G, Caldieri G, Tete S, Luini A, Buccione R: **Multiple regulatory inputs converge on cortactin to control invadopodia biogenesis and extracellular matrix degradation.** *Journal of cell science* 2008, **121(Pt 3):**369-378.
40. Bommarius B, Maxwell D, Swimm A, Leung S, Corbett A, Bornmann W, Kalman D: **Enteropathogenic Escherichia coli Tir is an SH2/3 ligand that recruits and activates tyrosine kinases required for pedestal formation.** *Molecular microbiology* 2007, **63(6):**1748-1768.
41. Tehrani S, Tomasevic N, Weed S, Sakowicz R, Cooper JA: **Src phosphorylation of cortactin enhances actin assembly.** *Proceedings of the National Academy of Sciences of the United States of America* 2007, **104(29):**11933-11938.
42. Okamura H, Resh MD: **p80/85 cortactin associates with the Src SH2 domain and colocalizes with v-Src in transformed cells.** *The Journal of biological chemistry* 1995, **270(44):**26613-26618.
43. Alto NM, Weflen AW, Rardin MJ, Yarar D, Lazar CS, Tonikian R, Koller A, Taylor SS, Boone C, Sidhu SS, *et al.*: **The type III effector EspF coordinates membrane trafficking by the spatiotemporal activation of two eukaryotic signaling pathways.** *The Journal of cell biology* 2007, **178(7):**1265-1278.
44. Martinez-Quiles N, Rohatgi R, Anton IM, Medina M, Saville SP, Miki H, Yamaguchi H, Takenawa T, Hartwig JH, Geha RS, *et al.*: **WIP regulates N-WASP-mediated actin polymerization and filopodium formation.** *Nature cell biology* 2001, **3(5):**484-491.

Cortactin, an oncoprotein targeted by pathogens during infection

E. Nieto-Pelegrín[1], E. Meiler[1], and N. Martínez-Quiles[1, 2]

[1] Department of Microbiology, Facultad de Farmacia, Universidad Complutense de Madrid, Avda de la Complutense s/n, 28040 Madrid, Spain.
[2] Corresponding author: narcisaquiles@farm.ucm.es

1. Introduction

Cell motility and locomotion are important for many cellular functions. The cell skeleton or cytoskeleton remodels itself during multiple cellular tasks. For example, the actin cortical cytoskeleton undergoes significant changes during endocytosis, cell migration, adhesion and bacterial invasion [1].

The cytoskeleton is made up of actin, intermediate and tubulin filaments. There is crosstalk among these constituents, allowing then to behave as a complex network. We are just beginning to understand some of the aspects of this network and to flesh out the broad strokes of how it is regulated. We are confronted by great biological complexity, so we must try to simplify it in order to understand it. Thus, it would contribute to our knowledge of the cytoskeleton as a whole if we focus on some details of a particular protein that helps to orchestrate some of these changes. This review focuses on cortactin, a protein that has emerged as an important convergence node in the regulation of the cytoskeleton during numerous biological tasks. More than to give an exhaustive review, our intention is to give a general vision of the best known aspects of this protein, while highlighting with a personal view some more controversial aspects that may require further studies. We recommend some recent reviews of cortactin that complement the present one [2,3].

2. From the first studies of cortactin to the present

Cortactin was originally described as a protein located at the cell cortex and as a substrate of the Src kinase [4]. At nearly the same time, it was identified as the product of the CTTN gene (formerly EMS1), located in a chromosomal region, 11q13, frequently amplified in different human carcinomas [5]. Today, cortactin is considered an oncoprotein and a *bona fide* invadopodia marker. Invadopodia are actin-rich protrusions of the cell membrane that penetrate the extracellular matrix and degrade it, mainly through the accumulation and action of metalloproteinases [6,7]. At the same time, cortactin is a preferential target for bacterial and viral pathogens that subvert the cytoskeleton to their own benefit. For this reason, it has been called 'the Achilles' heel of the actin cytoskeleton' [8].

3. Cortactin is an important node in the regulation of the actin cellular network

Cortactin is a modular protein that participates in many signals that converge on the alteration of the actin cytoskeleton. Actin polymerization occurs when the globular monomeric form (G-actin) ensembles into a filamentous form (F-actin). The initial formation of a dimeric or a trimeric nucleus is unstable, and it is promoted and controlled by proteins that facilitate the process. One such protein is the Arp2/3 complex, which comprises two subunits, called actin-related proteins 2 and 3, as well as five other subunits. This complex is able to add a 'branch' to the side of a preexisting filament, giving rise to branched filaments with a characteristic 70-degree angle [1].

Cortactin has an N-terminal acidic motif (NTA) that directly binds and activates the Arp2/3 complex, thereby behaving as a nucleation-promoting factor (NPF). The NTA domain is followed by a six and a half repeats of amino acids that bind to F-actin, binding that is required for cortactin activity [3]. However cortactin is a weak activator of the Arp2/3 complex *in vitro*, which raises the question of whether wild-type (WT) cortactin is active or whether it requires some post-translational modification to be fully active. Indeed, although cortactin has a predicted molecular weight of approximately 65 kDa, it migrates as an 80/85 kDa doublet in SDS-PAGE. To add to the complexity, cortactin is expressed as several isoforms that differ in the number of repeats, which seems to be related to the location of these isoforms to cell-cell contacts in epithelial cells [9]. In particular, a detailed analysis of cortactin expression is needed for immunological cells, since in most situations it is assumed that a paralog protein HS1 plays the role of cortactin. We favor the hypothesis that the pattern of expression of cortactin is similar to that of N-WASP/WASP (see next paragraph). Clearly, we do not understand some basic aspects of cortactin expression and post-translational modification.

There is another way in which cortactin can promote actin nucleation: its SH3 terminal domain binds directly and activates the neural Wiskott-Aldrich syndrome protein (N-WASP) [10, 11]. The first described activators of the Arp2/3 complex were the WASP family of proteins. The representative member of the family, WASP, which is expressed exclusively in the immune system, is mutated in the immune deficiency called Wiskott-Aldrich syndrome (WAS). N-

WASP is more ubiquitous than WASP and is coexpressed with this protein in some cell types, such as macrophages and dendritic cells. The mechanism by which these proteins promote actin polymerization (NPFs class I) differs from that of cortactin: they bind G-actin and activate the Arp2/3 complex through a verprolin cofilin acidic (VCA) domain [10].

4. Cellular location of cortactin

Following various stimuli such as growth factor stimulation, binding and integrin engagement, cortactin translocates from a perinuclear/Golgi location to areas of cytoskeleton remodeling, such as lamellipodia at the leading edge [3]. The molecular mechanism of this translocation is still unknown. More recently, cortactin has been detected in the nucleus, where it has been proposed to participate in the separation of the centrosomes in preparation for mitosis [12]. Again the details of this translocation remain to be elucidated.

5. Post-translational modifications of cortactin

5.1 Cortactin phosphorylation

As previously mentioned, cortactin is traditionally known as a substrate of Src kinase. Until the past decade, that was the only known cortactin post-translational modification of cortactin. In the murine protein the major phosphorylation sites are tyrosines 421, 466 and 482. It is assumed that Src phosphorylation of cortactin stimulates cortactin activity. More recent data, however, paint a more complicated picture of the effect of Src-mediated phosphorylation of native cortactin [3].

In addition to Src kinase, one study has indicated that extracellular response-activated kinase (Erk) phosphorylates cortactin on serines 405 and 418 [13]. Long forgotten, this report came to light again in view of the action of cortactin on N-WASP activity, which we discuss later in this review.

In a comprehensive and meritorious effort, the Cell Migration Consortium mapped cortactin phosphorylation sites [14] describing 17 new ones. This gives us a more realistic perspective on the complexity of the regulation of this protein. Most of these sites are serines and threonines.

At the present it is known that cortactin is phosphorylated by various kinases, including Fer, Abelson and related kinases (Abl/Arg), p21-activated kinases (Paks) [15], and protein kinase D (PKD) [3]. In contrast, protein-tyrosine phosphatase 1B (PTP1B) is the sole phosphatase known to act on cortactin [16,17]. The physiological importance of cortactin dephosphorylation has probably been misrepresented due to the scarce data on the subject.

5.2 Cortactin acetylation

Recently, regulation of cortactin by reversible lysine acetylation has been described [18]. It can be acetylated by the acetyltransferase PCAF and p300, and deacetylated by histone deacetylase 6 (HDAC6) and SIRT1. According to this study, 11 lysines can be acetylated. When acetylated, the molecule loses two otherwise positively charged patches of lysines, most of which are located in the area of the repeats. Consequently, the ability of cortactin to bind F-actin diminishes. The authors of that study proposed that acetylation of cortactin inactivates the protein. However, it is very important to address the consequences of this acetylation on cortactin activity using *in vitro* actin polymerization assays and an acetylation mimic cortactin mutant. In this way, some important conclusions might be drawn about the activity of the protein and the effect of the acetylation on cortactin structure.

This regulation has already been implicated in quality control (QC) autophagy, a mechanism that, under physiological conditions, is important for removal of protein aggregates and turnover of organelles, such as mitochondria. HDAC6 recruits and deacetylates cortactin, which promotes the F-actin remodelling required for the fusion of autophagosome and lysosome and subsequent substrate degradation [19].

6. Cortactin as a cytoskeletal switch

Apart from its intrinsic activity, cortactin can activate the WASP/N-WASP family of nucleators, which establishes a functional connection between the two main families of proteins capable of activating the Arp2/3 complex.

It was shown that cortactin binds and activates N-WASP through its SH3 terminal domain. However, full-length cortactin was less potent than the isolated SH3 domain in activating N-WASP, which suggests that cortactin, at least *in vitro*, is in a closed conformation that masks the SH3 domain. The interaction between cortactin and N-WASP was studied using *in vitro* actin polymerization assays involving both phosphomimetic mutants and non-phosphorylatable mutants of cortactin, as well as recombinant cortactin phosphorylated *in vitro*. Erk-mediated serine phosphorylation of cortactin opens the molecule, and allows the cortactin SH3 to interact with N-WASP. This interaction is terminated by Src-mediated tyrosine phosphorylation of cortactin. These findings led to the proposal of an 'on/off switching' mechanism called the 'S-Y Swicth' model, in which phosphorylation of cortactin by Erk and Src kinases controls the

ability of cortactin to activate N-WASP. Thus, cortactin binds and activates N-WASP only when phosphorylated at serines 405 and 418. The phosphorylation of cortactin by Src at tyrosines 421, 466 and 482 terminates this interaction (Fig. 1) [11].

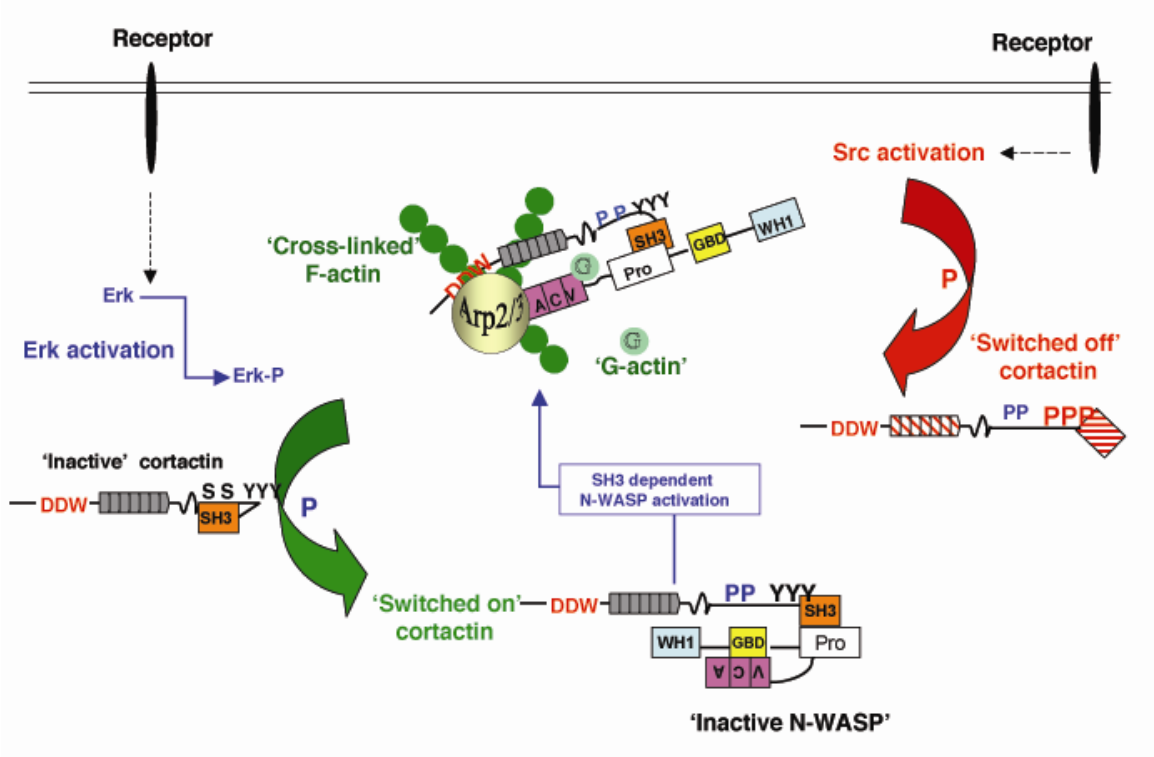

Figure 1. Coupled cortactin-N-WASP activation according to the 'S-Y Switch' model proposed by Martinez-Quiles *et al* (2004).

The most easily testable prediction of the 'S-Y Switch' model is the understanding that cortactin can be regulated by a conformational change. The structure of cortactin has been resolved by circular dicroism, chemical crosslinking and X-ray scattering. These results showed that cortactin adopts a closed globular conformation through interaction between the cortactin SH3 domain and the repeats region [20]. These results are in agreement with our proposed 'S-Y Switch' model and contradict a previous description of cortactin as a thin elongated monomer [21]. It would be very important to use structural techniques to asses how Src-mediated phosphorylation of cortactin affects its structure and activity. As mentioned above, it seems that the *in vitro* effect of this phosphorylation is different from that of Erk phosphorylation, which seems to open the molecule and liberate the SH3 domain.

Immediately after Erk- and Src-mediated phosphorylation was shown to regulate cortactin, these findings were tested in different *in vivo* settings because of their repercussions on the fields of cellular motility and molecular microbiology [8, 22]. In a clear relation to the 'S-Y Switch' model, studies examined the effects of different serine and tyrosine phospho-mutations in cortactin on lamellipodial protrusion, actin assembly within cells, and focal adhesion dynamics. Cortactin mutants mimicking serine phosphorylation appeared to affect predominantly actin polymerization, whereas mutation of tyrosine residues altered turnover of focal adhesions [23].

The 'S-Y Switch' model was also tested in different settings [24, 25], and phosphorylation of cortactin not only by Erk and Src but also by Pak was shown to be important for invadopodia formation, where 'a fine balance between different phosphorylation events induces subtle changes in structure to calibrate cortactin function during invadopodia formation' [24].

Finally, the importance of studying the different states of cortactin phosphorylation during bacterial invasion has been highlighted [8]. Under the new prism of the 'S-Y Switch' model, our group decided to assess the contribution of cortactin to actin polymerization during pedestal formation by enteropathogenic *Escherichia coli* (EPEC). We chose EPEC as a model system in order to analyze signaling to the actin cytoskeleton across the plasma membrane in response to external stimuli.

7. Cortactin and bacterial pathogens

7.1 Role of cortactin in pedestal formation by EPEC and EHEC

Numerous pathogens have evolved mechanisms to subvert for their own benefit the cellular regulatory complexes that control actin polymerization. Among such bacteria, enteropathogenic *Escherichia coli* (EPEC) and enterohemorrhagic *E. coli* (EHEC) are non-invasive pathogens. EPEC are responsible for severe diarrhoea and EHEC can cause bloody diarrhoea, haemorrhagic colitis and haemolytic uremic syndrome. Both food-borne pathogens are an important cause of infant mortality in developing countries. These bacteria colonize the intestinal epithelium through the formation of attaching and effacing (AE) lesions, which are characterized by a localized loss of microvilli, close adherence of bacteria to the host cell membrane and the generation of filamentous (F)-actin-rich structures beneath these bacteria called pedestals [26,27].

To generate these actin pedestals both pathogens translocate their bacterial effectors into the mammalian cell using a type III secretion system (TIIISS). Translocated intimin receptor (Tir) is a translocated receptor that inserts into the plasma membrane with a hairpin loop topology. The extracellular domain binds to the bacterial outer membrane protein intimin inducing clustering of Tir. Tyrosine 474 in the C-terminal cytoplasmic domain is phosphorylated. This phosphotyrosine recruits the SH2 domain-containing mammalian adapter proteins Nck1 and Nck2 (hereafter referred to collectively as Nck). Nck recruits and is thought to activate N-WASP, which in turns binds and activates the Arp2/3 complex to promote actin polymerization [28].

For many years this has been the only pathway considered both necessary and sufficient for actin polymerization. When our research group as new comers to the field, examine the literature on this pathway, several questions occur to us. When does the phosphorylation of Tir occur? After the insertion in the membrane or is it a necessary step for insertion? Does it occur before or after clustering? If we extrapolated from signaling in immune receptors, we would expect the clustering to precede the phosphorylation. A more general question is, why, ultimately, do these bacteria form pedestals? This is an intriguing question because bacteria also adhere without them. Are pedestals made for the sole purpose of strengthening bacterial adhesion? If so, why are then many other proteins recruited to pedestals, including cortactin [29,30]? What is the reason for recruiting two activators of the Arp2/3 complex, when one (N-WASP) is sufficient [31]?

It is known that cortactin localizes to actin pedestals, and that overexpression of truncated forms of the protein blocks pedestal formation [31]. This indicates that cortactin is an important player whose role should be reconsidered in view of its newly described capacity to directly activate both the Arp2/3 complex [21] and N-WASP [11]. Greater importance for cortactin is also suggested by the recently proposed 'S-Y Switch' model of regulation [11]. Indeed, using a very similar approach two research groups [32, 33] examined the effect of serine and tyrosine phospho-mimic and non-phosphorylatable mutants of cortactin on pedestal formation. Both studies concluded that tyrosine phosphorylation inhibits pedestal formation. However, the Erk phospho-mimic mutant had no effect on pedestal formation, in contrast to the inhibitory effect of the corresponding non-phosphorylatable mutant [33]. Therefore it seems that serine phosphorylation of cortactin is needed for pedestal formation, whereas tyrosine phosphorylation inhibits it.

A very important finding reported independently by both groups is that EPEC infection induces tyrosine phosphorylation of cortactin [32, 33]; this phosphorylation is abolished in N-WASP-deficient cells [33] but not in Nck-deficient cells (our own unpublished results). Therefore cortactin tyrosine-phosphorylation depends on the presence of N-WASP, more than on the presence of the pedestal itself, because pedestals do not form in the absence of either N-WASP or Nck. On the contrary, serine phosphorylation of cortactin does not require N-WASP. Moreover, the N-terminal domain of cortactin directly binds the N-terminal part of Tir *in vitro* [33, 32], in a tyrosine and serine phosphorylation independent manner [32, 33]. More importantly, the interaction between cortactin and Tir_{EPEC} promotes Arp2/3 complex-mediated actin polymerization by activating cortactin [33].

We propose a model of cortactin action on pedestals induced by EPEC (Fig. 2) [33]. Taking into account that cortactin binds and activates N-WASP though its SH3 domain, and that this activation by cortactin is regulated by tyrosine and serine phosphorylation of cortactin, we proposed that cortactin binds Tir through the N-terminus and N-WASP through the SH3 domain. In this situation, cortactin phosphorylated on serine would bind both Tir and N-WASP, whereas cortactin phosphorylated on tyrosine would bind only Tir. In other words, cortactin may act on the Tir-Nck-N-WASP pathway by controlling a possible cycling activity of N-WASP that may underlie pedestal motility (Fig. 2) [33].

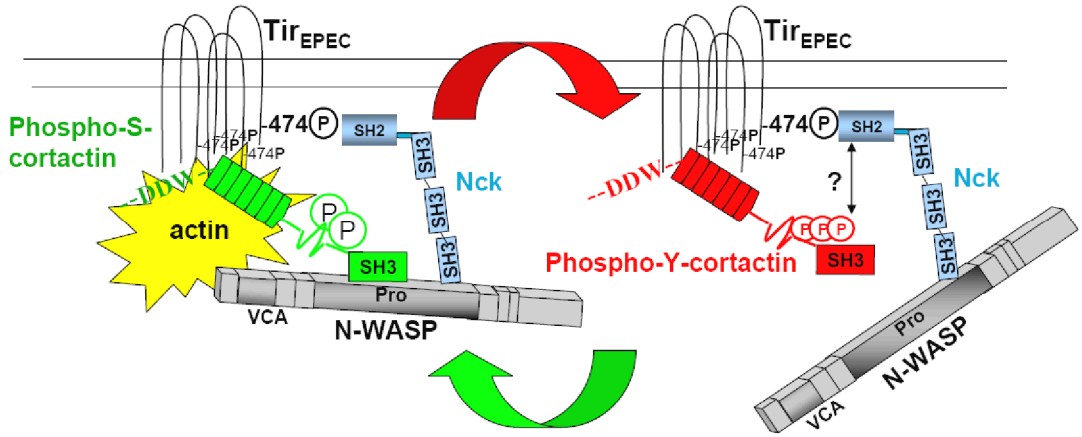

Figure 2. Proposed model of the coordinated actions of cortactin and N-WASP during EPEC infection. Modified from Cell Commun Signal. 2009 May 6; 7:11.

Current research on pedestal signaling to trigger actin polymerization shows an increasingly complicated picture: no longer is there a reassuringly linear Tir-Nck-N-WASP pathway. EspF is another translocated effector of both EPEC and EHEC that seems to participate in pedestal formation. EspF contains several C-terminal repeats, each of which possesses a segment for N-WASP binding and a proline-rich sequence. The latter is recognized by sorting nexin 9 (SNX9), a protein that contains an SH3 domain and a highly conserved Bin-Amphysin-Rvs (BAR) domain that binds and deforms membranes inwardly. The role of EspF-SNX9 interaction is intuitively difficult to understand because pedestals are structures that protrude [34]. The implication of cortactin in this recently described and apparently secondary pathway has not been addressed. Therefore it would be very interesting to test whether cortactin contributes to actin assembly through EspF.

Despite the high homology between the Tir proteins from EPEC and EHEC strains, the latter lack tyrosine 474 which has 'forced' the development of a distinct mechanism to promote actin synthesis in EHEC. In this pathotype, Tir_{EHEC} does not require Nck for actin assembly. Two groups reported that the effector encoded within prophage U, EspFu [35], also known as Tir cytoskeleton coupling protein, Tccp [36], is able to recruit and to activate N-WASP. EspFu is recruited to sites of bacterial attachment, and this recruitment depends on the NPY_{458} (Asn-Pro-Tyr_{458}) motif located in the C-terminal domain of Tir_{EHEC}. It is unclear how the motif recruits EspFu, since EspFu does not bind directly to it.

Interestingly, this motif is homologous to tyrosine 454 on Tir_{EPEC}, which is responsible for a minor Nck-independent pathway whose physiological importance is uncertain. This raises the possibility that both EPEC and EHEC use a common Nck-independent pathway for actin polymerization. How can it be that what is an inefficient mechanism in EPEC has turned into the major mechanism in EHEC? The expression of EspFu by EHEC has converted this otherwise secondary pathway into the principal one. The picture gets even more complicated when we consider that EHEC express both EspFu and EspF effectors which share 25% sequence identity and 35% similarity.

As another example of bacterial molecular mimicry, EspFu is able to activate N-WASP by disrupting the intramolecular interaction that maintains N-WASP in a closed conformation [37]. Although WIP is known to keep N-WASP in a closed conformation [38], the role of WIP in modulating the effect of EspFu on N-WASP has not been addressed.

7.1.1 Cortactin as the 'missing link' in EHEC

Although N-WASP and EspFu complex with Tir neither protein binds Tir directly. An important area of investigation in EHEC signaling to actin is the search for the 'missing link' that bridges Tir and N-WASP. Cortactin has been suggested as an appropriate candidate [39]. Cortactin binds both Tir_{EHEC}, and EspFu simultaneously: the C-terminal SH3 domain of cortactin is responsible for binding EspFu [39]. Subsequently, in *in vitro* organ cultures (IVOC) of human terminal ileal tissue, it was shown that cortactin is recruited to the site of EHEC adhesion independently of EspFu and N-WASP. This suggests that cortactin plays a more important role during infection of mucosal surfaces *in vivo* than has been observed using *in vitro* cultured cells [40].

Interestingly, at early stages of infection, EHEC induces the tyrosine phosphorylation of cortactin, after which it is rapidly dephosphorylated [40]. The authors proposed a model where at early stages of infection cortactin binds Tir and EspFu. Soon thereafter, cortactin is tyrosine-dephosphorylated and released from EspFu. Finally this liberated cortactin helps to activate N-WASP, promoting actin polymerization through the Arp2/3 complex [40] (Fig. 3).

Various other proposed 'missing links' has been proposed, such as the 53KDa insulin receptor substrate (IRSp53) and insulin receptor tyrosine kinase substrate (IRTKS), which are homologous to each other [41-43]. Both contain inverse-BAR (I-BAR) domains that deform PI(4,5)P(2)-rich membranes outwardly, mainly through electrostatic interactions [44]. We should also take into account that Tir_{EPEC} phosphorylated on tyrosine 454 forms complexes with an active phosphatidylinositol 3-kinase (PI3K), probably to stimulate the production of PI(3,4,5)P(3) beneath EPEC attachment sites [45]. If we extrapolate this mechanism to the tyrosine 458 of EHEC, we can speculate that IRSp53 is implicated in the deformation of the membrane, which in turn is coupled to actin remodeling through a process involving the WAVE family of proteins [46]. Although researchers that advocate for these missing links tend to underestimate the contribution of cortactin, we think that both IRSp53/IRTKs and cortactin might participate in the process, and that contradictory views arise from the incompleteness of the data at presently known. To be sure, we could propose many different models to support various views of the signaling process and of the identity of the missing link in EHEC. However, we believe that when doing research on signal transduction it is important to keep an open mind [47] and to interpreter incomplete findings cautiously. Dogmas are sustained until knowledge abrogates them, and one example is the finding that a recently described category of EPEC forms intracellular pedestals [48].

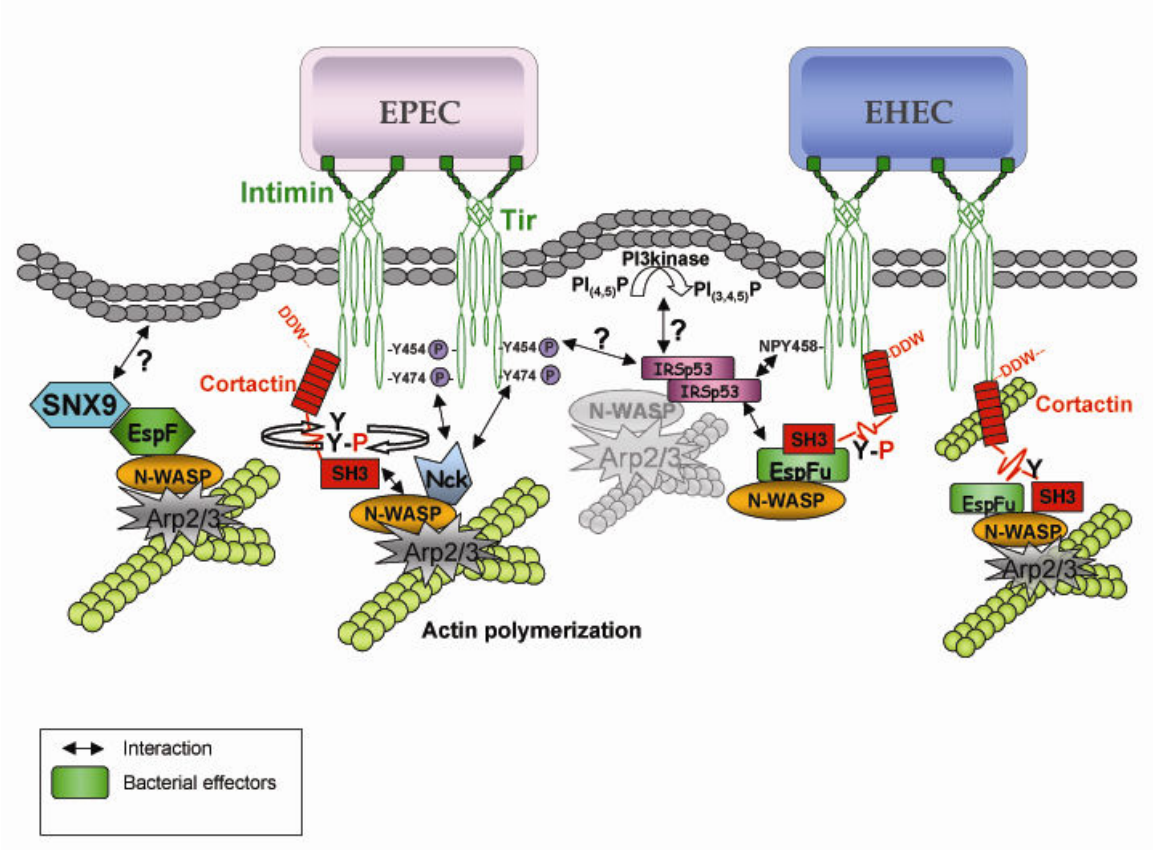

Figure 3. Signaling during pedestal formation by EPEC and EHEC

7.2 Cortactin phosphorylation during the invasion of other pathogens

During *Chlamydia trachomatis* infection, pathways involving Abl kinase or platelet-derived growth factor receptor (PDGFR) are activated, leading to tyrosine phosphorylation of cortactin. Tyrosine phosphorylation of cortactin likely participates in the remodelling of actin cytoeskeleton in order to internalize bacteria. Phospho-cortactin is also recruited to the site of bacterial entry [49]. There are many other examples where bacteria control cortactin phosphorylation as part of a complex mechanism of entry, such as *Shigella* [8]. Many other pathogens will be shown to alter not only cortactin tyrosine phosphorylation but many other post-translational modifications.

7.2.1 Cortactin as a bacterial target for acetylation

To block the immune response, the acetyltranferase YopJ, an effector of *Yersinia* species, acetylates the critical serine or threonine of the activation loop of a MAP kinase, impeding its subsequent activation by phosphorylation [50].

It would be very interesting to test whether *Yersinia* also inhibits cortactin by acetylating it. In addition to deacetylating cortactin, HDAC6 deacetylates alpha-tubulin and this is required for invasion by uropathogenic

Escherichia coli (UPEC) [51]. Future studies will probably establish many situations in which acetilation/deacetilation is subverted by pathogens [52].

7.2.2. Cortactin and the innate immune response to *Candida*

Immature dendritic cells (DC) express C-type lectins that recognize fungi. A newly described type of protrusion, named fungipod, has been implicated in the recognition of *Candida parapsilosis*. Fungipods are dynamic structures that contain clathrin, actin and cortactin. They may promote yeast phagocytosis by DCs [53].

Acknowledgments
This work was supported by grants to NMQ from Fundación Médica Mutua Madrileña (FMMM) and the Instituto de Salud Carlos III (PS0900080). ENP and EM are predoctoral UCM fellows.

References

[1] Pollard TD, Cooper JA. Actin, a central player in cell shape and movement. *Science*. 2009;326(5957):1208-12.
[2] Ren G, Crampton MS, Yap AS. Cortactin: Coordinating adhesion and the actin cytoskeleton at cellular protrusions. *Cell Motil Cytoskeleton*. 2009;66(10):865-73.
[3] Ammer AG, Weed SA. Cortactin branches out: roles in regulating protrusive actin dynamics. *Cell Motil Cytoskeleton.* 2008;65(9):687-707.
[4] Wu H, Reynolds AB, Kanner SB, Vines RR, Parsons JT. Identification and characterization of a novel cytoskeleton-associated pp60src substrate. *Mol Cell Biol*. 1991;11(10):5113-24.
[5] Schuuring E, Verhoeven E, Mooi WJ, Michalides RJ. Identification and cloning of two overexpressed genes, U21B31/PRAD1 and EMS1, within the amplified chromosome 11q13 region in human carcinomas. *Oncogene*. 1992;7(2):355-61.
[6] Weaver AM. Cortactin in tumor invasiveness. *Cancer Lett*. 2008;8;265(2):157-66.
[7] Caldieri G, Ayala I, Attanasio F, Buccione R. Cell and molecular biology of invadopodia. *Int Rev Cell Mol Biol*. 2009;275:1-34.
[8] Selbach M, Backert S. Cortactin: an Achilles' heel of the actin cytoskeleton targeted by pathogens. *Trends Microbiol*. 2005;13(4):181-9.
[9] Katsube T, Togashi S, Hashimoto N, Ogiu T, Tsuji H. Filamentous actin binding ability of cortactin isoforms is responsible for their cell-cell junctional localization in epithelial cells. *Arch Biochem Biophys*. 2004;1;427(1):79-90.
[10] Kurisu S, Takenawa T. The WASP and WAVE family proteins. *Genome Biol*. 2009;10(6):226.
[11] Martinez-Quiles N, Ho HY, Kirschner MW, Ramesh N, Geha RS. Erk/Src phosphorylation of cortactin acts as a switch on-switch off mechanism that controls its ability to activate N-WASP. *Mol Cell Biol*. 2004;24(12):5269-80.
[12] Wang W, Chen L, Ding Y, Jin J, Liao K. Centrosome separation driven by actin-microfilaments during mitosis is mediated by centrosome-associated tyrosine-phosphorylated cortactin. *J Cell Sci.* 2008;15;121(Pt 8):1334-43.
[13] Campbell DH, Sutherland RL, Daly RJ. Signaling pathways and structural domains required for phosphorylation of EMS1/cortactin. *Cancer Res*. 1999;15;59(20):5376-85.
[14] Martin KH, Jeffery ED, Grigera PR, Shabanowitz J, Hunt DF, Parsons JT. Cortactin phosphorylation sites mapped by mass spectrometry. *J Cell Sci*. 2006;15;119(Pt 14):2851-3.
[15] Buday L, Downward J. Roles of cortactin in tumor pathogenesis. *Biochim Biophys Acta.* 2007;1775(2):263-73.
[16] Stuible M, Dubé N, Tremblay ML. PTP1B regulates cortactin tyrosine phosphorylation by targeting Tyr446. *J Biol Chem.* 2008;6;283(23):15740-6.
[17] Mertins P, Eberl HC, Renkawitz J, Olsen JV, Tremblay ML, Mann M, Ullrich A,Daub H. Investigation of protein-tyrosine phosphatase 1B function by quantitative proteomics. *Mol Cell Proteomics*. 2008;7(9):1763-77.
[18] Zhang X, Yuan Z, Zhang Y, Yong S, Salas-Burgos A, Koomen J, Olashaw N, ParsonsJT, Yang XJ, Dent SR, Yao TP, Lane WS, Seto E. HDAC6 modulates cell motility by altering the acetylation level of cortactin. *Mol Cell*. 2007;20;27(2):197-213.
[19] Lee JY, Koga H, Kawaguchi Y, Tang W, Wong E, Gao YS, Pandey UB, Kaushik S,Tresse E, Lu J, Taylor JP, Cuervo AM, Yao TP. HDAC6 controls autophagosome maturation essential for ubiquitin-selective quality-control autophagy. *EMBO J.* 2010;3;29(5):969-80.
[20] Cowieson NP, King G, Cookson D, Ross I, Huber T, Hume DA, Kobe B, Martin JL.Cortactin adopts a globular conformation and bundles actin into sheets. *J Biol Chem*. 2008;6;283(23):16187-93.
[21] Weaver AM, Karginov AV, Kinley AW, Weed SA, Li Y, Parsons JT, Cooper JA. Cortactin promotes and stabilizes Arp2/3-induced actin filament network formation. *Curr Biol*. 2001;6;11(5):370-4.
[22] Lua BL, Low BC. Cortactin phosphorylation as a switch for actin cytoskeletal network and cell dynamics control. *FEBS Lett*. 2005;31;579(3):577-85.
[23] Kruchten AE, Krueger EW, Wang Y, McNiven MA. Distinct phospho-forms of cortactin differentially regulate actin polymerization and focal adhesions. *Am J Physiol Cell Physiol*. 2008;295(5):C1113-22.
[24] Ayala I, Baldassarre M, Giacchetti G, Caldieri G, Tetè S, Luini A, Buccione R. Multiple regulatory inputs converge on cortactin to control invadopodia biogenesis and extracellular matrix degradation. *J Cell Sci*. 2008;1;121(Pt3):369-78.
[25] Jia L, Uekita T, Sakai R. Hyperphosphorylated cortactin in cancer cells plays an inhibitory role in cell motility. *Mol Cancer Res*. 2008;6(4):654-62.
[26] Croxen MA, Finlay BB. Molecular mechanisms of Escherichia coli pathogenicity. *Nat Rev Microbiol*. 2010;8(1):26-38.
[27] Hayward RD, Leong JM, Koronakis V, Campellone KG. Exploiting pathogenic Escherichia coli to model transmembrane receptor signalling. *Nat Rev Microbiol*. 2006;4(5):358-70.

[28] Caron E, Crepin VF, Simpson N, Knutton S, Garmendia J, Frankel G. Subversion of actin dynamics by EPEC and EHEC. *Curr Opin Microbiol*. 2006;9(1):40-5.
[29] Dean P, Kenny B. The effector repertoire of enteropathogenic E. coli: ganging up on the host cell. *Curr Opin Microbiol*. 2009;12(1):101-9.
[30] Sal-Man N, Biemans-Oldehinkel E, Finlay BB. Structural microengineers: pathogenic Escherichia coli redesigns the actin cytoskeleton in host cells. *Structure*. 2009;14;17(1):15-9.
[31] Cantarelli VV, Takahashi A, Yanagihara I, Akeda Y, Imura K, Kodama T, Kono G, Sato Y, Iida T, Honda T. Cortactin is necessary for F-actin accumulation in pedestal structures induced by enteropathogenic Escherichia coli infection. *Infect Immun*. 2002;70(4):2206-9.
[32] Cantarelli VV, Kodama T, Nijstad N, Abolghait SK, Iida T, Honda T. Cortactin is essential for F-actin assembly in enteropathogenic Escherichia coli (EPEC)-and enterohaemorrhagic E. coli (EHEC)-induced pedestals and the alpha-helical region is involved in the localization of cortactin to bacterial attachment sites. *Cell Microbiol*. 2006;8(5):769-80.
[33] Nieto-Pelegrin E, Martinez-Quiles N. Distinct phosphorylation requirements regulate cortactin activation by TirEPEC and its binding to N-WASP. *Cell Commun Signal*. 2009;6;7:11.
[34] Campellone KG. Cytoskeleton-modulating effectors of enteropathogenic and enterohaemorrhagic Escherichia coli: Tir, EspF and actin pedestal assembly. *FEBS J*. 2010;27.
[35] Campellone, K. G., D. Robbins, et al.. "EspFU is a translocated EHEC effector that interacts with Tir and N-WASP and promotes Nck-independent actin assembly". *Dev Cell*. 2004;7(2):217-228.
[36] Garmendia, J., A. D. Phillips, et al.. "TccP is an enterohaemorrhagic Escherichia coli O157:H7 type III effector protein that couples Tir to the actin-cytoskeleton". *Cell Microbiol.* 2004;6(12):1167-83
[37] Daugherty-Clarke K, Goode BL. WASp identity theft by a bacterial effector. *Dev Cell*. 2008;15(3):333-4.
[38] Martinez-Quiles N, Rohatgi R, Antón IM, Medina M, Saville SP, Miki H,Yamaguchi H, Takenawa T, Hartwig JH, Geha RS, Ramesh N. WIP regulates N-WASP-mediated actin polymerization and filopodium formation. *Nat Cell Biol*. 2001;3(5):484-91.
[39] Cantarelli VV, Kodama T, Nijstad N, Abolghait SK, Nada S, Okada M, Iida T,Honda T. Tyrosine phosphorylation controls cortactin binding to two enterohaemorrhagic Escherichia coli effectors: Tir and EspFu/TccP. *Cell Microbiol*. 2007;9(7):1782-95.
[40] Mousnier A, Whale AD, Schüller S, Leong JM, Phillips AD, Frankel G. Cortactin recruitment by enterohemorrhagic Escherichia coli O157:H7 during infection in vitro and ex vivo. *Infect Immun*. 2008;76(10):4669-76.
[41] Weiss SM, Ladwein M, Schmidt D, Ehinger J, Lommel S, Städing K, Beutling U,Disanza A, Frank R, Jänsch L, Scita G, Gunzer F, Rottner K, Stradal TE. IRSp53 links the enterohemorrhagic E. coli effectors Tir and EspFU for actin pedestal formation. *Cell Host Microbe*. 2009;19;5(3):244-58.
[42] Yi CR, Goldberg MB. Putting enterohemorrhagic E. coli on a pedestal. *Cell Host Microbe*. 2009;19;5(3):215-7.
[43] Vingadassalom D, Kazlauskas A, Skehan B, Cheng HC, Magoun L, Robbins D, Rosen MK, Saksela K, Leong JM. Insulin receptor tyrosine kinase substrate links the E. coli O157:H7 actin assembly effectors Tir and EspF(U) during pedestal formation. *Proc Natl Acad Sci U S A*. 2009;21;106(16):6754-9.
[44] Takenawa T. Phosphoinositide-binding interface proteins involved in shaping cell membranes. Proc Jpn Acad Ser *B Phys Biol Sci*. 2010;86(5):509-23.
[45] Sason H, Milgrom M, Weiss AM, Melamed-Book N, Balla T, Grinstein S, Backert S,Rosenshine I, Aroeti B. Enteropathogenic Escherichia coli subverts phosphatidylinositol 4,5-bisphosphate and phosphatidylinositol 3,4,5-trisphosphate uponepithelial cell infection. *Mol Biol Cell*. 2009;20(1):544-55.
[46] Miki H, Yamaguchi H, Suetsugu S, Takenawa T. IRSp53 is an essential intermediate between Rac and WAVE in the regulation of membrane ruffling. *Nature* 2000;7;408(6813):732-5.
[47] Mayer BJ, Blinov ML, Loew LM. Molecular machines or pleiomorphic ensembles: signaling complexes revisited. *J Biol*. 2009;16;8(9):81.
[48] Bulgin R, Arbeloa A, Goulding D, Dougan G, Crepin VF, Raymond B, Frankel G. The T3SS effector EspT defines a new category of invasive enteropathogenic E. coli (EPEC) which form intracellular actin pedestals. *PLoS Pathog*. 2009;5(12):e1000683.
[49] Elwell, C. A., A. Ceesay, et al. "RNA interference screen identifies Abl kinase and PDGFR signaling in Chlamydia trachomatis entry." *PLoS Pathog*. 2008;4(3):e1000021.
[50] Ukherjee S, Keitany G, Li Y, Wang Y, Ball HL, Goldsmith EJ, Orth K. Yersinia YopJ acetylates and inhibits kinase activation by blocking phosphorylation. *Science*. 2006;26;312(5777):1211-4.
[51] Dhakal BK, Mulvey MA. Uropathogenic Escherichia coli invades host cells via an HDAC6-modulated microtubule-dependent pathway. *J Biol Chem*. 2009;2;284(1):446-54.
[52] Linda I H, Bruno P L, Alan J W. Bacterial protein acetylation: the dawning of a new age. *Mol Microbiol*. 2010;12.
[53] Neumann AK, Jacobson K. A novel pseudopodial component of the dendritic cell anti-fungal response: the fungipod. *PLoS Pathog*. 2010;12;6(2):e1000760.

OPEN ACCESS Freely available online

PLoS one

Cortactin Tyrosine Phosphorylation Promotes Its Deacetylation and Inhibits Cell Spreading

Eugenia Meiler, Elvira Nieto-Pelegrín, Narcisa Martinez-Quiles*

Departamento de Microbiología II, Facultad de Farmacia, Universidad Complutense de Madrid, Madrid, Spain

Abstract

Background: Cortactin is a classical Src kinase substrate that participates in actin cytoskeletal dynamics by activating the Arp2/3 complex and interacting with other regulatory proteins, including FAK. Cortactin has various domains that may contribute to the assembly of different protein platforms to achieve process specificity. Though the protein is known to be regulated by post-translational modifications such as phosphorylation and acetylation, how tyrosine phosphorylation regulates cortactin activity is poorly understood. Since the basal level of tyrosine phosphorylation is low, this question must be studied using stimulated cell cultures, which are physiologically relevant but unreliable and difficult to work with. In fact, their unreliability may be the cause of some contradictory findings about the dynamics of tyrosine phosphorylation of cortactin in different processes.

Methodology/Principal Findings: In the present study, we try to overcome these problems by using a Functional Interaction Trap (FIT) system, which involves cotransfecting cells with a kinase (Src) and a target protein (cortactin), both of which are fused to complementary leucine-zipper domains. The FIT system allowed us to control precisely the tyrosine phosphorylation of cortactin and explore its relationship with cortactin acetylation.

Conclusions/Significance: Using this system, we provide definitive evidence that a competition exists between acetylation and tyrosine phosphorylation of cortactin and that phosphorylation inhibits cell spreading. We confirmed the results from the FIT system by examining endogenous cortactin in different cell types. Furthermore, we demonstrate that cell spreading promotes the association of cortactin and FAK and that tyrosine phosphorylation of cortactin disrupts this interaction, which may explain how it inhibits cell spreading.

Citation: Meiler E, Nieto-Pelegrín E, Martinez-Quiles N (2012) Cortactin Tyrosine Phosphorylation Promotes Its Deacetylation and Inhibits Cell Spreading. PLoS ONE 7(3): e33662. doi:10.1371/journal.pone.0033662

Editor: Laszlo Buday, Hungarian Academy of Sciences, Hungary

Received January 4, 2012; **Accepted** February 14, 2012; **Published** March 30, 2012

Funding: This work was funded by an Instituto de Salud Carlos III grant (PS09/0080) and a Fundación Médica Mutua Madrileña Personnel grant (01754/2008) to NMQ. NMQ is also funded by the I3 program [Ministerio de Ciencia e Innovación (MICINN)]. EMR and ENP are predoctoral fellows supported, respectively, by the Formación Personal Universitario (FPU) program of MICINN and by the Universidad Complutense de Madrid (UCM). The funders had no role in study design, data collection and analysis, decision to publish, or preparation of the manuscript.

Competing Interests: The authors have declared that no competing interests exist.

* E-mail: narcisaquiles@farm.ucm.es

Introduction

The actin cytoskeleton remodels to accomplish many cellular processes and therefore undergoes significant changes during cell migration, adhesion, endocytosis and bacterial invasion [1]. The cortactin protein has emerged as an important node in the network regulating the actin cytoskeleton during numerous biological processes [2,3]. It was originally described as a substrate of Src kinase located primarily at the cell cortex [4]. Almost simultaneously, cortactin was cloned as the product of the *CTTN* gene (formerly *EMS1*), located in chromosomal region 11q13, which is frequently amplified in different human carcinomas [5]. Today, cortactin is considered an oncoprotein and a *bona fide* invadopodial marker [6].

Cortactin is a modular protein that contains an N-terminal acidic (NTA) domain with a $_{20}$DDW$_{22}$ motif that directly binds and activates the Arp2/3 complex. The NTA domain is followed by six and a half amino acid 'repeats' that bind to F-actin and define the actin-binding region (ABR) [7]. Since cortactin only weakly activates the Arp2/3 complex *in vitro* [8], it is unclear whether cortactin requires post-translational modifications to be fully active. The ABR is followed by a helical, proline-rich region, followed in turn by a C-terminal Src homology (SH3) domain. Cortactin binds several proteins through its SH3 domain, such as WIP [9] and neural Wiskott-Aldrich syndrome protein (N-WASP) [10,11].

Cortactin regulation is very complex [12]. Although traditionally studied as a substrate of Src family kinases (SFKs) [4], it can also be phosphorylated by other tyrosine kinases such as Fer [13] and Abl/Arg [14]. The effects of tyrosine phosphorylation on cortactin structure and function remain largely unknown. This phosphorylation was shown to decrease cortactin binding to F-actin [15], and this binding is required for cortactin activation of the Arp2/3 complex [16]. This phosphorylation is also required for inducing bone metastasis of breast cancer cells in nude mice [17], and it appears to be involved in bacterial invasion of cells, such as for the adhesion of enteropathogenic *Escherichia coli* (EPEC) [18]. Protein phosphatase 1B (PTB-1B) dephosphorylates tyrosine 421 in cortactin [19], suggesting reversible regulation. The data seem to indicate that tyrosine phosphorylation of cortactin is

tightly controlled, but the details of this regulation are far from clear. Tyrosine phosphorylation-dephosphorylation of cortactin may regulate its ability to form complexes with other proteins [20,21].

Cortactin is also the target of serine-threonine kinases, including ERK [22] and Pak [23,24]. In fact, phosphoproteomic analysis has revealed numerous phosphorylation sites, most of which are serines and threonines [25].

Cortactin promotes actin polimerization through two pathways: directly, by activating the Arp2/3 complex; and indirectly, when the SH3 domain binds and activates N-WASP [10]. *In vitro*, cortactin binds and activates N-WASP only when phosphorylated on serines by ERK, whereas phosphorylation by Src at tyrosines 421, 466 and 482 terminates cortactin activation of N-WASP, which suggests that phosphorylation indeed affects cortactin structure. Based on studies by our group [10] and others [22], we proposed a model in which serine/tyrosine phosphorylation controls the accessibility of the SH3 domain of cortactin [10]. This model was subsequently named the 'S-Y Switch' model [26], and its most easily testable prediction is that cortactin can be regulated by a conformational change. The structure of unmodified cortactin [27] reveals a closed, globular conformation achieved mainly through interactions between the SH3 domain and ABR region.

Studies with mutant forms of cortactin have been carried out to understand the functional consequences of serine and tyrosine phosphorylation. Indeed it has been proposed that different cortactin phosphoforms have distinct cellular functions: in this proposal, tyrosine-phosphocortactin mainly regulates focal adhesion turnover, whereas serine-phosphocortactin controls actin polimerization [28]. More recently, antibodies specific for phospho-serine have been used to show that serine phosphorylation of cortactin is essential for lamellipodial persistence [29].

Adding another layer of complexity to cortactin regulation, studies have shown that the protein is also regulated by reversible acetylation. The protein can be acetylated by histone acetyltransferase p300/CBP-associated factor (PCAF) and deacetylated mainly by Histone Deacetylase 6 (HDAC6). Acetylated cortactin has a reduced capacity to bind F-actin [30].

Although numerous studies of cortactin have suggested a complex network of regulatory post-translational modifications, they have been unable to indicate definitively how Src-mediated phosphorylation affects cortactin structure and activity, and how this phosphorylation relates to other post-translational modifications. These difficulties may reflect the low basal level of phosphotyrosine cortactin in most cell types, which makes cell culture-based studies of cortactin challenging. Here we attempt to overcome this problem using the Functional Interaction Trap (FIT) system [31,32]. The FIT system involves fusing a kinase and a substrate of interest to complementary leucine zippers; cotransfection with the two expression vectors allows for specific and efficient phosphorylation of the substrate.

Methods

Cells, reagents and antibodies (Abs)

The following cell lines were obtained from the American Type Culture Collection (ATCC): human epithelial HeLa cells; mouse fibroblasts deficient in Src, Yes, and Fyn kinase ($Src^{-/-}$, $Yes^{-/-}$, $Fyn^{-/-}$; abbreviated SYF); and SYF fibroblasts rescued for Src ($Src^{+/+}$, $Yes^{-/-}$, $Fyn^{-/-}$; abbreviated Rsrc). Wild-type (WT) and HDAC6-deficient MEFs immortalized by p53 gene deletion [33] were obtained from Dr. Tso-Pang Yao (Department of Pharmacology and Cancer Biology, Duke University). Cells were grown in Iscove's modified Dulbecco's medium (IMDM) supplemented with 10% fetal bovine serum (FBS) and antibiotics. The deacetylase inhibitor Trichostatin A (TSA) from *Streptomyces sp* was purchased from Sigma. The selective Src-family kinase inhibitor PP2 was purchased from Calbiochem.

The following commercial Abs were purchased from Millipore: mouse cortactin 4F11 MoAb; mouse Src GD11 MoAb; mouse myc 4A6 MoAb; Platinum phospho-tyrosine (for WB), which is a mixture of two generic phosphotyrosine Abs: PY20 and 4G10; vinculin MoAb; and FAK 2A7 MoAb (for IPs). For immunoprecipitations (IPs), we used phosphotyrosine MoAb and for FAK WB, the Ab from Cell Signaling. Mouse actin C4 MoAb was from MP Biomedicals, and rabbit cortactin MoAb was from Novus Biologicals. The rabbit cortactin polyclonal Ab (Applied Biological Materials) was raised against an unphosphorylated peptide around tyrosine 466. This Ab recognizes both unphosphorylated and tyrosine-phosphorylated cortactin. Rabbit phosphocortactin Y466 polyclonal Abs were obtained from Santa Cruz Biotechnology and from Abcam (data not shown). Myc (A14) Ab was from Santa Cruz. pY421 cortactin Ab was from Abcam. Rabbit Ab against acetyl-cortactin was initially obtained from Dr. Edward Seto (H. Lee Moffitt Cancer Center and Research Institute, Tampa, Florida) and subsequently from Millipore.

IRDye 800CW-labeled goat rabbit and mouse secondary Abs (Fisher Scientific) were used to give green signal. IRDye 680CW-labeled goat rabbit Ab (Fisher Scientific) and Alexa 680-labeled goat mouse Ab (Invitrogen) were used to give red signal. All secondary Abs were purchased at a concentration of 1 mg/ml and used at 1:5,000 dilution.

Constructs

All FIT constructs used, including MycCortactin, were a generous donation of Dr. Bruce J. Mayer (Connecticut Health Center, CT, USA). Cortactin with mutations of all three tyrosines that can be phosphorylated by Src (Y421/466/482F, referred to as the 3F mutant) was produced using the QuikChange site-directed mutagenesis kit (Stratagene). Mutations were produced sequentially: first the 421F mutant was generated, and then this was used as template to mutate Y466 and Y482 (primer sequences available upon request). After verifying the sequence, the insert was subcloned into an empty ZipB vector. WT GFP-cortactin and 3F-GFP constructs were previously described [10].

Cell transfection and Western blotting (WB)

For transfection, plasmid DNAs were purified with endotoxin-free, transfection-grade JetStar 2.0 Midi columns (Genomed) as per the manufacturer's instructions. Cell transfections were carried out using Lipofectamine 2000 (Invitrogen) or Fugene HD transfection reagent (Roche). Briefly, cells were grown to 60–75% confluence for Lipofectamine transfections or to 50–60% confluence for Fugene transfections in 6-well plates using 2 μg of the indicated plasmids per well. Transfections were incubated for approximately 20 h in medium containing 10% FBS but no antibiotics.

WB was carried out on cells from a single well or, when necessary, from a 100-mm plate. Cells were washed once with cold Dulbecco's phosphate-buffered saline (D-PBS) with calcium and magnesium (Invitrogen) and scraped into 300 μl 2× Laemmli buffer. Samples were homogenized by three passages through a syringe with a 25-gauge needle and then centrifuged at 21,000×*g* for 5 min at 4°C. Samples were resolved by 10% SDS-PAGE and transferred to nitrocellulose membranes (Amersham) using a BioRad transfer system. Membranes were blocked for 1 h with Odyssey blocking buffer and incubated overnight with primary Ab

in blocking buffer containing 0.1% Tween 20. Membranes were washed 4 times for 5 min with PBS containing 0.1% Tween 20, then incubated for 1 h with the appropriate secondary antibody, and washed as before. Membranes were scanned with the Odyssey infrared system (Lycor, Fisher Scientific) using the red (700 nm) and green (800 nm) channels. When required, membranes were stripped using Odyssey stripping buffer according to the manufacturer's instructions. When significantly different intensities were observed between the two color signals, we performed sequential Ab incubations. After stripping membranes, we incubated them with secondary Ab alone and scanned them to confirm the efficiency of stripping before incubating them with another primary Ab.

Quantification of the bands was performed on the scanned images using the Odyssey Scan band tool. The results were analyzed by the two-tailed Student's t test and displayed graphically using GraphPad Prism software (version 5.0).

Pervanadate treatment

Pervanadate solution was prepared by mixing 1 mM Na_3VO_4 with 1% H_2O_2 (both from Sigma), diluting two-fold with IMDM medium and used for 30 min at 37°C and 5% CO_2.

Immunoprecipitation (IP) experiments

Cells were grown on 150-mm plates and transfected as described above with 20 μg of each plasmid. After transfection cells were washed once with D-PBS and scraped into 700 μl modified RIPA buffer [50 mM Tris-HCl (pH 7.4), 150 mM NaCl, 15% glycerol, 2 mM EDTA, 0.1% SDS, 1% Triton X-100, 1 mM Na_3VO_4, 10 mM NaF, 1 mM PMSF, protease inhibitor cocktail (Amersham), phosphatase inhibitor (PhosSTOP, Roche)]. When indicated, TSA was added to the RIPA buffer at a final concentration of 400 ng/ml to detect cortactin acetylation [30], except in the case of lysates from WT or HDAC6-deficient cells.

Magnetic mouse or protein G Dynabeads (30 μl/IP, Invitrogen) were washed and blocked with PBS containing 0.1% BSA for 10 min, then incubated 1 h with 4 μg Ab per IP. After one wash with PBS-0.1% BSA, the beads were added to 200–300 μl cell lysate and incubated with rotation at 4°C for 4 h. The beads were washed 3 times with the help of a magnet (Invitrogen) and 200 μl lysis buffer diluted 1:10 in PBS supplemented with TSA, except in the case of lysates from WT or HDAC6-deficient cells, when TSA was omitted. The beads were resuspended in 40 μl 2× Laemmli buffer and processed for SDS-PAGE or frozen at −80°C until further analysis.

Pull-down (PD) experiments

GST and the GST-cortactin SH3 domain were produced in BL21 *E. coli*, purified and coupled to GSH-beads [10]. The proteins were added to 200 μl cell lysate and incubated for 3 h with tumbling at 4°C. Pull-downs were washed twice with 200 μl lysis buffer diluted 1:10 in PBS.

Immunofluorescence microscopy

Cells were fixed for 20 min at room temperature with 4% formalin (Sigma) and permeabilized with 0.1% Triton X-100 for 5 min. After three washes with PBS, cells were blocked with 2% BSA in PBS for 10 min, stained at room temperature (RT) with the appropriate primary Ab for 1 h, washed 3 times with PBS, and finally incubated 1 h with secondary Ab. Actin cytoskeleton was visualized with 1 μg/ml tetramethyl-rhodamine-isothiocyanate (TRITC)-phalloidin (Sigma) or a 1:25 dilution of Alexa Fluor 350-phalloidin (Invitrogen). The secondary Abs (Invitrogen) were Alexa Fluor 405-labelled mouse (blue), Alexa Fluor 488-labeled mouse and -rabbit (green), and Alexa 568-labeled rabbit (red).

Counting was done using a Nikon Eclipse TE 200-U fluorescence microscope equipped with a Hamamatsu camera. Images were processed with Adobe Photoshop. Confocal microscopy was performed at the Parque Científico de Madrid microscopy facility with a Leica Confocal SP2/DMEIR2, using Leica software (version 2.61).

Spreading experiments

Cells were transfected for 20 h, trypsinized and washed once with trypsin inhibitor at 0.5 mg/ml (Sigma). For immunofluorescence studies, 2.5×10^5 cells per time point were replated on 4 coverslips previously treated with 30 μg/ml fibronectin (Calbiochem) in each well of a 6-well plate. After fixation they were processed for immunofluorescence. For FAK pull-down and IP experiments, transfections were carried out in 150-mm plates, and cultures were trypsinized 20 h later. For each condition, 2.5×10^6 trypsinized cells were kept in suspension or replated on fibronectin-treated 100-mm plates.

Results

Efficient tyrosine phosphorylation of cortactin by Src in cells transfected with the FIT system

To specifically phosphorylate cortactin in cells with Src kinase, we used the FIT system (Fig. 1, schematic cartoon). HA-tagged Src kinase lacking the SH2 and SH3 domains was expressed with a C-terminal leucine zipper from the Leucine-ZipA vector (ZipAHA-ΔSrc), while myc-tagged cortactin was expressed with an N-terminal leucine zipper from the Leucine-ZipB vector (ZipBMyc-Cortactin) (Fig. 1, lane 5). As controls, we transfected different vector combinations (Fig. 1A) and left cells untransfected (lane 9). We performed these transfections in SYF fibroblasts, which lack the three SFKs (Src, Yes, Fyn) predominant for that cell type [34]. We also performed these transfections in control cells reconstituted with Src (Rsrc cells).

WB of cell lysates was carried out using the Odyssey two-color infrared scanning system. Src targets tyrosines 421, 466, and 482 of mouse cortactin [35]. We observed strong tyrosine phosphorylation of transfected cortactin using a phospho-specific Ab against tyrosine 466 (pY466 Ab). Simultaneously we detected both endogenous cortactin, migrating at 80–85 kDa, and transfected cortactin using the 4F11 mouse MoAb (Fig. 1A). We next merged the images to show that the phosphorylated band superimposes on the transfected cortactin band, and that the mobility of both bands was slightly lower than that of unphosphorylated cortactin. Actin was detected as a loading control. Similar results were obtained with a different cortactin pY466 Ab (data not shown). Using the FIT system, we found no appreciable differences in the levels of cortactin phosphorylation between SYF and Rsrc cells.

To analyze how efficiently the FIT system generated phosphorylated cortactin, we transfected truncated Src kinase and cortactin without the ZipA or ZipB domains, respectively (Fig. 1A, lines 4 and 8). The results show that cotransfection of Src and cortactin increases tyrosine phosphorylation of cortactin, and that the phosphorylation level is much higher when the leucine zipper domains are used, in agreement with previous studies using the FIT system [32].

We also analyzed the phosphorylation of position 421 using a pY421 Ab (Fig. 1B). The results in Fig. 1A and 1B indicate that the FIT system allows efficient phosphorylation of cortactin on tyrosines 421 and 466. In subsequent experiments, we used the pY466 Ab because it gave a stronger signal than the pY421 Ab.

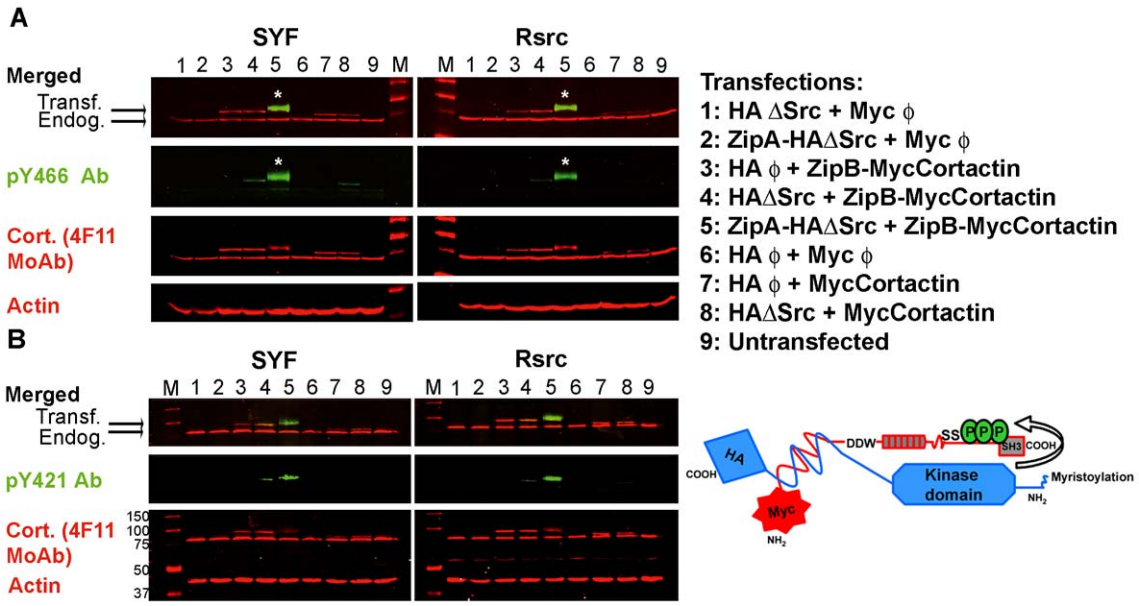

Figure 1. Efficient tyrosine phosphorylation of cortactin by Src in cells using the FIT system. SYF and Rsrc cells were transfected with different combinations of Src and cortactin FIT fusion vectors (lanes 1–8) or left untransfected (lane 9). Cell lysates were blotted for actin as a loading control and with different Abs, then blotted with the respective conjugated secondary antibodies and finally visualized with the Odyssey system. The lysates were blotted with (**A**) pY466 or (**B**) with pY421 cortactin Abs. In both cases, we observed a clear specific phosphorylation band (in green) when ZipA-HA-ΔSrc and ZipB-MycCortactin were cotransfected (transfection 5), and this band superimposes (asterisks) on the cortactin band detected with the 4F11 MoAb (in red). Sizes of the molecular weight markers (denoted M) are shown in kDa. A schematic cartoon of the FIT system is shown.
doi:10.1371/journal.pone.0033662.g001

To specifically detect transfected cortactin, we performed WB with mouse myc 4A6 MoAb and rabbit cortactin MoAb. Fig. S1A shows that transfected cortactin is recognized equally well by both Abs. This was further confirmed by the superposition of bands generated with the 4F11 Ab and the rabbit cortactin MoAb (data not shown). These results show that endogenous and transfected ZipBMyc-Cortactin can be detected by either MoAb, though the signal intensity was greater with the rabbit MoAb.

As a control for the transfections we blotted with antibodies against the HA tag to detect both HA-ΔSrc (Fig. S1B, lanes 1, 4 and 8) and ZipAHA-ΔSrc (lanes 2 and 5). We confirmed the genotype of the SYF and Rsrc cells by blotting with Src MoAb GD11 (Fig. S1B).

Substrate specificity of Src kinase in the FIT system

To determine whether cortactin is the primary Src substrate phosphorylated in cells transfected with the FIT system, we analyzed the cell lysates by WB using mouse MoAbs against generic phospho-tyrosine (Platinum Ab: 4G10+PY20) (Fig. S2). The same membrane was also incubated with rabbit cortactin MoAb. We observed a strong phospho-tyrosine band that comigrated with transfected cortactin (lane 5, asterisk). When Src kinase is activated, it is phosphorylated on tyrosines, which explains why we observed in lanes 2 and 5 a band of slightly higher molecular weight than actin that corresponds to ZipAHA-ΔSrc. Similarly, we observed Src kinase in the reconstituted Rsrc cells. These results demonstrate that the major phospho-protein in our lysates is transfected ZipBMyc-Cortactin that is tyrosine-phosphorylated by ZipAHA-ΔSrc (lane 5, asterisk).

As a second control of phosphorylation specificity, we analyzed whether the Src substrate paxillin [36] is phosphorylated by our transfected Src kinase. We performed WB using a phospho-paxillin (p-paxillin) Ab. In Fig. 2A we show the most relevant transfections (lanes 4 and 5) from two FIT experiments (FIT8 and FIT9), after blotting with p-paxillin Ab. As an internal control, we treated both cell types with pervanadate, a generic phosphatase inhibitor that induced a strong signal for p-paxillin. While untreated cell lysates did not show detectable paxillin phosphorylation, lysates of treated cells did. Thus we can conclude that our transfected cells express a basal level of phospho-paxillin.

Positional specificity of Src kinase in the FIT system

Src phosphorylates tyrosines 421, 466 and 482 in mouse cortactin [35]. After detecting cortactin phosphorylation at positions 421 and 466, we wanted to exclude the possibility of phosphorylation at other tyrosines. For this purpose we used a non-phosphorylatable mutant in which the three major residues targeted by Src kinase were replaced by phenylalanine (3F). We carried out our experiments in HeLa cells because the experiments described above showed similar results in SYF and Rsrc cells, and HeLa cells are easier to handle and widely used.

We cotransfected cells with ZipAHA-ΔSrc and either ZipBMyc-Cortactin or ZipBMyc-Cortactin 3F, and performed WB using Abs against generic phospho-tyrosine and cortactin. Cortactin was phosphorylated on tyrosines, while the 3F mutant was not (Fig. 2B, lanes 4 and 5), indicating that cortactin is phosphorylated specifically on the expected tyrosines.

Relationship between tyrosine phosphorylation and acetylation of cortactin

Cortactin is acetylated mainly in the cortactin repeat region, and this modification decreases the ability of cortactin to bind F-actin [30]. Because cortactin phosphorylation by Src has a similar effect [15], we wanted to analyze whether a relationship exists between the two post-translational modifications.

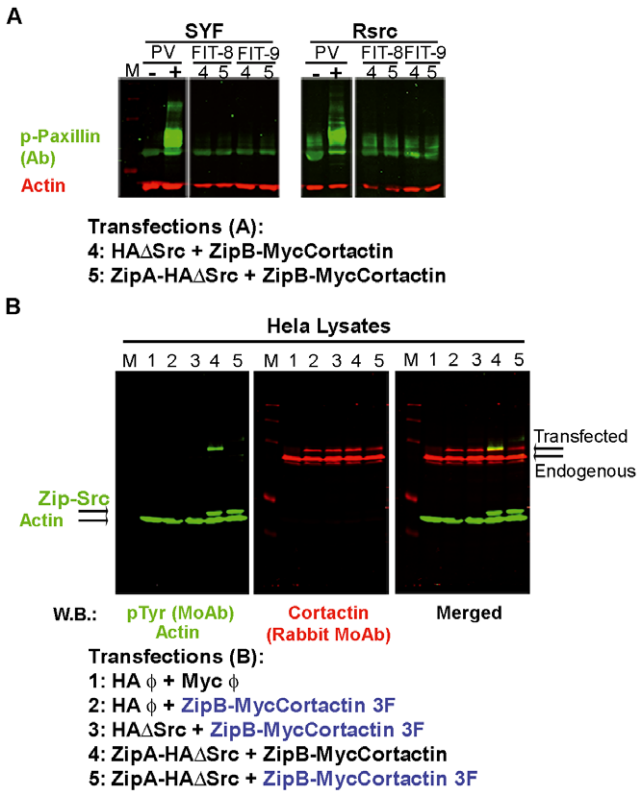

Figure 2. Specificity of tyrosine phosphorylation in the FIT system. (**A**) Detection of the phosphorylation status of paxillin, another Src kinase substrate. SYF and Rsrc cells were transfected with FIT fusion vectors and the most relevant lysates (4 and 5) from two different experiments (FIT 8 and 9) were analyzed by WB with a rabbit Ab against phospho-paxillin (in green) and with a MoAb against actin (in red). As controls, cells were left untreated or treated with pervanadate (PV), a potent phosphatase inhibitor that induces the phosphorylation of paxillin. Rsrc cells showed a higher basal level of phospho-paxillin than did SYF cells, though in both cell lines, this basal level was enhanced by treatment with PV. The FIT system did not increase the basal level of phospho-paxillin. (**B**) Tyrosine phosphorylation of cortactin occurs on the expected tyrosines (Y421, Y466 and Y482). HeLa cell lysates were transfected with ZipA-HA-ΔSrc and ZipB-MycCortactin (lane 4) or with ZipA-HA-ΔSrc and ZipB-MycCortactin with the triple mutation Y421/466/482F (3F) (lane 5). Several control cotransfections were done (lanes 1–3). WB with generic pTyr MoAb demonstrated that only ZipB-Myc WT cortactin, and not the 3F mutant, was phosphorylated (in green). Cortactin was detected with a rabbit MoAb (in red). Actin is shown as a loading control.
doi:10.1371/journal.pone.0033662.g002

For this purpose, we decided to use HeLa cells because cortactin acetylation was previously detected in this cell type [30]. Cells were transfected with empty vectors (Fig. 3, lane 1), with ZipBMyc-Cortactin plus HA empty vector (lane 2), or with ZipBMyc-Cortactin together with HA-ΔSrc (lane 3) or ZipAHA-ΔSrc (lane 4). Transfected cells were left untreated or treated with Trichostatin A (TSA), a deacetylase inhibitor previously used to prevent deacetylation of cortactin [30]. WB experiments were performed to confirm tyrosine phosphorylation of cortactin using the pY466 Ab (Fig. S3A). As expected, cortactin was strongly phosphorylated when ZipBMyc-Cortactin was cotransfected with ZipAHA-ΔSrc (lane 4), and the phosphorylation signal was much lower when ZipBMyc-Cortactin was cotransfected with HA-ΔSrc (lane 3).

To analyze whether phospho-cortactin was simultaneously acetylated, we performed IPs of transfected cortactin using a myc MoAb, followed by WB with an Ab specific for acetyl-cortactin (Fig. 3A). The results show that cortactin was efficiently immunoprecipitated in all samples, while it was undetectable in the isotype control IP (Fig. 3A, right panels). Acetyl-cortactin was nearly undetectable in the sample in which cortactin was strongly phosphorylated (lane 4), whereas it was clearly detectable when cortactin was not phosphorylated (lane 2). Treating cells with TSA increased the apparent level of acetyl-cortactin, suggesting that it prevents the deacetylation of cortactin as previously described [30].

In addition to checking cortactin phosphorylation in the lysates used to perform the IPs (Fig. S3A), we wanted to check the phosphorylation status in the immunoprecipitates (Fig. 3A). The membrane was gently stripped until the green acetyl signal was lost and then reprobed with pY466 Ab and myc MoAb. As expected, the myc immunoprecipitates showed cortactin phosphorylation mainly when ZipAHA-ΔSrc and ZipBMyc-Cortactin were cotransfected (lane 4). When transfected alone, ZipBMyc-Cortactin was not detectably phosphorylated, yet it presented a strong acetylation signal (Fig. 3A, lane 2). The results suggest that acetylation and phosphorylation of cortactin occur antagonistically.

To confirm these results separate IPs were carried out in parallel with myc MoAb and generic phospho-tyrosine MoAb (pTyr MoAb) (Fig. 3B). To simplify the experiment we used only TSA-treated cells and the most relevant vector combinations: empty vectors (lane 1), empty HA-vector and ZypBMyc-Cortactin (lane 2), and ZipAHA-ΔSrc and ZipBMyc-Cortactin (lane 3). IP with pTyr MoAb was performed only in the cotransfection of ZipAHA-ΔSrc and ZipBMyc-Cortactin, where cortactin should be phosphorylated. Again, we observed that tyrosine-phosphorylated cortactin was not acetylated and *vice versa*. Thus no signal for acetylation was detected in the phospho-tyrosine IP, which pulled down only tyrosine-phosphorylated cortactin. In contrast, a very faint acetylation signal was detected in the myc IP, which pulled down primarily phosphorylated cortactin but also a small fraction of unphosphorylated protein. We found a statistically significant difference in acetylation signal between unphosphorylated cortactin (transfection 2) and tyrosine-phosphorylated protein (transfection 3; Fig. 3B).

To verify these results with tyrosine-phosphocortactin by a different approach we performed IPs with the pY466 cortactin Ab (Fig. S3B) using the same vector combinations as above (Fig. 3B). The immunoprecipitates and lysates were blotted with cortactin 4F11 MoAb, which detects both transfected and endogenous cortactin in lysates. Tyrosine-phosphorylated cortactin was efficiently immunoprecipitated when ZipAHA-ΔSrc and ZipB-Myc-Cortactin were cotransfected (lane 3). WB with acetyl-cortactin Ab revealed that pY466 immunoprecipitates did not contain acetylated cortactin, which is consistent with previous results (Fig. 3A, B). These results indicate that the two modifications did not occur simultaneously, suggesting that a competition exists between phosphorylation and acetylation of cortactin.

To exclude any non-specific effects due to the fusion tag and to further characterize how these two post-translational modifications relate to each other, we performed transfections using GFP-tagged cortactin constructs (Fig. 4). We transfected HeLa cells with empty vector and a vector encoding GFP-WT cortactin or GFP-3F cortactin, and we blotted the lysates with acetyl-cortactin Ab. We observed that WT and GFP-3F cortactin were acetylated (Fig. 4A) and found no statistically significant difference in acetylation level between the two constructs (data not shown). This indicates that

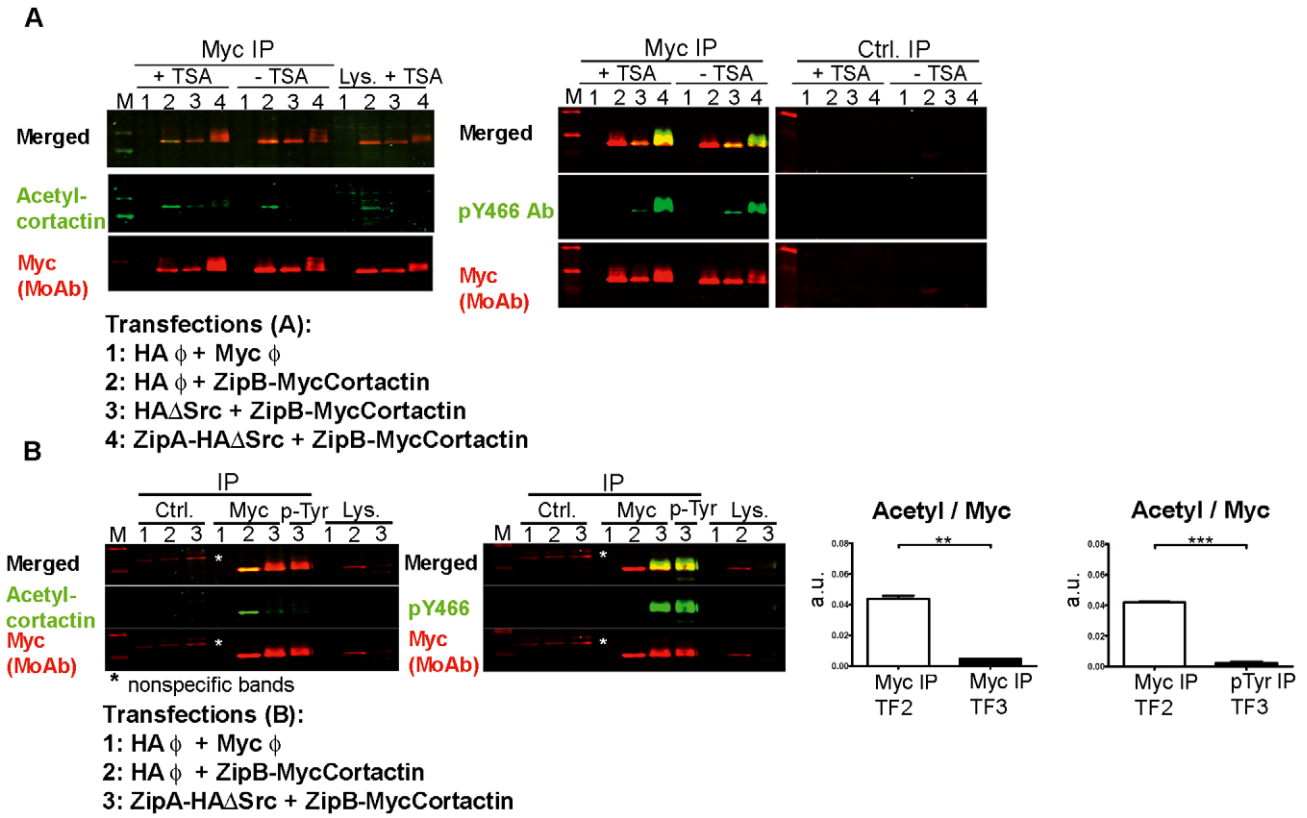

Figure 3. Analysis of acetylation and tyrosine phosphorylation of transfected cortactin. (**A**) Lysates from various transfection combinations (lanes 1–4), treated or not with the deacetylase inhibitor Trichostatin A (TSA), were used to perform IPs using a myc MoAb that were examined by WB first with acetyl-cortactin Ab (in green) and second with myc MoAb (in red). The merge of both images is shown. After the membrane was gently stripped to remove the acetyl signal, it was blotted with pY466 Ab. The isotype control IP (Ctrl.) is also shown. (**B**) TSA-treated cell lysates from various transfection combinations (lanes 1–3) were subjected to parallel IP experiments with the myc MoAb and the generic pTyr MoAb. The IPs were blotted first with acetyl-cortactin Ab, and second with the myc MoAb; then the membranes were stripped and reprobed with pY466 Ab and myc MoAb. The asterisks denote non-specific bands. Quantification of the signals from cortactin immunoprecipitates showed a statistically significant inverse relationship between acetylation and tyrosine phosphorylation signals. a.u.: arbitrary units. *, $p<0.05$; **, $p<0.01$.
doi:10.1371/journal.pone.0033662.g003

phosphorylation of cortactin at positions 421, 466 and 482 is not required for cortactin acetylation.

We next examined the effects of pervanadate (PV) and TSA on GFP-cortactin; these compounds induce phosphorylation and acetylation, respectively (Fig. 4B). Lysates of cells transfected with GFP-cortactin were left untreated or treated with PV or TSA, and subjected to WB with the acetyl-cortactin Ab first, followed by gentle stripping and then reprobing with the pY466 cortactin Ab. As a transfection control, lysates were also blotted with GFP MoAb. Treating lysates with TSA increased the amount of acetyl-cortactin over basal levels. However, we cannot determine whether it simultaneously decreased the level of phospho-cortactin because the basal level of the phospho-protein is undetectable. In contrast, PV strongly induced tyrosine phosphorylation of cortactin, and this was accompanied by a decrease in the level of acetyl-cortactin, such that the ratio of the two forms of cortactin differed significantly from basal conditions (Fig. 4B). These results indicate that induction of tyrosine phosphorylation of cortactin decreases its acetylation.

Analysis of the acetylation and phosphorylation status of endogenous cortactin

The experiments described so far established that acetylation and phosphorylation of transfected cortactin are mutually exclusive events. We next analyzed whether the same relationship holds for endogenous cortactin (Figs. 5, 6). First we performed experiments in WT and HDAC6-deficient mouse embryonic fibroblasts (MEFs), because HDAC6 is the major cortactin deacetylase in cells [30]. IPs using 4F11 MoAb were blotted with acetyl-cortactin Ab, then the membranes were stripped and blotted with pY466 Ab (Fig. 5A). IPs from HDAC6-deficient cell lysates using 4F11 MoAb showed a significantly higher basal level of acetylated cortactin than did IPs from WT cell lysates. In addition, the ratio of the acetyl:pY466 signals was significantly higher in the HDAC6-deficient cells. These results indicate that the lack of HDAC6 deacetylase significantly increases the acetyl:pY466 cortactin ratio and that HDAC6-deficient cells are a valuable reagent to characterize how acetylation and tyrosine phosphorylation of cortactin relate to each other. Consequently, we performed cortactin IPs using the acetyl-cortactin Ab and blotted them with pY466 Ab and 4F11 MoAb. No signal was detected by pY466 Ab in the immunoprecipitates in which cortactin was detectable with the 4F11 MoAb (Fig. 5B). To confirm this result, acetyl-cortactin immunoprecipitates were analyzed using generic pTyr mouse MoAb or cortactin rabbit MoAb on separate membranes. Similar results were obtained (Fig. S4). We confirmed the HDAC6-deficient phenotype of the MEFs by WB with HDAC6 Ab (Fig. 5C). These results show that

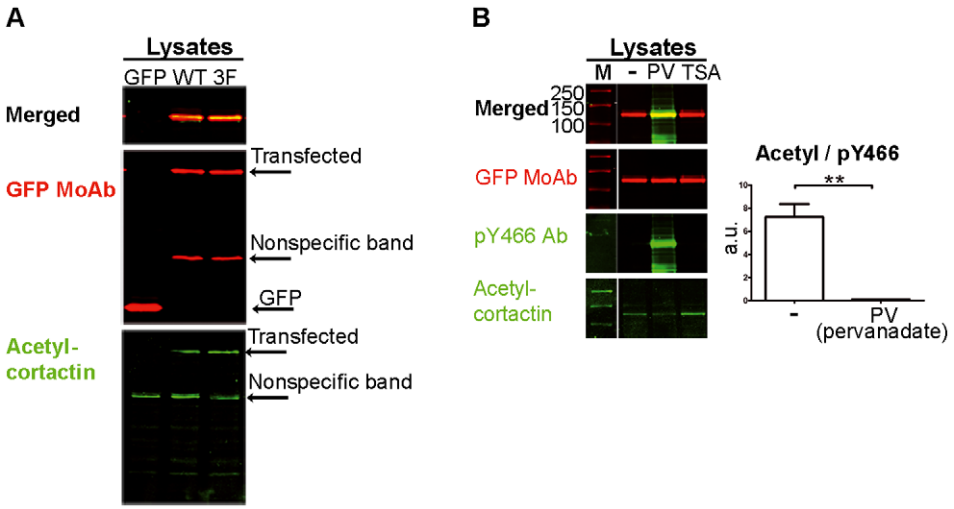

Figure 4. Analysis of acetylation and tyrosine phosphorylation of transfected GFP-cortactin. (**A**) Tyrosine phosphorylation of cortactin is not required for acetylation of the protein. HeLa cells were transfected with vectors encoding GFP fused with WT cortactin or the Y421/466/482F non-phosphorylatable cortactin mutant (3F). Lysates were blotted with acetyl-cortactin Ab and GFP MoAb. Transfected cortactin was acetylated and no statistically significant difference was found in acetylation level between WT and 3F transfectants (data not shown). (**B**) Tyrosine phosphorylation of cortactin decreases acetylation of the protein. HeLa cells were transfected with a vector encoding GFP fused with WT cortactin. Transfectants were left untreated (-) or treated with pervanadate (PV), a generic phosphatase inhibitor, or with Thrichostatin A (TSA), a deacetylase inhibitor. Lysates were blotted with acetyl-cortactin Ab and with GFP MoAb. After stripping, the membrane was incubated with pY466 cortactin, which was merged with the GFP cortactin signal. The ratio of acetyl:pY466 cortactin is shown for untreated (-) and PV-treated cells. a.u.: arbitrary units. **, $p<0.01$.
doi:10.1371/journal.pone.0033662.g004

endogenous acetylated cortactin is not tyrosine-phosphorylated in WT or HDAC6-deficient cells.

We next examined cortactin acetylation in SYF and Rsrc MEFs, because they represent cell types with different levels of tyrosine-phosphorylated cortactin (Fig. 6). Separate IPs were carried out in parallel using 4F11 and pTyr MoAb and blotted first with rabbit acetyl-cortactin Ab. Then the blot was stripped and reprobed with pY466 cortactin Ab. To detect immunoprecipitated cortactin the membrane was stripped again and reprobed with a cortactin Ab (Fig. 6A). We detected acetyl-cortactin in immunoprecipitates prepared from SYF and Rsrc cell lysates using cortactin 4F11 MoAb. Parallel IPs performed with the pTyr MoAb showed that endogenous tyrosine-phosphorylated cortactin was present only in Rsrc cell lysates, as expected. Furthermore, this cortactin fraction was not acetylated (see asterisks, Fig. 6A). We quantified three independent experiments and found that 4F11 immunoprecipitates from SYF and Rsrc cells differed significantly in the ratio of acetyl:pY466 cortactin (Fig. 6A). These results indicate that when most of the immunoprecipitated cortactin is tyrosine-phosphorylated, then is not concomitantly acetylated.

To confirm these results, we performed IPs from SYF and Rsrc cell lysates with pY466 cortactin Ab (Fig. 6B). The immunoprecipitates were blotted with acetyl-cortactin Ab and cortactin 4F11 MoAb, gently stripped, and then reprobed with pY466 cortactin antibody (Fig. 6B). As detected in Fig. 6A, tyrosine-phosphorylated cortactin was immunoprecipitated only from Rsrc cell lysates. More importantly, cortactin phosphorylated on Y466 was not acetylated (Fig. 6B). Again as detected in Fig. 6A, when cortactin was immunoprecipitated with a generic antibody such as 4F11 MoAb, the immunoprecipitates contained both acetylated and tyrosine-phosphorylated cortactin. On the contrary, when cortactin was immunoprecipitated with a generic phospho-tyrosine MoAb or a specific pY466-cortactin Ab, only tyrosine-phosphorylated cortactin was immunoprecipitated and it was not acetylated. Together these results demonstrate that the majority of endogenous cortactin is acetylated or tyrosine-phosphorylated, consistent with the results obtained with transfected cortactin.

Analysis of cortactin acetylation and tyrosine phosphorylation during cell spreading

We performed FIT transfections of SYF and Rsrc cells to visualize the location of nonphosphorylated cortactin (transfection 2) and phosphorylated protein (transfection 3). As negative controls, we left cells untransfected and we transfected them with empty vectors (Fig. S5 and data not shown). We visualized cell morphology with TRICT-phalloidin (Fig. S5). We also examined high-magnification images to study cell morphology in detail. We detected cortactin expression using myc MoAb and cortactin phosphorylation using pY466 Ab. As in the IPs (Fig. 6), the level of endogenous cortactin that was tyrosine-phosphorylated in SYF cells under our experimental conditions was nearly undetectable; the level of phosphorylation was similar to that observed in cells transfected only with cortactin (transfection 2, TF2). Cotransfection of cortactin and Src kinase in the FIT system (TF3) increased the level of phospho-cortactin in cells, and this level was easier to observe in SYF cells because of their null background level. In SYF cells, cortactin localized to the cell periphery and around the nucleus, as previously described for endogenous cortactin [7].

In contrast to SYF cells, untransfected Rsrc cells showed, as expected, a detectable level of tyrosine-phosphorylated cortactin (data not shown), as did Rsrc cells transfected in the TF2 experiment. Some cells showed clusters of actin and phospho-cortactin (arrows, Fig. S5). Images from TF3 showed that Rsrc cells were somewhat more retracted and detached than their TF2 counterparts. These results demonstrate that transfected and endogenous tyrosine-phosphorylated cortactin show similar localization, and suggest a role for phospho-cortactin in cell adhesion.

To test this hypothesis, we examined the spreading of transfected SYF and Rsrc cells on fibronectin (Fig. 7). Fig. 7A shows representative spread and non-spread SYF and Rsrc cells

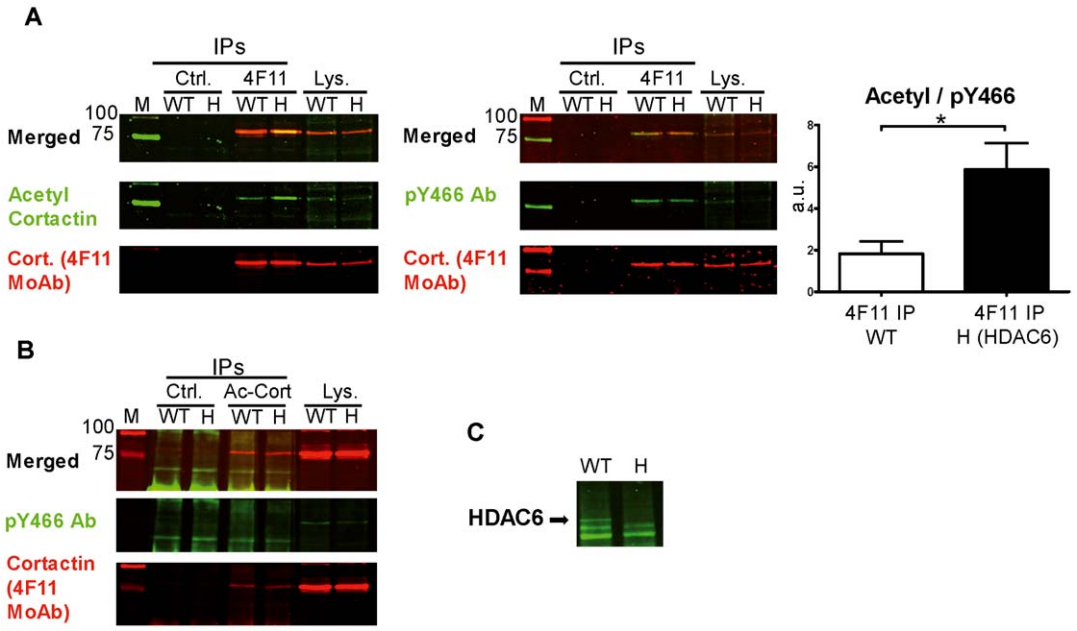

Figure 5. Analysis of acetylation and tyrosine phosphorylation of endogenous cortactin in WT and HDAC6-deficient MEFs. (**A**) Isotype control (Ctrl.) and 4F11 immunoprecipitates from cell lysates of WT and HDAC6-deficient MEFs (H) were blotted first with acetyl-cortactin Ab (in green) and second with the 4F11 cortactin MoAb (in red). The merge of both images is shown. After gentle stripping to remove the acetyl signal, the membrane was blotted with pY466 Ab and 4F11 MoAb. Quantification and statistical analysis of three independent 4F11 immunoprecipitates and the ratio of acetyl:pY466 cortactin signals are shown. a.u.: arbitrary units. *, $p<0.05$. (**B**) Immunoprecipitates obtained with acetyl-cortactin Ab were blotted with pY466 Ab and 4F11. The phosphorylation signal did not coincide with acetylated cortactin. (**C**) Blotting of WT and HDAC6-deficient cell lysates with HDAC6 Ab is shown as a control of cell phenotype.
doi:10.1371/journal.pone.0033662.g005

transfected with ZipB-MycCortactin and empty HA vector (TF2) or ZipB-MycCortactin and ZipAHA-ΔSrc (TF3). We counted 100 transfected cells and classified then as spread or non-spread for two different time points under three transfection conditions [TF1 (empty vectors), TF2 (cortactin) and TF3 (tyrosine-phosphorylated cortactin)]. In TF3 we counted only transfected cells that also showed significant phosphorylation signal. Quantification of the results showed that at 1 h after replating, cells overexpressing cortactin (TF2) showed significantly more cell spreading than did TF1 or TF3 cells. More importantly, expression of tyrosine-phosphorylated cortactin (TF3) significantly inhibited cell spreading compared to TF1 or cortactin-transfected cells (TF2). This pattern of spreading was also observed at 3 h after replating. Analysis of cells that did not spread confirmed that cortactin favors spreading, while tyrosine-phosphorylated cortactin inhibits it. Indeed, at 6 and 18 h after replating, most Rsrc cells in TF3 were detached (data not shown). Similar results were found in SYF cells, although the differences among the three transfection conditions did not reach statistical significance. These results suggest that cortactin expression favors cell spreading, while cortactin phosphorylation counteracts this effect (Fig. 7A).

To further understand the role of tyrosine phosphorylation of cortactin and explore how it relates to cortactin acetylation during cell spreading, we analyzed the spreading of Rsrc cells on fibronectin in the presence and absence of PP2, a widely used Src family kinase inhibitor (Fig. 7B). Untreated cells were plated and allowed to spread for 1 and 3 h. Cells on a third plate were allowed to spread for 1 h and then they were cultured for 2 h in the medium containing 10 μM PP2. Cell lysates were subjected to IPs with cortactin 4F11 MoAb or isotype control Ab. The membranes were first blotted with acetyl-cortactin Ab, the acetyl signal was stripped, and then the membranes were reprobed with pY466 cortactin Ab and 4F11 cortactin MoAb. We observed that PP2 treatment nearly abolished cortactin tyrosine phosphorylation (right panel IPs, Fig. 7B) and increased the intensity of the acetyl-cortactin signal (left panel IPs). Quantification of three independent experiments showed that treatments with PP2 significantly increased the ratio of acetyl:pY466 cortactin. These results indicate that inhibition of tyrosine phosphorylation of cortactin during cell spreading induces cortactin acetylation.

To characterize how cell spreading is altered by tyrosine phosphorylation of cortactin, we stained focal adhesions using vinculin as a marker (Fig. 8). We performed FIT transfections of SYF and Rsrc cells as before and allowed them to spread on FN for 3 hours (Fig. 8). We visualized focal adhesions by immunofluorescence staining with vinculin MoAb and detected expressed protein using myc Ab in cells transfected with empty vectors (TF1) or in cells overexpressing unphosphorylated cortactin (TF2) or tyrosine-phosphorylated cortactin (TF3). We observed that cells overexpressing tyrosine-phosphorylated cortactin (TF3) showed markedly fewer focal adhesions than under the TF1 and TF2 conditions, and these differences were more apparent in Rsrc cells (Fig. 8) than in SYF cells. Many cells in TF3 had an elongated morphology, in agreement with previous observations (Fig. 7).

Cell spreading induces the interaction of cortactin with focal adhesion kinase (FAK), and this interaction is lost upon tyrosine phosphorylation of cortactin

To understand how tyrosine phosphorylation of cortactin may affect the formation of focal adhesions, we focused on a recently described cortactin partner, focal adhesion kinase (FAK) [37], which plays important roles in focal adhesion dynamics [38].

We examined the spreading of HeLa cells on fibronectin, and in parallel left them in suspension as a negative control (Fig. 9). Since

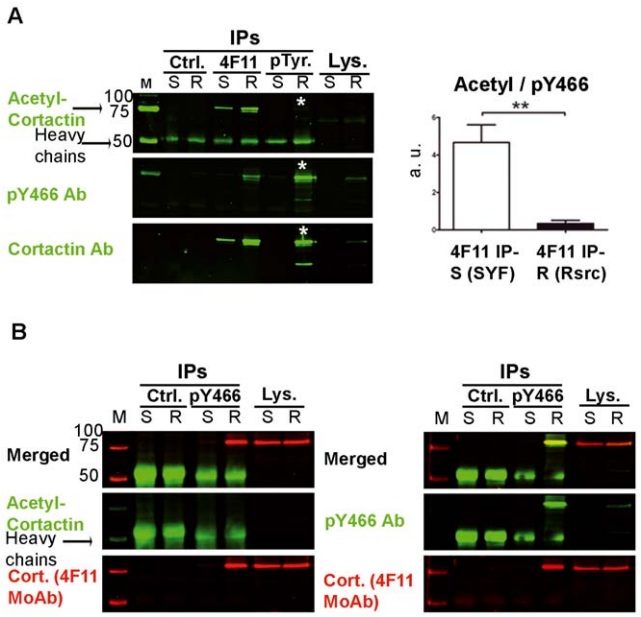

Figure 6. Analysis of acetylation and tyrosine phosphorylation of endogenous cortactin in SYF and Rsrc MEFs. Cell lysates of SYF and Rsrc MEFs were subjected to IPs using (**A**) isotype control Ab (Ctrl), 4F11 MoAb and generic phospho-tyrosine (pTyr) MoAb. These IPs were performed in parallel by probing first with acetyl-cortactin Ab (in green), after a gentle stripping, with pY466 and at last, the membrane was stripped and reprobed with cortactin Ab. Statistical analysis of the ratio of acetyl:pY466 cortactin signals is shown for 4F11 immunoprecipitates. a.u.: arbitrary units. **, $p<0.01$. Asterisks denote evidence that pTyr immunoprecipitates from Rsrc cell lysates contain phospho-cortactin but not acetyl-cortactin. (**B**) IPs with pY466 and isotype control Abs were probed with acetyl-cortactin Ab and 4F11 cortactin MoAb, and reprobed, after gentle stripping, with pY466 Ab and 4F11 MoAb.
doi:10.1371/journal.pone.0033662.g006

previous work has shown that WT cortactin interacts with FAK, while cortactin lacking the SH3 domain does not [37], we performed pull-down experiments on the lysates using recombinant purified cortactin SH3 domain fused to GST (GST-SH3) or GST alone as a negative control (Fig. 9A). We found that cortactin SH3 domain was able to pull down much more FAK from the lysates of spread cells than from lysates of suspended cells. Similar results where obtained with Rsrc lysates (data not shown). These results indicate that focal adhesion formation during cell spreading induces cortactin-FAK association (Fig. 9B).

To confirm the cortactin-FAK interaction during cell spreading and to determine whether it is affected by tyrosine phosphorylation of cortactin, we performed IPs from cell lysates overexpressing cortactin (TF2) or tyrosine-phosphorylated cortactin (TF3) (Fig. 9C). We immunoprecipitated FAK using a FAK mouse MoAb. The immunoprecitates were blotted sequentially, first with myc Ab and secondly with FAK Ab, and lastly with pY466 cortactin Ab. Interestingly, we observed that FAK immunoprecipitated cortactin but not tyrosine-phosphorylated cortactin (see asterisk, Fig. 9C). This result implies that FAK is associated with cortactin, but not when it is tyrosine-phosphorylated.

Discussion

Cortactin phosphorylation is predicted to have important physiological consequences [26] that are not yet fully understood. Although cortactin is a classical Src kinase substrate, the functional consequences of its tyrosine phosphorylation remain unclear. The low basal level of tyrosine-phosphorylated cortactin, and poor reproducibility of results when stimulating cell cultures with growth factors such as EGF and PDGF, have made it challenging to understand how tyrosine phosphorylation regulates cortactin activity. To avoid these problems, we used the FIT system to study the effect of Src-mediated phosphorylation of cortactin in cells. In this system, a leucine zipper motif, consisting of a pair of complementary amphipathic helices [39], is added to both Src and its substrate, in this case cortactin.

Src kinase targets tyrosines 421, 466 and 482 of murine cortactin [35]. Src family kinases (SFKs) are composed of separable modules that include SH2 and SH3 domains [34]. Different systems have been used to study SFK substrates and signal transduction pathways. The hemopoietic cell Src kinase (Hck) was reengineered by substituting the SH2 and SH3 domains with a PDZ domain to alter the kinase's substrate specificity [40]. In another study, a temperature-sensitive vSrc mutant was found to increase tyrosine phosphorylation of cortactin [41]. The FIT system has been used successfully to force efficient phosphorylation of desired substrates in cells [31], including Src-mediated phosphorylation of paxillin, p130Cas and cortactin [32].

In the present study, we set up the FIT system and simultaneously detected levels of total cortactin and tyrosine-phosphorylated protein, both transfected and endogenous, using two commercial Abs against phospho-Y466 and the 4F11 MoAb (Fig. 1A). Transfected cortactin was also detected using a rabbit cortactin MoAb and a MoAb to recognize the myc tag on our cortactin constructs. Western blots were visualized with the Odyssey scanning system, which allowed unambiguous double labeling of cortactin and phospho-cortactin. We performed these experiments in SYF and Rsrc fibroblasts to exclude any contribution from endogenous Src kinases. When cells were cotransfected with Src and cortactin, both fused to leucine zipper interaction motifs, we observed a strong phosphorylation signal at positions 421 and 466 that superimposed on the transfected cortactin band (Fig. 1A, B).

We next performed various analyses to determine the phosphorylation specificity of our FIT system. We determined that cortactin is the major phosphoprotein in our samples, based on experiments using two generic phospho-tyrosine MoAbs (Fig. S2). We also showed that our FIT system is specific to cortactin: the transfections did not affect the phosphorylation status of paxillin, a known Src substrate (Fig. 2A). Finally, using the non-phosphorylatable triple cortactin mutant Y421/466/482F (3F), we verified that Src-mediated phosphorylation of cortactin occurs at the expected tyrosines (Fig. 2B).

Like phosphorylation, acetylation regulates numerous cellular functions. In fact, many proteins related to cytoskeletal dynamics are regulated by acetylation, such as Arp2/3, tubulin, cofilin and coronin [42]. Cortactin is regulated by reversible acetylation that occurs mainly in the ABR of the protein [30], and this acetylation was recently confirmed by "acetylome" analysis [42]. Acetylation of lysines in the ABR was shown to reduce binding to F-actin, which inhibits cell migration [30].

Like cortactin acetylation, Src-mediated phosphorylation of cortactin decreases its binding to F-actin [15]. This binding is required to activate the Arp2/3 complex [16]. We hypothesized that the two modifications are interrelated since they have similar effects on cortactin function, and we explored this idea in the present study. Using the FIT system, we overexpressed phosphorylated or unphosphorylated cortactin in cells, immunoprecipitated the protein, and performed WB experiments with Abs against

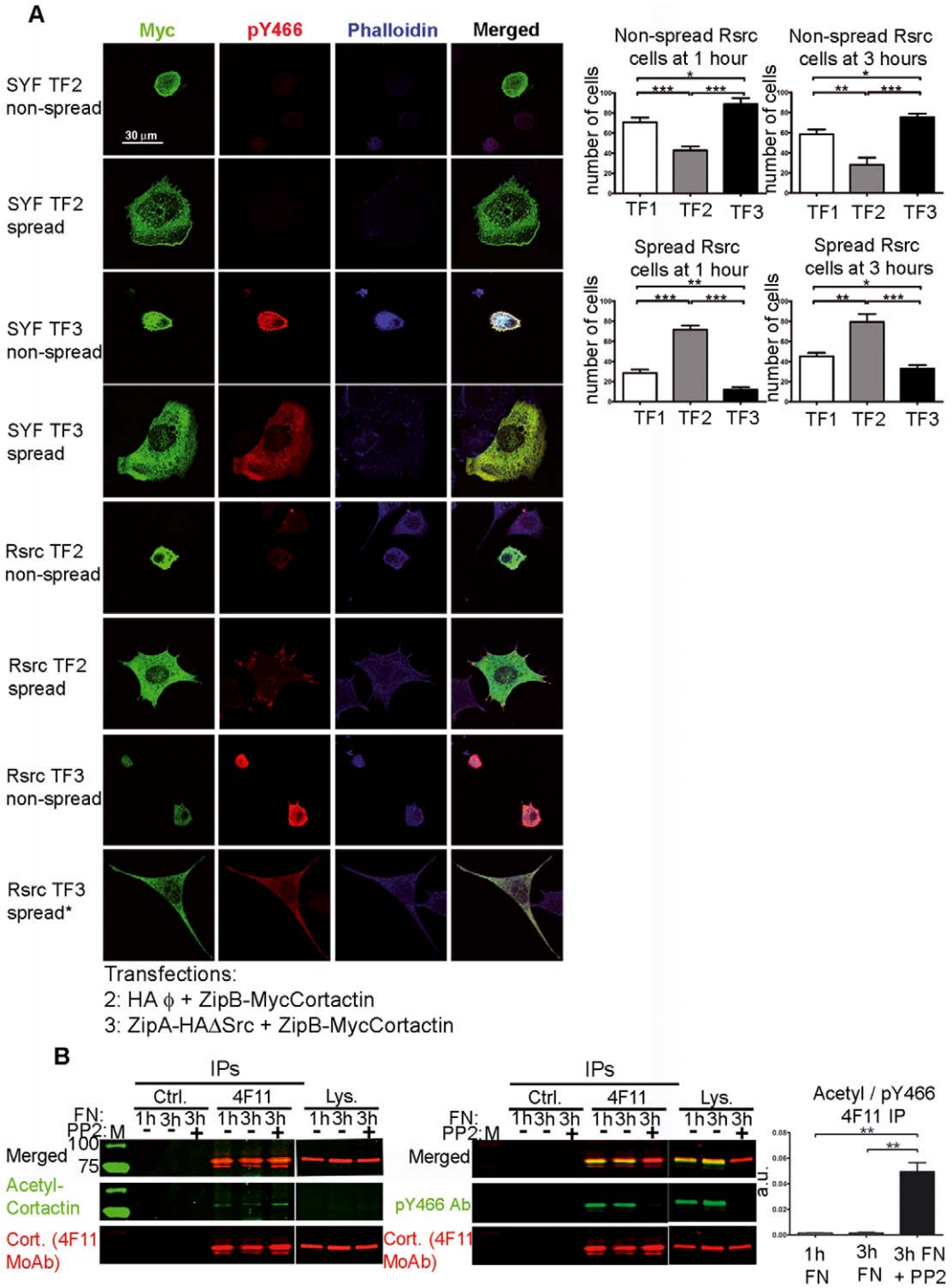

Figure 7. Tyrosine phosphorylation of cortactin affects cell spreading. (**A**) SYF and Rsrc cells were transfected for 20 h with empty vectors (not shown), ZipB-MycCortactin and empty vector (TF2), or ZipB-MycCortactin and ZipA-HAΔSrc (TF3). Cells were then trypsinized, replated on fibronectin-treated coverslips, and fixed at 1 and 3 h. Pictures were taken in a confocal microscope at 600× magnification. Immunofluorescence staining was done using myc MoAb (in green), pY466 cortactin Ab (in red) and Alexa Fluor 350-phalloidin (in blue). For each experimental condition, a representative image of a non-spread and spread cell is shown. * Denotes that spreading of Rsrc cells is incomplete. Images were merged using Leica software. Scale bars are shown. A total of 100 transfected cells were quantified and classified into two categories: spread or non-spread. Statistical analysis from 7 independent experiments at 1 and 3 h after replating Rsrc cells is shown for tranfections TF1 (empty vectors), TF2 (cortactin) and TF3 (phosphorylated cortactin). *, $p<0.05$; **, $p<0.01$; ***, $p<0.001$. (**B**) Inhibition of cortactin phosphorylation increases its acetylation during cell spreading. Rsrc cells were replated on fibronectin (FN)-coated coverslips and allowed to spread for 1 or 3 h. A third plate was allowed to spread for 1 h and then treated with PP2 for 2 h. The lysates were subjected to IPs using isotype control (Ctrl.) MoAb or 4F11 MoAb and were blotted first with acetyl-cortactin Ab and second with anti 4F11 MoAb. After gentle stripping, the membrane was incubated with pY466 cortactin Ab and 4F11 MoAb. Quantification of the ratio of acetyl:pY466 cortactin signals indicated a significantly higher ratio after PP2 treatment. a.u.: arbitrary units. **, $p<0.01$.
doi:10.1371/journal.pone.0033662.g007

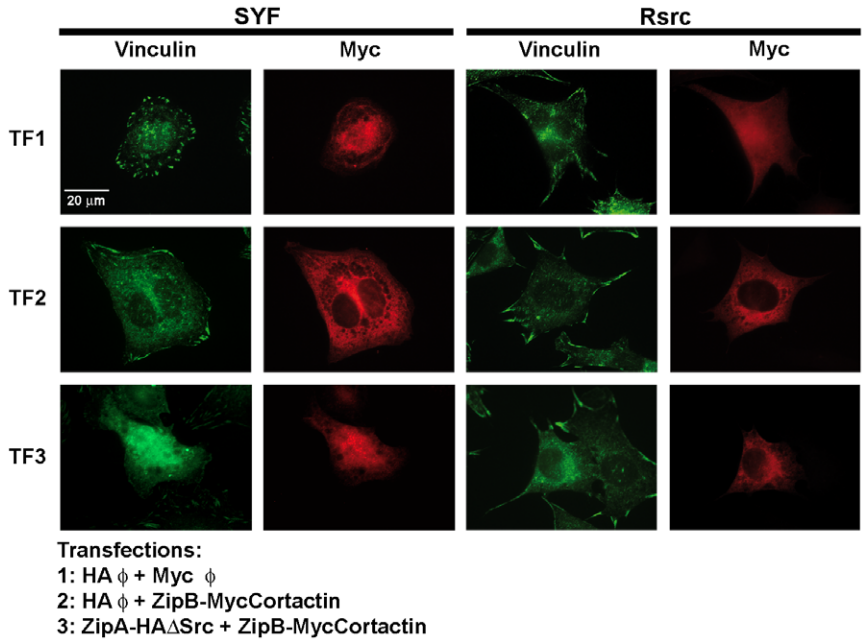

Figure 8. Tyrosine phosphorylation of cortactin affects focal adhesion formation: staining for vinculin. SYF and Rsrc cells were transfected with empty vectors, with ZipB-MycCortactin and empty vector (TF2) or with ZipB-MycCortactin and ZipA-HAΔSrc (TF3). Cells were fixed and visualized by immunofluorescence using vinculin MoAb (in green) and myc Ab (in red). Photographs were taken using a Nikon Eclipse TE 200-U fluorescence microscope equipped with a Hamamatsu camera. Images were processed with Adobe Photoshop. A scale bar is shown.
doi:10.1371/journal.pone.0033662.g008

acetyl-cortactin and pY466-cortactin (Fig. 3). To be sure of our results, we performed the IPs using a myc MoAb, and then again using a generic phospho-tyrosine MoAb (Fig. 3A, B) and pY466 cortactin Ab (Fig. S3). The first set of IPs brought down phosphorylated and unphosphorylated cortactin, whereas the second set brought down only phosphorylated cortactin. Blotting with pY466 Ab detected cortactin phosphorylation mainly in the sample transfected with Zip-cortactin and Zip-Src. These experiments show that acetylation and phosphorylation of cortactin are mutually exclusive: acetylated cortactin is not phosphorylated and *vice versa* (Fig. 3). Another major finding of our study is that when WT cortactin is expressed in transfected cells, at least some of it is acetylated (Figs. 3 and 4) and therefore predicted to be inactive [30].

To determine whether the competition observed between acetylation and phosphorylation of transfected cortactin also holds for the endogenous protein, we carried out experiments in two cell types. The first was WT and HDAC6-deficient MEFs. HDAC6 is the major deacetylase acting on cortactin [30]. As expected, we found the HDAC6-deficient cells to have a significantly higher basal level of acetylated cortactin than did WT cells, as previously described using siRNA techniques [30]. More importantly, we confirmed in both cell types our finding of a competition between acetylation and tyrosine phosphorylation. We did this in two types of IP experiments, one using the 4F11 MoAb and the other using an Ab against acetyl-cortactin (Fig. 5). In the latter IPs, acetyl-cortactin did not show detectable tyrosine phosphorylation, as assessed by either pY466 cortactin Ab or generic pTyr MoAb (Fig. S4). These two IP experiments were repeated on endogenous cortactin in a second cell type, SYF cells, for which Rsrc cells served as control (Fig. 6). Since SYF and Rsrc cells have different levels of tyrosine-phosphorylated cortactin, we performed IPs with 4F11, pTyr Ab and pY466 Ab. As in WT and HDAC6 deficient MEFs, endogenous tyrosine-phosphorylated cortactin was not acetylated.

A major conclusion of our work is that phosphorylation of cortactin has important repercussions on cell spreading, extending the insights of a previous study showing that cortactin mutants mimicking tyrosine phosphorylation affect focal adhesion turnover [28]. Using the FIT system to control tyrosine phosphorylation of cortactin, we analyzed the effect of phosphorylating cortactin on cell location (Fig. S5) and cell spreading (Fig. 7). We found that phosphorylated and unphosphorylated cortactin expressed through transient transfection has an intracellular distribution similar to that of endogenous protein [12]. More importantly, phosphorylation affects cell spreading: cortactin expression facilitated cell adhesion, while tyrosine phosphorylation inhibited it. This phenotype was more noticeable in Rsrc cells, which express Src, than in SYF cells, which do not contain the major SFKs expressed in fibroblasts (Src, Yes and Fyn). This difference between the cell lines is understandable given that many proteins besides cortactin participate in cell adhesion, and many of them are regulated by Src-mediated phosphorylation [43].

In an effort to understand the molecular mechanism underlying the inhibitory effect of tyrosine phosphorylated cortactin on cell spreading, we hypothesized that this post-translational modification would affect the binding of cortactin SH3 domain to interacting proteins that function in cell spreading. One obvious candidate was FAK [37]. Our results in the present study demonstrate that *in vivo*, as previously proposed *in vitro* [10], tyrosine phosphorylation of cortactin prevents the SH3 domain from interacting with FAK and potentially other proteins as well.

While we were preparing this manuscript for submission, researchers reported that a tyrosine phosphorylation-mimicking mutant of cortactin no longer binds FAK and promotes cell motility [44]. This result is comparable to our results obtained with cortactin mutants and with the endogenous protein after

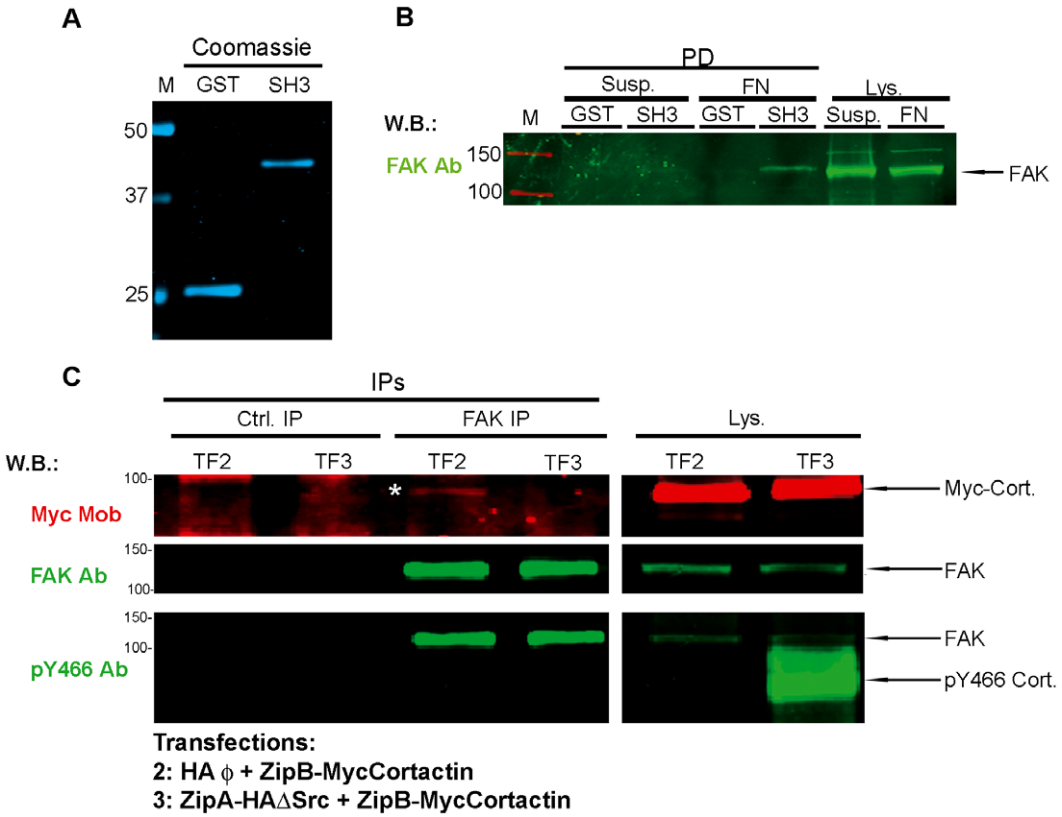

Figure 9. Tyrosine phosphorylation of cortactin terminates its interaction with focal adhesion kinase (FAK) during cell spreading. (**A**) Coomassie staining of purified GST and GST-cortactin SH3 domain was scanned in the Odyssey system. (**B**) HeLa cells were detached with trypsin-EDTA, washed with trypsin inhibitor and kept in suspension (susp.) or allowed to spread for 3 h on fibronectin (FN)-treated 100-mm plates. RIPA cell lysates were used for pull-down experiments with GST or GST-SH3, which were analyzed by SDS-PAGE and WB with focal adhesion kinase (FAK) Ab, followed by labeling with a 800CW-conjugated goat rabbit Ab. (**C**) HeLa cells were transfected with ZipB-MycCortactin and empty vector (TF2) or with ZipB-MycCortactin and ZipA-HAΔSrc (TF3). After 20 h cells were detached with trypsin-EDTA, washed with trypsin inhibitor and allowed to spread on FN-coated 100-mm plates for 3 h. Cell lysates were subjected to immunoprecipitation with FAK MoAb. The immunoprecipitates were subjected to WB and probed in three steps: (1) with myc Ab to detect transfected cortactin, followed by a 680CW-labeled goat mouseAb (red); (2) with FAK Ab, followed by a 800CW-labeled goat rabbit Ab (green); and (3) with pY466 cortactin Ab, followed by a 800CW-labeled goat rabbit Ab. Transfected cortactin was immunoprecipitated by FAK (asterisk) only when the protein was not tyrosine-phosphorylated.
doi:10.1371/journal.pone.0033662.g009

Helicobacter infection [37]. In the present study, we used not mutant forms of cortactin but the phosphorylated form of the WT protein to demonstrate directly that phosphorylation inhibits cortactin binding to FAK and cell spreading. Our results point to a significant role for tyrosine phosphorylation of cortactin in regulating cell adhesion to fibronectin. This further suggests the possibility that cortactin and its phosphorylation contribute to integrin signaling.

Model

We propose a model for the 'sequential' activation of cortactin (Fig. 10). The major tyrosines targeted by Src are located in the proline-rich region at the C-terminus of the protein. Cortactin has a closed, globular conformation, achieved mainly through interactions among the SH3 domain, the ABR and helical region [27]. This agrees with previous studies showing that in unmodified cortactin, the SH3 domain is masked [10,22]. Since acetylated cortactin has also been proposed to be inactive [30], we hypothesize that acetylated cortactin has a closed conformation as well.

Based on our observation that acetylation and tyrosine phosphorylation are not present simultaneously, we propose that in acetylated cortactin, the tyrosines targeted by Src are hidden. Analysis of the tertiary structure of cortactin suggests that both acetyl and phosphate groups can be close to each other in space [45], which may explain why one process excludes the other. Acetylation of the ε-amino group of lysines has already been suggested to "rival" phosphorylation in some cases [46]. Some examples of phosphorylation-acetylation switches in the regulation of proteins are already known. For example, Signal Transducers and Activators of Transcription 1 (STAT1) is activated by phosphorylation and inactivated by acetylation [47]. We further propose that upon appropriate stimulation, such as focal adhesion formation during cell spreading, cortactin is deacetylated, mainly by HDAC6, which like cortactin can translocate to the cell periphery [48]. This deacetylated status would be maintained by rapid Src-mediated tyrosine phosphorylation, although we cannot exclude the possibility that other post-translational modifications contribute to inhibiting reacetylation. In essence, we propose that tyrosine-phosphorylated cortactin is a 'pre-activation state'. At the present moment we do not know whether this species has an open or closed configuration; this will require high-resolution structural analysis.

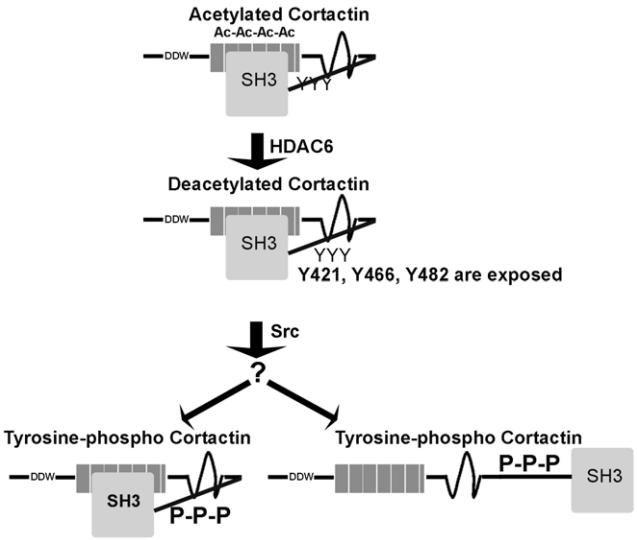

Figure 10. Model for sequential activation of cortactin by deacetylation and phosphorylation. Acetylated cortactin is inactive and probably has a closed conformation that masks the tyrosines targeted by Src. Upon appropriate stimulation, cortactin is deacetylated by HDAC6, exposing the tyrosines, which are then rapidly phosphorylated by Src. This phosphorylation keeps cortactin deacetylated. Whether this tyrosine-phosphorylated cortactin has an open or closed configuration is unknown (question mark).
doi:10.1371/journal.pone.0033662.g010

Supporting Information

Figure S1 Western-blotting controls for the transfections of the FIT vectors. (**A**) To detect our transfected protein, lysates were analyzed by WB with a rabbit cortactin MoAb and a mouse myc MoAb. Both MoAbs recognize transfected cortactin. (**B**) Transfection and cell phenotype controls were performed by WB with HA Ab (in green), and myc and Src MoAbs (in red).
(TIF)

Figure S2 Specificity of the FIT system as detected with phosphotyrosine generic antibodies. SYF and Rsrc cells were transfected with different combinations of Src and cortactin FIT fusion vectors (lanes 1–8) or left untransfected (lane 9). The cell lysates were blotted for actin as a loading control, and with a mixture of two generic phosphotyrosine MoAbs: 4G10 and PY20 (Platinum). The major tyrosine-phosphorylated band observed in our lysates corresponded to cortactin detected with rabbit cortactin MoAb (in red) in the lysates cotransfected with ZipA-HA-ΔSrc and ZipB-MycCortactin (lane 5, asterisks).
(TIF)

Figure S3 Analysis of acetylation and tyrosine phosphorylation of transfected cortactin. (**A**) Lysates from various transfection combinations (lanes 1–4), treated or not with the deacetylase inhibitor Trichostatin A (TSA), were blotted using pY466 cortactin Ab (pY466) (in green) and 4F11 MoAb (in red) to analyze the phosphorylation of transfected cortactin. (**B**) TSA-treated cell lysates from various transfection combinations (lanes 1–3) were subjected to IP experiments with the pY466 Ab or isotype control Ab (Ctrl.). The IPs were blotted first with acetyl-cortactin Ab, and second with the cortactin 4F11 MoAb; then the membrane was stripped and reprobed with pY466 Ab and with cortactin 4F11 MoAb. The asterisk denotes nonspecific bands.
(TIF)

Figure S4 Analysis of acetylation and tyrosine phosphorylation of endogenous cortactin in WT and HDAC6-deficient MEFs. Immunoprecipitates obtained with acetyl-cortactin Ab were blotted with phospho-tyrosine generic mouse MoAb (pTyr) and cortactin rabbit MoAb. There was not phosphorylation signal to coincide with acetylated cortactin.
(TIF)

Figure S5 Localization of tyrosine-phosphorylated cortactin. SYF and Rsrc cells were transfected with empty vectors (not shown), with ZipB-MycCortactin and empty vector (TF2) or with ZipB-MycCortactin and ZipA-HAΔSrc (TF3). Cells were fixed and visualized by immunofluorescence using myc MoAb (in blue), pY466 cortactin Ab (in green) and TRITC-phalloidin to label actin cytoskeleton (in red). Pictures were taken on a confocal microscope at 600× magnification. Images were merged and a zoomed view was generated using Leica software. Scale bars are shown. Some cells showed clusters of actin and phospho-cortactin (arrows).
(TIF)

Acknowledgments

We are indebted to Dr. Bruce J. Mayer (Connecticut Health Center, CT, USA) for providing the FIT vectors and Dr. Tso Pang Yao (Duke University, NC, USA) for WT and HDAC6-deficient MEFs. We are very grateful to Dr. Seto (H Lee Moffitt Cancer Center, FL, USA) for sharing the acetyl-cortactin Ab.

Author Contributions

Conceived and designed the experiments: NMQ EM ENP. Performed the experiments: EM ENP NMQ. Analyzed the data: EM ENP NMQ. Contributed reagents/materials/analysis tools: EM ENP NMQ. Wrote the paper: NMQ. Revised the manuscript: EMR ENP NMQ.

References

1. Pollard TD, Cooper JA (2009) Actin, a central player in cell shape and movement. Science 326: 1208–1212.
2. Daly RJ (2004) Cortactin signalling and dynamic actin networks. Biochem J 382: 13–25.
3. Ren G, Crampton MS, Yap AS (2009) Cortactin: Coordinating adhesion and the actin cytoskeleton at cellular protrusions. Cell Motil Cytoskeleton 66: 865–873.
4. Wu H, Reynolds AB, Kanner SB, Vines RR, Parsons JT (1991) Identification and characterization of a novel cytoskeleton-associated pp60src substrate. Mol Cell Biol 11: 5113–5124.
5. Schuuring E, Verhoeven E, Litvinov S, Michalides RJ (1993) The product of the EMS1 gene, amplified and overexpressed in human carcinomas, is homologous to a v-src substrate and is located in cell-substratum contact sites. Mol Cell Biol 13: 2891–2898.
6. Weaver AM (2008) Cortactin in tumor invasiveness. Cancer Lett 265: 157–166.
7. Weed SA, Parsons JT (2001) Cortactin: coupling membrane dynamics to cortical actin assembly. Oncogene 20: 6418–6434.
8. Uruno T, Liu J, Zhang P, Fan Yx, Egile C, et al. (2001) Activation of Arp2/3 complex-mediated actin polymerization by cortactin. Nat Cell Biol 3: 259–266.
9. Kinley AW, Weed SA, Weaver AM, Karginov AV, Bissonette E, et al. (2003) Cortactin interacts with WIP in regulating Arp2/3 activation and membrane protrusion. Curr Biol 13: 384–393.
10. Martinez-Quiles N, Ho HY, Kirschner MW, Ramesh N, Geha RS (2004) Erk/Src phosphorylation of cortactin acts as a switch on-switch off mechanism that controls its ability to activate N-WASP. Mol Cell Biol 24: 5269–5280.
11. Mizutani K, Miki H, He H, Maruta H, Takenawa T (2002) Essential role of neural Wiskott-Aldrich syndrome protein in podosome formation and degradation of extracellular matrix in src-transformed fibroblasts. Cancer Res 62: 669–674.

12. Ammer AG, Weed SA (2008) Cortactin branches out: roles in regulating protrusive actin dynamics. Cell Motil Cytoskeleton 65: 687–707.
13. Sangrar W, Gao Y, Scott M, Truesdell P, Greer PA (2007) Fer-mediated cortactin phosphorylation is associated with efficient fibroblast migration and is dependent on reactive oxygen species generation during integrin-mediated cell adhesion. Mol Cell Biol 27: 6140–6152.
14. Boyle SN, Michaud GA, Schweitzer B, Predki PF, Koleske AJ (2007) A critical role for cortactin phosphorylation by Abl-family kinases in PDGF-induced dorsal-wave formation. Curr Biol 17: 445–451.
15. Huang C, Ni Y, Wang T, Gao Y, Haudenschild CC, et al. (1997) Down-regulation of the filamentous actin cross-linking activity of cortactin by Src-mediated tyrosine phosphorylation. J Biol Chem 272: 13911–13915.
16. Weaver AM, Karginov AV, Kinley AW, Weed SA, Li Y, et al. (2001) Cortactin promotes and stabilizes Arp2/3-induced actin filament network formation. Curr Biol 11: 370–374.
17. Li Y, Tondravi M, Liu J, Smith E, Haudenschild CC, et al. (2001) Cortactin potentiates bone metastasis of breast cancer cells. Cancer Res 61: 6906–6911.
18. Nieto-Pelegrin E, Martinez-Quiles N (2009) Distinct phosphorylation requirements regulate cortactin activation by TirEPEC and its binding to N-WASP. Cell Commun Signal 7: 11.
19. Mertins P, Eberl HC, Renkawitz J, Olsen JV, Tremblay ML, et al. (2008) Investigation of protein-tyrosine phosphatase 1B function by quantitative proteomics. Mol Cell Proteomics 7: 1763–1777.
20. Oser M, Yamaguchi H, Mader CC, Bravo-Cordero JJ, Arias M, et al. (2009) Cortactin regulates cofilin and N-WASp activities to control the stages of invadopodium assembly and maturation. J Cell Biol 186: 571–587.
21. Tehrani S, Tomasevic N, Weed S, Sakowicz R, Cooper JA (2007) Src phosphorylation of cortactin enhances actin assembly. Proc Natl Acad Sci U S A 104: 11933–11938.
22. Campbell DH, Sutherland RL, Daly RJ (1999) Signaling pathways and structural domains required for phosphorylation of EMS1/cortactin. Cancer Res 59: 5376–5385.
23. Grassart A, Meas-Yedid V, Dufour A, Olivo-Marin JC, Dautry-Varsat A, et al. (2010) Pak1 phosphorylation enhances cortactin-N-WASP interaction in clathrin-caveolin-independent endocytosis. Traffic 11: 1079–1091.
24. Webb BA, Zhou S, Eves R, Shen L, Jia L, et al. (2006) Phosphorylation of cortactin by p21-activated kinase. Arch Biochem Biophys 456: 183–193.
25. Martin KH, Jeffery ED, Grigera PR, Shabanowitz J, Hunt DF, et al. (2006) Cortactin phosphorylation sites mapped by mass spectrometry. J Cell Sci 119: 2851–2853.
26. Lua BL, Low BC (2005) Cortactin phosphorylation as a switch for actin cytoskeletal network and cell dynamics control. FEBS Lett 579: 577–585.
27. Cowieson NP, King G, Cookson D, Ross I, Huber T, et al. (2008) Cortactin adopts a globular conformation and bundles actin into sheets. J Biol Chem 283: 16187–16193.
28. Kruchten AE, Krueger EW, Wang Y, McNiven MA (2008) Distinct phosphoforms of cortactin differentially regulate actin polymerization and focal adhesions. Am J Physiol Cell Physiol 295: C1113–1122.
29. Kelley LC, Hayes KE, Ammer AG, Martin KH, Weed SA (2010) Cortactin phosphorylated by ERK1/2 localizes to sites of dynamic actin regulation and is required for carcinoma lamellipodia persistence. PLoS One 5: e13847.
30. Zhang X, Yuan Z, Zhang Y, Yong S, Salas-Burgos A, et al. (2007) HDAC6 modulates cell motility by altering the acetylation level of cortactin. Mol Cell 27: 197–213.
31. Sharma A, Antoku S, Fujiwara K, Mayer BJ (2003) Functional interaction trap: a strategy for validating the functional consequences of tyrosine phosphorylation of specific substrates in vivo. Mol Cell Proteomics 2: 1217–1224.
32. Sharma A, Mayer BJ (2008) Phosphorylation of p130Cas initiates Rac activation and membrane ruffling. BMC Cell Biol 9: 50.
33. Kawaguchi Y, Kovacs JJ, McLaurin A, Vance JM, Ito A, et al. (2003) The deacetylase HDAC6 regulates aggresome formation and cell viability in response to misfolded protein stress. Cell 115: 727–738.
34. Parsons SJ, Parsons JT (2004) Src family kinases, key regulators of signal transduction. Oncogene 23: 7906–7909.
35. Huang C, Liu J, Haudenschild CC, Zhan X (1998) The role of tyrosine phosphorylation of cortactin in the locomotion of endothelial cells. J Biol Chem 273: 25770–25776.
36. Weng Z, Taylor JA, Turner CE, Brugge JS, Seidel-Dugan C (1993) Detection of Src homology 3-binding proteins, including paxillin, in normal and v-Src-transformed Balb/c 3T3 cells. J Biol Chem 268: 14956–14963.
37. Tegtmeyer N, Wittelsberger R, Hartig R, Wessler S, Martinez-Quiles N, et al. (2011) Serine phosphorylation of cortactin controls focal adhesion kinase activity and cell scattering induced by Helicobacter pylori. Cell Host Microbe 9: 520–531.
38. Parsons JT, Martin KH, Slack JK, Taylor JM, Weed SA (2000) Focal adhesion kinase: a regulator of focal adhesion dynamics and cell movement. Oncogene 19: 5606–5613.
39. Arndt KM, Pelletier JN, Müller KM, Alber T, Michnick SW, et al. (2000) A heterodimeric coiled-coil peptide pair selected in vivo from a designed library-versus-library ensemble. J Mol Biol 295: 627–639.
40. Yadav SS, Yeh BJ, Craddock BP, Lim WA, Miller WT (2009) Reengineering the signaling properties of a Src family kinase. Biochemistry 48: 10956–10962.
41. Kelley LC, Ammer AG, Hayes KE, Martin KH, Machida K, et al. (2010) Oncogenic Src requires a wild-type counterpart to regulate invadopodia maturation. J Cell Sci 123: 3923–3932.
42. Choudhary C, Kumar C, Gnad F, Nielsen ML, Rehman M, et al. (2009) Lysine acetylation targets protein complexes and co-regulates major cellular functions. Science 325: 834–840.
43. Parsons JT, Horwitz AR, Schwartz MA (2010) Cell adhesion: integrating cytoskeletal dynamics and cellular tension. Nat Rev Mol Cell Biol 11: 633–643.
44. Wang W, Liu Y, Liao K (2011) Tyrosine phosphorylation of cortactin by the FAK-Src complex at focal adhesions regulates cell motility. BMC Cell Biol 12: 49.
45. Yang XJ, Seto E (2008) Lysine acetylation: codified crosstalk with other posttranslational modifications. Mol Cell 31: 449–61.
46. Yang XJ, Gregoire S (2007) Metabolism, cytoskeleton and cellular signalling in the grip of protein Nepsilon - and O-acetylation. EMBO Rep 8: 556–562.
47. Kramer OH, Knauer SK, Greiner G, Jandt E, Reichardt S, et al. (2009) A phosphorylation-acetylation switch regulates STAT1 signaling. Genes Dev 23: 223–235.
48. Gao YS, Hubbert CC, Lu J, Lee YS, Lee JY, et al. (2007) Histone deacetylase 6 regulates growth factor-induced actin remodeling and endocytosis. Mol Cell Biol 27: 8637–8647.